THE ROLE OF INHIBITORS OF APOPTOSIS (IAPs) IN RETINAL GANGLION CELL DEATH AND DENDRITE REMODELLING

Lilian Kisiswa

Thesis submitted to Cardiff University in accordance with the requirements for the degree of Doctor of Philosophy

Visual Neuroscience and Molecular Biology Group
School of Optometry and Vision Sciences
Cardiff University
2010

ProQuest LLC
789 East Eisenhower Parkway
P.O. Box 1346
Ann Arbor, MI 48106-1346

CARDIFF UNIVERSITY
PRIFYSGOL CAERDYDD

DECLARATION

This work has not previously been accepted in substance for any degree and is not being currently submitted in candidature for any degree.

Signed ..... Date 24.1.11

STATEMENT 1

This thesis is being submitted in partial fulfillment of the requirements for the degree of PhD.

Signed ..... Date 24.1.11

STATEMENT 2

This thesis is the result of my own investigation, except where otherwise stated. Other sources are acknowledged by footnotes giving explicit references. A bibliography is appended.

Signed ..... Date 24.1.11

STATEMENT 3

I hereby give consent for my thesis, if accepted, to be available for photocopying and for inter-library loan, and for the title and summary to be made available to outside organisations.

Signed ..... Date 24.1.11

Dedicated to my father, Mr. Guðmundur Kristján Þorvarðarson.

Acknowledgements

Firstly, I would like to thank my supervisors Professor James E. Morgan, Dr. Michael A. Wride and Dr. Julie Albon for their supervision, support, encouragement and continuous guidance throughout the course of my studies.

I would also like to express my profound gratitude to Professor Alun M. Davies for giving me an opportunity to work in his laboratory. I wish to thank Dr. Humberto Gutierrez for sharing his knowledge and expertise in neuroscience methods. Thanks to my advisor, Dr. Malgorzata Rózanowska for her guidance throughout my studies.

Very special thanks to Drs. Debbie Tudor and Kate Powell for fruitful discussion and for their moral support and encouragement. Thanks to Elaine for her support and encouragement.

Many thanks to all the members of the Davies' group who have been very helpful during my study, especially Dania. I'm also thankful to all the members of Morgan's group, past and present for their laughs, support and discussion.

Thanks to my dear friends, Helen, Catarina and Miguel for listening to me complaining and being ready to help in every possible way.

My sincere thanks goes to my dear sister Susan Kagai, although being stubborn, she has always given me unconditional love, laughs, encouragement and support.

Last but not least, I'm grateful to my dad Mr Guðmundur Kristján Þorvarðarson for giving me unconditional love and care. I would have not made this far without his faith and encouragement.

Abstract

Neuronal viability and connectivity is essential for neuronal function in heath and disease. The aim of this study was to elucidate factors and mechanisms that govern the maintenance and remodelling of RGC dendrites, as well as neuronal cell death in ageing and neurodegenerative diseases. Using PCR technique, the expression pattern of caspases 3,6-9 and inhibitors of apoptosis (IAPs), namely neuronal IAP (NIAP), cellular IAP1 and 2 (cIAP1 and 2), X-chromosome linked IAP (XIAP), Survivin, Bruce and Livin was determined in young adult (6 weeks), mature (24-52 weeks), old (88 weeks) and diseased retinae of Wistar albino and Brown Norway (BN) rats. Caspase expression was not altered during maturation and ageing in both strains. In ageing Wistar, NIAP, cIAP2 and XIAP and cIAP1 were decreased in 88 compared to 24-52 weeks, while Survivin, Bruce and Livin were slightly increased with age. IAPs expression was generally decreased in mature (24-52 weeks) BN retinae compared to younger (6 weeks). Furthermore, validation of the expression of these molecules at protein level was carried out using western blotting and immunofluoroscence techniques. cIAP1 protein levels were downregulated in RGCL of BN rats. Reduction of cIAP1 did not alter caspase activity but led to impairment in the survival pathway. Older BN retinae demonstrated compromised RGC morphology, but there was no retinal cell loss. Microbead experimental glaucoma model demonstrated no alteration in caspase expression upon induction of glaucoma. NIAP, cIAP2, Survivin and Livin were up-regulated, while Bruce was down-regulated in glaucomatous eyes. cIAP1 and XIAP expression remain similar between control and experimental eye. In conclusion, reduction in IAPs, which may lead to impairment in survival pathways might be the underlaying cause of reduction in dendrite complexity. Compromised RGC morphology makes a preparatory platform for neurodegenerative process observed in glaucoma disease where age is a major risk factor.

Table of contents

List of figures

List of tables

Abbreviations

γ	Gamma
AD	Alzeheimers' disease
AMPAR	α-amino-3-hydroxy-5-methylisoxazole-4-propionic acid receptors
ANOVA	Analysis of variance
Apaf-1	Adaptor molecule apoptosis protease activated factor
ARVO	Associassion of research in vision and ophthalmology
ATP	Adenosine-5'-triphosphate
Bcl-2	B cell lymphoma 2
BDNF	Brain derived neurotrophic factor
BIR	Baculovirus Inhibitor of apoptosis protein Repeat
BN	Brown Norway
Bp	Base pair
BSA	Bovine serum albumin
BSS	Balanced salt saline
Ca^{2+}	Calcium
CaMII &IV	Calcium calmodulin kinase II and IV
cAMP	Cyclic adenosine monophosphate
CARD	caspase recruitment domain
cDNA	Complementary DNA
CED	Caenorhabditis elegance defective
cGMP	Cyclic nucleotide guanosine 3`/5`-monophosphate
cIAP1&2-	Cellular inhibitor of aopotosis 1 and 2
CMA	Chaperone-mediated autophagy
CNS	Central nervous system
CO_2	Carbon dioxide
COOH	Carboxyl group
CREB	cAMP response element binding protein
Ct	Threshold cycle
Cx43	Connexin 43
Dasm1	Dendrite arborization and synapse maturation 1
DED	Death effector domain
DIABLO	Direct IAP binding protein with low pI
DIAP1	Drosophila inhibitor of apoptosis 1
DIC	Differential interference contrast microscopy
DiI	1,1'-dioctadecyl-3,3,3',3'-tetramethylindocarbocyanine
DmIKKε	Drosophila IKK- related kinase
DNA	Deoxyribonucleic acid
DPX	Digital Picture Exchange mounting medium
DRONC	Drosophila effector caspase
dt	Delta
e.g	exempli gratia (for the sake of example)
EDTA	Ethylenediaminetetraacetic acid
EtBr	Ethidium bromide

FADD	Fas activated death domain
Fe_3O_4	Ferrous-ferric oxide
g	Gram
GAPDH	Glyceraldehyde 3-phosphate dehydrogenase
GFAP	Glial fibrillary acidic protein
GTP	Guanosine triphosphate
H&E	Hemotoxilin and eosin
HD	Huntington's disease
i.e	id est(that is
IAP	Inhibitor of apoptosis
IgG	Immunoglobulins
IGL	Intergeniculate leaflet
IKK	Inhibitor of NF-kB (IkB) kinase
INL	Inner nuclear layer
IOP	Intraocular pressure
IP3	Inositol phosphatidyl 3
JNK1	c-Jun N-terminal kinase 1
kDa	Kilodalton
LAMP-2A	Lysosomal membrane receptor lysosomal-associated membrane protein 2A
LGN	Lateral geneculate nucleus
mA	Miliampere
MAP2	Microtubuli associated protein
MAPK	Mitogen-activated protein (MAP) kinases
Max	Maximum
MESA	MOPS electrophoresis buffer
mL	Mililiters
Mm	Milimeter
MOPS	4-Morpholinepropanesulfonic acid
mRNA	Messenger ribonucleic acid
NF-kB	Nuclear factor kappa-light-chain-enhancer of activated B cells
NGF	Nerve growth factor
NIAP	Neuronal inhibitor of apoptosis
NK	Natural killer cells
Nm	Nanometer
NMDAR	N-methyl D aspartate receptor
NT3&4	Neurotrophin-3 and 4
ns	Non significant
OC	Optic tract
OCT	Ocular coherence tomography
OD	Optical density
OH	Hydroxide
ON	Optic nerve
ONH	Optic nerve head
ONL	Outer nuclei layer
OPN	Olivary pretectal nucleus

Opn4	Melanopsin
OT	Optic chiasma
PAGE	Polyacrylamide gel electrophoresis,
PBS	Phosphate buffer saline
PCR	Polymerase chain reaction
PD	Parkinson's disease
PEG	Polyethylen glycol
PFA	Paraformaldehyde
pH	Power of hydrogen
PMB	paramagnetic beads
PMSF	Phenylmethanesulfonylfluoride or phenylmethylsulfonyl fluoride
PNS	Peripheral nervous system
pRGC	Melanopsin containing retinal ganglion cells
Psi	Pound per square inch
PVP	Poly-4-vinylphenol
QPCR	Quantitative PCR
RGC	Retinal ganglion cells
RGCL	Retinal ganglion cell layer
RIPA	Radioimmunoprecipitation assay buffer
RNA	Ribonucleic acid
RPM	Revolutions per minute
RT-PCR	Reverse transcriptase polymeras chain reaction
SC	Superior collicullus
SCN	Suprachiasmatic nuclei
SD	Standard devietion
SDS	Sodium dodecyl sulfate
SEM	Standard error
Sema3A	Semaphorin 3A
Shh	Sonic hedghog
SMA	Spinal cord muscle atrophy
Smac	Second mitochondria activator of caspase
SOP	Sensory organelle precursor
SPSS16	Self-Propelled Semi-Submersible 16
Ta	Annealing temperature
TBS	Tris Buffered Saline
TBST	Tris-Buffered Saline and Tween 20
TdT	Deoxynucleotidyl Transferas
TE	Tris EDTA
Tm	Melting temperature
TM	Trabecular meshwork
TNF	Tumor necrosis factor
TNFR	Tumor necrosis factor receptor
TRADD	Tumor necrosis receptor assossiated death domain
TRAF2	Tumor necrosis factor receptor assossiated factors 2
Trk	Tyrosin kinase receptor
TsIAP	Testis inhibitor of apoptosis

TUNEL	Terminal deoxynucleotidyl transferas-mediated deoxyuridine triphosphate (dUTP)-biotin nick end labelling
U	unit
Uba1	Ubiquitin activation enzyme
UbcD1	Ubiquitin-conjugating enzyme
UK	United Kingdm
UPS	Ubuquitin system
UTP	Uridine-5'-triphosphate
UV	Ultraviolet
V	volt
XIAP	X-chromosom linked inhibitor of apoptosis
µG	Micrograms
µL	Microliters

Chapter 1

General Introduction

1.1 General introduction

The viability of the cell body and interneuronal connections are required for neural function in health and disease. Work performed by various group, including ours has emphased the importance of the viability of the neuronal cell body and interneuronal connections in neuronal pathologies. Neurons receive and processes incoming signals through the dendritic tree and convey the information to other neurons or parts of the body via axons (Brown, 2001). Dendrites are unique because they occupy a large three-dimensional space in a relationship to the cell body and axon and are highly plastic (Stuart, 2008), which increases susceptibility to any changes. In many neurodegenerative diseases (Alzheimer's disease (AD),Parkinson's disease (PD) and glaucoma), changes in the dendritic tree are taken as an early sign of disease. In AD remodelling of the dendritic tree is seen as a foundation of the disease etiology (Knobloch and Mansuy, 2008). Changes in the dendritic tree also occur in PD, where the loss of dopaminergic neuron input induces changes in the dendrites in the affected striatal regions (Deutch, 2006, Zaja-Milatovic et al., 2005).

In retinal pathologies such as glaucoma, dendrite remodelling occurs as an early event (Liets et al., 2006). Studies carried out in primates and murine models of glaucoma confirm that the changes have functional consequences (Weber and Harman, 2005). Despite this, the molecular mechanisms that control these changes are still unclear. The rapid development of non-invasive bio-imaging techniques as such ocular coherence tomography (OCT) and Optophysiology gives a promising sign of providing a way to detect these changes in the early stages of disease in the near future (Bizheva et al., 2006). That is why it is very important to elucidate the molecular mechanisms that modulate the changes in the dendrite during ageing and disease. The knowledge that will be obtained from this study might be essential for design of more effective therapeutic drugs for neuroprotection.

1.2 Neuronal cell death

Cell death is defined by failure of a cell to maintain crucial life functions. One of the early sign of cell death is irreversible damage to the plasma membrane (Golstein and Kroemer, 2007). There are three types of cell death based on morphological criteria: Type I programmed cell death (apoptosis) that is a cell intrinsic mechanism for suicide; Type II cell death (autophagy) is characterised by the accumulation of double-membrane autophagic vacuoles in the cytoplasm; and Type III cell death (necrosis) is defined by the absences of the features observed in type I and type II cell death and is adenosine-5'-triphosphate (ATP)-independent (Edinger and Thompson, 2004). In addition to these modes of cell death, cells can be eliminated by other mechanisms including mitotic catastrophe, dark cell death, paraptosis, chondroptosis and autoschizis. Mitotic catastrophe is a type of cell death that occurs during mitosis (Castedo et al., 2004). Dark cell death is death usually observed in Huntington's disease (Wolszon et al., 1994). It is defined by strong cytoplasmic condensation, chromatin lumping and ruffling of the cell membrane, but blebbling of the nucleus or plasma membrane is not observed (Turmaine et al., 2000).

Paraptosis is a variant of apoptosis that is characterised by formation of cytoplasmic vacuoles and mitochondrial swelling (Yamashima, 2004); (Sperandio et al., 2004). This kind of cell death is observed in amyotrophic lateral sclerosis (Sperandio et al., 2004). Similar to paraptosis, chondroptosis is a variant of classical apoptosis with features such as cell shrinkage, chromatin and involvement of apoptosis but is phagocytosis-independent (Roach et al., 2004). In autoschizis, the cell membrane splits allowing the cytoplasma to leak (Gilloteaux et al., 1998, Gilloteaux et al., 1995, Jamison et al., 2002). The aim of this introduction is to briefly summarise the literature on necrosis and autophagic cell death and to discuss apoptosis in detail, its components and involvement in dendrite remodelling because it is becoming apparent that regulated apoptosis signalling has a role in dendrite remodelling (Williams et al., 2006). The links between the three types of cell death in the context of neurodegenerative disease will also be discussed, focusing on glaucoma.

1.2.1 Necrosis

Necrosis occurs as a consequence of pathological insults secondary to toxin exposure or physical damage (Edinger and Thompson, 2004). It is defined by disruption of the plasma membrane and spillage of intracellular contents into the surrounding milieu with the consequence of initiating inflammation around the necrotic cell. The physiological importance of necrotic cell death has yet to be determined. Necrosis can be triggered by an apoptotic signal, such as activation of tumour necrosis factor (TNF) receptor; cells will die even in the presence of anti-apoptotic molecules and the cell will display all the morphological hallmarks of a necrotic cell (Jaattela and Tschopp, 2003). Indeed, Chan et al., studied cell death in *Vaccinia* infected cells to demonstrate the physiological significance of necrosis (Chan et al., 2003). *Vaccinia* encodes for anti-apoptotic proteins to preserve host cell viability. Addition of the proinflammatory cytokine, TNF to *Vaccinia* infected cells resulted in necrosis in the face of inhibition of apoptotic pathways (Chan et al., 2003).

1.2.2 Autophagy

Autophagy means "eat oneself". Most cells have a basal level of active autophagy where it has a housekeeping role in maintaining the integrity of intracellular organelles and proteins (Jin, 2006). However, nutrients deprivation strongly induces activation of autophagy and this has been postulated to be an adaptive response of cells to starvation that promotes survival (Glick et al., Levine and Klionsky, 2004). Autophagic cell death involves formation of double membrane vesicles in the cytosol in which whole organelles and bulk cytoplasm are encapsulated. The vesicles are then fused with the lysosome in which the contents of the autophagosome is degraded and recycled (Edinger and Thompson, 2004). Thus, physiologically, autophagy is thought to play a role in degeneration of damaged organelles and long-lived proteins in order to provide energy in times of starvation.

There are three modes of autophagy, namely macro-, micro- and chaperone-mediated autophagy, all of which promote proteolytic degradation of organelles and proteins in the lysosomes. Marco-autophagy transfers cytoplasmic cargo to the lysosomes through autophagosomes (double membrane bound vesicles) that fuses to lysosomes and forms an autolysosome. In micro-autophagy, on the other hand, the organelles and proteins are directly taken up by the lysosome itself. In chaperone-mediated autophagy (CMA), targeted cytoplasmic components are bound to chaperone proteins (such as heat shock (HSP)-70) forming a complex that is translocated across the lysosomal membrane. This is facilitated by the recognition of HSPs by lysosomal membrane receptors such as lysosomal associated membrane protein (LAMP-2A) leading to unfolding and degradation cytoplasmic cargo (Saftig et al., 2008).

1.2.3 Apoptosis

1.2.3.1 Introduction to apoptosis

Apoptosis is a type programmed cell death, which is orchestrated by a series of biochemical occurrences as part of signalling cascade (Fig 1.1). The biochemical and morphological hallmarks of apoptotic cells are chromatin condensation, cell shrinkage, plasma membrane blebbling, mitochondrial disruption, DNA fragmentation, and formation of apoptotic bodies (Kerr et al., 1972). In contrast to necrotic cell death, apoptosis is an active, energy consuming process carried out in an ordered manner. Apoptosis is essential for the development and viability of a healthy organism. The initiation of the apoptotic process may occur extrinsically or intrinsically. The extrinsic pathway involves the activation of death receptors such as Fas, a member of the TNF receptor superfamily,on the cell membrane (Ashkenazi and Dixit, 1998). The activation of death receptors leads to activation of Fas activated death domain (FADD), which in turn activates initiator caspases. Active, initiator caspases then activate effector caspases (see next paragraph for details on initiator and

effector caspases). Once the effector caspases are activated ("point of no return"), the cell is designated to die (Guerin et al., 2006).

The key organelle for the intrinsic pathway is the mitochondrion. In addition to being the energy station for the cell, the mitochondrion houses a proapoptotic molecule including the members of the B cell lymphoma 2 (Bcl-2) family (such as Bax and Bim) and cytochrome c. Bcl-2 family members controls mitochondrial integrity which, if compromised results in the release of cytochrome c to the cytosol resulting in its association with the adaptor molecule apoptosis protease activated factor (Apaf-1). The outcome is formation of a multimeric complex called the apoptosome that recruits caspase 9 and builds an active holoenzyme (Jiang and Wang, 2004). Once activated, caspase 9 is then capable of activating the effector caspase (Slee et al., 1999). It is important to note that crosstalk between the two pathways is possible and is mediated by truncated Bid molecules that are activated by caspase 8. Activated Bid promotes release of cytochrome c through activation of Bax (Li et al., 1998).

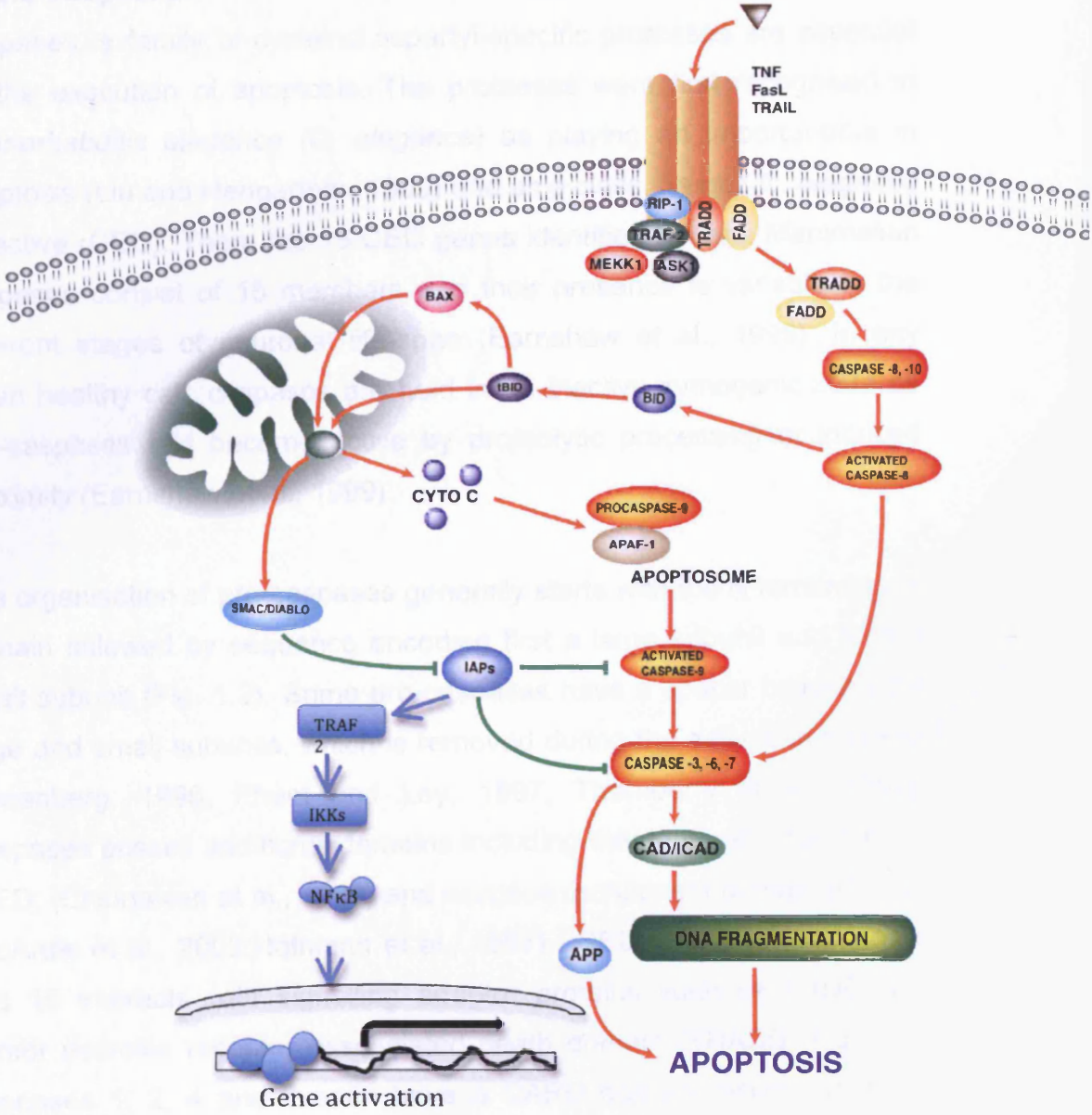

Fig. 1.1. Apoptosis cascade. Programmed cell death can be activated via extrinsic factors (TNF receptor activation) or intrinsically by the relise of cytochrome c release from mitochondria. Both pathways lead to activation of effector caspases (including caspases 3, 6 and 7) that activate apoptotic protein cleavage. The IAP family of proteins inhibit, both initiator and effector caspases activation, but they in turn can be inhibited by smac/Diablo relise from damaged mitochondria. It is hypothesis for this project that IAPs may have a role in activation of NFκB, which is survival pathway. This activation in turn has an inhibitory effect on apoptotic pathway. Figure adapted with modification from Kisiswa et al., (2009). Picture courtesy of Dr. Adrian G Dervan.

1.2.3.2 Caspases

Caspases, a family of cysteine aspartyl-specific proteases are essential for the execution of apoptosis. The proteases were first recognised in *Caenorhabditis elegance (C. elegance)* as playing an importantrole in apoptosis (Liu and Hengartner, 1999) and as a class, named *C. elegance* defective (CED). There are 15 CED genes identified to date. Mammalian caspases consist of 15 members and their presence is variable in the different stages of neuronal life-span (Earnshaw et al., 1999). In any given healthy cell, caspases are held in an inactive zymogenic state as pro-caspases and become active by proteolytic processing or induced proximity (Earnshaw et al., 1999).

The organisation of pro-caspases generally starts with the N-terminal pro-domain followed by sequence encoding first a large subunit and then a small subunit (Fig. 1.2). Some pro-caspases have a spacer between the large and small subunits, which is removed during the activation process (Greenberg, 1996, Pham and Ley, 1997, Thornberry et al., 1997). Caspases posses additional domains including the death effector domain (DED; (Chinnaiyan et al., 1995) and caspase recruitment domain (CARD; (McArdle et al., 2002:Hofmann et al., 1997). DED, found in caspases 8 and 10 interacts with signalling adaptor proteins such as FADD and Tumor necrosis receptor assossiated death domain (TRADD, Fig. 1.2). Caspases 1, 2, 4 and 9 each have a CARD domain, which facilitates interaction between different caspases and between caspases and other regulatory and adaptor proteins (Earnshaw et al., 1999). There are two categories of caspases, namely initiator caspases (caspase 1, 2, 6, 8 and 9) and effector caspases comprising caspase 3, 4 and 7 in mammalian cells (Table 1.1). Initiator caspases tends to have large pro-domain and require oligomerisation and conformational change in order to be activated. Activation of effector caspases (caspases with a smaller pro-domain) involves cleavage on the carboxyl side of aspartate residues and assembly of peptide fragments that gives rise to an activated enzyme (Prunell and Troy, 2004).

Once activated, caspases induce cell death by cleaving cytoskeletal and associated proteins including kinases, members of the Bcl-2 family of apoptosis-related proteins, presinilins, amyloid precursor protein and DNA repair enzymes as well as by indirectly activating chromosomal endonucleases (Guerin et al., 2006). The expression of caspases varies depending on age of the organism. Recently, it has been shown that older mouse retinas are more resistant to apoptosis *in vitro*. This is due to lower expression of proapototic factors, such as caspase 3 and 9 in the older compared to the younger animals (McKernan et al., 2006). This clearly indicates that the caspase profile differs during development and adulthood.

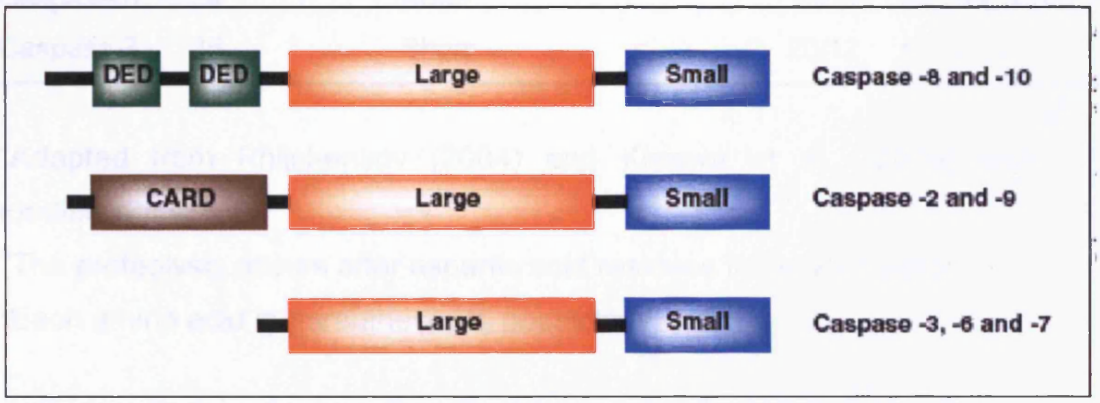

Figure 1.2. Structure of mammalian caspase family. Caspases 2,8-10 containes a pro-domain followed by a large and small subunit while caspases 3,6and 7 lacks pro-domain. The pro-domain, which varies in length may consists of two DEDs (found in caspase 8 and 10) and CARD (found in caspase 2 and 9). Both DED and CARD are absent in caspases 3, 6 and 9. Figure, a courtesy of Dr. Adrian G Dervan was adapted from Kisiswa et al., (2009).

Table 1.1. Structural and functional characteristic of mammalian neuronal caspases[a]

Caspase	Size of pro-caspase (kDa)	Prodomain type	Active subunit (kDa)	Caspases proteolytic specificities
Apoptotic initiator caspase				
Caspase-2	51	Long with CARD domain	19/12	VDVAD[a]
Caspase-8	55	Long with two DED domains	18/11	(L/V/D)E(T/V/I)D[b]
Caspase-9	45	Long with CARD domain	17/10	(L/V/I)EHD
Caspase -10	55	Long with two DED domains	17/12	(I/V/L)EXD
Apoptotic effector caspase				
Caspase-3	32	Short	17/12	DE(V/I)D
Caspase-6	34	Short	18/11	(T/V/I)E(H/V/I)D
Caspase-7	35	Short	20/12	DE(V/I)D

[a]Adapted from Philchenkov (2004) and Kisiswa et al., (2009) with modifications.

[b]The proteolysis occurs after aspartic acid residues in the P_1 position

[c]Each amino acid in parentheses is possible

Table 1.2. Protein substrate of caspases[a]

Protein substrates	Caspases	Cleavage motif	Function of substrate
PARP	3,7	DEVD↓G	DNA repair enzyme
U1-70kDa	3	DGPD↓G	Splicing of RNA
DNA-PKcs	3	DEVD↓N	DNA double-strand-break repair
Gas2	3,7[b]	SRVD↓G	Component of microfilament system
Protein kinase C δ	3	DMQD↓N	Cleaved to active form in apoptosis
Pro-IL-1β	3	DELD↓S	Regulator of Rho GTPases
Lamin A	6	VEID↓N	Assist in maintaining nuclear shape
Heteroribonuclear proteins C1 and C2	3,7	?	Process of pre-RNA
Huntingtin	3	DXXD	Huntington disease gene product
Frodin	3[c]	DEAD↓S	Membrane associated cytosketal protein

[a]Table adapted from (Cohen, 1997)and Kisiswa et al., (2009) with modifications

[b](Sgorbissa et al., 1999)

[c](Tahzib et al., 2004)

1.2.3.3 Inhibitors of apoptosis (IAPs)

To prevent unnecessary cell death, cells are equipped with molecules called IAPs, which are the only known endogenous proteins that modulate the activity of both initiator and effector caspases. IAPs are members of a protein family characterised by the presence of one or more 70-80 amino-acids baculoviral IAP repeats (Vonsattel et al.)domains (Fig 1.3). The BIR domains are defined by cysteine and histidine-rich protein folding domain that chelates zinc and forms a

compact globular structure consisting of four to five alpha helices and variable number of anti-parallel beta-pleated sheets (Liston et al., 2003). There are two types of BIR domains: Type I domains posses a high homology with the BIR domains in baculovirus IAPs and are capable of binding and inhibiting caspase; by contrast type II domains bind to caspases but affect the cell cycle i.e, they are expressed only during mitosis where they regulate cell division (Verhagen et al., 2001).

IAPs exert their functions either by binding to pro-caspases and preventing their activation, or by binding activated caspases to block their activity. Eight mammalian IAPs has been identified, namely, X-chromosome-linked IAP (XIAP), cellular IAP (cIAP) 1 and 2, testis-specific IAP (TsIAP), neuronal IAP (NAIP), Survivin Bruce and Livin have been characterised (Prunell and Troy, 2004). With the exception of Survivin and Bruce, all mammalian IAPs contain type I BIR domains. Different IAPs may contain additional domains, such as the caspase recruitment domain (McArdle et al. 2002), which is found in cIAP1 and 2, and the RING finger domain, which is present in XIAP, cIAP1 and cIAP2 (Uren et al., 1996). In addition to their apoptosis inhibition properties, IAPs can also function as caspase substrates. In this case, caspases cleave IAPs in order to enhance their activity. For example, full-length XIAP is a less potent inhibitor of caspase 9 compared to the BR3-RING portion (Deveraux et al., 1997). Furthermore, there are a number of factors that are able to suppress the IAP activity.

Three mammalian negative IAP regulators have been identified; Smac [second mitochondria activator of caspase; known as DIABLO (direct IAP binding protein with low pI) in mouse], XIAP-associated factor 1 (XAF1) and Omi, a mitochondrial IAP-binding protein. Smac/Diablo positively regulates caspase activity by binding IAPs which results in the dissociation of IAPs from caspases, which in turn primes the execution phase of apoptosis (Duckett, 2005).XAF1 and Omi negatively regulated XIAP function by directly binding to XIAP preventing caspase 3 inhibition(Liston et al., 2001). Interestingly, Omi is also involved in

caspase-indipendent cell death (Liston et al., 2003). A summary of all mammalian IAPs, caspase activity and identified bonding protein can be seen in table 3

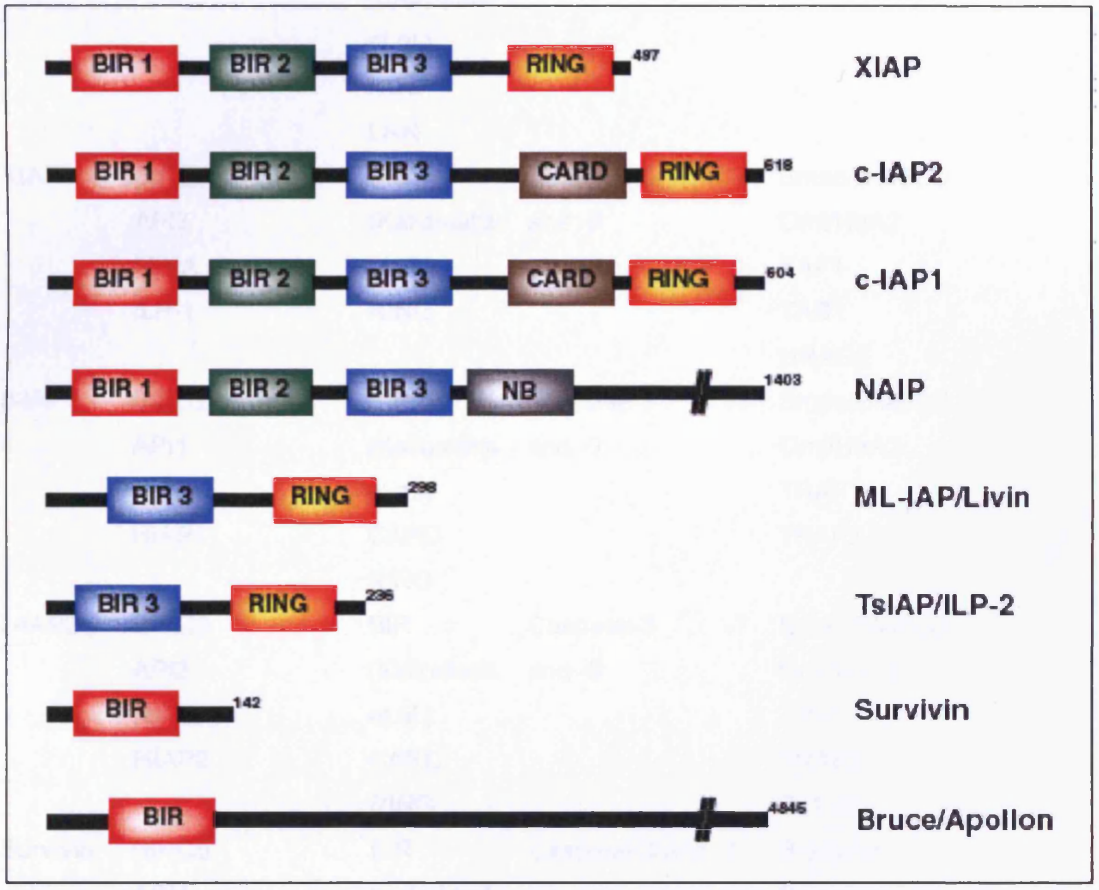

Figure 1.3 The mammalian IAPs structure. The IAPs contain one or more BIR domains of either type I or II. In addition to the BIR domains, some IAP contains a RING zinc-finger domain, which employs E3 ubiquitin ligase activity and enables the IAP to catalyze ubiquitination, and a CARD domain that allows for homotypic protein-protein interaction. The "survivin-like" IAPs (Survivin and Bruce) are the simplest IAPs containing only one BIR domain. Figure adapted from Kisiswa et al., (2009) and is a courtesy of Dr. Adrian G Dervan.

Tabel 1.3. IAPs normenclature and their properties. Table adapted from Liston et al., (2003).

IAP	Alternative names	Domains	Caspase specificity	Identified binding proteins
NIAP	BIRC1	BIR (Kalloniatis et al.) NOD LRR	Caspase-3 and -7	Hippocalcin
XIAP	BIRC4 API3 MIHA ILP-1	BIR (Kalloniatis et al.) RING	Caspase-3 , -7 and -9	Smac/DIABLO Omi/HtrA2 XAF1 TAB1 NRAGE
c-IAP1	BIRC2 API1 MIHB HIAP1	BIR (Kalloniatis et al.) CARD RING	Caspase-3 , -7 and -9	Smac/DIABLO Omi/HtrA2 TRAF1 TRAF2
c-IAP2	BIRC3 API2 MIHB HIAP2	BIR (Kalloniatis et al.) CARD RING	Caspase-3 , -7 and -9	Smac/DIABLO Omi/HtrA2 TRAF1 TRAF2 Bc110
Survivin	BIRC5 API4 TIAP (mouse)	BIR Coiled coil	Caspase-3 and -7	B-tubulin Smac
Livin	BIRC7 KIAP ML-IAP	BIR RING	Caspase-3 , -7 and -9	Smac
Ts-IAP	BIRC8 ILP-2	BIR RING	Caspase-9	

1.2.3.4 Non-Apoptotic role of caspases

It is important to emphasise that caspase activation does not always have lethal consequences. A large body of literature has documented that caspases are involved in various cellular process, including cell proliferation and differentiation (Sadowski-Debbing et al., 2002, Schwerk and Schulze-Osthoff, 2003).

1.2.3.4.1 Role of caspases in cell proliferation

Several reports suggest that caspases are essential for proliferation of immune cells. Utilising caspase inhibitors, it was demonstrated that caspase 8 is required for T lymphocyte proliferation (Kennedy et al., 1999, Alam et al., 1999). In line with this, work carried out on patients bearing inactivation mutations in caspase 8 revealed that these patients had abnormal proliferation of several immune cells including T and B lymphocytes and natural killer (NK) cells (Chun et al., 2002).

1.2.3.4.2 Role of caspases in cell differentiation

The first studies linking caspases to cell differentiation were perfomed in lens fibre cells (Ishizaki et al., 1998, Wride et al., 2006). Based on these observations it was hypothesised that caspases are involved in cell differentiation in various cells including erythrocytes, platelets, osteocytes and keratinocytes in addition to lens fibre cells (Oliver and Vallette, 2005). In keratinocyte differentiation, Okuyama and colleagues demonstrated that caspase 3 is required (Okuyama et al., 2004), while it was also reported that caspase 3 is important for efficient erythropoiesis (Carlile et al., 2004). Caspases 3 and 9 are also been suggested to be crucial for maturation of monocytes to macrophages but not to dendritic cells (Sordet et al., 2002). In osteoblast differentiation, caspases 8, 2 and 3 are required (Mogi and Togari, 2003)

1.3 Retina

The retina represents the critical first stage for the transduction of visual signals. It is a highly organised multilayered part of the central nervous system (CNS) and maintains a high level of metabolic activity. A fully developed normal retina is approximately 500 microns thick in human and 250 microns thick in rat. Morphologically, the retina is composed of RGCs which are the output neurons of the retina, photosensors, consisting of the rods and cones, horizontal, bipolar, amacrine cells and Müller glia (Masland, 2001, Becker et al., 1998). RGCs are located closest to the lens, while the photoreceptors are situated against to the epithelium and choroid (Guerin et al., 2006).Alteration in viability in RGCs and interneuronal connections plays an important role in retinal disorders. Investigations performed on the retina over the past few years have elucidated the importance of a viable cell body, but little is know about the significance of neuronal connectivity in maintaining retinal function

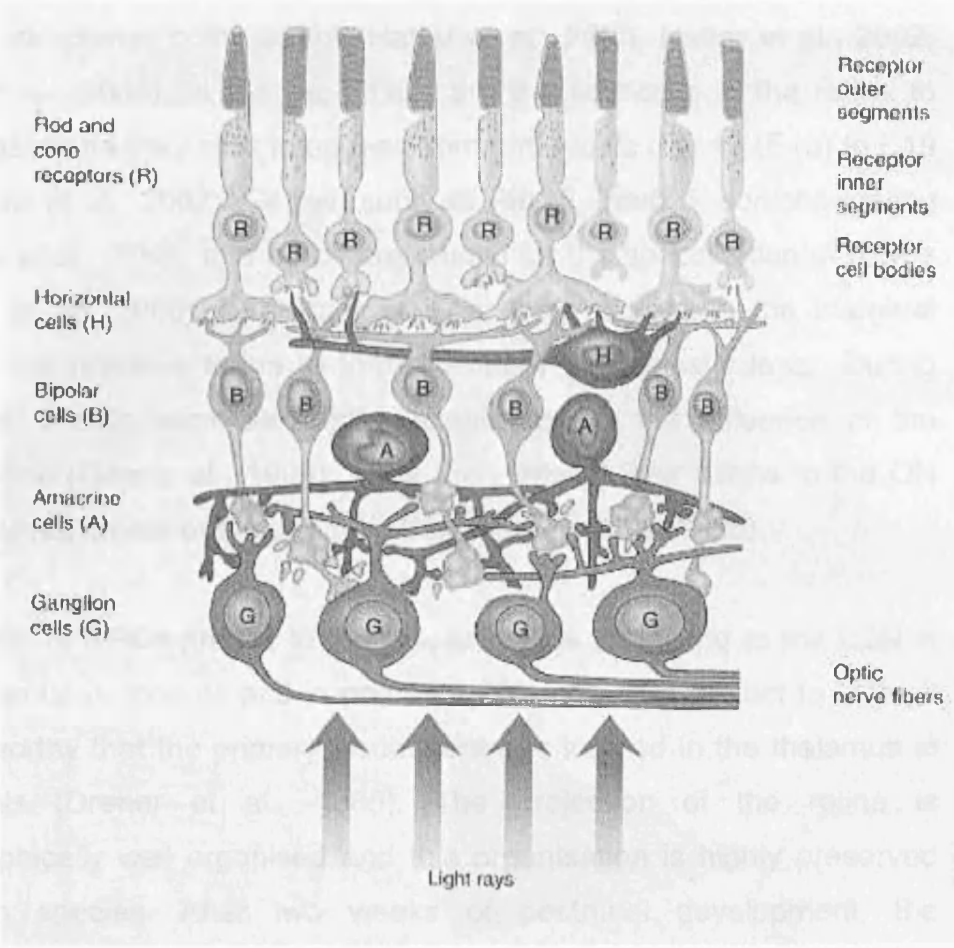

Figure 1.4. Mammalian retinal structure. Retina comprises of different cells including photoreceptors, horizontal cells, bipolar cells, amacrine cells, ganglion cells and glial cell (not shown on the picture). Picture adapted from www.owlnet.rice.edu/~psyc351/imagelist.htm. Accessed on 1.6.2010.

1.4 Retinal ganglion cells (RGCs)

RGCs represent 1% of the total number of retinal cells in the adult retina (Young, 1985) and comprise up to 70% of the cells in the ganglion cell layer (RGCL; (Isenmann et al., 2003). They are the only retinal neurons that project their axons through the optical nerve (ON), optic chiasm (OC) and the optic tract (OT) to their main targets, the superior colliculus (SC) and lateral geniculate nucleus (LGN) in the midbrain (Isenmann et al., 2003). Other RCGs targets in the brain include suprachiasmatic nucleas (SCN), intergeniculate leaflet (IGL), olivary pretectal nucleas (OPN),

lateral hypothalamus and preoptic regions, which are classified as "non imaging structures in the brain" (Hattar et al., 2006, Hattar et al., 2002, Morin et al., 2003). In the rat, RGCs are the first cells in the retina to differentiate and they start to appear from embryonic day 13 (E13) to E19 (Dallimore et al., 2002). Genes, such as *Pax 6*, *math 5*, *sonichedgehog (Ashhab et al., 2001)* and *notch* are crucial for the specification of RGCs (Guerin et al., 2006). After specification, they migrate to the marginal zone of the primitive retina to form the inner neuroblastic layer. During migration, RGCs terminates differentiation under the influence of the *brn36* gene (Gan et al., 1999). They then extend their axons to the ON before development of the dendritic tree (Maslim et al., 1986).

Over 90% of RGCs project to the SC, with 10% projecting to the LGN in the thalamus in rodents and in primates 90% of RGCs project to LGN. It is noteworthy that the primary visual centre is located in the thalamus in mammals (Dreher et al., 1985). The projection of the retina is topographically well organised and this organisation is highly preserved between species. After two weeks of postnatal development, the development and fine-tuning of the retino-tectal projections is completed and is in the adult state (Isenmann et al., 2003). The retino-tectal map is defined by the presence of both an anterior-posterior and a nasal-temporal orientation. Axons from the temporal retina project to the rostral SC, while the axons from the nasal retina innervate the caudal SC. Axons from the ventral retina project to the dorsal SC, while axons from the dorsal retina project to the ventral SC (Isenmann et al., 2003).

Morphologically, RGCs are classified into different types based on soma size and the architecture of the dendrite arbour (Fig. 1.5). These include two major groups: monostratified cells and bistratified cells. The groups are further subdivided into subtypes and have different nomenclature depending on the species (Sun et al., 2002). In the primate retina, the monostratified cells class consists of midget and parasol cells. The vast majority of RGCs in primates are the midget cells, which represents 80% of the RGCs. They have a medium-sized soma and a fairly small but

compact and bushy dendritic tree. The second biggest population is comprised of the parasol cells that represent 10% of RGCs in the primate retina. They have the largest soma and dendritic field among the neurons in the ganglion cell layer (Weber et al., 1998). Bistratified cells in the rat are small in size with recursive and loop-forming dendrites (Sun et al., 2002).

Recently, a small number of RGCs that contain an opsin-like protein called melanopsin (Opn4) were identified and named melanopsin RGC (pRGC; Berson et al., 2002, Sekaran et al., 2005, Semo et al., 2003, Hattar et al., 2002). These cells represent approximately 1% of the RGCs population in rodents (Hattar et al., 2002, Sollars et al., 2003). It was suggested that these cells may serve as photoreceptors that provides the SCN of the hypothalamus with photic information (Provencio et al., 2000). Further studies demonstrated that this was indeed the case, where it was demonstrated that most of the RGCs that project to the SCN were Opn4 positive(Gooley et al., 2001, Sollars et al., 2003). There are several central sites that receive input from the pRGCs. Among these are the SCN, IGL, OPN, lateral hypothalamus and preoptic regions (Hattar et al., 2006, Hattar et al., 2002, Morin et al., 2003). These sites are known to be involved in determination of light levels. The Opn4-containing RGCs also project to the ventral subparaventricular region and the ventrolateral preoptic zone, compartments that participate in acute modulation of behaviour and sleep (Gooley et al., 2003). Thus, pRGCs are involved in circadian rythme (Barnard et al., 2004, Freedman et al., 1999), suppression of pineal melatonin (Lucas et al., 1999), pupil construction (Lucas et al., 2001), negative masking behaviour (Thompson et al., 2008) and modulation of sleep (Altimus et al., 2008, Lupi et al., 2008).

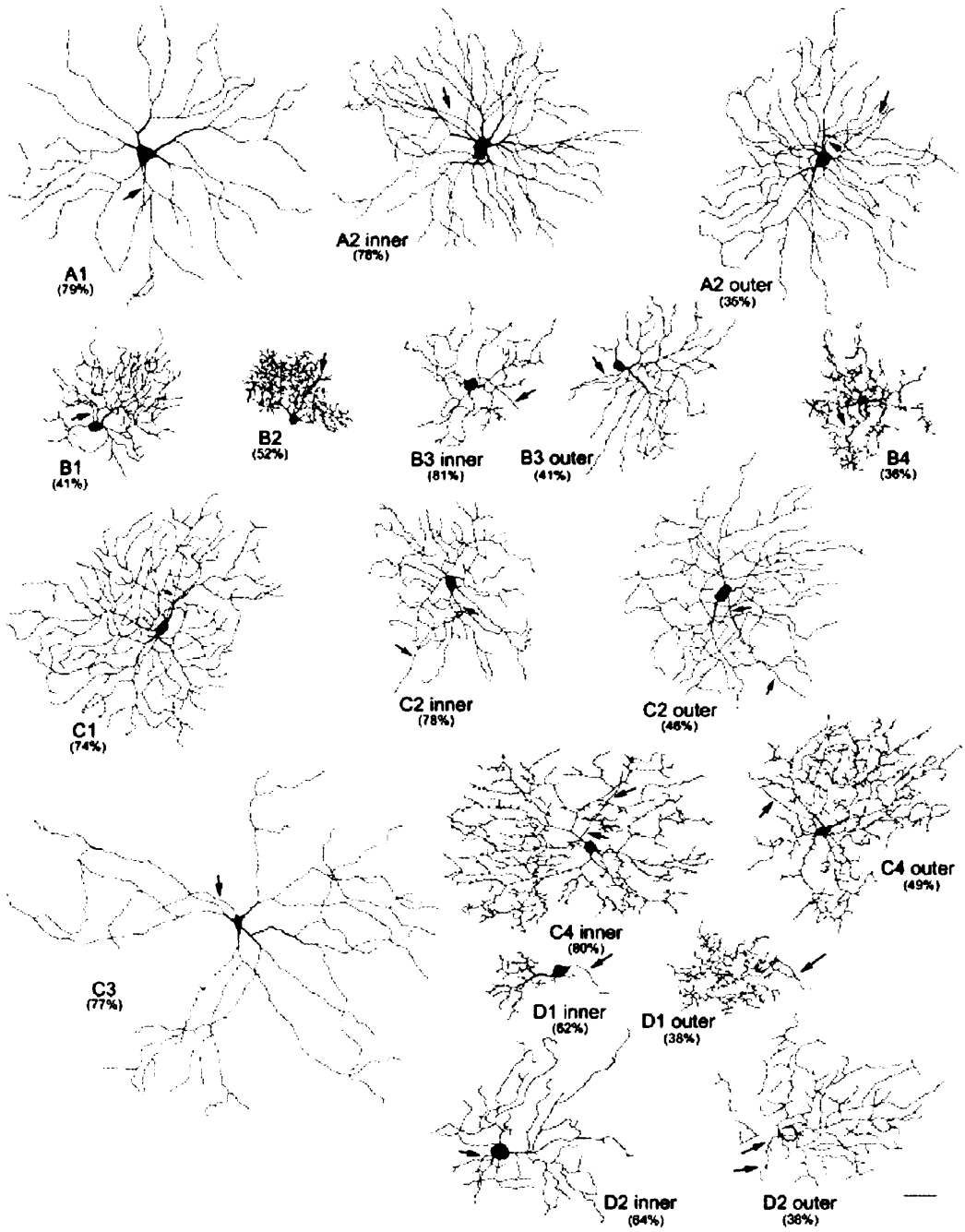

Figure 1.5. Types of RGC found in the rat retina. Four groups and 12 subtypes have been identified to date. Percentile in the parenthesis indicates average depth of dendritic stratification in the inner plexiform layer of the particular subtype. Figure adapted form Sun et al., (2002).

1.5 RGC death during development

In common with other parts of the CNS, RGCs undergo a substantial phase od cell death during development. There are two phases of RGC death during development. The first one, an early phase occurs immediately after neuronal birth, differentiation and migration, while the second one, a late phase, involves physiological cell death, which coincides with target innervations (Guerin et al., 2006). The late phase has been suggested to occur as a "fine-tuning" cell death, which ensures that only target-innervated cells survive. It has been estimated that 90% of RGCs undergo apoptosis during development (Galli-Resta and Ensini, 1996). Interestingly, it has been shown that pRGC population is not affected by developmentalcel death, suggesting that the absolute number remain the same(Gonzalez-Menendez et al., 2010, Sekaran et al., 2005).Sekaran and colleagues suggested that the high number of light-responsive neurons in eary postnatal days in RGCL in mice is a result of overproduction of pRGC (Sekaran et al., 2005).Neurotrophic factors are crucial for RGC survival, differentiation and regeneration and are expressed by RGCs themselves and other cells in the primary visual centre (Herzog and von Bartheld, 1998).

Other factors that are involved in RGC death during development are gap junctions. Gap junctions are intracellular channels that allow the cell to exchange small molecules including, inositol phosphatidyl 3 (IP3), Ca^{2+} and second messengers such as cyclic nucleotide. Due to the small size of the channels, transfer of proteins and nucleic acid is excluded (Bennett et al., 1991). The channels are formed through each cell providing a hemichannel, which unites and form a two hemichannels called connexons. Each connexon consist of six subunits termed connexins (Cx's) (Sohl et al., 1998). Gap junctions, found throughout the CNS are involved in different processes including neurogenesis (Becker and Mobbs, 1999), cell death (Lin et al., 1998), pattern formation (Paul et al., 1995), synaptogenesis (Allen and Warner, 1991, Walton and Navarrete, 1991) and the synchronization of impulses essential for the sharpening

ofthe central visual projection (Cook, 1991). Most cells in the retina are coupled to each other via gap junctions (Becker et al., 1998).

During early development of chick retina the coupling is heterogenous and by E14 only cells with the same morphology are coupled to each other (Becker et al., 2002). It has been suggested that Cx43 mediates communication between RGCs during development, which may influence cell proliferation (Becker and Mobbs, 1999, Ilia and Jeffery, 1996). However, the expression decline during mid embryonic stages correlates with the end of proliferation and the beginning of the apoptotic period (Becker et al., 1998). In other regions of the developing CNS, the junctions have been suggested to be utilised for signalling apoptosis to the neighbouring cells by permitting the spreading of calcium waves suggesting involvement of calpains in cell death (Wolszon et al., 1994). The same might applies to RGCs.

1.6 Neurodegenerative diseases

Neurodegenerative diseases are classically defined by the presence of neuronal cell death. The group includes AD, which is characterised by death of neurons in cerebral cortex (Wenk, 2003), PD where the dopaminergic midbrain neurons are deceased (Isenmann et al., 2003), HD where neurons in the basal ganglia and cerebral cortex are degenerated (Vonsattel et al., 1985) and glaucoma (which will be discussed in detail below). In these diseases, neurons die predominately through apoptotic mechanisms though other cell death types cannot be exclusively ruled out. Terminal deoxynucleotidyl transferas-mediated deoxyuridine triphosphate (dUTP) nick end-labelling (TUNEL), which has been used for detection of apoptosis in neurodegenerative diseases, is a technique used to determine apoptosis by labelling fragmented DNA, but this method does not detect alterations in cell morphology. There is substantial evidence suggesting that this technique also positively labels cell that are undergoing necrosis. Thus, the TUNEL assay is not specific for detection of apoptosis. Additionally, there are many reports concluding

that caspases are required for necrotic death (Yamashima, 2004) and activation of other proteases, in particular calpains and cathepsins are detected in necrosis (Golstein and Kroemer, 2007).

Calpains are calcium-dependent neutral proteases that are found in two isozymes, m- and μ-calpains. Calpain is synthesised as an inactive heterodimer comprising 30 kDa and 80 kDa subunits. Upon activation, the 30 kDa subunit is cleaved to a final active fragment of 17 kDa while the 80 kDa is converted to 76 kDa enzymatic active form (Yamashima, 2004). Calpains are activated both during physiological and pathological conditions, such as phosphorylation (Melloni et al., 1996), muscular dystrophy (Kinbara et al., 1998), AD (Lee et al., 2000) and PD (Mouatt-Prigent et al., 1996). Once activated, calpains target cytoskeletal and associated proteins, kinases andphosphatases, membrane receptors and transporters and steroid receptors (Yamashima, 2004). In neurons, calpains are located in the somatodendritic area and in the axons. Increased free Ca^{2+} leads to overactivation of calpains and this result in loss of neuronal cell structure integrity and alterations in axonal transport (Yamashima, 2004).

Lysosomes house 80 different types of hydrolytic enzymes including various isoforms of cathepsins (cathepsins D (aspartyl), B, H and L (cysteine)) proteases. In neurons, sustained calpain activation may lead to disruption of the lysosome, releasing its contents. Cathepsin D mediates neuronal death, which is induced by ageing (Adamec et al., 2000), while cathepsins B and L execute hippocampal neuronal death after global ischemia (Yamashima, 2000). Moreover, in AD and PD in particular, cells in an advanced stage of autophagy are frequently observed (Yuan et al., 2003).

1.7 Glaucoma

1.7.1 Introduction to glaucoma

Glaucoma comprises a collection of eye diseases that commonly features cupping of the optical nerve head and death of RGCs (Quigley, 1999), which in turn leads to blindness in patients. It is the second commonest cause of blindness in the world and the leading cause of irreversible blindness. Various factors contribute to development of glaucoma including age, race, myopia, central cornea thickness and genetics (Pang and Clark, 2007). However, the major symptom frequently associated with glaucoma is elevated intraocular pressure (IOP), which is influenced by the balance between aqueous humoral production inside the eye and the aqueous drainage out of the eye through the trabecular meshwork (TM). Healthy individuals have IOP between 10-21mm Hg while some individuals may have hypotony low pressure in the eye that can drop to 0mm Hg. In some glaucoma patients the IOP can exceed 70 mm Hg (Khaw et al., 2004).

Different mechanisms have been proposed to contribute to RGC death. These include withdrawal of neurotrophic factors, vascular insufficiency, immune abnormality, glutamine toxicity and glial activation (Pang and Clark, 2007). While there are many dictinct subtypes in human, glaucoma can broadly be divided into two groups, namelyprimary open angle glaucoma and acute angle closure glaucoma

1.7.2 Primary open angle glaucoma

Primary open andgle glaucoma is defined by the increases resistant of the aqueous outflow in the trabecular meshwork or in Schlemm's canal. It is important to note that the precise anomarlity in this type of glaucoma is yet to be elucidated. Patients suffering from primary open angle glaucoma lose their vision gradually and the manifestation of the clinical symptoms usually occurs after severe damage to the retinal ganglion cell

layer (RGCL). Primary open angle glaucoma has been estimated to be the third cause of blindness in the UK (Khaw et al., 2004).

1.7.3 Acute angle closure glaucoma

In acute angle closure glaucoma is characterised by the blockade of the aqueous flow from the posterior chamber to the anterior chamber. The patients' eyes become red and painful and they may also experience nausea and severe pain or headache (Khaw et al., 2004).

1.8 Experimental models of glaucoma

1.8.1 Introduction

The genetic and pathophysiological complexity of glaucoma has led to the need to employ a diverse range of experimental approaches and models to understand the molecular mechanisms involved in the disease. Several experimental animal models for glaucoma exist including monkey, mice and rat each with distinct advantages and pitfalls. The disease is induced in these animals by either surgical or genetic elevation of IOP (Weinreb and Lindsey, 2005, Morrison et al., 1995, Morrison et al., 1997, John et al., 1999). Although the animal glaucoma models may not reflect the pathophysiology of human glaucoma, they enable the comparison of the prosess leading RGC death caused by elevated IOP, which may highlight pathways that are specific to increased IOP related guacoma versus glaucoma that occurs in absence of elated IOP. Elevated IOP causes structural, biochemical and functional changes that resemble the changes in the human disease. These modifications include disorganisation and compositional alterations in the optic nerve head (Bonhoeffer and Yuste, 2002), RGC death and visual deficit (Kuehn et al., 2005).

1.8.2 Experimental glaucoma in monkeys

Glaucoma can be induced in monkeys in different ways. The most useful method is by argon laser photocoagulation treatment to the TM, but the most effective technique is diode laser photocoagulation (Wang et al., 1998, Gaasterland and Kupfer, 1974). Treatment results in whitening of the TM and also formation of bubbles. The treated eyes in this model develop moderately elevated IOP similar to that one observed in humans, varying between 25-60 mmHg (Quigley et al., 1995, Quigley, 1983). The elevated IOP can last for weeks to years. Damage to the RGCL can be assessed by RGC loss, but there are other ways of evaluating the damage in this model (Levkovitch-Verbin, 2004). Quigley and Addicks developed another model for producing chronic experimental glaucoma in monkeys. They injected autologous, fixed red blood cells into the anterior chamber in order to maintain elevated IOP. This model however, has a disadvantage of poor visibility of the retina and the ONH (Quigley and Addicks, 1980b, Quigley and Addicks, 1980a).

1.8.3 Experimental glaucoma in rats

In rats, experimental glaucoma is induced by translimbal laser photocoagulation. This model is postulated to be more reliable, simple to produce, reproduce and inexpensive (Levkovitch-Verbin et al., 2002, Levkovitch-Verbin, 2004). The treatment is carried out using a diode laser to damage the venous drainage from the TM of the animal, which is under general anaesthesia. This procedure is very quick; therefore more animals can be treated in a short period of time. It is important to measure the IOP before the treatment and every 3 days in the first two weeks and weekly thereafter. More than two measurements are performed and the final IOP value is obtained from the mean calculated from all measurements. Immediately after the laser treatment the retina and the choroidal blood vessels are observed focusing attention for signs of retina oedema and haemorrhage.

The IOP peak in this model is between 34-40mm Hg, but unfortunately IOP goes up and then tends to drop. The axonal loss is gradual with a mean loss of axons of approximately 20% at the third week, 25% at the sixth week and 50% at the ninth week. Despite the closure of the intra-becular spaces and the major out flow channels, the retina and choroid continues to appear normal at all times (Levkovitch-Verbin, 2004, Levkovitch-Verbin et al., 2002).

The second rat model of experimental glaucoma, which is established in our group, was developed by Morrison and colleagues in which they increased outflow resistant by microinjecting hyperosmotic saline into the episcleral vein of Brown Norway rats (Johnson et al., 1996, Morrison et al., 1995, Morrison et al., 1997, Sohl et al.). Initially, the technique was effective in half of the animals treated and repetitive injections were required in order to increase IOP, but the method has been improved notably. The advantage of using BN rats is that the IOP can be measured on awake animals (Moore et al., 1995) since anaesthetic has been shown to decrease IOP (Jia et al., 2000). Two other models were also developed. In the first model, the limbus-draining veins were exposed by incising the conjunctiva in order to obtain increased IOP. The elevated IOP observed was twice normal and was maintained for a long time and at 6 months the loss of RGCs was 40% (Sawada and Neufeld, 1999, Shareef et al., 1995). In the second model, the increase in IOP was achieved by injecting India ink into the anterior chamber one week prior to laser photocoagulation treatment (Ueda et al., 1998).

1.8.4 Experimental glaucoma in mice

The most valuable mouse model of glaucoma is the genetically manipulated DBA/2J mouse strain (John et al., 1999). This strain develops glaucoma as a result of changes in the anterior chamber. The advantage of this model is that it exhibits similar features to pigmentary dispersion glaucoma in humans. These DBA/2J mice develop pigment dispersion, iris transillumination, iris atrophy, anterior synechiae and

elevated IOP. Older animals are more likely to get glaucoma and the severity also increases with age. The RGC death in these animals is mainly by an apoptotic process and the degeneration of the RGCL is observed. The genes that contribute to glaucoma in this model are linked to chromosome 4 and 6 (John et al., 1998); (John et al., 1999).The disadvantage of DBA/2J model is that axon loss in these mice is not observed until 9 months, which requires housing the animals for long periods increasing experimental cost.

Furthermore, Mabuchi et al induced elevated IOP in mice employing a limbal laser photocoagulation technique. The IOP increased by 1.5 fold and was maintained for 2 to 12 weeks (Mabuchi et al., 2003). The magnitude and duration of elevated IOP correlated with axonal damage. Reitsamer developed an acute model by injected hyperosmatic saline in the mice limbal to induce glaucoma. At 8 weeks 20% of the axons were degenerated (Reitsamer et al., 2004)

1.9 RGCs in glaucoma

A large body of data demonstrates that RGCs in glaucoma undergo apoptosis (Cecconi et al., 1998, Neufeld and Gachie, 2003, Quigley et al., 1995, Spear, 1993). Whether these cells die in a selective or random manner is still debatable. There are reports showing that in human and monkey glaucoma the large RGCs are more susceptible to apoptosis. These findings are based on histological results (Kalloniatis et al., 1993). However, findings from psychophysical investigations do not support histological data since magnocellular and parvocellular pathway deficits lead to similar results (Johnson, 1994, Graham et al., 1996). Morgan and colleagues challenged the hypothesis that there is a selective cell loss in the RGCs in primates (Morgan, 1994, Morgan, 2002, Morgan et al., 2000). The authors demonstrated using cell soma analysis that both parasol and midget RGCs undergo cell shrinkage to the same extend prior to apoptosis (Morgan, 2002).

Several mechanisms have been suggested to be involved in initiation and progression of RGC death. Axonal damage is one of the well recognised clinical features of glaucoma (Osborne et al., 1999). The axonal damage in the animal model is caused by elevated IOP, but it is important to acknowledge that in some glaucoma patients, RGC death occurs despite normal IOP. An estimation showed that a third of glaucoma patients do not show any defects in IOP (Douglas, 1998, Gupta and Weinreb, 1997). Insults to the vascular supply to the ONH can lead to ischemia/hypoxia-like effects on the RGC axons. Due to the complexity of the vascular supply, this can easily be achieved. It has been shown that the blood flow to the ONH is altered in glaucoma. These findings clearly support the notion that axonal damage in glaucoma is a result of defective vascular supply (Osborne et al., 1999). Once the axon injury has occurred, the retrograde transport of growth factors is inhibited. In fact, it is suggested that the RGCs die because the soma is deprived of growth factors, such as brain derived neurotrophic factor (BDNF) that are provided by postsynaptic neurons (Jacobson, 1991). Thus, degeneration of RGCs in glaucoma occurs as a result of insufficient supply of trophic factors. This theory is also supported by studies performed in the rat ONL demonstrating that RGCs show a high capacity for axon regrowth and survival after treatment with BDNF (Osborne et al., 1999).

The retina contains three different kinds of glial cells; astrocytes, microglia and müller cells (Kuehn et al., 2005). Glial cell function under normal conditions is to support neurons. Excessive activation of glial cells has been suggested to contribute to RGC death. This was shown by the increased expression of glial fibrillary acidic protein (GFAP) in astrocytes and müller cells in glaucoma (Wang et al., 2000). The decreased glial cell support of neuronal function was proposed to be a mechanism underlying activated glial-dependent RGC death (Kuehn et al., 2005). This can be mediated by decreased biosynthesis of glutamate receptors (Martin et al., 2002) or increased synthesis of harmful substances such us pro-inflammatory cytokines, TNF-alpha (TNF-α; (Tezel et al., 2001), reactive

oxygen species or nitric oxide (Morgan et al., 1999a). Down-regulation of synthesis of glutamate receptors may result in increased glutamate concentrations. Excessive amounts of glutamate are toxic to neurons. Investigations carried out on cultured RGCs showed that these cells are more susceptible to glutamate excitoxicity (Caprioli et al., 1996).

Interestingly, recent discovered pRGCs has been suggested to have a preferential survival in glaucoma compared to the rest of RGCs (Li et al., 2006, Robinson and Madison, 2004, Wang et al., 2008a). The injury-resistant feature of pRGC in glaucoma is yet to be eludidated but there has been suggestion that the non-uniform immediate early gene espression of pRGCs might contribute to the injury-resistant phenotype (Robinson and Madison, 2004, Semo et al., 2003). The sparsely branching dendritic field property of pRGC may also contribute to their increased survival (Berson et al., 2002). Li and colleagues showed after ONT and OH, the surviving pRGCs expressed activated Akt (Li et al., 2008). Previous work from other groups demonstrated that delayed RGC death is a result of injury-mediated activation of PI3/Akt signalling pathway (Cheung et al., 2004, Huang et al., 2008, Nakazawa et al., 2002). In contrary, there other reports suggesting that mRGCs are equally affect by axotomy as the rest of RGC population (Drouyer et al., 2008, Jakobs et al., 2005). This discrepancy account for different models, survival periods and method of mRGCs quantification has been imployed in the different studies.

1.10 Dendrites in development

Neurons are polarised cells consisting of a cell body (also known as soma), axons and dendrites. The dendrites are extensions of neurons and the collective name for dendrites is the dendritic tree. While the axon is the important part of the neuron for transmission of information, in the form of action potentials, dendrites are essential for receiving the information from the surrounding milieu. For proper function of a neuron, the presence of a healthy dendritic tree is essential.

The development of dendrites is divided into five stages which are: *1)* polarisation, in which the dendrite attains characteristics such as diameter, length, growth rate and molecular composition almost similar to those found in the axon (Craig and Banker, 1994); *2)* elongation, in which they extend in a defined direction and increase their diameter; *3)* branching, involving the elaboration of the dendritic tree and formation of dendritic spines; *4)* tiling, involving the spatial segregation of dendrite arbours into non-overlapping spatial territories observed in some classes of neurons; and *5)* synapse formation (Jan and Jan, 2003, Scott and Luo, 2001).

Actin and the microtubule cytoskeleton are the major components that regulate dendritic development. In the cortex, filamentous actin (F-actin) is ubiquitously expressed in the dendrites, but is enriched in the dendritic spines. Microtubulin on the other hand, fills the interior of the dendrites (Fischer et al., 1998). Similar to the axon growth cone, dendritic growth cones consist of filopodia containing densely packed F-actin bundles. The filopodia allows the dendrites to sense the signals in the environment (Dailey and Smith, 1996). Thus, the molecules that regulate the actin cytoskeleton are also important in dendritic development. These molecules includes Rho small family guanosine triphosphate-ase (GTPase; Rac, Rho, Cdc42; (Hall, 1998). In their active form (GTP-bound), they function as molecular switches and signal transducers (Scott and Luo, 2001). Microtubules provide structural integrity for the dendrite. It was demonstrated that by silencing microtubule-associated protein (MAP2) utilising antisence oligonucleotides, the cultured neurons failed to form dendrites (Caceres et al., 1992). Moreover, microtubules in dendrites have a bi-directional orientation; they have both a plus-end-distal and minus-end-distal orientation (Craig and Banker, 1994). This has been suggested to be important for the differentiation and maintenance of dendritic structure (Scott and Luo, 2001).

Dendrite pruning is essential for development of neurons of both the CNS and peripheral nervous system (PNS). In general, an increased dendrite

complexity is thought to enhance the number of synapses made on the neuron. Thus, a neuron with a highly complex dendritic tree is more susceptible to changes in its input structure from a variety of sources (Hickmott and Ethell, 2006, Kolb and Whishaw, 1998). Different factors can influence dendrite structure. These include external factors such as neurotrophins, Semaphorin 3A (Sema3A) and dendrites arborisation and synapsematuration1 (Dasm1) as well as internal factors, including synaptic activity among others (Hickmott and Ethell, 2006).

1.10.1 External factors

Neurotrophins. Neurotrophins are a group of growth factors that comprise of nerve growth factor (NGF), Brain-derived neurotrophic factor (BDNF), neurotrophin-3 (NT-3) and neurotrophins-4 (NT-4) in mammals. They are involved in diverse cellular processes, such as neuronal survival, proliferation, axonal and dendrite growth, membrane trafficking, synapses formation and plasticity (Herzog and von Bartheld, 1998). Neurotrophins mediate their effects though interaction with a high affinity receptor tyrosine kinases (Trk receptors) and a low affinity receptor p75 (Guerin et al., 2006). NGF was first shown to mediate axonal growth in the PNS, but later it was demonstrated to induce dendritic growth and maintain dendrites in the PNS (Huang and Reichardt, 2003). Other studies demonstrated that neurotrophins control dendritic growth and arbourisation in the CNS, in particular pyramidal neurons in the developing visual cortex. BDNF increases the length and complexity of basal dendrites in pyramidal neurons of layer IV, whereas NT-4 exerts its effect on neurons in layers V and VI. On the other hand, apical dendrites respond to all four neurotrophins (McAllister et al., 1995).

Sema 3A. Sema3A is a soluble protein that belongs to the Semaphorin family, which consists of 20 membrane-bound and soluble proteins. Sema3A was characterised as an axonal guidance protein, but this protein is also directly involved in growth of apical dendrites of pyramidal neurons towards layer 1 in the cerebral cortex (Polleux et al., 2000). The mechanism behind the changes of Sema3A status (i.e. from being an

axonal growth factor dendrite growth factor) is thought to involve cyclic nucleotide gunosine 3`/5`-monophosphate (cGMP). When the concentration of cGMP is increased in the axon, Sema3A becomes axonal repulsive and converts to a dendrite attractant (Song et al., 1998). It was shown that the enzyme that produces Sema3A is asymmetrically localised to the apical dendrite and it seems to be essential for dendrite attraction (Polleux et al., 2000). Sema3A knockout mice showed impaired orientation of pyramidal axons and dendrites in the cortex. Moreover, others investigations performed on Sema3A demonstrated reduced dendrite length and branching in Sema3A null mice. The authors postulated that the protein is required for development of dendrite arbours in the neocortex (Fenstermaker, 2003). The promiscuous effect of Sema3A is mediated by neuropilin-plexin receptor complex (He et al., 2002) but the mechanism remains elusive.

Dasm 1. Dendrite arborization and synapse maturation 1 (Dasm1) has also been suggested to be involved in dendrite remodelling (Shi et al., 2004b). Although still uncharacterised, its resemblance to Robo, a cell-surface receptor involved in axonal guidance, suggested Dasm 1 to be a receptor (Falls, 2005). The receptor was shown to regulate dendrite elongation and branching and also strengthen the glutamergic synapses. Downregulation of Dasm 1 using RNA interference inhibited the elongation and branching of dendrites but had no effect on axons in cultured hippocampal neurons. Furthermore, reduction of Dasm 1 leads to a decreased number of α-amino-3-hydroxy-5-methylisoxazole-4-propionic acid receptors (AMPAR) receptors (a type of glutamergic receptors). Overall, Dasm 1 is involved in controlling neuronal input and might also be involved in neuronal plasticity throughout life (Shi et al., 2004a, Shi et al., 2004b).

1.10.2 Internal factors

Synaptic activity, NMDAR, Calcium (Ca^{2+}), CaMII and CaMIV. Changes in intracellular Ca^{2+} have been suggested to regulate dendrite morphology (Wong and Ghosh, 2002). Increased intracellular Ca^{2+} following activation of N-methyl D aspartate (NMDAR) receptors or voltage-gated Ca^{2+} channels leads to activation of Ca^{2+s}-dependent kinases; calcium calmodulin kinase II (CaMII) and CaMIV. CaMII induces Ras- and mitogen-activated kinase (MAPK)-mediated structural changes in dendritic morphology, whereas CaMIV activates cyclic adenosine monophosphate (Balosso et al.)response element binding protein (CREB)-mediated transcription (Redmond and Ghosh, 2005). In hippocampal neurons, it was shown that constant changes in dendritic architecture following multiple depolarisation was dependent on Ras and MAPK activation inducing local cytoskeletal changes (Wu et al., 2001). Activation of CaMIV and CREB-mediated gene expression in cortical neurons *in vitro* play a role in calcium-induced dendritic growth (Redmond et al., 2002). The overexpression of active CaMIV induces dendritic growth while a kinase-dead form of CaMIV or dominant-negative form of CREB suppressed calcium-dependent dendritic growth (McAllister, 2000).

1.11 Dendritic spines

Dendritic spines are small protrusions on dendrites that receive over 90% of excitatory input and are highly dynamic. Generally spines consist of a head attached to a dendrite through a stalk. They are morphologically divided into several types namely; stubby, thin, mushroom-shaped and cup-shaped (Dunaevsky et al., 1999). The formation of a spine is believed to involve dendrite filopodia and growth of presynaptic elements, although all dendrite filopodia seen at early stages do not transform to spines in adults. This suggests that both extrinsic and intrinsic factors regulate spine formation (Bonhoeffer and Yuste, 2002). The motility of the spines is highly dependent on the polarisation of actin filament. Various molecular families are known to regulate actin dynamics which in return plays a crucial role in dendritic spine morphogenesis (Fischer et al.,

1998). These include receptors, scaffolding proteins and regulators of the cytoskeleton (Lippman and Dunaevsky, 2005). Changes in spine number and morphology are associated with changes in neuronal activity (Bonhoeffer and Yuste, 2002) while the size of the spine head correlates with synaptic strength (Lippman and Dunaevsky, 2005).

1.12 Dendrite remodelling of RGCs

All neurodegenerative diseases exhibit alterations in dendrite structure. In AD, progressive loss of dendritic spines is observed (Fiala et al., 2002). Fewer dendritic spines are observed in PD (McNeill et al., 1988), while in moderate HD, the striatal neurons show an increased in the density of dendritic spines, progressing to a marked loss of spines in advanced disease (Ferrante et al., 1991)

Dendrite atrophy and remodelling have been revealed to be the earliest sign of glaucoma in primates (Liets et al., 2006, Morgan, 2002) and also in a feline model of glaucoma (Shou et al., 2003). Dendrite atrophy occurs primarily due to axotomized RGCs. This axonal damage deprives the RGCs of neurotrophin support and the first part to be affected by the insufficient nutrients supply is the dendritic tree (Brannstrom et al., 1992, Thanos, 1988, Yawo, 1987). There is evidence pointing to a reduction of axonal thickness occurring at the same time as changes in the soma, but after alterations in dendrite structure. The structural changes include slimming of both proximal and distal dendrites and generally decreased complexity of the dendritic tree (Weber et al., 1998).

Morgan and colleagues showed that dendrite remodelling also occurs in the experimental rat glaucoma model (Morgan, 2002). The authors postulated that this observation suggests that global remodelling takes place prior to cell loss in glaucoma. Primate and mouse studies confirmed that alteration of the dendritic structure results in alterations in neuronal function; in particular, the action potential becomes more randomly (Jakobs et al., 2005, Weber and Harman, 2005) and contrast sensitivity

and receptive field size are reduced, contributing to decreased efficient spatial summation. These alterations correlate with the symptoms seen in glaucoma in which variability in visual field sensitivity is manifested as an early feature of disease.

To date, very little attention has been paid to elucidating the molecular mechanisms that are involved in dendrite self-destruction. Whitmore suggested that the possible mechanisms could BCL-2 proteins, which are critical for regulation of apoptosis and appear not to be involved in axonal degeneration. This was demonstrated by experiments on explants culture in the absence of pro-apoptotic BCL-2 family members, where Bax and Bak did not show axonal degeneration (Whitmore et al., 2005).

1.13 Caspases and IAPs in dendrite remodelling

Alpha-Fodrin (α-fodrin) is a neuronal cytoskeleton protein that is targeted by caspase 3 (Tahzib et al., 2004). It is the first protein to be cleaved during apoptosis. α-Fodrin has been shown to co-localise with neurofibrillary tangle in AD. Recent research found a large accumulation of abnormal deposits of caspase 3 cleaved α-fodrin in many viable neurons (Tahzib et al., 2004). Furthermore, a significant investigation carried out by Williams and colleagues revealed that in *Drosophila* neurons during development, dendrite pruning was modulated by local caspase activity. The authors also reported that overexpression of *Drosophila* inhibitor of apoptosis 1 (DIAP1), which is a negative regulator of the *Drosophila* effector caspase DRONC, resulted in suppressed removal of the dendrites (Williams et al., 2006).

Moreover, other additional caspase regulation levels have been proposed (Montell, 2006). A mutation in the ubiquitin activation enzyme (Uba1) and the proteasome complex protein (mov34) is capable of hindering efficient remodelling of *Drosophila* C4da peripheral sensory neuron in larval metamorphosis (Kuo et al., 2005). A follow up study carried out by the same group revealed that the ubiquitin proteasome system (UPS)

activation of the C4da neurons likely results in E2 ubiquitin-conjugating enzyme (UbcD1) mediated degradation of DIAP (Kuo et al., 2006). Additionally, another mechanism for degradation of DIAP has been discovered in which a newly described kinase called Drosophila IKK-related kinase (DmIKKε) is involved. Elimination of DmIKKε in sensory organelle precursor (SOP) development resulted in stabilisation of endogenous DIAP and this had a negative effect on *Drosophila* SOP development (Kuranaga et al., 2006). Furthermore, Oshima and colleagues revealed that IKKε regulates F-actin assembly, which plays an important role in cell morphogenesis. F-actin is required for maintenance of polarised elongation of the cell during morphogenesis (Oshima et al., 2006).

Taken together, these data indicate that tight regulation of local caspase activity is very important for dendrite pruning in *Drosophila* development. How this process is restricted to dendrites without affecting the other parts of the cell may be explained by the dendrite-specific trafficking of UPS components resulting in the local degradation of dendritic IAPs and activation of caspases (Kuo et al., 2006). The other possibility is that activated DRONC cleaves a dendrite-specific substrate (Kuo et al., 2006). It is still unclear as to whether the same mechanisms as those in *Drosophila* apply to vertebrates and also whether similar mechanisms for dendrite remodelling occur during development and disease. However, elevated IOP in glaucoma leads to drastic environmental changes. Dendrites are susceptible to these changes and this leads to the remodelling and subsequent removal of dendrites prior to cell death.

Moreover, there is accumulating evidence supporting the role of apoptosis in regulating synaptic plasticity (Gilman and Mattson, 2002, Mattson and Duan, 1999). Mitochondria are key organelles that control synaptic plasticity through various mechanisms, including regulation of apoptosis signalling pathways (Mattson, 2006). Activation of caspase 3 has been shown to cleave glutamate receptor or associated protein,

which, in turn, leads to synaptic plasticity (Glazner et al., 2000, Lu et al., 2002, Lu et al., 2006).

1.14 Summary

Generally, neural function in health and disease is dependent on a viable cell body and inteneuronal connections. Recent studies have made it clear that the changes in the dendritic tree occur as an early event in most neurodegenerative diseases including AD, PD and glaucoma (Deutch, 2006, Knobloch and Mansuy, 2008, Liets et al., 2006, Morgan et al., 2006, Zaja-Milatovic et al., 2005).And yet our understanding of the molecular mechanisms that modulate this changes is limited. The rapid development of non-invasive imaging techniques such as ocular coherence tomography (OCT) and Optophysiology shows a promising future in detecting changes in dendrites in the near future (Bizheva et al., 2006).

There is a possibility of rescuing cells yet to undergo apoptosis; i.e. before they reach the point of no return, which is characterised by activation of effector caspases. Removal of dendrites results in the cell losing its support from the surrounding cellular milieu and this can facilitate cell death. The possibility of detecting the changes in dendritic structure associated with early stages of disease provides a window of opportunity for rescuing the cell from undergoing apoptosis. Attempts to rescue the cell by manipulation of the neurotrophin axis (Chen and Weber, 2001); (Martin et al., 2002) and cognate receptor trkB6 (Cheng et al., 2002) have shown low efficiency and clearly additional therapeutic strategies are required. Therefore, it is important to elucidate the molecular mechanisms underlying dendrite pruning in neurodegenerative diseases because this could provide insights into which molecules to target in order to obtain efficient therapeutic effects for neuroprotection.

1.15 Hypothesis and aims of the study

1.15.1 Hypothesis

It is hypothesised that IAPs are differently expression in RGC which leads to differential modulation of caspase activity in these neurons, thereby providing molecular control of dendrite maintenance and remodelling as well as neuronal cell death in ageing and neurodegenerative diseases.

1.15.2 Aims

1. To characterise the expression pattern of caspases and IAPs At RNA level during maturation and ageing of BN and Wistar albino rat retinae.
2. To determine wether the expression pattern at RNA level correlates with expression pattern at protein level.
3. To evaluate the involvement of differently expressed IAP in maintenance of the cells in the BN RGCL.
4. To investigate whether there is any alteration in retinal cell density during retina maturation of BN rat.
5. To determine when dendrite pruning starts and the extent to which dendrite pruning occurs in adult rat retina.
6. To characterise the expression profile of pro-apoptotic and survival pathway molecules in glaucomatous eyes in order to identify molecules that could be targeted for therapeutic purposes in order to rescue RGC death.

Chapter 2

General Methods

2.1 Animal husbandry

Adult BN rats (retired male breeders) of age range: mature (male, 24-52 weeks), young adults (male, age 6 weeks), adult (male, age 10 and 16 weeks) and adult Wistar albino (male and female) rats 16-24 and 88 weeks in this study were fed rodent global diet pellet (Harlan, UK) and given water ad *libitum*. All experiments were conducted in accordance with Home Office (UK) regulations and ARVO Statement for the Use of Animals in Ophthalmic and Vision Research.

2.2 Retina dissection

2.2.1 Retina dissection for RNA analysis

Retinae were dissected before noon in order reduce variation that are caused by Circadiam rythme. BN rats (n = 3 for RT-PCR and n=6 for real time PCR in each group) and Wistar albino rats 16-24 months (n=4) and 88 months (n=5) were sacrificed using an overdose of CO_2. The eyes were immediately removed and stored in cold sterile RNA-free phosphate saline buffer (PBS), pH 7.4 (Sigma-Aldrich, Dorset, UK) awaiting dissection (2-5 minutes). The retina was dissected, removing the anterior chamber, the lens and vitreous (Kretz et al., 2007) in cold PBS under cold conditions and placed in RNase-later (Qiagen, West Sussex,UK) immediately after dissection. The samples were stored at 4°C until further analysis.

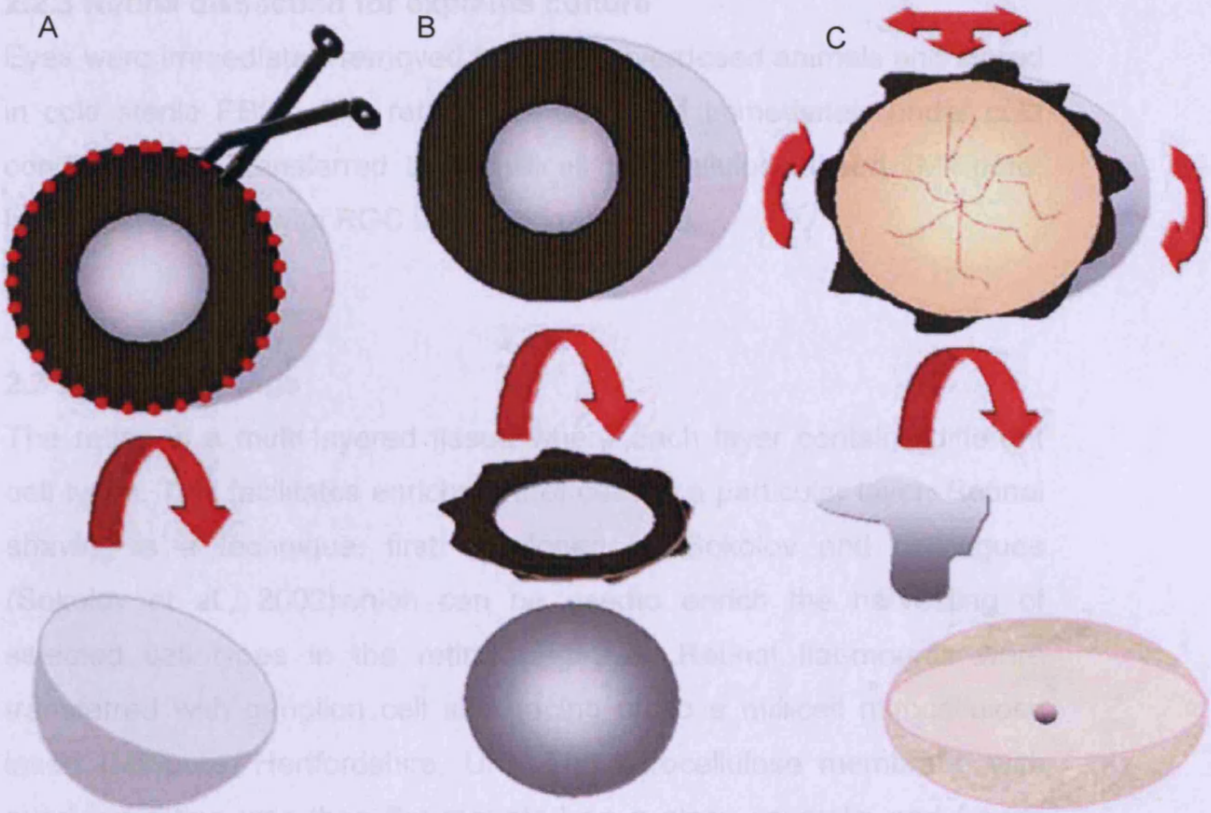

Figure2.1.A schematic diagram showing retina dissection.**A**. The cornea is cut along the corneo-scleral rim as indicated by the red dotted line. **B.** The iris and the lens are then removed. **C.** The vitreous is removed using fine forceps. The retina is then detached from the eye cup by insertion of forceps branches between retina and eye cup and shearing forceps and eye cup in opposite directions (red arrows). Figure adapted from Kretz et al., (2007).

2.2.2 Retina dissection for protein isolation and immunofluorescence

Animals (n = 6 for each experiment) were sacrificed using an overdose of CO_2. The eyes were immediately removed and stored in sterile PBS pH 7.4. The retina for protein isolation was dissected in sterile PBS under cold conditions and stored in sterile PBS immediately after dissection at -20°C. The eyes used for immunofluorescence were dissected and the eye-cups were stored in 4% paraformaldehyde solution for further analysis (see appendix). All samples were stored at 4°C for further analysis.

2.2.3 Retina dissection for explants culture

Eyes were immediately removed from CO_2 overdosed animals and stored in cold sterile PBS. The retina was dissected immediately under cold conditions and transferred to a millicell nitrocellulose insert (Millipore, Hertfordshire, UK) with RGC side facing upwards.

2.3 Retina shavings

The retina is a multi-layered tissue where each layer contains different cell types. This facilitates enrichment of cells in a particular layer. Retinal shaving is a technique, first developed by Sokolov and colleagues (Sokolov et al., 2002)which can be usedto enrich the harvesting of selected cell types in the retina (Fig 2.2). Retinal flat-mounts were transferred with ganglion cell side facing up to a millicell nitrocellulose insert (Millipore, Hertfordshire, UK). The nitrocellulose membrane with overlying retina was then flat mounted on a glass coverslip and frozen immediately frozen by putting the sample in the cryostat set at -20°C. The retina was aligned with the cutting surface of the cryostat and 20 microns of RGCL shaved from the retina and transferred directly to ice cold 0.1M PBS pH 7.4. Both retinae from a single animal were processed in this way to provide a single sample. The remaining retina was immediately thawed and washed off the membrane using PBS and retained for further analysis.

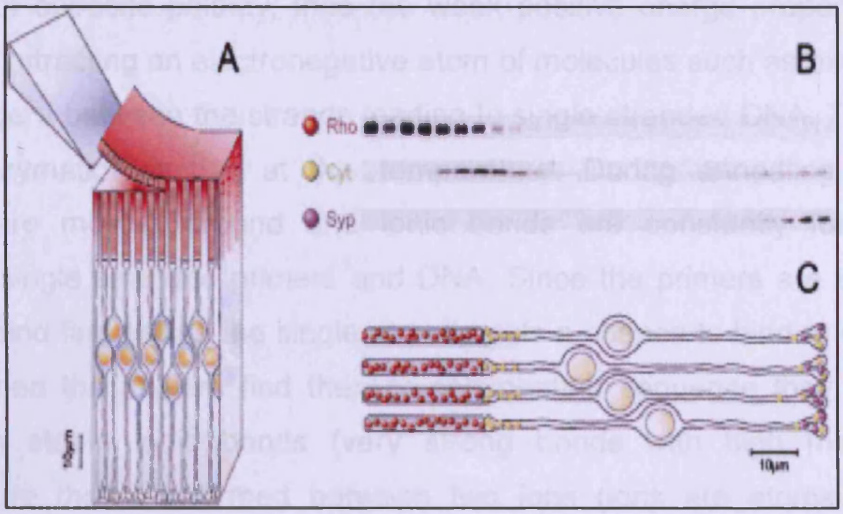

Figure 2.2. A schematic imaging showing retina shaving as done by Sokolov et al., (2002). A. The shaving technique. B. Staining of different photoreceptors markers. C. Schematic drawing of photoreceptors

2.4 Reverse transcriptase –PCR (RT-PCR)

2.4.1 Principle

The polymerase chain reaction (PCR) is a method that allows logarithmic amplification of a gene of interest (Fig. 2.3A-B). This is important because it generates enough starting material for subsequent analysis, such as gene sequencing and quantification of gene expression. PCR is divided into different sub-categories including RT- PCR, also known as conventional PCR, which is a semi quantitative PCR and real time-PCR, which is considered more quantitative (see section 2,4 for further details). The basic principle in both sub-categories is that a DNA template from the gene of interest is exponentially amplified over several (usually 20-35) cycles.

The three major steps of PCR are denaturation, annealing and extension (Fig 2.3B). Denaturation, which is usually performed at 94°C, is when the double stranded DNA is heated up, disrupting hydrogen bonds (a type of

attractive intermolecular force that exists between two partial electric charges of opposite polarity, thus the weak positive charge property of hydrogen attracting an electronegative atom of molecules such as oxygen and nitrogen) between the strands leading to single stranded DNA. There is no enzymatic reaction at this temperature. During annealing, the primers are moving around and ionic bonds are constantly formed between single stranded primers and DNA. Since the primers are small they will bind first before the single strands gets a chance to bind to each other. When the primers find their complementary sequence they bind and form stable ionic bonds (very strong bonds with high melting temperature that are formed between two ions (ions are atoms with unequal number of protons and electrons)) and this generate a small segment of double stranded DNA. This facilitates the attachment of polymerase (an enzyme used for creating a new DNA/RNA strand using an existing DNA/RNA strand as a templet so that the templet can be copied).

The annealing temperature (T_a) is usually 5-10^{0}C below the melting temperature (T_m) of the primers. T_a describes the temperature at which 50% of the oligonucleotide-target duplexes have formed. The third step of PCR is extension, which takes place at 72°C. This is the ideal working temperature for the tag polymerase. RT-PCR has a number of limitations including low sensitivity detection with ethidium bromide, which leads to unreliable results. The detection of the RT-PCR samples requires post-amplification processing, which can increases the cross-contamination of the samples. Amplicons can be visualised only after the amplification ends.

A

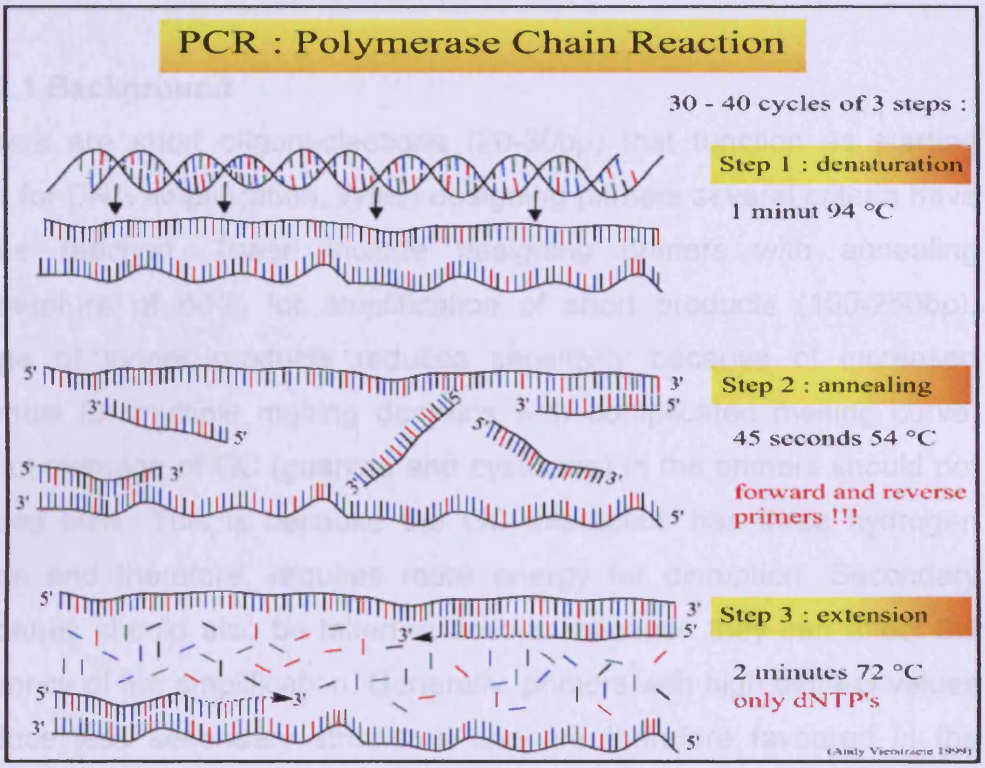

B

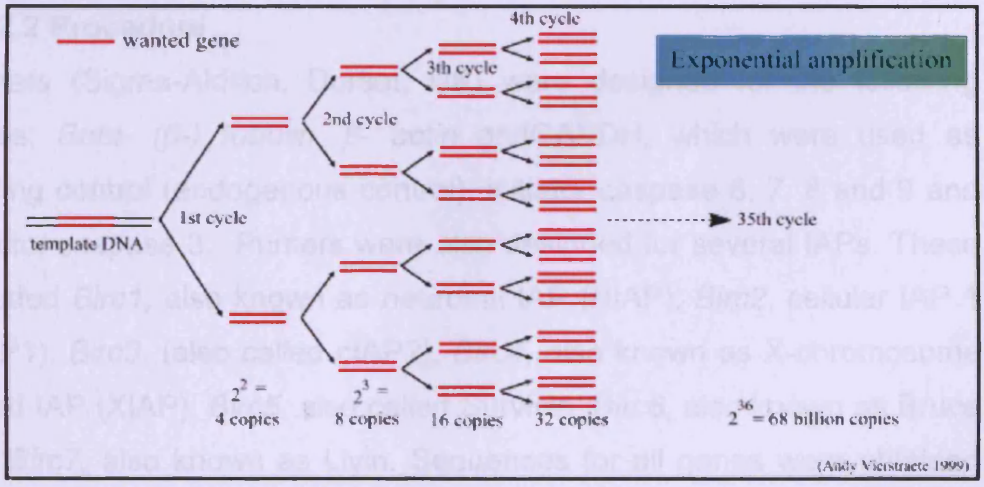

Figure 2.3. The principle of PCR. (A) there are three crucial steps required for DNA amplification. These are denaturation, annealing also know as hybridisation and extension. (B) Schematic representation of the method, from one molecule to hundreds.

2.4.2 Design of primers

2.4.2.1 Background

Primers are short oligonucleotides (20-30bp) that function as starting point for DNA amplification. When designing primers several criteria have to be reached. These include designing primers with annealing temperature of 60°C for amplification of short products (100-250bp). Usage of longer products reduces sensitivity because of increased potential for multiple melting domains with complicated melting curve. The percentage of GC (guanine and cystosine) in the primers should not exceed 50%. This is because the GC interaction has three hydrogen bonds and therefore, requires more energy for disruption. Secondary structures should also be taken in account because they can affect the efficiency of the amplification. Generally, primers with high delta-G values produce less secondary structures and are therefore favoured in the amplification reaction. Low delta-G values indicate a strong and high level of secondary structure and therefore values above -1 are favoured.

2.4.2.2 Procedure

Primers (Sigma-Aldrich, Dorset, UK) were designed for the following genes; *Beta- (β-) tubulin*, *β- actin* andGAPDH, which were used as loading control (endogenous control), initiator caspase 6, 7, 8 and 9 and effector caspase 3. Primers were also designed for several IAPs. These included *Birc1,* also known as neuronal IAP (NIAP), *Birc2*, cellular IAP 1 (cIAP1), *Birc3*, (also called cIAP2), *Birc4*, also known as X-chromosome linked IAP (XIAP), *Birc5*, also called Survivin, *Birc6*, also known as Bruce and *Birc7*, also known as Livin. Sequences for all genes were obtained from the NCBI (http://www.ncbi.nlm.nih.gov/SNP) or Ensemble database (http://www.ensembl.org/index.html). A portion of the Fasta (DNA and protein sequence alignment software) sequence was evaluated using BLAST (http://www.ensembl.org/Multi/blastview) to identify variation and intron-exon boundaries. The Fasta sequence with the least variation was copied and pasted in Primer 3 software

(http://fokker.wi.mit.edu/primer3/input.htm). Primer length (18-27), melting temperature (57-63°C) and product size (150-250bp) were selected. Primers with lowest percentage GC values were selected for further analysis. Secondary structure profiling software (http://www.bioinfo.rpi.edu/applications.hybrid/twostate-fold.php) was used to determine the secondary structure of both forward and reverse primers. The primers with delta-G value greater than -1 were chosen (Table 2.1).

Table 2.1: Primers used in this study

Gene	Primer sequence	T_a (°C)	Cycle no.
Caspase 3	Forward:AGGGGCATGTTTCTGTTTTG Reverse: CATTGCAGGCAGTGGTATTG	59	28
Caspase 6	Forward: TGAAGGAGCTGCTTTTCCAT Reverse: ATCAAGCAGGCTCGAGTTGT	61	35
Caspase 7	Forward: TACTGTGAGCATGGCCTCTG Reverse: CAACAGCCACCTTTTCCAAT	59	32
Caspase 8	Forward:TAAAAAGCAGCCCAGAGGAA Reverse: ATCAAGCAGGCTCGAGTTGT	61	35
Caspase 9	Forward:TCATTCTTGCAAAGCAGTGG Reverse: TGGGTGTTTCTGGTGTGAGA	59	28
Birc 1 (NIAP)	Forward: AAGGCAGGGCCAAAAGTTAT Reverse: GAGCATGCAGCAACTGTGTT	59	30
Birc 2 (cIAP1)	Forward: AGCTTGCAAGTGCTGGATTT Reverse: CTCCTGACCCTTCATCCGTA	59	34
Birc 3 (cIAP2)	Forward: TTCCCTCAGACCCTGTGAAC Reverse: GCAAAGCAGGCCACTCTATC	59	29
Birc 4 (XIAP)	Forward: GACAAATGTCCCATGTGCTG Reverse: CTAATGGACTGCGATGCTGA	59	30
Birc 5 (Survivin)	Forward: TGCAAAGGAGACCAACAACA Reverse: AAGCTGGGACAAGTGGCTTA	59	34
Birc 6 (Bruce)	Forward: GGTCACAGAACACGCTCAGA Reverse: CCTGCCTCAAAGAAGCAAAC	59	27
Birc 7 (Livin)	Forward: TCTTCTGCTACGGGGGTCTA Reverse: TCCTGTTCTTCCCGTTGTTC	59	29
GAPDH	Forward: GAAGGGCTCATGACCACAGT Reverse: GGATGCAGGGATGATGTTCT	61	35
Beta-Actin	Forward: TTGCTGACAGGATTGCAGAAG Reverse: TAGAGCCACCAATCCACACA	59	35
Beta tubulin	Forward:ACCGAAGCTGAGAGCAACAT Reverse:GAAACAAAGGGCAGTTGGAA	59	27

2.4.3 RNA extraction

RNA was extracted using the Qiagen mini kit (Qiagen, West Sussex, UK) according to manufactures' instructions. Briefly, the retina was homogenised in RTL buffer containing 1% β-mecaptoethanol. One volume of 70% ethanol was added to the homogenised lysate and the sample was mixed well by pippeting up and down. The samples were then transferred to a RNase mini column placed in a 2 ml collection tube and was centrifuged in a table centrifuge at max speed at 13000rpm (Jencons PLS, Leicestershire, UK) for 15 seconds. The flow through was discarded and DNASE1 (Qiagen, West Sussex, UK) added to the column and incubated at room temperature for 30 minutes.Further centrifugation was performed in order to remove the DNASE1 and RW1 buffer was then added to the column. Again the samples were centrifuged and the flow through was discarded. RPE buffer containing ethanol was added to the column and centrifuged at 2 minutes at max speed. More centrifugation was carried out to remove the remaining RPE buffer and RNase-free TE Buffer (Invitrogen, Paisley, UK; 30-50µl) was added directly to the column and incubated for 1-2 minutes. After incubation, the samples were centrifuged for 1 minute in order to elute RNA. The RNA was then stored at -20°C.

2.4.4 Quantification of RNA

RNA was quantified using either an Picodrop (3µl sample required; Picodrop limited, Saffron Walden, UK) or Nano-drop (1µl sample required; Labtech, East Sussex, UK) spectrophotometer. RNA concentration (ng/µl) and purity can be obtained using this methodology. The spectrometer measures total nucleic acid content at 260 and 280 nm. The machine then calculated the 260/280 ratio.A ratio between 1.9 and 2.3 suggested that the RNA is pure, thus no contamination. Unfortunately both DNA and RNA have the same wavelength (260nm), which makes it difficult to determine whether the RNA is free of DNA in case of contamination. Buffer contamination also gives poor 260/280 ratio. An

example of RNA concentration and purity can be seen in S1 in appendix III.

2.4.5 RNA denaturation gel

For assessing the quality and the yield of the RNA, denaturing agarose gel electrophoresis of RNA was employed. This system was also used to determine RNA secondary structure. Most RNA forms extensive secondary structure by intermolecular base pairing. MESA buffer containing 20mM MOPS solution, 2mM sodium acetate and 1mM EDTA (Sigma-Aldrich, Dorset, UK)were used for making the gel and running buffer. Agarose gel (1.2%) containing 37% (2.3M) formaldehyde was prepared and equilibrated for 30 minutes in running buffer (MESA buffer containing 37% (2.3M) formaldehyde) prior to running the gel. Meanwhile, RNA samples were prepared. RNA (5µl) was mixed with 10µl loading buffer and heated for 10 minutes at 65°C. The samples were then chilled on ice prior to loading. Ethidium bromide (EtBr, Promega, Hampshire, UK) is an intercalating agent that is used for staining nucleic acids and when exposed to UV light it fluorescence. Intact RNA will give two bands, 28S rRNA (the heavier band) and 18S rRNA (the smaller band). The heavier band should be more intense than the smaller band in a ratio of 2:1 (28S:18S) if the RNA is intact. In order to visualise the RNA with EtBr, at least 200ng of RNA should be loaded. Some RNA preparations such as preparation using needle biopsies may result in a low RNA yield. The RNA gel was initially run at 40V for 10 min and then at 80V for 30 minand visualized under UV light in (UVP-Bio Doc-It™ Systems, Cambridge, UK). Gel images were captured using VisiDoc-it Systems (UVP-Bio Doc-It™ Systems, Cambridge, UK) equipped with a thermal printer (Sony, Japan)

2.4.6 cDNA synthesis

Total RNA (50ng-1μg) was transcribed using the reverse transcriptase kit (BIOLINE, London, UK) according to manufactures' instruction. Briefly, RNA was primed at 65°C for 10 minutes. Reverse-transcription was then achieved at 42°C for 30 minutes. Oligo $(dt)_{18}$ was used for RT-PCR in order to distinguish mRNA from other RNA species. It is possible to use a higher temperature i.e. 50°C to increases the yield of cDNA synthesis if the sample has a complex RNA secondary structure but the yield of the majority of normal RNA molecules is reduced. No RT controls were included for all genes in this study.

2.4.7 cDNA amplification

The cDNA was amplified using 0.025 U/μl of Taq polymerase (Qiagen, West Sussex, UK). All products were optimized for cycle number to ensure a linear signal. All primers were used in a concentration of 0.25μM, unless indicated. PCR products were separated on a 1.5% agarose gel containing EtBr (Promega, Hampshire, UK) and visualized under UV light (UVP-Bio Doc-It™ Systems, Cambridge, UK). Gel images were captured using VisiDoc-it Systems (UVP-Bio Doc-It™ Systems, Cambridge, UK) equipped with a thermal printer (Sony, Japan)

2.4.8 Quantification the RT-PCR bands

Quantification was done using the ImageMaster ID prime program (Pharmacia Biotechnologies Inc, San Francisco, USA) where the band density was measured and normalised to β-tubulin band intensity.

2.5 Real-time PCR

2.5.1 Principle

In contrast to conventional RT-PCR, where the product can only be visualised after the amplification end, with real-time PCR (also known as quantitative PCR (QPCR)), the gene of interest is amplified and quantified while the reaction is running. This is accomplished by detection of fluoroscence emitted by accumulating PCR product at each PCR point. The intensity of fluoroscence is proportional to the concentration of the amplified gene of interest. There are two methods of detecting the amplification using real-time PCR. These includes using SYBR green (a fluorescent dye), which binds to the amplified cDNA or flourogenic probes, which are single stranded oligoneucleotid of 20-26 nucleotides and are designed to bind the DNA sequence between the two PCR primers. These fluorogenic probes allow only fluorescent signals from specific PCR products. The most used amplification detection method is uses SYBR green because of its high sensitivity, however it does not discriminate between the amplification of target gene and non-specific amplification of related sequence and/or primer artefacts.

2.5.2 cDNA synthesis

RNA obtained as described in section 2.3.3 was converted to cDNA. The cDNA synthesis was done as described in section 2.3.6, the difference here was that random hexamers were used instead of $oligo_{dt}$.

2.5.3 Real-time PCR procedure

The standard curve for the real time PCR was prepared with 6 weeks old BN retinae cDNA, which was synthesised as described above. The standard curve consisted of consecutive dilutions 1, 1/4, 1/16, 1/64 and 1/256, in RNase/DNase free water (Qiagen, West Sussex, UK). cDNA (2,5µl) was amplified in a 25-µl reaction volume using the SYBR@ Green

JumpStart™ Taq Readymix™(Sigma-Aldrich, Dorset, UK) kit according to manufactures' instructions. Primers were used at a concentration of 0.6μM. PCR was performed using a Cobrett PCR machine (Corbett research limited, Cambridge, UK) with an initial denaturation step at 95°C for 5 minutes and for 45 cycles of 94°C for 30 seconds, 59-61°C depending on the gene being amplified for 1 min, and 72°C for 30 seconds. Cycling was followed by a 1 minute hold at 65°C. A melting curve was obtained to confirm that the SYBR green signal corresponded to unique and specific amplicons (Fig 2.4A-B).

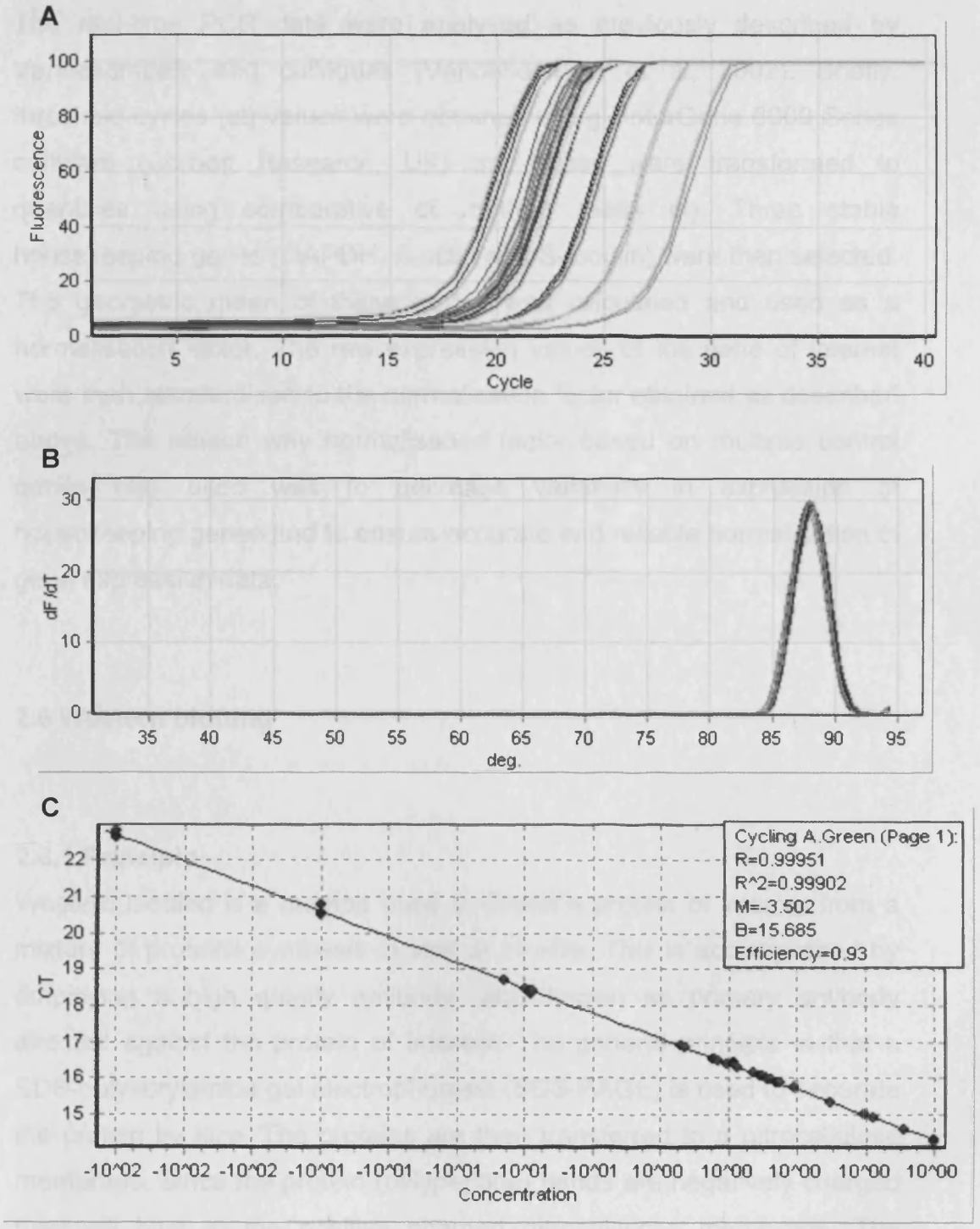

Figure 2.4: Real-time PCR program graphs obtained from Corbett PRC machine. (A) Amplification plot, (B) melting curve and (C) Standard curve

2.5.4 Data analysis

The real-time PCR data were analysed as previously described by Vandesompele and collegues (Vandesompele et al, 2002). Briefly, threshold cycles (ct) values were obtained using RotorGene 6000 Series software (Corbett Research, UK) and these were transformed to quantities using comparative ct method (delta ct). Three stable housekeeping genes (GAPDH, ß-actin and ß-tubulin) were then selected. The geometric mean of these genes was calculated and used as a normalisation factor. The raw expression values of the gene of interest were then standardised to the normalisation factor obtained as described above. The reason why normalisation factor based on multiple control genes was used was to decrease variability in expression of housekeeping genes and to ensure accurate and reliable normalisation of gene expression data.

2.6 Western blotting

2.6.1 Principle

Western blotting is a method used to detect a protein of interest from a mixture of proteins synthesis *in vivo* or *in vitro*. This is accomplished by employing a high quality antibody, also known as primary antibody directed against the protein of interest. The general principle is that a SDS-polyacrylamide gel electrophoresis (SDS-PAGE) is used to separate the protein by size. The proteins are then transferred to a nitrocellulose membrane. Since the protein (polypeptide) bands are negatively charged they will bind to the positive charged nitrocellulose membrane. The results will be a nitrocellulose membrane that is imprinted with the same protein bands as the gel. Primary antibody is applied to the membrane and the secondary antibody (directed against the primary antibody) with an enzyme (e.g. alkaline phosphates or horseradish peroxidase) conjugated to it is used to visualise the protein.

2.6.2 Protein extraction

Protein from retina was extracted using Qiagen Qproteome mammalian protein preparation kit (Qiagen, West Sussex, UK). Briefly, the retina was homogenised in cold PBS by trituration. The samples were then centrifuged for 5 minutes at 4500x g in a pre-cooled (4°C) centrifuge. The cell pellet was resuspended in lysis buffer containing 1U benzonase nuclease and a protease inhibitor. The samples were then incubated for 30 minutes at 4°C. After incubation, the suspension was centrifuged at 4°C for 10 minutes and the supernatant, containing total protein fraction transferred into a new tube and stored at -20°C for later analysis. In some cases, the retina was homogenised in RIPA lysis buffer (Upstate Millipore, Herts, UK) containing phenylmethanesulfonyl fluoride solution (PMSF, a protease inhibitor cocktail, Sigma Aldrich, Dorset, UK) using a pellet pestle motor (VWR international, Leicestershire, UK). The samples were then incubated on ice for 45 minutes, frozen and thawed in liquid nitrogen 3 times. The samples were centrifuged at 14000rpm for 15 minutes and supernatant containing protein was collected. The samples were stored at -20°C for further analysis.

2.6.3 Protein quantification

Protein quantification was carried out using the Bio-Rad Protein Assay (Bio-Rad, Hemel Hempstead, UK) with bovine serum albumin (BSA, Sigma-Aldrich, Dorset, UK) as standard (Table 2.2). The standard samples were prepared as shown in table 2.2 and the samples were diluted 1:10. The working reagent was prepared by adding 1 part reagent B with 50 parts reagent A (10mls reagent A to 200 µl reagent B). Working reagent (200µl) was then added to 96-well plate and 25 µl of each standard or unknown sample was also added. The mixture was incubated at 37°C for 30 minutes. The absorbance was then measured at 540nm using the plate reader. An example of protein concentration can be seen S2 in appendix III. In some cases, the Nano-drop spectophotometer was used to determine protein concentration.

Table 2.2. BSA standards.

Vial	Vol. Diluents (H2O)	Vol. BSA	Final BSA conc.
A	0 µl	300 µl of stock	2000 µg/ ml
B	125 µl	375 µl of stock	1500 µg/ ml
C	325 µl	325 µl of stock	1000 µg/ ml
D	175 µl	175 µl of vial B	750 µg/ ml
E	325 µl	325 µl of vial C	500 µg/ ml
F	325 µl	325 µl of vial E	250 µg/ ml
G	325 µl	325 µl of vial F	125 µg/ ml
H	400 µl	100 µl of vial G	25 µg/ ml
I	400 µl	0	0 µg/ ml

2.6.4 Western blotting procédure

In order to resolve the protein, 12% SDS-PAGE (see appendix II) was used and the protein transferred to a nitrocellulose membrane. Protein (10µg) was loaded to the immunoblot.The SDS-PAGE blot was run at 100V, 350mA for 1hour. Successful transfer was determined by incubated the nitrocellulose membrane (Amersham biosciences, Bucks, UK) with Ponceau S (Sigma-Aldrich, Dorset, UK) to visualise the protein bands (Fig. S1 in appendix III). The membrane was then washed in tris saline buffer (TBS) containing 0.1% Tween 20 (TBST, see appendixII) and blocked in 5% milk (Fluka, Biochemika, Buchs, Swisterland) in TBST for 1hour. After blocking, the membrane was washed and incubated in TBST with primary antibody (see dilution and incubation time in table 2.3). Following three washes in TBST, membranes were incubated in appropriate peroxidase-linked secondary antibodies (1.5000; Santa Cruz, Heidelberg, Germany) for 1h before substrate development using ECL-plus (GE Healthcare, Bucks, UK). Rabbit IgG was used as negative

control for TRAF2, caspase 3 and 9 antibody while cIAP1 blocking peptide was used as cIAP1 negative control. The blocking peptide was incubated together with cIAP1 primary antibody for 1h prior to incubation with the membrane. Another negative control (secondary antibody alone) was also included. The procedure used to detect the protein of interest was also used for the controls as well. Laser scanning densitometry was performed and bands were quantified using Labworks programme (UV BioImaging Systems, Cambridge, UK).

Table 2.3. Dilutions and incubation times of antibodies.

Antibody name	Antibody type	Company	Concentration	Incubation time
cIAP1	Polyclonal	Santa Cruz, Heidelberg, Germany	1:200	1h at room temperature
Active Caspase 3	Polyclonal	Abcam, Cambridge, UK	1µg	Overnight at 4°C
Caspase 3	Polyclonal	Cell Signalling, Hertfordshire, UK	1:1000	Overnight at 4°C
Caspase 9	Monoclonal	Cell Signalling, Hertfordshire, UK	1:1000	Overnight at 4°C
p53	Polyclonal	Santa Cruz, Heidelberg, Germany	1:1000	Overnight at 4°C
TRAF2	Polyclonal	Santa Cruz, Heidelberg, Germany	1:1000	Overnight at 4°C
Chx 10	Polyclonal	chemikon, Millipore, Hertfordshire, UK	1:500	Overnight at 4°C
Thy 1	Monoclonal	Abcam, Cambridge, UK	1:500	Overnight at 4°C
Actin	Polyclonal	Santa Cruz, Heidelberg, Germany	1:1000	1h at room temperature

2.6.5 Stripping the membranes

Stripping is a term used to describe removal of antibodies from a Western blot membrane. This is very useful since it allows investigation of more than one protein using the same blot. For example, a protein of interest and a loading control can be detected using the same membrane. Stripping has an advantage of saving samples, material and time. During the stripping process some protein will be lost, however. This is carried out by incubation of membrane in stripping buffer (see appendix II), two times, 10 minutes each. The membrane is then transferred to PBS and washed twice for 10 minutes each. And finally, washed in TBST, again twice for 5 minutes each time.

2.6.6 Quantification of IAPs and caspases protein in the retina

Laser scanning densitometry was performed and bands were quantified using Labworks programme (UV BioImaging Systems, Cambridge, UK). The values were normalised to the ß-actin band intensity.

2.7 Immunofluorescence

2.7.1 Principle

Immunoflourescence is a technique used to detect the location and the abundance of any protein using an antibody. It is very important for the entire process to be able to visualise the antibody when looking in through a microscope. In order to do this, a fluorescent dye is covalently (this bond is achieved when atoms share electrons) linked to the antibody. When the dye is illuminated, it absorbs light at the stimulation wavelength and emits a light at a longer wavelength, which can be imaged and quantified. In most experiments two antibodies are used. A primary antibody that recognise and binds to the protein of interest and a secondary antibody with a fluorescent dye attached to it that recognise and binds to the primary antibody.

2.7.2 Preparation of wax embedded retina sections

Eye-cups (anterior segment and lens removed) were dehydrated through a series of increasing methylated spirit (IMS, Fisher scientific, Leicestershire, UK) concentration (50%, 70%, 90% and 100%) with maximum incubation time of 1 h/concentration. The tissue was first immersed in an equal mixture of 100% ethanol (Fisher scientific, Leicestershire, UK) and xylene (VWR international, Leicestershire, UK) for 10 minutes. Thereafter, they were immersed in 100% xylene for 10 minutes and incubated warm wax for 1 h to remove xylene. Eye-cups were then transferred into fresh molten wax, incubated for 30 minutes and finally embedded in wax and sectioned at 7µm. Sections were incubated at 56°C overnight in order to dry.

2.7.3 De-wax the sections

Sections were immersed twice in 100% xylene for 10 minutes each and then twice in 100% alcohol for 5 minutes each. The samples were then transferred into a series of alcohol (90%, 70% and 50%) and incubated for 5 minute in each condition then washed in running water for 5 minutes.

2.7.4 Nuclei staining with Hoeschst 333542

Retinal wholemounts were stained with 3ng/µl Hoechst 33342 (Sigma-Aldrich, Dorset, UK) for 20 minutes and mounted in Prolong Gold antifade medium (Invitrogen, Paisley, UK).

2.7.5 Citrate buffer antigen retrieval

2.7.5.1 Principle

PFA fixation forms protein cross-links that can mask the epitopes in tissue samples. This may results into weak or false negative staining for immunohistochemical detection of certain proteins. Antigen unmasking was therefore undertaken to break protein cross-links, therefore unmask the antigens, which will enhance staining intensity of antibodies.

2.7.5.2 Procedure

De-waxed sections were washed in PBS and then put in a pressure cooker containing citrate buffer (15ml antigen unmasking solution in 1600 ml ddH_2O, Vector laboratories, Peterborough, UK) and heated to boiling point. Samples were removed after 15 minute of boiling, cooled for at least for 30 minutes at room temperature and washed in PBS for 5 minutes. In some cases, homemade citrate buffer was used (see appendix II). The sections were put in the citrate buffer and heated to boiling point using a microwave. The samples were then cooled for 5 minutes at room temperature and the procedure was repeated 2 more times.

2.7.6 Immunofluoroscence staining procedure

De-waxed sections were washed in PBS and blocked with 5% either rabbit (Sigma-Aldrich, Dorset, UK) goat (Sigma-Aldrich, Dorset, UK) or donkey (Sigma-Aldrich, Dorset, UK) serum in PBS containing 0.01% Triton x 100 (Sigma-Aldrich, Dorset, UK) for 1h at room temperature. Tissues were incubated overnight at 4°C with primary antibody in 1% blocking solution serum (anti-active caspase 3 (1µg, Abcam, Cambridge, UK) and anti-TRAF2 (1:100; Santa Cruz, Heidelberg, Germany)). After three washes, the sections were incubated with appropriate (donkey anti-goat, goat anti-rabbit) Alexa-Flour-labeled secondary antibody (1:1000, Invitrogen, Paisley, UK) for 1h at room temperature. All sections were counterstained with To-PRO 3 (Invitrogen, Paisley, UK) and mounted using Hydro-mount solution (National Diagnostic, England, UK).Controls (secondary antibody alone) were included in all studies.

2.7.7 Imaging

Sections were imaged using an Axioplan Zeiss laser scanning confocal microscopy (Zeiss, Heidelberg, Germany) equipped with the following absorption /emmision filters (nm); absorption at 494nm and emission 518nm filter, absorption at 555 nm and emission 575 filter for Alexa fluor (488nm) and (546nm), respectively and absorption 640 nm and emission 690 filter for

To-PRO3. Staining intensity was quantified utilising Adobe Photoshop (Adobe Systems Incorporated, Uxbridge, UK) and expressed in percentage of the staining intensity of the experimental sections after extracting the background staining intensity.

2.8 TUNEL assay

2.8.1 Principle

TUNEL assay is used to detected breakage in DNA strands by enzymatically labelling the free 3' –OH termini with modified nucleotides. The assay detects both single and double stranded DNA associated with apoptosis. Although the assay distinguishes apoptosis from necrosis, there are cases where cells exhibiting necrotic morphology may also stain lightly.

The underlaying principle is that digoxigenin-nucleotides are enzymatically added to DNA by terminal deoxynucleotidyl Transferas (TdT). TdT is then used as a catalytic factor to catalyse a templet-independent additional of nucleotides triphosphates to the 3'-OH end of double- and single- stranded DNA. The incoporated digoxigenin-nucleotides are the allowed to bind anti-digoxigenin antibody that is conjugated to a peroxidise reporter nucleotide, which can then be visualised (Fig 2.5)

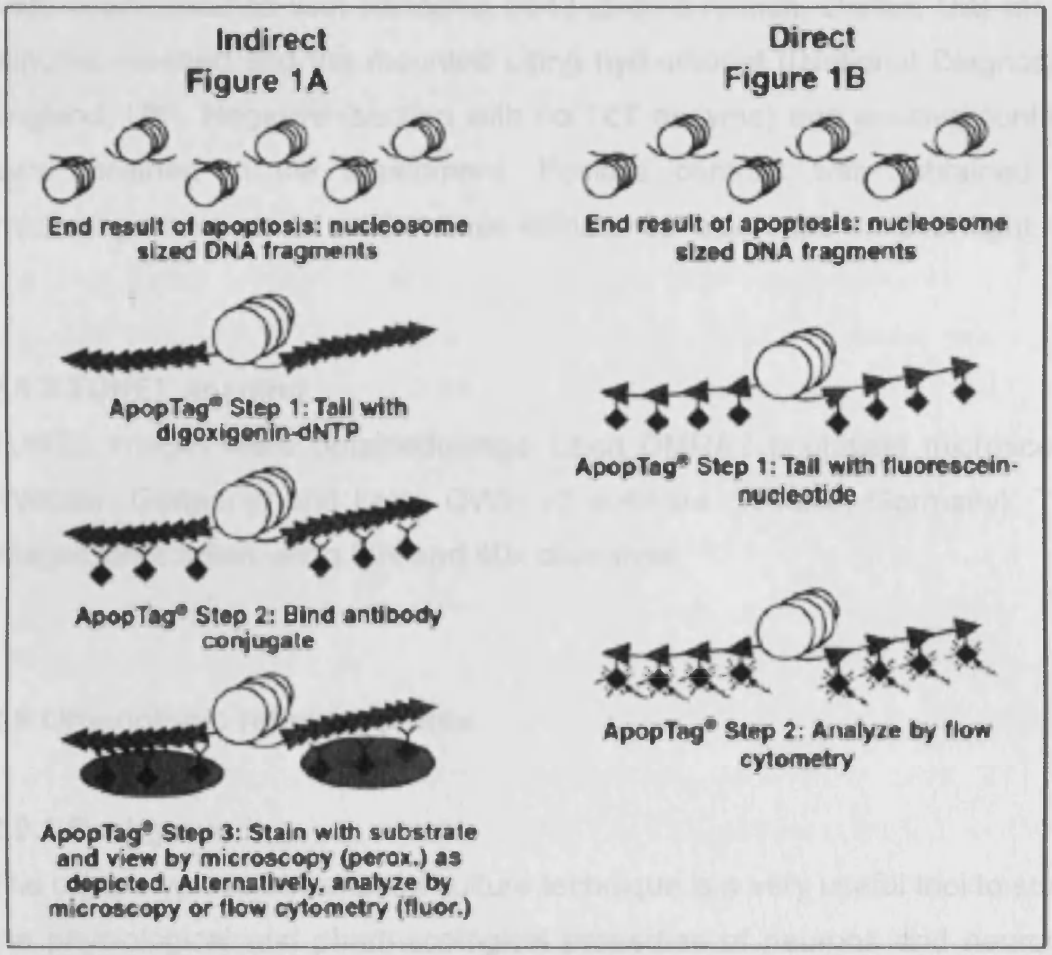

Figure2.5. ApopTag based TUNEL assay methodology (Figure adapted from Chemicon ApopTag Peroxidase *In situ* Apoptosis Detection Kit booklet).

2.8.2 Procedure

TUNEL assays were carried out according to manufacturer's instructions. Briefly, following three washes in PBS, dewaxed sections were incubated in 20µg/ml 60µl/5 cm ^{2} for 15 minutes. The sections were then washed using dH_2O and the endogenous peroxide blocked by additional of 3% hydrogen peroxidise for 5 minutes. Following washes in PBS, the sections were put in equilibration buffer for 30 seconds and the TdT enzyme was added to the sections. The reaction was stopped by adding working strength stop/wash buffer (see appendix II) and incubated to 10 minutes. Subsequently, the sections were incubated with anti-digoxignenin conjugate for 30 minutes, washed and working strength peroxidise substrate (see appendix II) applied to the sections and incubated for 15 minutes. Following washes, the samples

were counterstained with Hoeschst 3342 (Sigma-Aldrich, Dorset, UK) for 20 minutes, washed and the mounted using hydromount ((National Diagnostic, England, UK). Negative (section with no TdT enzyme) and positive controls were included in the experiment. Positive controls were obtained by incubating whole mount adult mouse retina in 3µl staurosporine overnight.

2.8.3 TUNEL imaging

TUNEL images were obtainedusinga Leica DMRA2 brightfield microscope (Wetzlar, Germany) and Leica QWin v3 software (Wetzlar, Germany). The images were taken using 20x and 40x objectives.

2.9 Organotypic retinal explants

2.9.1 Background

The organotypic retinal explant culture technique is a very useful tool to study the physiological and pharmacological properties of neurons and neuronal circuits. In contrast to dissociated retinal cells cultures, organotypic cultures have the advantage of retaining cytoarchitecture and neuronal circuits of the retina.

2.9.2 Medium preparation

Culture medium consisted of sterile Neurobasal medium (Gibco, Invitrogen, Paisley, UK) supplemented with 2% B27 (Invitrogen, Paisley, UK), 0,8mM L-glutamineand 0.1% penicilin/streptomycin (Sigma-Aldrich, Dorset, UK)

2.9.3 Explants cultures

The cultures used in the project were short-time with less than 1h incubation. After transferring the dissected retina on to a millicell nitrocellulose insert (Millipore, Hertfordshire, UK) with RGC side facing upwards the membrane was then inserted in a culture dish containing culture medium (see section

2.9.2). Explants were incubated at 37°C in the humidified 5% CO_2 incubator (ICN Flow Laboratories, Irvine, CA).

2.9.4 Pre-coating of tubing

Plastic tubing (Bio-Rad, Hertfordshire, UK, catalog number 165-2441) was pre-coated with 0.1mg/ml polyvinyl pyrolidone (PVP, Sigma-Aldrich, Dorset, UK). PVP was diluted in 100% ethanol and was freshly prepared each time before use. The tube was then hooked to a nitrogen tank (BOC, Bristol, UK) and left to dry for 30 minutes minimum.

2.9.5 Coating tungsten particles

1.1'-dioctadecyl-3,3,3',3'-tetramethylindocarbocyanine perchlorate (DiI, 25mg/ml, Molecular Probes, Eugene, OR) was dissolved in 400ml methylene chloride (Sigma-Aldrich, Dorset, UK). Tungsten particles (1.7µm diameter; BioRad, Hertfordshire, UK) were spread evenly on a glass slide. The DiI solution was then added to the particles until they were completely corvered with the solution. Menthylated choloride evaporated leaving the dye precipitated onto the tungsten particles. The particles were scraped from the glass slide giving a fine powder. The powder was then transferred into the pre-coated plastic tubing. The dye-coated particles were allowed to settle on to the wall for 20 minutes. The particle-coated tube was cut into 13mm pieces length using a tube cutter (Bio-Rad, Hertfordshire, UK) and stored at room temperature for further use.

2.9.6 Delivery of particles

The particles were delivered to the retinal explant using gene gun (Helios Gene-gun, BioRad Hercules, CA, USA). A membrane filter of size 11µm (black, gridded millipore filters, Millipore, Hertfordshire, UK) was placed between the gun and the culture to protect the retina from shock wave. In order to deliver the particles, 120psi helium gas pressure was used. The higher the pressure the more cells were labelled. Some tissues were shot several times (up to 3 times) in order to increase the labelling density but this was not preferred since several shooting may lead to tissue injury. Following

the delivery, the explants were incubated at 37°C in the humidified 5% CO_2 incubator for 30 minutes to allow the DiI to spread.

2.9.7 Fixing and counter staining

The explants were fixed overnight at 4°C in 4% paraformaldehyde (see appendix II) and counter stained and mounted on glass slides the following day as described in section 2.7.4.

2.9.8 Imaging

2.9.8.1 Analysis of RGCs dendrites

Diolistically labelled RGCs were imaged with an Axioplan Zeiss laser scanning confocal microscope 24 hours after labelling. Explant wholemounts were washed in PBS and mounted, ganglion cell side up on superfrost slides (Jencons, VWR International, UK). ProLong Gold (Invitrogen, Paisley, UK) was used as an antifade reagent. For every experimental age studied, the dendritic organisation of at least 60 neurons was reconstructed and analysed. For each RGC, 15 and 30 optical sections were obtained using 20x objective. Imaging was done at 565nm, obtaining slice thickness of 0.852µm.

2.9.8.2 Neuron nuclei imaging

Images of the RGCL were captured at 420/40nmin a systematic fashion using a fluorescent microscope (Leica 6000B,Wetzlar, Germany) linked to a Leica digital camera (Leica DFC350 FX, Wetzlar, Germany) and Stereo Investigator software (Microbrightfield, Magdeburg, Germany). Retinal specimens were placed on a motorized stage and the cells in the RGCL were imaged with a 20x objective in 12 fields (each with an area of 217141.75 μm^2)arranged in a grid centred on the optic disc (OD).

2.9.8.3 INL and ONL imaging and cell count

De-waxed wax embedded retinal sections (sections crossing the optic nerve (ON), see section 2.7.2-3) were stained with Hoeschst 3342 (Sigma-Aldrich, Dorset, UK) for 20 minutes. Images were obtained at 420/40nm utilising a fluorescent microscope (Leica 6000B, Wetzlar, Germany) linked to a Leica digital camera (Leica DFC350 FX, Wetzlar, Germany) and Stereo Investigator software (Microbrightfield, Magdeburg, Germany). The sections were imaged with a 20x objective in 10 fields per section.

2.9.9 Sholl analysis

Sholl analysis was performed on the Z-projection image of the neurons. The Sholl analysis programme is MATLAB based software that creates a series of 20μm a part concentric circles that were centred on the cell soma. The dendrites intersecting each ring were counted and plotted as a function a function of radial distance from the cell soma. In this thesis, Fast Sholl programme (Gutierrez and Davies, 2007), which is a simplified Sholl programme was used (Fig 2.6)

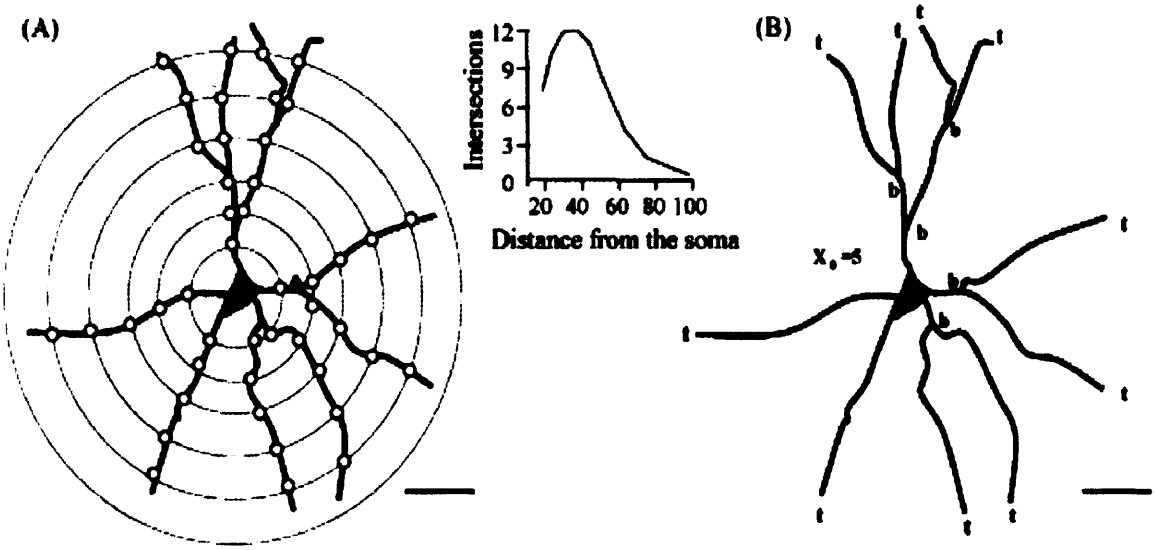

Figure 2.6.A schematic image of Conventional Sholl (A) and Fast Sholl (B). With conventional Sholl analysis, a number of concentric rings with increasing radial centred in the cell body are traced and the number Xi of neuritis (dendrite and axons) intersecting each ring of increasing radii is counted (shown as open circles). The data are then averaged over a population of sampled neurons and plotted vs. radial distance result in the characteristic Sholl profile (inset). Fast Sholl analysis, on the other hand, the entire Sholl profile is derived from the radial distance to bifurcations ('b' points in image B) and terminal points ('t' points in image B) and the number of processes emerging from the soma (X0). Figure adapted from Gutierres and Davies, (2007)

2.9.10 Cell counting

For RGC counting, the number of labelled cells in each image was counted manually using the Cell Counter plugin for ImageJ (NIK Images, NIH, USA). Approximately 5.2% of 6 week old and 4.2% of 24-52 week old BN retina was evaluated to estimate neuronal density. Standard morphologic criteria were applied for discriminating non-neuronal cells (endothelial and glial cells) from neuronal cellsINL and ONL cell count was also performed manually using the Cell Counter plug-in for ImageJ (NIK Images, NIH, USA). Total of 5 sections per retina in of 3 animals per study stage were imaged.

2.10 Experimental glaucoma

2.10.1 Principle

Experimental rat glaucoma model is a valuable tool for studying human glaucoma. Experimental glaucoma in animals is achieved by blocking the outflow of the aqueous humor produced by ciliary body from the anterior chamber. Different reagents have been used, these includes saline phosphate buffer, different types of beads among others. The reagents clog the trabecular meshwork, which serves as drainage. This leads to elevated IOP, which in return results in damage to the optic nerve head and to RGC.

2.10.2 Preparation of polystyrene paramagnetic beads

Ferro-magnetic microspheres (CHI Scientific, Inc., USA, bead diameter 5 microns) were reconstructed in sterile Balance Salt Solution (BSS, Alcon Corp, Hünenberg, Switzerland) resulting in an concentration of 30 mg/ml. Microspheres were then sterilised by γ-irradiation with a Gammacell 1000 Elite (Nordon International Inc. 22 TBq Caesium Source, Fleurus, Belgium).

2.10.3 Animal Acclimatisation

Ten retired male breeder BN rats were housed in a constant low-light environment (40-60 lux) to minimise diurnal fluctuations in IOP, with food and water provided ad libitum. IOPs were measured 3 times before injection using a handheld rebound tonometer (Tiolat, Oy, Finland) calibrated for use with the rat eye (Levkovitch-Verbin et al., 2002). All measurements were made in awake animals (Fig 2.7) in which the cornea was anaesthetised using topical 0.4% oxybuprocaine hydrochloride eye drops(Chauvin, UK).

Figure 2.7. An example of IOP being measured in awake rat. Figure adapted from http://www.colmedsupply.com/ophthalmology.html. Accessed on 15-04-2010

2.10.4 Injection of the beads to anterior chamber

Animals were first generally anaesthetised using Isoflurane anaesthesia. Topical chloramphenicol (0.5%, Cusi, Herts, UK) was administered pre and post injection. Approximately 20 μl of the bead solution was injected into the anterior chamber of the left eye, delivering approximately 0.6 mg of beads. The right eye served as an unoperated control. Injections were made using a sterile 32 (Hamilton) or 33-gauge (WPI Corporation) needle parallel to the iris. The 33-gauge needles were bevelled on 3 sides to facilitate injection through the cornea. A tunnelled injection was made with the needle running parallel to the anterior surface of the iris to minimise the risk of iris trauma. Since the beads tended to settle under the influence of gravity, the syringe and needle were agitated using a vortex stirrer (IKA® Werke GmbH & co.kg. Staufe, Germany), for approximately 10 seconds prior to injection to resuspend the beads in BSS.

Following completion of the injection, the needle was kept in position and the beads then drawn away from the injection site using a small hand held magnet (0.45 Tesla) which prevented the egress of beads from the injection track. The magnet was then used to distribute the microspheres around the iridocorneal angle to reduce the outflow of aqueous humour via the trabecular meshwork. Immediate increases in IOP could be minimised by leakage of aqueous around the injection cannula once the beads had been drawn away from the injections site. Injections of microspheres were performed up to four times, depending on the required level and duration of the IOP elevation.

2.10.5 IOP measurements

IOPs were taken the following days and then every 3 days after injection. Again all measurements were made in awake animals in which the cornea was anaesthetised using topical 0.4% oxybuprocaine hydrochloride eye drops(Chauvin, UK). The IOP were taken as the mean and standard deviation of 6 readings. The readings were recorded on online database named critter (Fig. S7; critters1.cf.ac.uk)

2.10.6 Staining of the beads in TM

Animals were sacrificed using overdose of CO_2. One injected eye was dissected removing the anterior chamber and the lens. Both the eye cup and the anterior chamber was then fixed in 4% PFA overnight and left in 10% sucrose (se appendix II) until it sank. Cryosections (10 µm) of the anterior chamber were obtained and put on gelatine-coated slides were stained with Haematoxylin and Eosin (H&E) or mounted under DPX (Raymond A Lamb, Thermo Fisher Scientific, Basingstoke, UK)for differential interference contrast (DIC) also known as Nomarski imaging. Section images were taken using a Leica DMRA2 brightfield microscope (Wetzlar, Germany) and Leica QWin v3 software (Wetzlar, Germany).

2.10.7 Retina dissection and RNA extraction

Rats were sacrificed using overdose of CO_2. Retina dissection and RNA extraction were done as described in sections 2.2.1 and 2.4.3.

2.10.8 cDNA synthesis and real-time PCR

cDNA synthesis and real-time PCR were done as described in sections 2.5.2 and 2.5.3, respectively.

2.11 Statistical analysis

Data were expressed as mean and standard errors. Following normality testing (Shapiro-Wilk test) and homogeneity of variance (Lavene test), group comparisons were made using independent student t-test (SPSS16, Chicago, Illinois) or one-way ANOVA as appropriate followed by Fisher's Tukey's post hoc test (SPSS16, Chicago, Illinois) for normal distributed data. Nonparametric test, Kruskal-Wallis with post-hoc test (SPSS16, Chicago, Illinois) was performed for data that was not normal distributed. Differences were considered significant for $p< 0.05$.

Chapter 3

Expression profiling of caspases and IAPs in ageing retinas of BN and Wister albino rats using Conventional and Real time PCR

3.1 Introduction

The survival of neurons is a complex balance between pro-survival and pro-death factors. Vision loss in ageing and diseases has been suggested to be a consequence of retinal ganglion cell (RGC) death (Morgan, 2002, Morgan et al., 2006, Quigley, 1999). The majority of RGCs are lost by apoptosis. Recent reports suggest that upon insult, for example elevated IOP and/or deprivation of neurotrophic factors, RGC simultaneously activates both apoptotic and survival pathways (Kim and Park, 2005, Levkovitch-Verbin et al., 2006, Levkovitch-Verbin et al., 2007, Yang et al., 2007), clearly highlighting cells' struggle for survival.

Moreover, there is evidence indicating that RGCs undergo a prolonged period of remodelling in which the dendritic tree is reduced in both extent and complexity prior to loss of the cell body (Morgan et al., 2006, Weber et al., 1998). For example, work carried out in rodents and primates has demonstrated dendrite remodelling during ageing and glaucoma both in RGCs and other cells of the retina including rod bipolar cell (Xu et al., Liets et al., 2006, Morgan et al., 2006, Weber and Harman, 2005). Using the DBA/2J mouse glaucoma model, it was shown that there is dendritic loss of RGC and the loss is more pronounced in the high order dendrites (A. Koizuma, 2010).

Moreover, dendrite pruning occurs in other CNC neurons (Solis et al., 2007, Ferrante et al., 1991, Moolman et al., 2004, Morgan et al., 2006). For example, dendrite pruning occurs in striatal neurons in HD, in pyramidal neurons in both AD and PD. Also experiments in monkey glaucoma, demonstrated reduction in dendritic field of the pyramidal neurons in LGN (Yucel et al., 2006, Yucel et al., 2003). Thus, dendrite pruning is a common theme in neurogenerative diseases.

In primate and murine RGCs, the changes in the dendritic tree have shown to have functional consequences. For instant, generation of action potential is more stochastic (Jakobs et al., 2005, Weber and Harman, 2005) and contrast sensitivity and receptive field size are reduced. Although these cells are compromised they are still functional and it is important to determine the

molecular mechanisms that governs dendrite pruning in ageing and disease in order to rescue these cells. It will be a challenge to determine these changes before the cells reach the "point of no return" defined by activation of caspase 3 in apoptotic pathway.

Although it is known that during ageing and neurodegenerative diseases cells are eliminated by apoptotic mechanisms, it is still not clear whether apoptotic mechanisms are responsible for dendrite remodelling. Work carried out in developing neurons, has suggested the involvement of the apoptotic pathway in dendrite pruning. There have been suggestions that apoptotic activity might be occurring at the dendrite level prior to the activation of cell death at the level of soma. Williams and colleagues demonstrated that during development of *Drosophila Melanogaster* sensory neurons, local caspase activity directs the engulfment of dendrites (Williams et al., 2006).

There are different methods of detecting gene expression. These include Northern Blotting, RNAse Protection Assay (RPA), In situ hybridisation, microarray and PCR (RT-PCR and quantitative, also known as real-time PCR). Northern blotting can be used to detect alternative splicing products and to evaluate transcript size. However, the methodology is limited by RNA degradation and low sensitivity (Streit et al., 2009). RNAse Protection Assay, on the other hand, is a single-stranded RNA based technique that allows simultaneous analysis of multiple mRNAs in the same total RNA sample (Burton et al., 1999). The major limitation of RPA is that it does not provide information on transcript size (Qu and Boutjdir, 2007). *In situ* hybridisation is utilised to localise DNA and RNA of the gene of interest to specific regions and cells within the regions (Montgomery, 2009). Thus, it allows analysis of the macroscopic distribution and cellular localisation of DNA and/or RNA sequence in heterogeneous cell populations. The disadvantage of this technique is that it is not very sensitive and also proper controls are essential for interpreting the results obtained.

For the past decade, microarrays have shown to be a powerful technology that allows parallel evaluation of thousands of genes in a short period of time (Schena et al., 1995).Microarrays can analyse up to 20000 genes. There are different types commercially available including microarrays or gene chip cDNA and oligo-nucleotide type (Pfaffl, 2003). The degree of the pitfalls of microarray made it unsuitable methodology for the screening of the genes of interest in this study. These pitfalls include, high variability, low sensitivity for low abundant expressed genes, inconsistent fidelity, discrepancy in "fold-changes calculations" and lack of specificity for differentially expressed genes and different isoforms (Bustin, 2000, DeRisi and Iyer, 1999, Harrington et al., 2000, Schena et al., 1995).Also, the methodology was economical unfavourable for tis study.

However, PCR-based screening of expression profile of the apoptotic pathway was a favourable methodology for this study because of its exquisite sensitivity. The PCR technique has been shown to be the most specific and sensitive for quantative analysis of gene expression (Pfaffl, 2003, Horikoshi et al., 1992, Livak and Schmittgen, 2001, Murphy et al., 1990). In fact, PCR has up to a 100-fold detection limit compared to other gene expression methods such as Northern hybridisation and RNA-Protection Assay (Bustin, 2000, Lockey et al., 1998, Orlando et al., 1998, Pfaffl, 2003). Thus, PCR is more powerful for the analysis of gene expression because it is rapid, simple, has a high sensitivity and reproducibility.

3.2 Aim

The aim of the experiments carried out in this chapter was to characterise the expression patterns of caspases and IAPs during maturation and ageing of BN and wistar albino rat retinae. This was done in order to identify molecules that can be of importance in maturation and maintenance of a healthy retina.

3.3 Experimental design

RNA was extracted from 6, 10, 16 and 24-52 weeks old BN and from 16-24 and 88 weeks old Wistar albino rats retinae as described in section 2.3.3. Following RNA quantification, purification and integrity evaluation (see sections 2.4.3 and 2.4.4), cDNA synthesis was carried out as describe in chapter 2.

RT-PCR was performed as described in chapter 2 section 2.4.7 on samples from 6 and 24-52 week retinae. Following optimisation of PCR conditions (cycle number and annealing temperature, Table 2.1), amplification of capsases 3,6,7,8 and 9 and IAPs, namely NIAP, cIAP1&2, XIAP, Survivin, Bruce and Livin was carried out. The products were then separated on a 1.5% agarose gel containing EtBr and visualized under UV light. Gel images were captured using VisiDoc-it Systems and the bands quantified using ImageMaster ID prime program.

Following, determination of housekeeping genes stability, the real-time method was carried out as described in chapter 2. Three housekeeping genes, GAPHD, Beta actin and Beta III tubulin were used for normalisation of the expression of genes of interest, caspase 3,6,7,8 and 9 and IAPs, NIAP, cIAP1&2, XIAP, Survivin, Bruce and Livin. RNA was extracted, quantified, and purity and integrity evaluated (see details of the methods in chapter 2). Real-time PCR was performed, using appropriate annealing temperature for each gene (Table 2.1) running 45-50 cycles using Corbett machine (see section 2.5.3). A melting curve was obtained for every run to ensure only one product was amplified (Fig. S6-8 in appendix III)

Threshold values (ct) obtained from Corbett machine were transformed to quantities. Geometric mean of the three housekeeping genes was calculated and was used as a normalisation factor for normalisation of relative expression of the genes of interest.

Following evaluation of normal distribution and homogeneity of the variance of the data, parametric (student t-test and ANOVA) and nonparametric (Kruskal-Wallis test) were performed. Data are shown as mean ± standard errors. Differences were considered significant when $p < 0.05$.

3.4 Results

3.4.1 RNA integrity

Following RNA isolation, quantification and purity evaluation, integrity was confirmed utilising RNA denaturation gel. Intact rat RNA should give two bands, the heavier band correspond to 28S and the smaller band corresponding to 18S ribosomal bands. The denaturation gel showed only two band indicating that the RNA was intact (Fig. 3.1). If the RNA samples were degraded there would have been a smear on the gel, which was not the case.

3.4.2 RT-PCR optimisation

Initial PCR reactions were performed to determine the annealing temperatures and duration of product elongation. All products were optimized for cycle number. The conditions were chosen so that all of the genes (housekeeping gene, caspases and IAPs) analysed were in the exponential phase of amplification (Fig. 3.2A-F and Fig. 3.3A-G).

3.4.3 Expression of caspases and IAPs in BN retina

No statistical significant change in mRNA levels of caspases 3,6,7,8 and 9 (Fig. 3.4A) or IAPs (NIAP, cIAP2, XIAP, Survivin, Bruce and Livin) were identified between 6 and 24-52 weeks old retinae with the exception of cIAP1 (Fig. 3.4B) using RT-PCR. cIAP1 mRNA levels were significantly down-regulated in mature retinae when compared to younger retinae ($p<0.001$, Fig. 3.4B).Real-time PCR confirmed the down-regulation of cIAP1 in mature compared to younger retina and this reduction was shown to be gradual (Fig. 3.5).

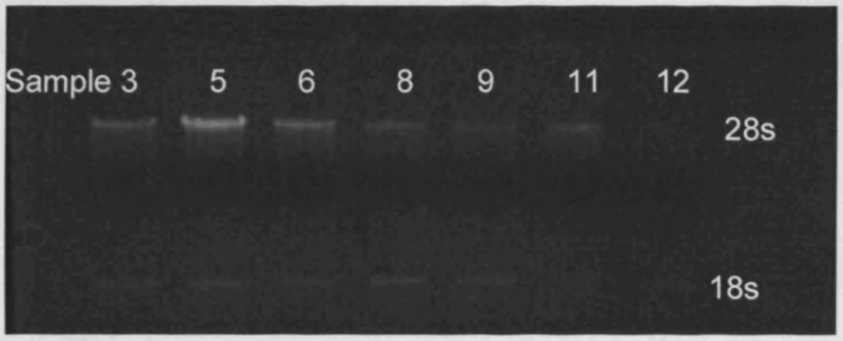

Figure 3.1. An example of an denaturing gel. Samples run on the gel were isolated from whole BN rat retina. Samples 3,5,6 and 8 are from 6 and samples 9,11 and 12 were isolated from 24-52 weeks old BN rat retina

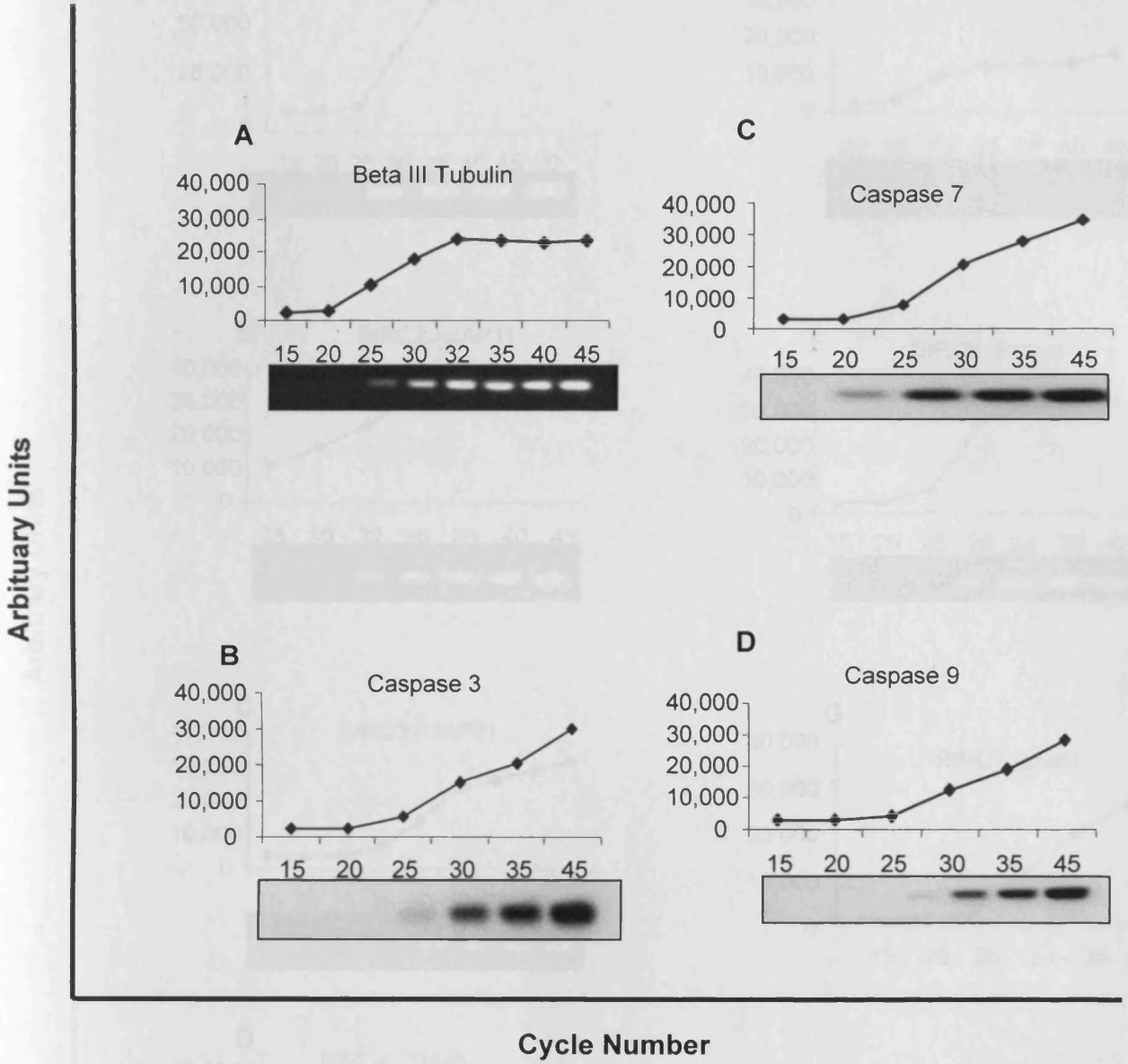

Figure 3.2. Optimisation of PCR conditions for β-tubulin (A), caspase 3 (B), 7 (C) and 9 (D) primers. The optimal cycle number was chosen in the exponential part of the curve.

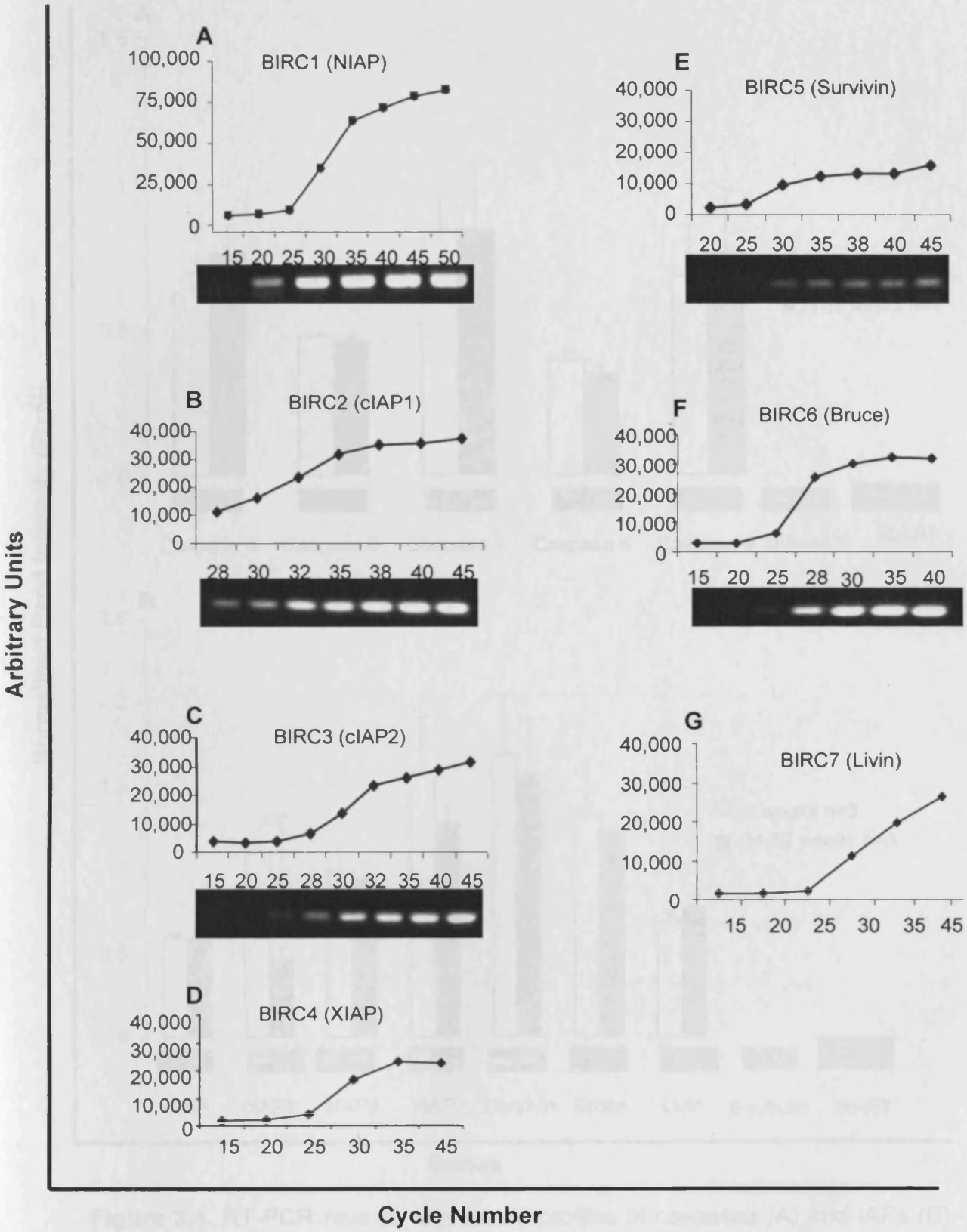

Figure 3.3. Optimisation of PCR conditions for NIAP (A), cIPA1 (B), cIAP2 (C), XIAP (D), Survivin (E), Bruce (F) and Livin (G). The optimal cycle number was chosen in the exponential part of the curve.

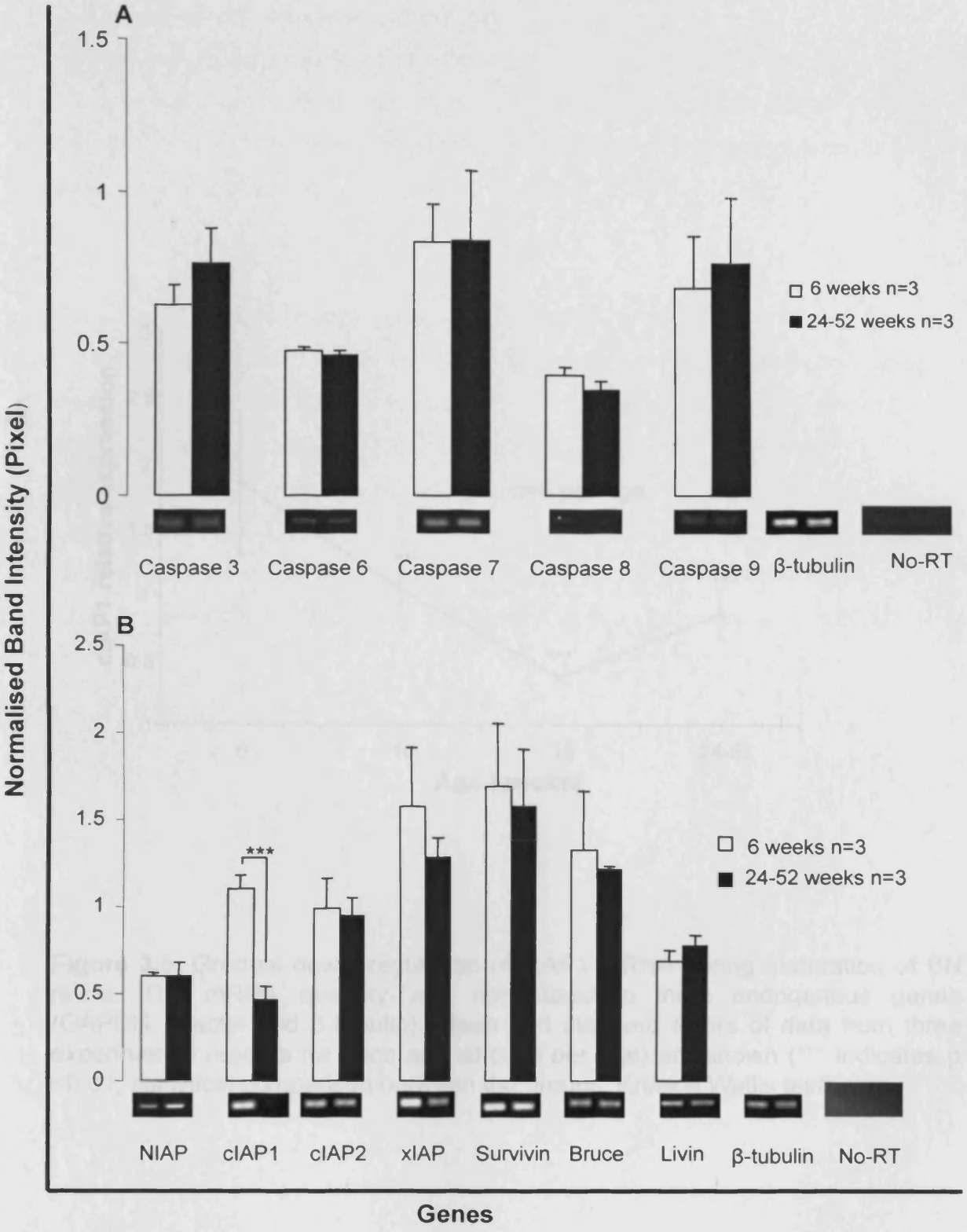

Figure 3.4. RT-PCR reveals expression profiles of caspases (A) and IAPs (B) in the ageing BN rat retina between 6 and 24-52 weeks of age. Samples were taken from total retinal extraction (6 eyes, 3 animals per group). Bands were normalized relative to β-tubulin mRNA. Mean and standard errors are shown (*** indicates $p < 0.01$, statistical comparison between the two ages, independent student's test)

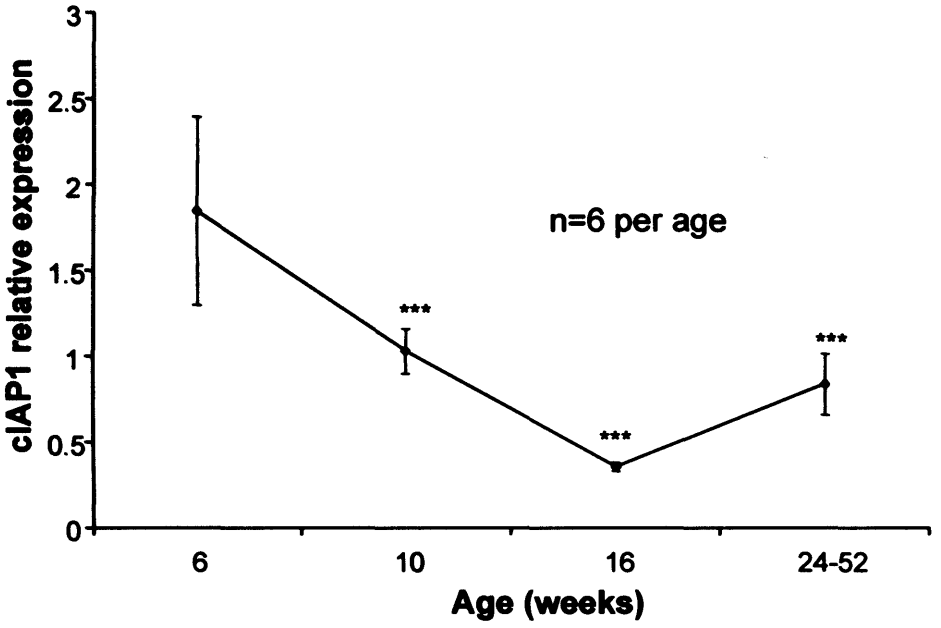

Figure 3.5. Gradual down–regulation of cIAP1 mRNA during maturation of BN retina. The mRNA quantity was normalized to three endogenous genes (GAPDH, β-actin and β-tubulin). Mean and standard errors of data from three experimental repeats for each animal (n=6 per age) are shown (*** indicates $p < 0.01$, statistical comparison between the groups, Kruskal Wallis test)

3.4.4 Evaluation of housekeeping gene costistency

Housekeeping gene expression was determined by plotting the ct values. The results show a trend towards a lower expression in older Wistar retinae (n = 5) but the difference was marginal indicating that their expression is not altered as a consequence of ageing (Fig. 3.6).

3.4.5 Expression of caspases and IAPs in Wistar albino rat retinae

Caspses 3,6,7,8 and 9 did not show alteration in their expression during ageing of Wistar albino rat retinae (Fig. 3.7A). Caspase 3 and 6 showed a trend towards increase in older (88 weeks) compared to younger (16-24 weeks) retinae but this was not statistical significant. NIAP, cIAP2 and XIAP were dramatically decreased in older compared to younger Wistar retinae (Fig 3.7B). cIAP1 was marginal decreased (Fig 3.7B). Survivin, Bruce and Livin showed a trend towards an increased but this was marginal (Fig 3.7B)

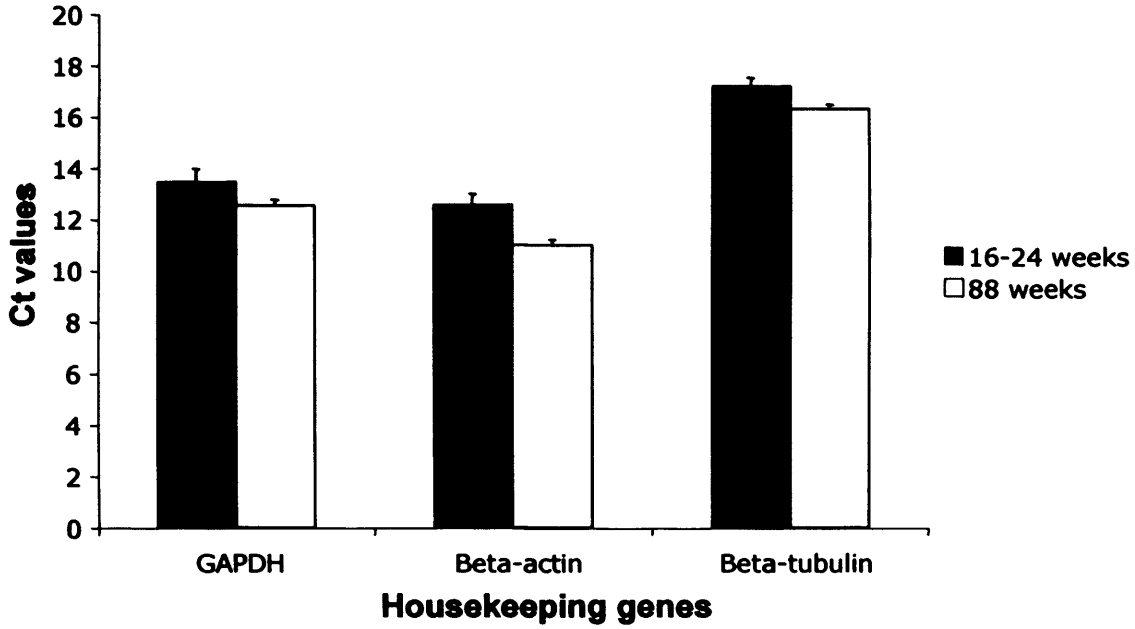

Figure 3.6. Stability of housekeeping genes (GAPDH, beta-actin and beta-III tubulin) in ageing wistar albino rat retinae. Determination of housekeeping genes in the two stages studied by plotting their ct-values.

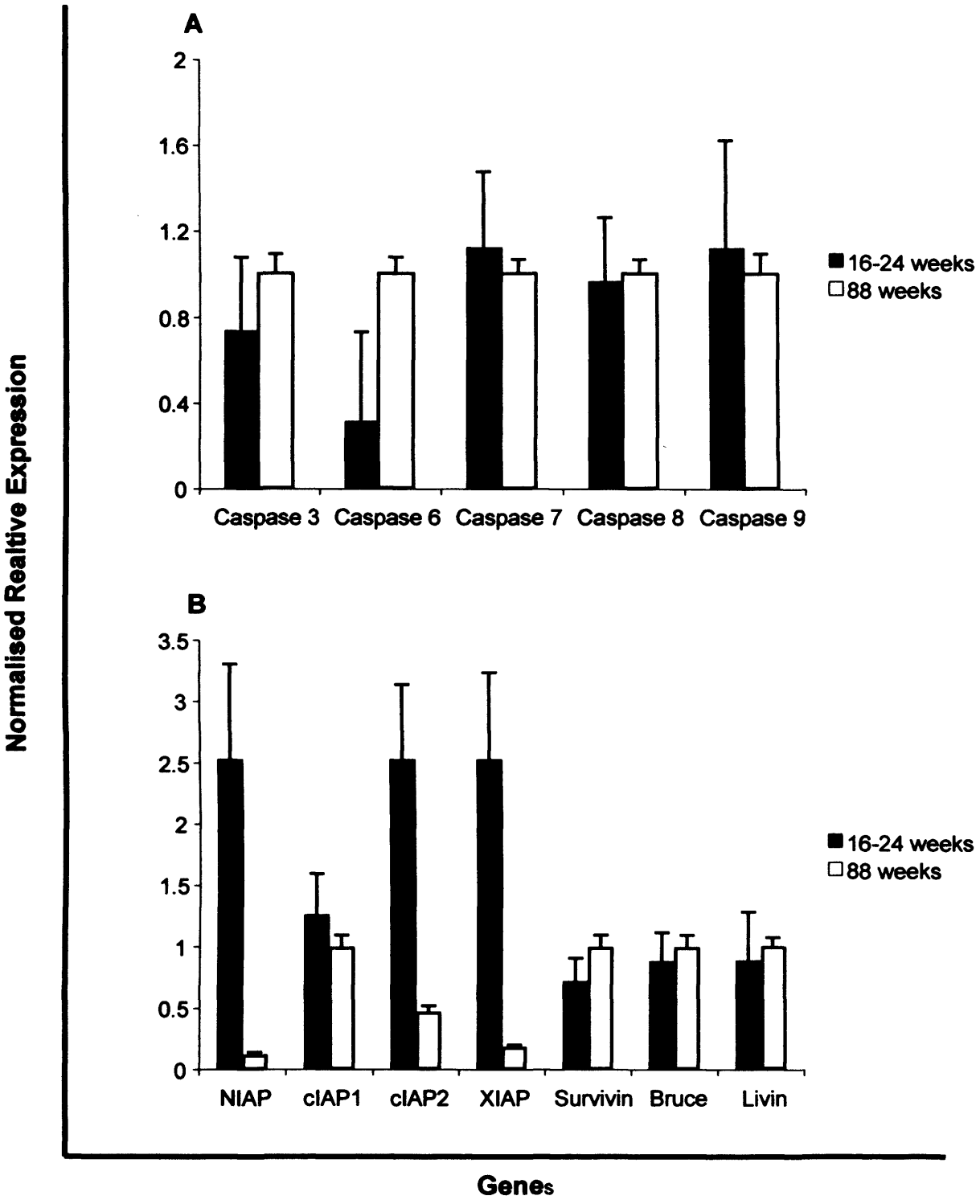

Figure 3.7. Real-time PCR on expression profiles of caspases (A) and IAPs (B) in the ageing wistar albino rat retina between 16-24 and 88 weeks of age. Samples were taken from total retinal extraction (4 and 5 animals for younger and older, respectively). The levels of mRNAs were calculated relative to three endogenous genes, namely, GAPHD, β-actin and β-tubulin mRNA. Mean and standard errors are shown.

3.5 Discussion

Understanding the expression pattern of genes is prerequisite for determining and elucidation of their function. The work reported in this chapter started by looking at the expression profile of caspases and IAPs utilising conventional PCR. This was carried out because it was unclear of what would be found and also to reduce experimental costs. The profile expressions were initially performed in BN rats.

Firstly, RNA integrity was determined, which showed that the RNA used to for cDNA was intact. This is important since fragmented RNA may introduce errors in cDNA generation, which in turn will affect the amplification of cDNA.

In order to eliminate false negative or positive signals during cDNA amplification, it is important to determine an optimal cell cycle. This was only done once and before the main experiments. Since the optimal cycle number was chosen in the exponential part of the curve, it is clear that the signal that obtained reflects the expression of the genes of our interest. All primers were designed to give a product of 150-250 base pair. A weight marker was used in the initial experiments just to confirm that the products obtained are of the correct size.

Using conventional PCR, caspase expression remained similar in the two stages studied.Densitometry quantification confirmed no statistically significant changes in caspase expression in mature compared to younger retinae. These data are not in line with observations made by McKernan and colleagues where they reported that caspase 3 and 9 expression is significantly reduced during ageing of the mouse retina between p6 and p60 (McKernan et al., 2006). This contradicting data could have several explanations. It is possible that species-specific difference in caspase 3 and 9 expression could be responsible for this apparent difference. A more likely explanation is that the differences is due to the different ages examined in the two studies; this study examined animals at 6 weeks at the earliest stage and did not include animals as young as P6 where one would expect to see

changes in caspase activity arising during development (Silver and Hughes, 1973, Silver and Robb, 1979).

Another possible explanation is that McKernan et al worked on cultured retinal tissue to determine expression of caspases, whereas the present study the expression was performed on freshly isolated tissue. The retinae in culture are traumatised and may not necessary reflect *in vivo* processes. During trauma, the cells respond by activating apoptotic/necrotic processes (Edinger and Thompson, 2004, Kerr et al., 1972). This includes activation of caspases. Additional explanation could be that BN rats have a high genetic variation despite inbreeding attempts (Gibbs et al., 2004) while genetic variation is absent in inbreed mice.

On the other hand, IAPs showed a general reduction in 24-52 compared to 6 weeks retinae in BN rat. IAP expression was generally decreased in mature compared to younger retinae suggesting that inhibition of apoptosis is compromised during ageing which could explain why neuronal degeneration is a common feature during ageing. In particular, cIAP1 is significantly down-regulated in mature compared to younger BN retinae. The data were validated using real-time PCR, which not only demonstrated a reduction in mature compared to younger retina but also showed that the reduction was gradual.

cIAP1 together with cIAP2 have been shown to control apoptosis triggered by multiple stimuli when introduce into mammalian cells (Eckelman and Salvesen, 2006). These two proteins are unusual among the BIR family proteins in their ability to bind to TRAF-family adapter proteins that have a role in TNF-receptor signaling (Li et al., 2002, Rothe et al., 1995, Shu et al., 1996). The TRAF-family consists of 6 members, TRAF1-6, but cIAPs only binds to TRAF1 and 2 through the BIR domain (Chung et al., 2002, Samuel et al., 2006). Although cIAPs bind to effector caspase 3 and 7 and initiator caspase 9 they are incapable of directly inhibiting their proteolytic activity (Eckelman and Salvesen, 2006). An emerging theory is that these two

proteins regulate apoptosis indirectly by inhibiting activation of survival pathways (Varfolomeev et al., 2006), which would be interesting to confirm in the retinal samples.

The majority of investigations on cIAP1 protein have mainly focus on tumour cells where it is highly expressed. Recently, it was shown that kockdown of cIAP1 either by an antagonist antibody or a knockout, leads to NF-kB activation and increased TNF- alpha expression, which result in cell survival. NF-kB is a transcriptional factor that is ubiquitously expressed (Vince et al., 2007). NF-kB is involved in different cellular processes including the stress response, innate and adaptive immune responses and cell survival and proliferation (Baldwin, 1996, Karin, 1996). Gutierrez and colleagues demonstrated that NF-kB signaling is involved in growth of neuronal processes in the developing PNS and CNS (Gutierrez et al., 2005). They observed reduced size and complexity of the neurite arbours of sensory neurons through inhibiting NF-kB activation. The hypothesis here is that the neurons of older animals have a less complex dendritic tree compared to younger animals. The suggestion put forward here is that the absence of cIAP1 may lead to reduced activation of NF-kB signaling. This in turn, contributes to decreased complexity of the dendritic tree.

There are two different methods for quantifying expression of genes using real-time PCR; absolute and relative quantification. Absolute quantification is critically dependent on the external standard material. The problem with external standard is that it lacks internal control for real-time and PCR inhibitors. Real-time PCR works on the basis that all samples are amplified with similar efficiency (Bustin, 2000, Livak and Schmittgen, 2001), which does not hold true for unknown samples. Relative quantification, which is the most commonly used method, evaluated the changes in steady-state mRNA of the gene and provides a result relative to the levels of the internal control (housekeeping gene; (Pfaffl, 2003).

Living cells are subject to fluctuation in their environments, which, in turn, influences the level of gene expression. Therefore, it is important to identify

genes whose expression remains constant in the tissue or cells under investigation, or in response to experimental treatment, that can be used as housekeeping genes in order to produce accuracy of RNA transcription analysis that real-rime PCR offers (Radonic et al., 2004). There have been suggestions that the expression of commonly used genes varies in different cell types, tissues, in diseases and during development and senescence (Spanakis, 1993, Suzuki et al., 2000, Bustin, 2000, Ishii et al., 2006, Thellin et al., 1999, Warrington et al., 2000)indicating that the use of single control gene is not suitable for evaluation expression of the target gene. Therefore, the use of multiple housekeeping genes as used in this chapter for analysis is advisable (De Boever et al., 2008). 18s and 28s rRNA have also been used as internal controls. These are not proper controls because of the imbalance between rRNA and mRNA. Also, they are absent in the highly purified mRNA samples (Vandesompele et al., 2002).

IAPs and caspase expression profile was also determined in very old (88 weeks) Wistar albino rat retina. Caspase expression remain similar in the two ages studied with the exception of caspase 6, which was up-regulated in older compared to younger retinae. NIAP, cIAP2 and XIAP were significantly down-regulated, whilst the expression of the rest of IAPs was not altered with age.

The pattern of expression was different in Wistar albino compared to the pattern observed in BN rat retinae. This could be owing to strain difference, but the more likely explanation is the different ages of the animals. The oldest BN rats used for the study were 52 weeks while the oldest Wistar rats were 88 weeks. The degree of apoptotic activity in senescence has been suggest to be more pronounced in 88 compared to 24 weeks retinae. Thus, the age difference could be the determining factor in the difference between caspases and IAPs expression in the two rodents strains used in this study.

Although Wistar albino rats have been used for glaucoma studies, are not favorable model for studying glaucoma. This is because they have other natural complications that occur as a result of ageing. These complications

include elevated cell death in the retina (Ricci et al., 1988, Neufeld and Gachie, 2003). For example, it was reported that neuronal loss during ageing in the retina is more pronounced in Wistar albino rats compared to pigmented rat strains (Weisse, 1995). In addition they show an increase in ultrastructural detrimental changes in the RPE (Adams, 1987). Although we did not observed any changes in caspase expression this does not exclude that there were changes in apoptotic activity in the two groups that were studied.

Caspases are stored in the cell as zymogens and are activated upon apoptotic signals (Kisiswa et al., 2009). It will be interesting to examine caspase and IAPs protein levels in order to determine whether the mRNA levels correlated with protein levels. Also it remains a challenge to evaluate activation in apoptotic pathway in Wistar albino rat retinae.

In summary, caspase expression, both in BN and Wistar albino rat retina is not significantly altered during maturation and senescence. IAPs expression, on the other hand, in BN rat retina show a general down-regulation in mature compared to younger retina with an exception of cIAP1, which was statistically significantly down-regulated in older mature compared to younger retina. IAPs expression pattern in wistar albino rat retina differs from the pattern observed in BN rat retina. NIAP, cIAP2 and XIAP significantly decreased in older compared to younger Wistar retinae. cIAP1 expression remained similar in the two ages studied. Survivin, Bruce and Livin showed a trend towards an increased but this was not significant. This suggests that the cell may respond differently to different stimuli.

Chapter 4

Impaired activation of survival pathway in BN RGCL during maturation

4.1 Introduction

Age-related loss of retinal ganglion cells (RGCs) is a consistent feature of the ageing mammalian visual system (Harman et al., 2000, Jonas et al., 1990, Jonas et al., 1989, Morrison et al., 1990, Neufeld and Gachie, 2003, Sanchez et al., 1986, Sohl et al., 1998).This non-pathological loss of RGCs is thought to contribute to the age-related decline in visual function (Neufeld and Gachie, 2003, Spear, 1993). Although the involvement of apoptosis in the elimination of RGCs in development, ageing and retinal pathology has been well documented (Cecconi et al., 1998, Neufeld and Gachie, 2003, Quigley et al., 1995, Spear, 1993), it is still unclear whether apoptosis is the main pathway of RGCs elimination during ageing (Kisiswa et al., 2009). Other modes of cell death namely, autoghagy and casapase-independent cell death, have been suggested to occur in glaucoma (Whitmore et al., 2005). The key regulators of apoptosis are caspases. Although essential for cell death, caspases have also been shown to participate in non-apoptotic processes including cell proliferation (Sadowski-Debbing et al., 2002, Schwerk and Schulze-Osthoff, 2003), differentiation (Carlile et al., 2004, Ishizaki et al., 1998, Okuyama et al., 2004, Oliver and Vallette, 2005, Wride, 2000, Wride et al., 2006, Wride et al., 1999) and maturation (Sordet et al., 2002). There is evidence that caspase expression in the retina is reduced following early post-natal development (McKernan et al., 2006).

Inhibitors of apoptosis (IAPs) comprise a family of proteins characterised by the presence of a variable number of Baculoviral IAP Repeats (BIR) domain (Clem, 2001). Early work showed that IAPs are involved in the inhibition of apoptosis by binding directly to caspases through their BIR domains and preventing their activation and activity (Liston et al., 2003). Recent evidence demonstrate that IAPs are involved in other cellular processes including cell division, morphogenesis, nuclear factor-kB (NF-kB) activation and mitogen-activated proteins (MAP) kinase signalling (Srinivasula and Ashwell, 2008). Substantial evidence indicates that cIAP1 and 2 form a multicomplex with tumor necrosis factor receptor associated factor 2 and 3 (TRAF2 and 3), resulting in the activation of NF-kB (Chu et al., 1997, Rothe et al., 1995, Tang et al., 2003). TRAF2 is an adaptor protein involved in signal transduction by

most members of the tumour necrosis factor receptor (TNFR) family (Wajant et al., 2003). The binding of cIAP1 to TRAF2 leads to ubiquitin-dependent degradation of TRAF2 as a feedback signal for NF-kB activation (Li et al., 2002).

Work in the ageing and age related diseases such as glaucoma suggest that RGCs undergo a prolonged process of degeneration prior to cell death, manifest as a reduction in the complexity of the dendritic tree and the elimination of terminal processes (Kisiswa et al., 2009, Watts et al., 2003, Whitmore et al., 2005, Williams et al., 2006). These observations are consistent with those in other neuronal systems where parts of the neuron degenerate at different rates raising the possibility that the early stages of degeneration, neuronal damage is associated with partial activation of programmed cell death (Whitmore et al., 2005).

It has been hypothesis that these chronic changes in neuronal morphology indicating a balance between the factors that initiate program cell death and those that inhibit the process (Kisiswa et al., 2009). In support of this theory there is evidence that caspase activation, which is a consistent trigger to apoptosis is countered by IAPs, whose expression and activation increases in the cells that are entering into the apoptosis process (Kisiswa et al., 2009).

4.2 Aims

To clarify the relationship between caspase activation and inhibition in the maturation process, the expression of cIAP1 protein was measured in healthy young adult and mature BN rat retina. This was done since there was a significant reduction in cIAP1 expression at mRNA levels in BN retinae as shown in previous work (see chapter 3 for details). The involvement of cIAP1 in maintenance of the cells in BN RGCL was also determined. The analysis was performed in the whole retina and in isolated RGCL preparation. The cIAP1-dependent regulation of TRAF2 was also exploited.

4.3 Experimental design

Retinae was dissected from eyes of 6 and 24-52 weeks animals for protein isolation as described in chapter 2, section 2.2.2. Protein was isolated and its concentration determined.

Protein samples (10µg) were resolved using a 12% SDS-PAGE electrophoresis followed by transfer onto a nitrocellulose membrane. Membranes were blocked for 1h in 5% dried milk in Tris buffered saline-Tween 20 (TBST). The blocked membranes were then incubated in either anti-cIAP1 or anti-actin at room temperature for 1h, anti-caspase 3, anti-caspase 9, anti-TRAF2, anti-Thy 1, anti-Chx 10 at 4°C overnight. Following washes in TBST, membranes were incubated in appropriate peroxidase-linked secondary antibodies (anti-goat or anti-rabbit depending on the source of primary antibody) for 1hour before substrate development using the ECL-plus Kit according to manufactures instruction. Laser scanning densitometry was performed and bands were quantified using Labworks programme.

For immunofluorescence analysis, eye-cups (anterior segment and lens removed; see section 2,2,2) were wax embedded (see details in chapter 2) and serially sectioned at 7 µm. They were then de-waxed, washed in PBS and blocked with 5% BSA in PBS containing 0.01% Triton x 100 for 1h at room temperature. The cIAP1 staining, dewaxed sections were subjected to antigen retrival (see section 2.7.5). Tissues were incubated overnight at 4°C with primary antibody in 1% blocking solutions and anti-TRAF2. After three washes, the sections were incubated with Alexa-Fluor-labeled secondary antibody for 1h at room temperature. All sections were counterstained with To-PRO 3 and mounted using Hydro-mount solution. Sections were imaged using an Axioplan Zeiss laser scanning confocal microscopy. Staining intensity was quantified utilising Adobe Photoshop and expressed in percentage of the staining intensity of the experimental sections after extracting the background staining intensity.

Subsequently, dewaxed sections were washed in PBS and subjected to TUNEL assay analysis as described 2.8.3. The samples were imaged using Leica bright field microscopy.

Following normality testing, group comparisons were made using independent student t-test or one-way ANOVA as appropriate followed by Fisher's Tukey's post hoc test.

4.4 Results

4.4.1 cIAP1 protein level in the whole BN retina

Investigation of cIAP1 protein levels in the whole retina revealed reduction of cIAP1 protein in mature BN retinae. Levels of cIAP1 protein in whole retinal lysate were statistically significantly ($p=0.040$) reduced in mature compared to younger retinae (Fig. 4.1A-B; $n=3$).

4.4.2 Enrichment of RGCL cells

Cells in RGCL were enriched employing retinal shaving technique described in chapter 2. The purity of the RGCL shaves was confirmed by immunoblotting for the RGC marker (Thy 1) and bipolar marker (Chx 10). Staining for Thy-1 was more intense and the Chx 10 was below the level of detection in the RGCL lysate compared to the non-GCL lysate (Fig.4.2A) confirming precise isolation of the cells in RGCL. Chx 10 staining was absent in the RGCL sample (Fig.4.2B) confirming that there was no bipolar cell contamination.

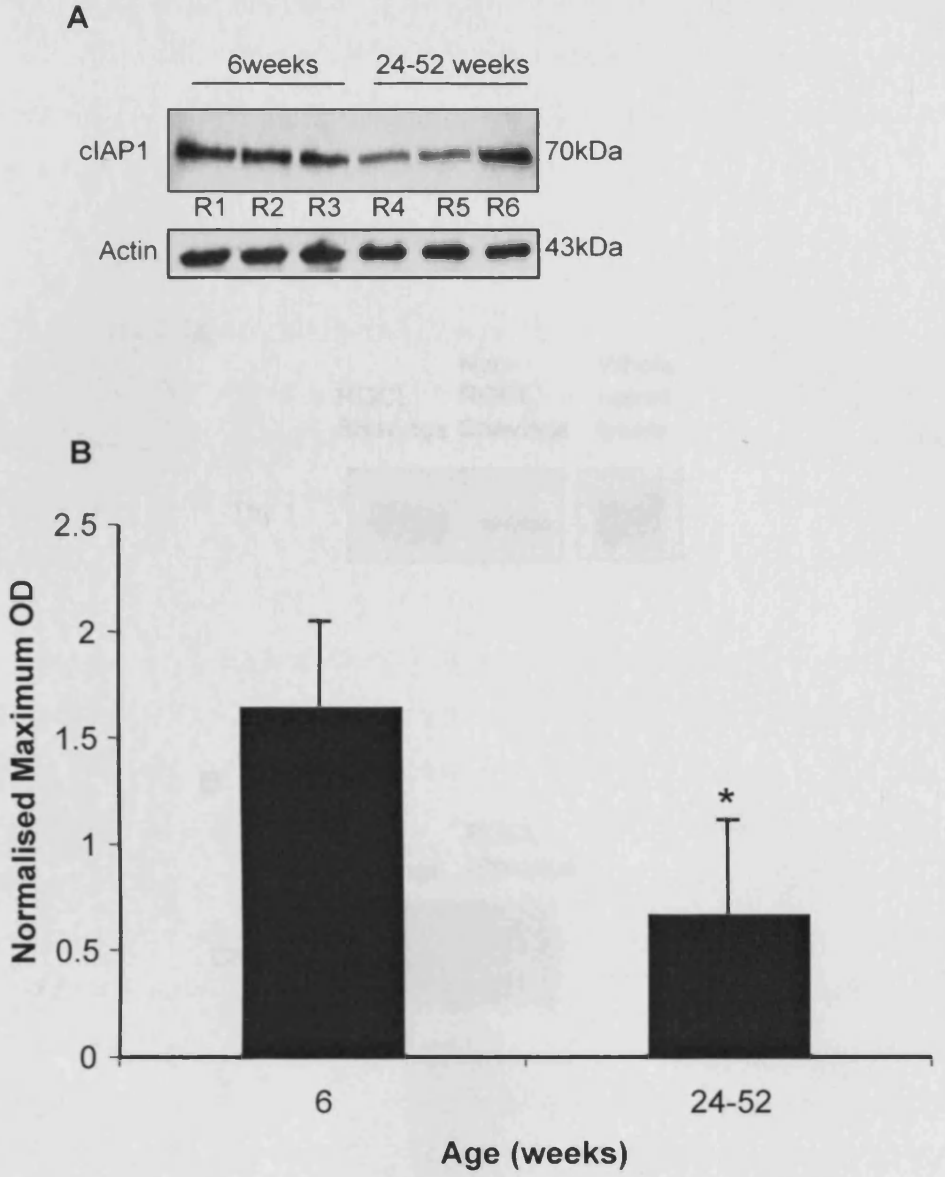

Figure 4.1. Reduced cIAP1 protein levels in the whole retina in 24-52 compared to 6 weeks animals. (A) shows the bands for individual animals (R1-3 at 6 weeks and R4-6 and 24-52 weeks). (B) shows the densitometry data for cIPA1 as a ratio value relative to actin levels (mean and standard errors, n-3 for each group (3 readings were taken for each animal; * indicates $p < 0.04$, statistical comparison between the two ages, independent student's test). Abbreviations: R1-6, rat 1-6.

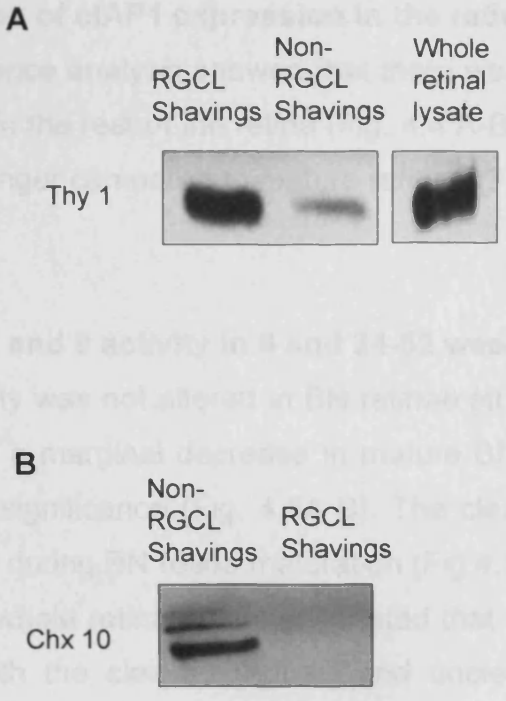

Figure 4.2. Enrichment of cells in the RGCL. The RGCL samples were obtained from retinal shavings and the purity was confirmed by staining for a RGC marker Thy1 (A) and Chx 10 (B), a bipolar marker (absent in RGCL).

4.4.3 Comparison of cIAP1 protein expression in RGCL and non-RGCL of BN rat retinae

Expression of cIAP1 protein in the non-RGCL remained constant (Fig. 4.3A-B; n=6) while cIAP1 protein amounts were statistically significantly ($p < 0.004$) decreased (Fig. 4.3C-D, n=6) in the mature compared to younger animals in the RGCL.

4.4.4 Localisation of cIAP1 expression in the retina

Immunofluoroscence analysis showed that there was staining of cIAP1 in the RGCL but none in the rest of the retina (Fig. 4.4 A-B). The staining was more visible in the younger compared to mature retinae (Fig. 4.4 A-B).

4.4.5 Caspase 3 and 9 activity in 6 and 24-52 weeks BN retinae

Caspase 9 activity was not altered in BN retinae studied. Inactive caspase 9 (50kDa) showed a marginal decrease in mature BN retinae but this did not reach statistical significance (Fig. 4.5A-B). The cleaved caspase 9 (37kDa) remained similar during BN retina maturation (Fig.4.5 A, C). Western blotting of caspase 3 in whole retinal lysate suggested that there was a trend for up-regulation of both the cleaved (active) and uncleaved (inactive) forms in mature compared to younger retina, but this did not reach statistical significance (Fig. 4.6A-B). Immunohistochemical analysis confirmed that there was a slight increase of cleaved caspase 3 expression in 24-52 weeks old RGCL (Fig. 4.6C).

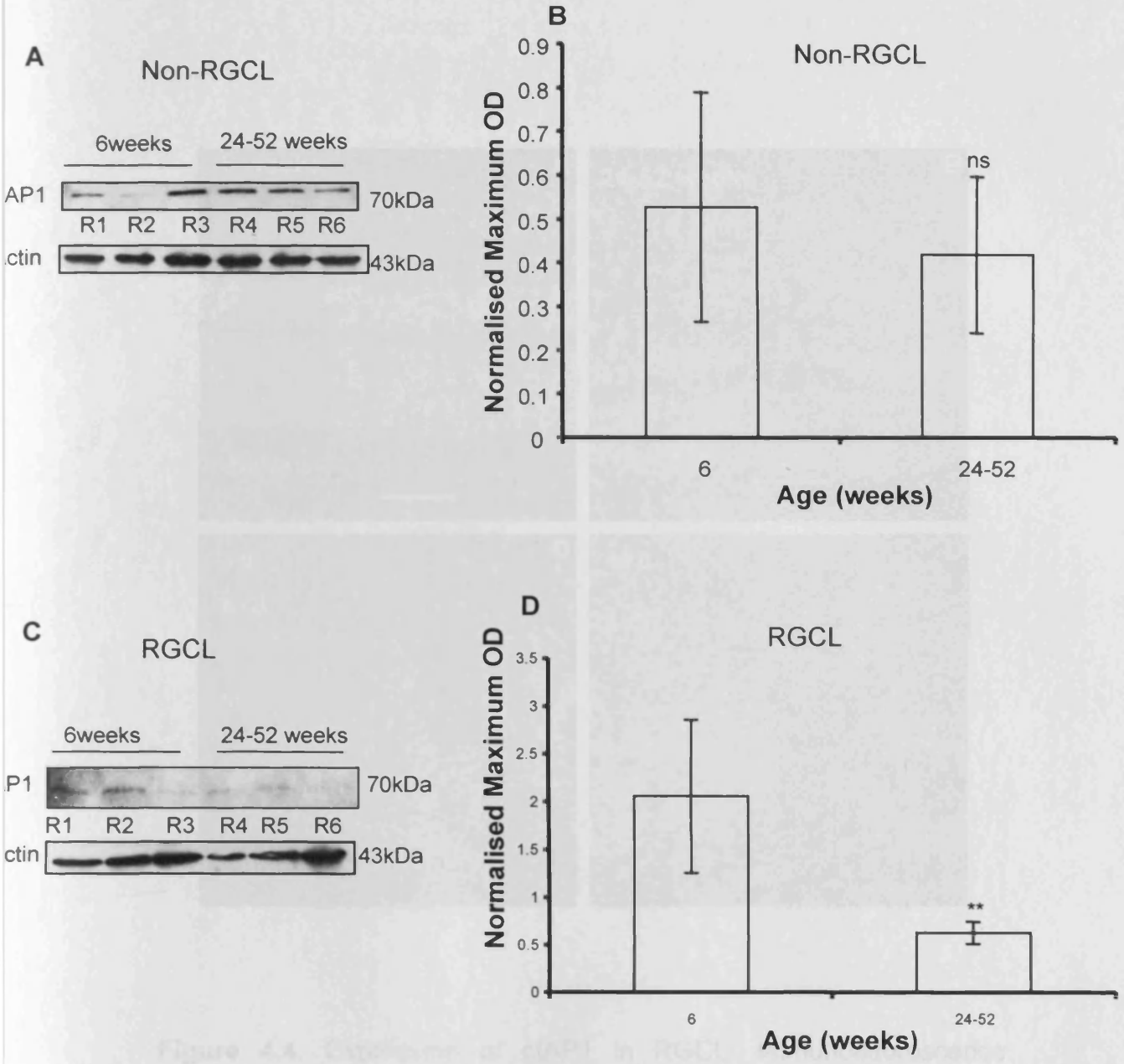

Figure 4.3. cIAP1 down-regulation is restricted for cells in the RGCL. No changes were observed in cIAP1 protein levels in non-RGCL (A-B) but there was a significant ($p < 0.02377$) reduction in RGCL (C-D) in 24-52 compared 6 weeks. Densitometry data reflect the expression level for cIAP1 as a ratio value relative to actin levels (mean and standard errors, n=6 for non-RGCL and n=9 for RGCL (3 readings were carried out for each animal; ** indicates $p < 0.02$ statistical comparison between the two ages, independent student's test). Abbreviations: R1-6, rat 1-6; RGCL, retinal ganglion cell layer; ns, non significant.

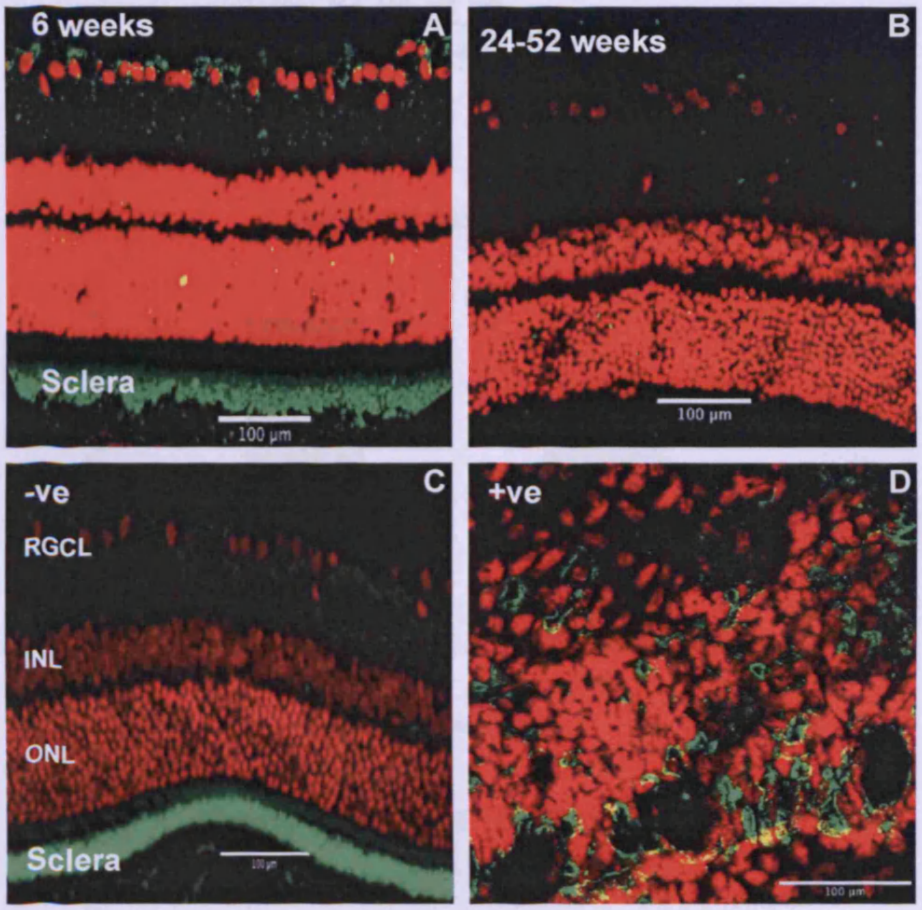

Figure 4.4. Expression of cIAP1 in RGCL. Immunofluoroscence analysis showed staining of cIAP1 in RGCL of 6 weeks retinae (A) and almost none in 24-52 weeks retinae (B). Negative (C, secondary antibody only) and positive (D, cIAP1 expression in p0 CD1 mouse brain controls were included in the study, Representative sections are shown (3 sections crossing the optic nerve per animal per age; n=3). Abbreviations; ONL, outer nuclear layer; INL, inner nuclear layer; RGCL, retinal ganglion cell layer. Scale bar: 100µm

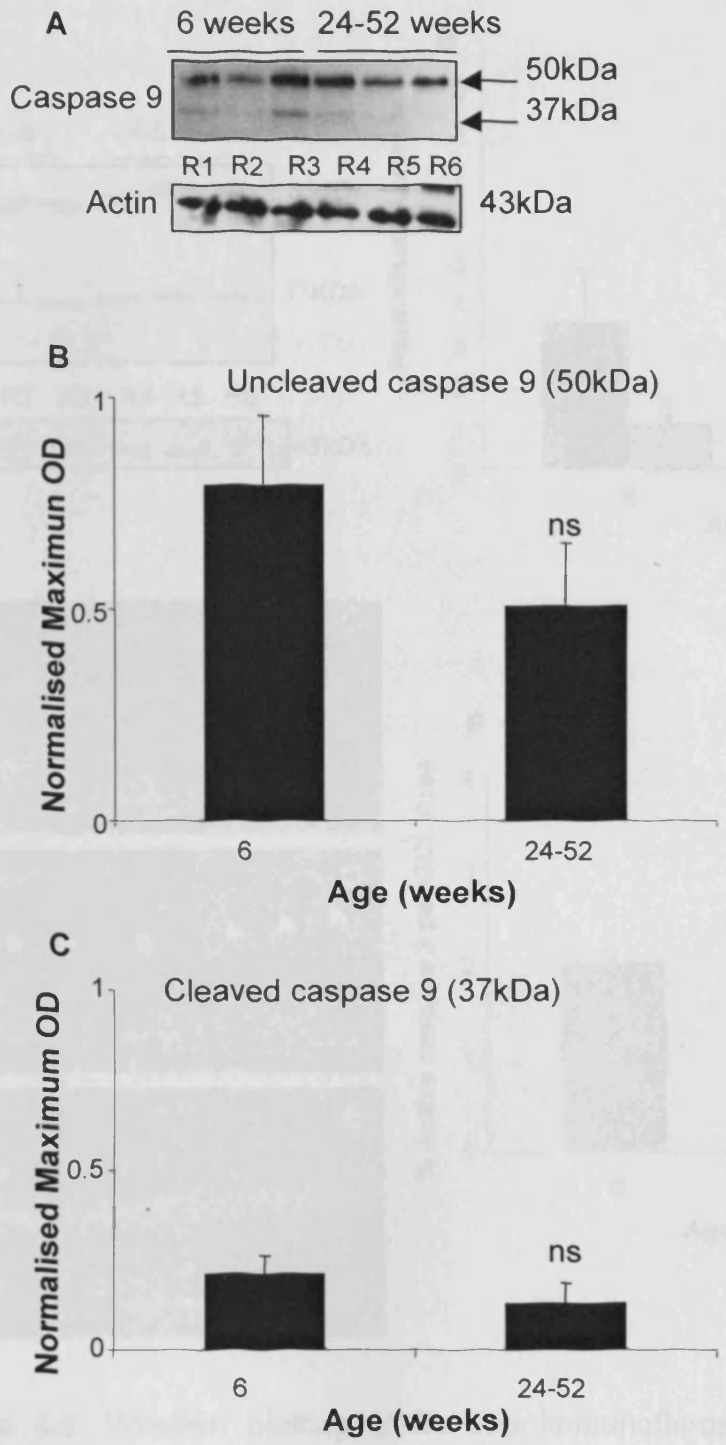

Figure 4.5. Western blotting reveal no changes in expression of in caspase 9 activity during ageing of BN retina. (A) an example of western blots. Both uncleaved (B) and cleaved (C) caspase 9 expression was not altered. The densitometry data reflect the expression level for cleaved and uncleaved forms of caspase 9 as a ratio value relative to actin levels (mean and standard errors, n=3 for each group: 3 readings were taken for each animal). Abbreviations; R1-6, rat 1-6; ns, non significant.

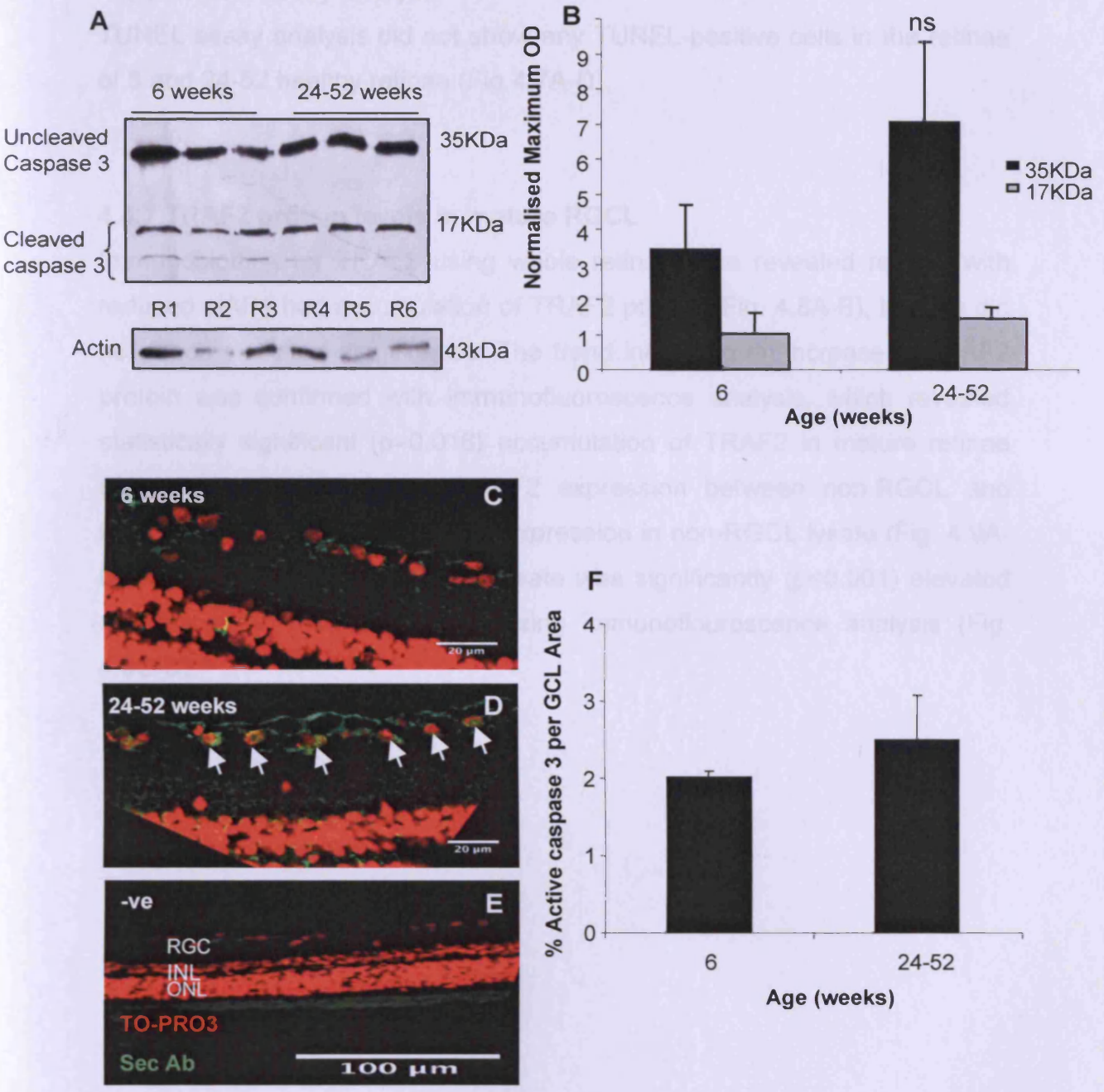

Figure 4.6. Western blotting (A-B) and immunofluroscence analysis (C-F) reveal no changes in expression of in caspase 3 activity during ageing of BN retina. The densitometry data reflect the expression level for cleaved and uncleaved forms of caspase 3 as a ratio value relative to actin levels (mean and standard errors, n=3 for each group: 3 readings were taken for each animal). Representative sections are shown (3 sections per animal per age (total 18 sections)). Images were taken with 20x objective. Arrows indicate nucleai that are positive for active caspase 3. Abbreviations; R1-6, rat 1-6; ONL, outer nuclear layer; INL, inner nuclear layer; RGCL, retinal ganglion cell layer; ns, non significant.

4.4.6 TUNEL assay analysis

TUNEL assay analysis did not show any TUNEL-positive cells in the retinae of 6 and 24-52 healthy retinae (Fig 4.7A-D).

4.4.7 TRAF2 protein levels in mature RGCL

Immunoblotting for TRAF2 using whole retina lysate revealed retinae with reduced cIAP1 had accumulation of TRAF2 protein (Fig. 4.8A-B), but this did not reach statistical significance. The trend indicating an increase in TRAF2 protein was confirmed with immunofluoroscence analysis, which revealed statistically significant ($p=0.018$) accumulation of TRAF2 in mature retinae (Fig. 4.8C). Comparison in TRAF2 expression between non-RGCL and RGCL showed consistent TRAF2 expression in non-RGCL lysate (Fig. 4.9A-B). TRAF2 expression in RGCL lysate was significantly ($p<0.001$) elevated confirming the results obtained using immunoflouroscence analysis (Fig. 4.9C-D).

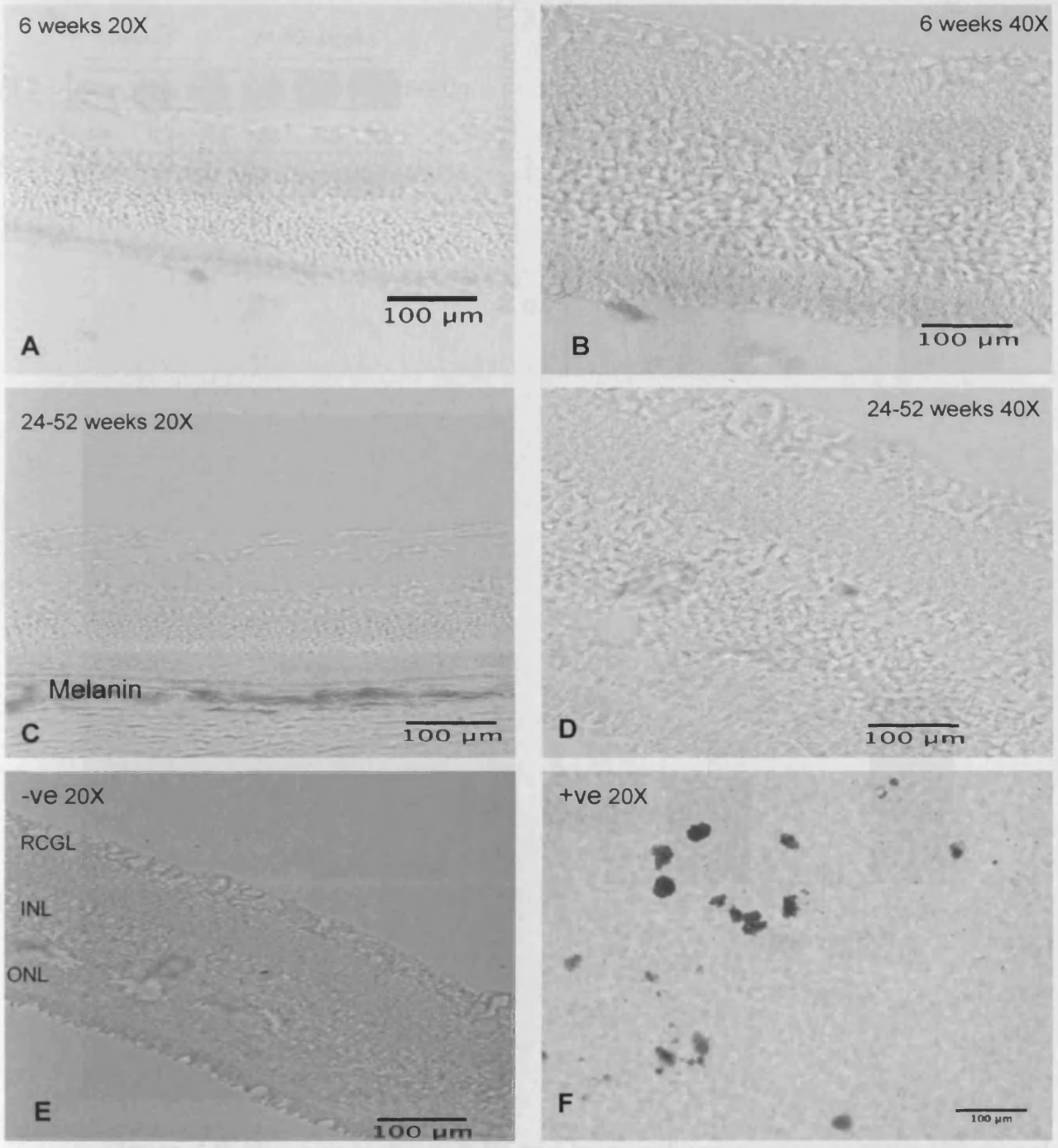

Figure 4.7. TUNEL assay analysis of 6 and 24-52 weeks BN rat retinae. There were no TUNEL positive cells in 6 (A-B) and 24-52 weeks (C-D) retinae. Negative (E) and positive (F: whole amount retina treated with staurosporine overnight) were included in the experiment. Representative sections are shown (3 sections crossing the optic nerve per animal per age; n=3). Abbreviations; ONL, outer nuclear layer; INL, inner nuclear layer; RGCL, retinal ganglion cell layer.

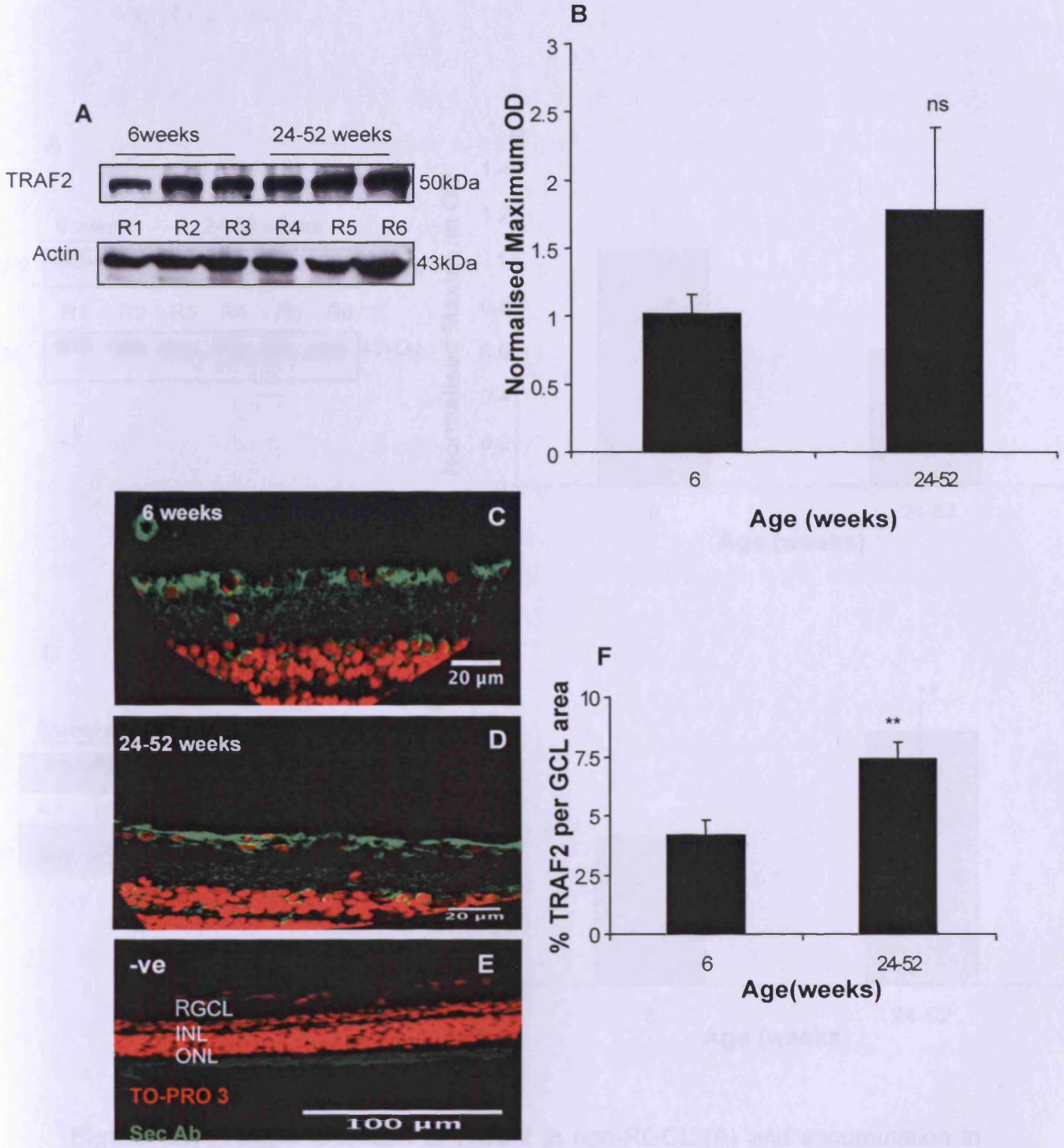

Figure 4.8. Western blotting (A-B) and immunofluoroscence analysis (C) reveal accumulation of TRAF2 in 24-52 compared to 6 weeks retinae. Immunofluoroscence data revealed a statistically significant (p=0.018) accumulation of TRAF2 in the RGCL. The densitometry data reflect the expression level for TRAF2 as a ratio value relative to actin levels (mean and standard errors, n=3 for each group: 3 readings were taken for each animal). Representative sections are shown (3 sections per animal per age (total 18 sections)). Abbreviations; R1-6, rat 1-6; ONL, outer nuclear layer; INL, inner nuclear layer; RGCL, retinal ganglion cell layer; ns, non significant

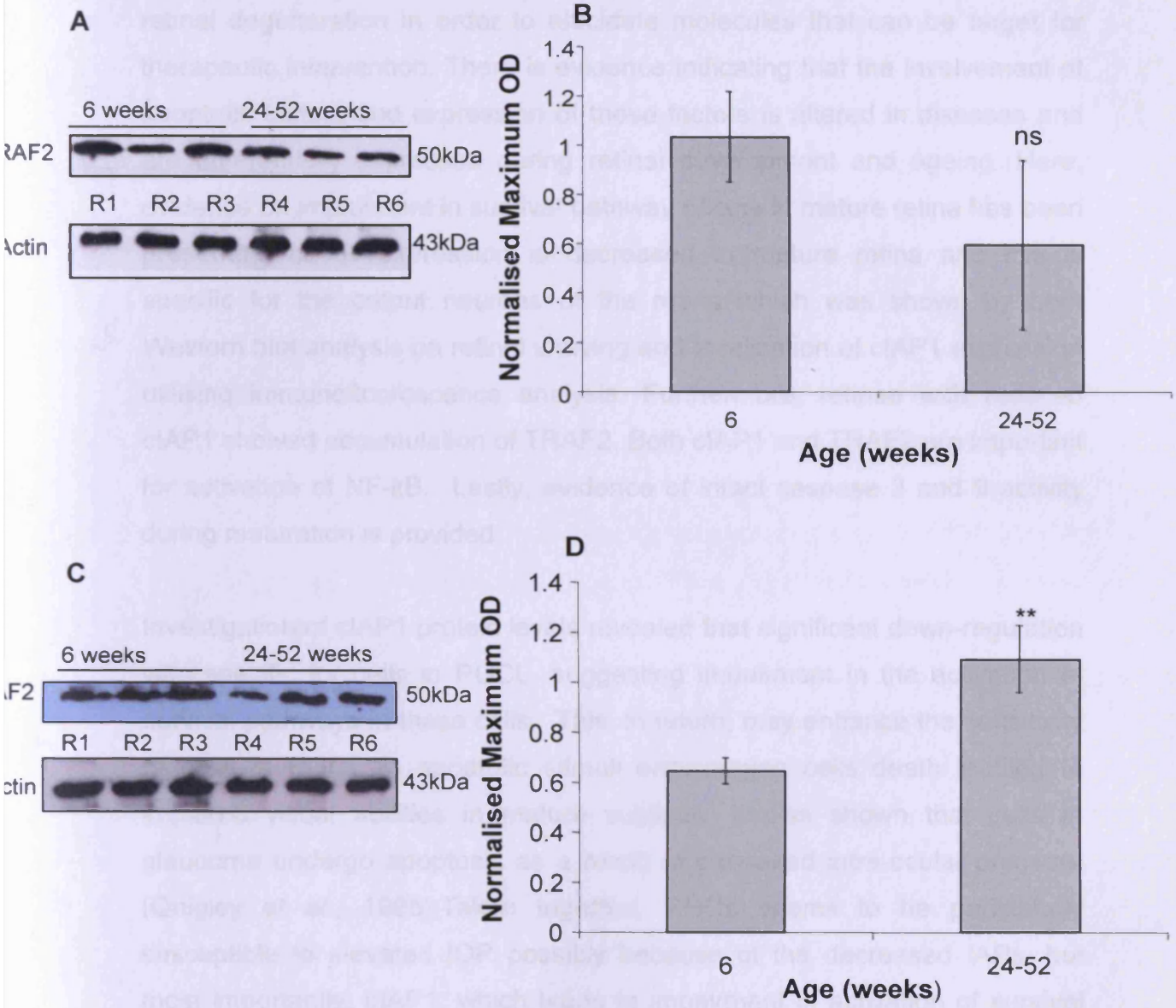

Figure 4.9. A slight reduction of TRAF2 in non-RGCL (A) and accumulation in RGCL (B) in mature compared to younger retina. The densitometry data reflect the expression level for TRAF2 as a ratio value relative to actin levels (mean and standard errors, n=6 per age; ** indicates p <0.02 statistical comparison between the two ages, independent student's test). Abbreviations: R1-6, rat 1-6, RGCL, retinal ganglion cell layer; ns, non significant.

4.5 Discussion

The present study has focused on understanding the molecular mechanisms underlying cell death in ageing and neurodegenerative disease including retinal degeneration in order to elucidate molecules that can be target for therapeutic intervention. There is evidence indicating that the involvement of apoptotic factors and expression of these factors is altered in diseases and are differentially expressed during retinal development and ageing. Here, evidence on impairment in survival pathway occurs in mature retina has been presented. cIAP1 expression is decreased in mature retina and this is specific for the output neurons of the retina which was shown by both Western blot analysis on retinal shaving and localisation of cIAP1 expression utilising immunofluoroscence analysis. Furthermore, retinae with reduced cIAP1 showed accumulation of TRAF2. Both cIAP1 and TRAF2 are important for activation of NF-kB. Lastly, evidence of intact caspase 3 and 9 activity during maturation is provided.

Investigation of cIAP1 protein levels revealed that significant down-regulation was specific for cells in RGCL, suggesting impairment in the activation of survival pathways in these cells. This, in return, may enhance the sensitivity of cells in RGCL to apoptotic stimuli encouraging cells death leading to impaired visual abilities in mature subjects. It was shown that cells in glaucoma undergo apoptosis as a result of increased intra-ocular pressure (Quigley et al., 1995).Taken together, RGCs seems to be particularly susceptible to elevated IOP possibly because of the decreased IAPs, but most importantly, cIAP1, which leads to impairment in activation of survival pathways.

In this study, the involvement of cIAP1 in both the intrinsic and extrinsic apoptotic pathway was investigated by evaluating capsase 3 and 9 (representative to intrinsic pathway). Evidence on that the expression of caspase 3 and 9 protein, both the active and inactive form, remains constant during ageing of BN rat retina has been provided. The data are not consistent with reports showing that caspase 3 expression is significantly reduced during ageing of the mouse retina between p6 and p60 (McKernan et al.,

2006). This could be explained by that fact that the model used for the study was mouse while in this study rat retina was utilised for the investigation, suggesting caspase expression pattern varies between different species. This raises an interesting question to whether IAPs and caspase expression in the central and peripheral nervous system vary during human lifespan. However, a more likely explanation is that the difference is due to the different ages examined in the two studies; our study examined animals at 6 weeks at the earliest stage and did not include animals as young as P6 where we would expect to see changes in caspase expression arising during development (Silver and Hughes, 1973, Silver and Robb, 1979).

There was no alteration in caspase 3 and 9 activity as a consequence of reduced cIAP1. Thus, there was no alteration in activation of caspase 3 and 9. Early reports on cIAP1 and 2, which are homologous, suggest that these proteins protect cells against apoptotic signals (Orth and Dixit, 1997, Roy et al., 1997) through direct binding to caspases via their BIR domains. Protein structure analysis of caspase 3, 7 and 9 revealed that these proteins have a binding site for cIAP1 and 2 (Roy et al., 1997, Santoro et al., 2007). However, recent work demonstrates that although cIAP1 is capable of binding caspases, it does not inhibit their activity (Eckelman and Salvesen, 2006), suggesting that the cIAP1 BIR domains that interact with caspase have evolutionarily lost their protease inhibition sequence that is found in other IAPs such as XIAP. Consistent with this, data obtained in this study support the notion that cIAPs inhibits apoptosis by enhancing activation of survival pathways. There are substantial reports emphasising the importance of cIAP1 in NF-kB activation (Mahoney et al., 2008, Varfolomeev et al., 2007, Varfolomeev and Vucic, 2008, Dupoux et al., 2009, Shu et al., 1996, Zarnegar et al., 2008). For example, it was shown that cIAP1 regulates NF-kB activation in endothelial cells, which, in turn, regulates vascular homeostatis in zebrafish (Santoro et al., 2007). Zarnegar and collegues demonstrated that activation of non-canonical NF-kB requires assembly of a regulatory complex, in which cIAP1 is a member of the complex (Zarnegar et al., 2008).

Upon activation of TNFR1 and 2, TRAF 2 builds a multicomplex with cIAP1, 2 and TRAF3 leading to activation of NF-kB and JNK pathways (Eckelman and Salvesen, 2006, Rothe et al., 1995). Furthermore, TRAF2 interact with TRADD leading to NF-kB activation (Hsu et al., 1996, Hsu et al., 1995, Shu et al., 1996), suggesting that TRAF2 is involved in both TNF-R1 and TNF-R2-mediated NF-kB activation. In this study there was an increase in TRAF2 protein levels in RGCL where cIAP1 was significantly reduced. This increase might be caused by impairment in cIAP1-dependent ubiquitination of TRAF2 upon survival signal activation. Thus, the reduction of cIAP1 might lead to inhibition of survival pathways depriving cells with death protection mechanism and enhancing apoptotic activity.

TRAF2 has been linked to other neurodegenerative disease such as Alzeimer's diseases (AD). Interestingly, TRAF2 is increased in neurons of AD patients and is associated with neuritic plaques and neurofibrary tangles, suggesting either a continual recruitment of TRAF2 due to persistent in NF-kB activation pathway or lack of proteosomal degradation of TRAF2 leading to accumulation of TRAF2 in these neurons (Culpan et al., 2009). It would be interesting to evaluated cIAP1 expression in AD brain and determine whether there is alteration in cIAP1 expression in these neurons and if the alterations are in line with the data obtained in this study. Interestingly, TRAF2 has been suggested to be involved in inhibition of seizures in rodent (Balosso et al., 2005) but the molecular mechanisms underlying this inhibition are yet to be elucidated.

Although there was no alteration in caspase activity, it is reasonable to postulate that caspase-independent apoptosis may occur in RGCs. Several groups have shown that caspase-independent apoptosis occurs in adult neurons (Okuno et al., 1998, Selznick et al., 2000, Zhang et al., 2002). Bcl-2 family proteins are known to regulated apoptosis by inhibiting capsase activation (Merry and Korsmeyer, 1997), there is evidence indicating that this family of proteins is capable of preventing cell death via a caspase-independent mechanism (Okuno et al., 1998). Moreover, other forms of cell death have been suggested to occur in neurodegenerative disease.

Autophagy is one of these cell death modalities that has been largely studied in neurodegeneration. Autophagy has been shown to occur in AD (Moreira et al., 2007, Nixon, 2007), PD (Pan et al., 2008, Xilouri et al., 2009) and HD (Kegel et al., 2000, Ravikumar et al., 2004, Sarkar et al., 2007). Furthermore, autohpagic bodies have been reported to increase with age in mice (White et al., 2009). Taken these findings together with data shown here, this suggests that caspases may play a limited role in neuronal cell death in ageing rat retina.

The negative results obtained in this study using TUNEL assay analysis emphasise that other forms of cell death may play an important role during retinal maturation and ageing. It is important to note that even in human glaucoma, very few TUNEL-positive cells are detected (Kerrigan et al., 1997). Another explanation to these negative results could be that the cells were already dead or at a very early stage of cell death that it was impossible to detected using TUNEL assay. However, according to the manufactures' instruction, these cells should be detectable with TUNEL kit.

Whilst this study demonstrates reduction of cIAP1 in the RGCL of mature BN retina, it remains still unclear at present to what extend cIAP1 contribute to death of the cells in RGCL. The precise point when the cells in RGCL start to be eliminated and whether the death correlates with reduction of cIAP1 are still to be elucidated. Determining the magnitude of cIAP1 contribution to RGC cell death is of high interest. As already demonstrated by several groups, cIAP1 seems to be a common player in facilitating cell death and activation of survival pathways (Eckelman and Salvesen, 2006, Hsu et al., 1996, Hsu et al., 1995, Rothe et al., 1995, Shu et al., 1996). Furthermore, there is evidence that exogenous IAPs may protect neurons during glaucoma. Gene therapy delivery of XIAP/BIRC4 to the retinae of chronical ocular hypertensive (COH) model of rat glaucoma significantly promoted optic nerve axon survival (Kugler et al., 1999, Kugler et al., 2000, McKinnon et al., 2002).

The limitation of this study is that it has not clarified whether the cIAP1 reduction occurs as early as 24 weeks. The age range in the mature sample is too big to draw any definitive conclusions. The reason that the age range was used is because the company (Charles River, UK) where the animals were purchased from could not provide the specific age of the animals

At present, what determines the balance between cell death and activation is still unknown. Further investigation into the subject will highlight the molecules that may be targeted for therapeutic intervention in order to arrest RGC cell death. Thus, it remains a challenge to determine the specific contribution of cIAP1 to cell death of ageing and diseased RGCs.

Chapter 5

Age-related dendrite pruning in Adult BN rat retina

5.1 Introduction

Age-related functional changes in mammalian CNS vary between different regions of the brain, as reflected by the decline in motor, sensory and cognitive functions associated with senescence (Hofer et al., 2003, Mattson and Magnus, 2006). These changes include modification and/or loss of neuronal structure, function, cell loss of a specific neuronal population and/or loss of cells that support neurons such as glial cells (Adams, 1987, Ball, 1977, Coleman and Flood, 1987, Morgan et al., 1999b, Morrison and Hof, 1997, Nakamura et al., 1985, Poe et al., 2001, Wong et al., 1998).

Neuronal loss during normal ageing is a universal phenomenal, which is associated with cognitive function decline (McArdle et al., 2002, Finch, 2009). Recently, it was suggested that cognitive function decline start in early adulthood (Coleman et al., 1990, Finch, 2009, Li et al., 2001, McArdle et al., 2002). There have been reports indicating that neuronal loss start at middle-age, at 25 years in humans (Salthouse, 2009) and at 3 months for rodents (Severson and Finch, 1980). Severson and Finch showed a well defined decline in dopamine D2, Serotonin 2A and other binding sites in striatum and cortex in middle-aged rodents (Severson and Finch, 1980). Although there is substantial evidence of neuronal loss at early adulthood in different regions of the brain, it is still unclear whether this is the course of decline of motor, sensory and cognitive function associated with senescence.

Vision is one of the first functions that are affected by age (Dandona and Dandona, 2006). Although there are reports indicating that there is a neuronal loss in the retina with age (Neufeld and Gachie, 2003, Spear, 1993), it has also been suggested that the loss is subtle (Harman et al., 2000, Mann, 1996). Work carried out on human wholemounted or sectioned retina demonstrated a decrease in neuronal density with age in the retina (Gao and Hollyfield 1992). Similarly, reduction in cell density in retinal ganglion cell layer (RGCL) in rat (Katz and Robison, 1986), quokka wallaby and the horse has been demonstrated (Harman et al., 2000, Harman et al., 2003, Harman et al., 1999). In rats the reduction was up to 60% in RGCL, 27-30% in INL and 38-50% in ONL. Although there have been many reports

suggesting that cell loss in the retina occurs in aged rodents and humans, very little investigation has been carried out to determine the time of onset of cell loss. Thus, it is important to elucidate when the decline begins because this may indicate to which period in adulthood is likely to be informative for learning about the causes of, not only age-related visual impairment, but also age-related motor and cognitive function impairment.

5.2 Aims

The aim of this study was to investigate whether there is any alteration in retinal cell density during retina maturation of BN rat. The BN rat is a valuable model to study normal ageing since it has a low incidence of age-related pathologies (Sprott and Austad, 1995). The second goal of this study was to determine when dendrite pruning starts and the extent in which dendrite pruning occurs in adult rat retina.

5.3 Experimental design

Eyes from 6 and 24-52 weeks animals were removed immediately after sacrificing the animal. The anterior segment and vitreous were removed and retina carefully dissected as described in chapter 2, section 2.2.3. Once the retina was out of the eye-cup, four cuts were made in order to open up the retina. Dissection was carried out quickly and under cold conditions. The retina was then transferred to a nitrocellulose membrane with RGC side facing up and then inserted in a culture dish containing culture medium (see section 2.9.2)

The retina was incubated at 37°C under humidified 5% CO_2 for 20 minutes in order to allow the adjustment of the retina to dissection stress. Following diolistic labelling using BioRad gene gun, the retina was incubated for maximum 30 minutes at 37°C in the humidified 5% CO_2 incubator in order to allow the DiI dye to spread. Before incubation, the retina was visualised with Ziess confocal microscope to evaluated transfection success. Following 30 minutes incubation, the retina was fixed in 4% PFA overnight at 4°C, washed

and then transfared to a glass slide, again with the RGC side facing up and mounted using ProLong Gold antifade reagent. Imaging was carried out using Zeiss confocal microscope and images stack of the retina were obtained for cells of interest.

Following imaging, the retina was carefully removed from the slide washed in PBS and counter stained for Hoeschst 3342 for 20 minutes. Subsequently, three washes in PBS were carried out and the retina was mounted once again on glass slide with RGC side facing up and mounted with ProLong Gold antifade reagent. Imaging was carried out utilising Leica fluoroscence microscope. Cells were counted using Cell Counter plugin for ImageJ (see Chapter 2, section 2.9.8).

For determining the cell density in the INL and ONL, the anterior segment was removed and the eye-cup was fixed overnight in 4% PFA. Following standard paraffin embedding of the eye-cups, 7 µm sections were obtained. Following dewax, the sections were stained for Hoeschst 3342 for 20 minutes. The sections were washed and mounted on glass slide and mounted with ProLong Gold antifade reagent. Leica fluoroscence microscope was used to obtain images. Nuclei were counted using a Cell Counter plugin for ImageJ.

Data in this chapter are expressed as mean and standard error. Normality test was carried out for all data before performing any statistical test. Statistical analysis was done using SPSS program. For comparison between two groups, independent student test was utilised. Comparison among multiple groups was performed using one-way ANOVA followed by Fisher's Tukey's post hoc test. Differences were considered significant for $p<0.05$.

5.4 Results

5.4.1 Decreased RGC density in 24-52 week old retinae

Systematic imaging of RGCs in the whole retinal mount (Fig 1A-C) revealed that there was a significant decrease in cell number (n = 4; per studied group; p>0.001; Fig 5.2A) and density (p>0.001) in the whole retina (Fig 5.3A). Percentage-wise, RGCL cell loss was 16% in the whole retina (Fig 5.2A). When the different areas of the retina were investigated, there was a significant reduction in the central (1mm from the OD, p>0.001, Fig 5.2B and 5.3B). This reduction was up to 24%. The density of the peripheral (2mm and 3mm from the OD) retina remained similar during retinal maturation (Fig 5.2B and 5.3B).

5.4.2 Decreased cell density in INL and ONL 24-52 week old retinae

Evaluation of cell number and density revealed that there was a statistically significant decreased cell number in the INL and ONL cells (n = 4; p>0.001, and p>0.001, respectively) counted from the retinal slices crossing the optic nerve (Fig 5.4A-C). These corresponded to 25% decrease in INL and 20% decrease in ONL (Fig 5.4A-C).

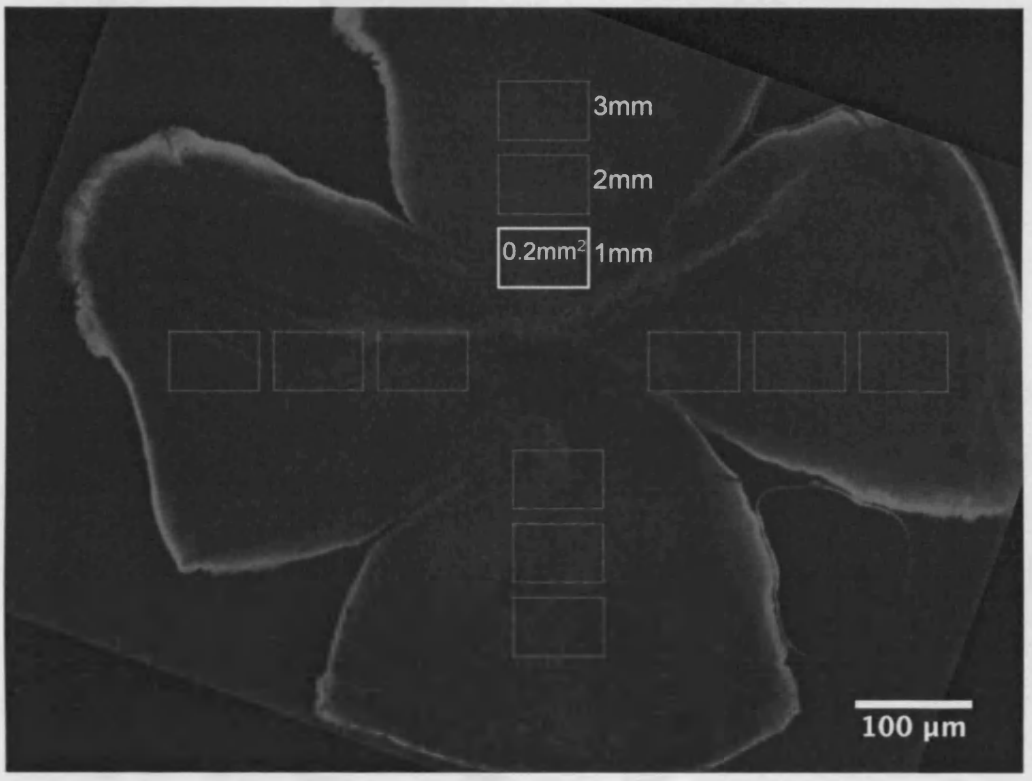

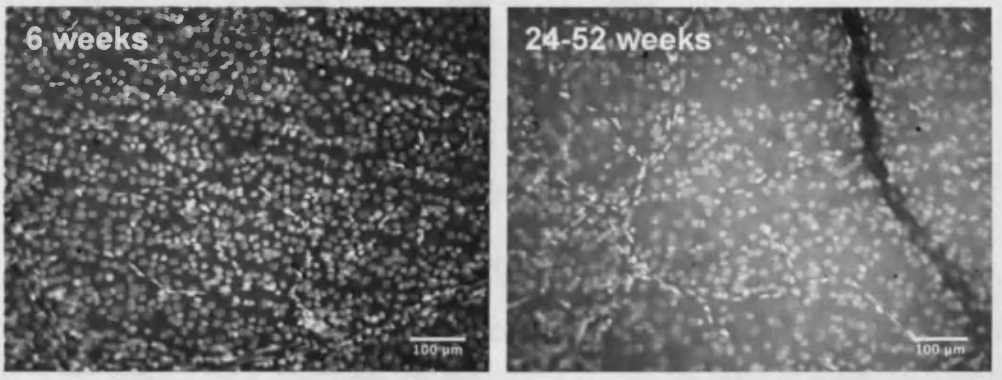

Figure 5.1. Hoeschst 3342 stained retinal ganglion cells. (A) Schematic picture of the imaging areas. (B) RCGs in 6 weeks (C) RGCs in 24-52 weeks. The scale bar is the same for all figures and represents 100µm

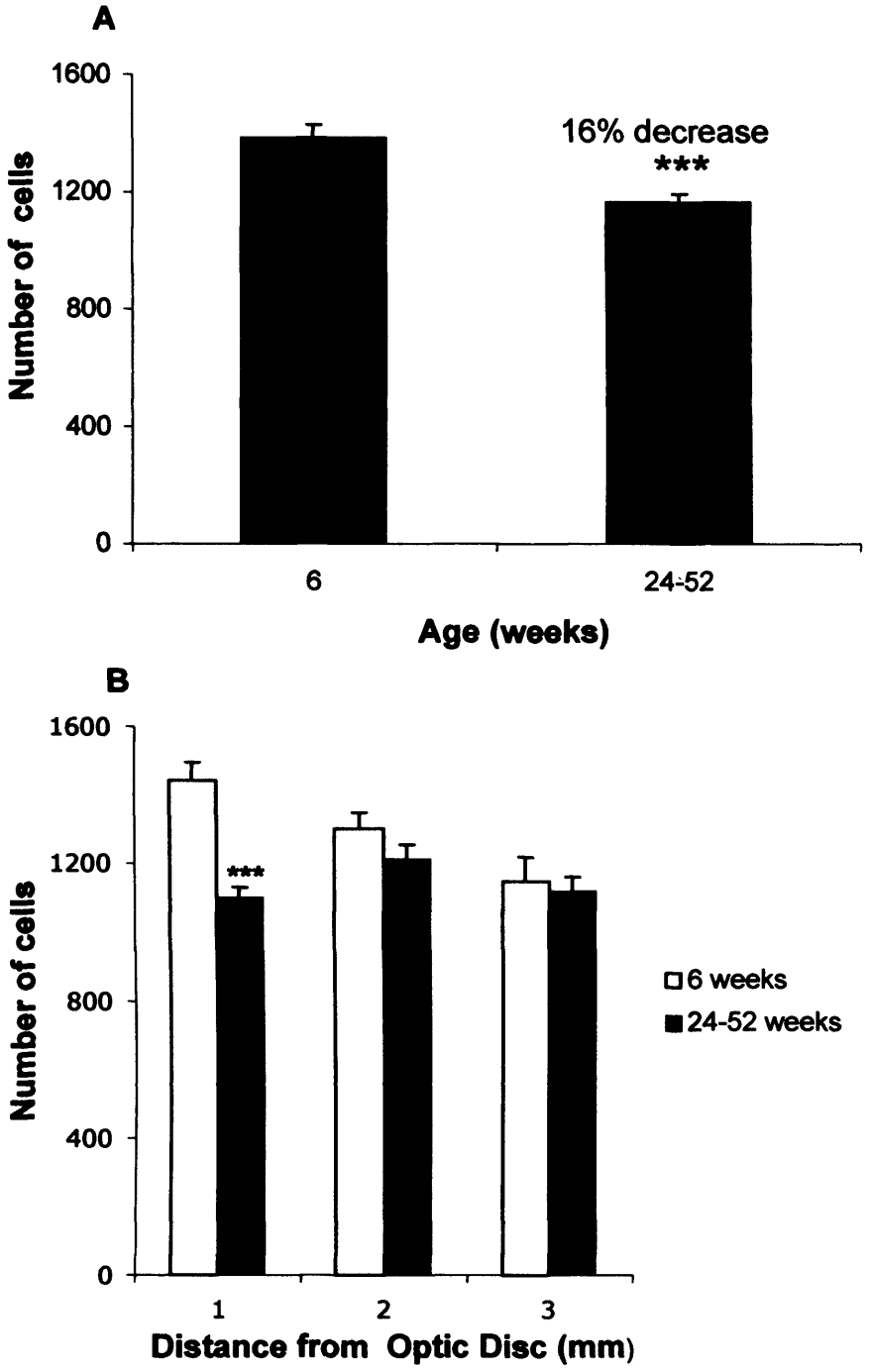

Figure 5.2. Decreased RGC number in the central but not peripheral BN retina during ageing. (A) The total RGC number in the whole retina was statistical significantly reduced. (B) RGC cell in three different areas of the retina in the two studied stages. There was a statistical significant reduction of RGC number in the central area (1mm from the Optic disc) of the retina of 24-52 compared to 6 week old retina. Mean and standard errors are shown on data from 4 animals per age (total 8 retinae per age) to produce the results (*** indicates $p < 0.001$ statistical comparison between the two ages, independent student's test).

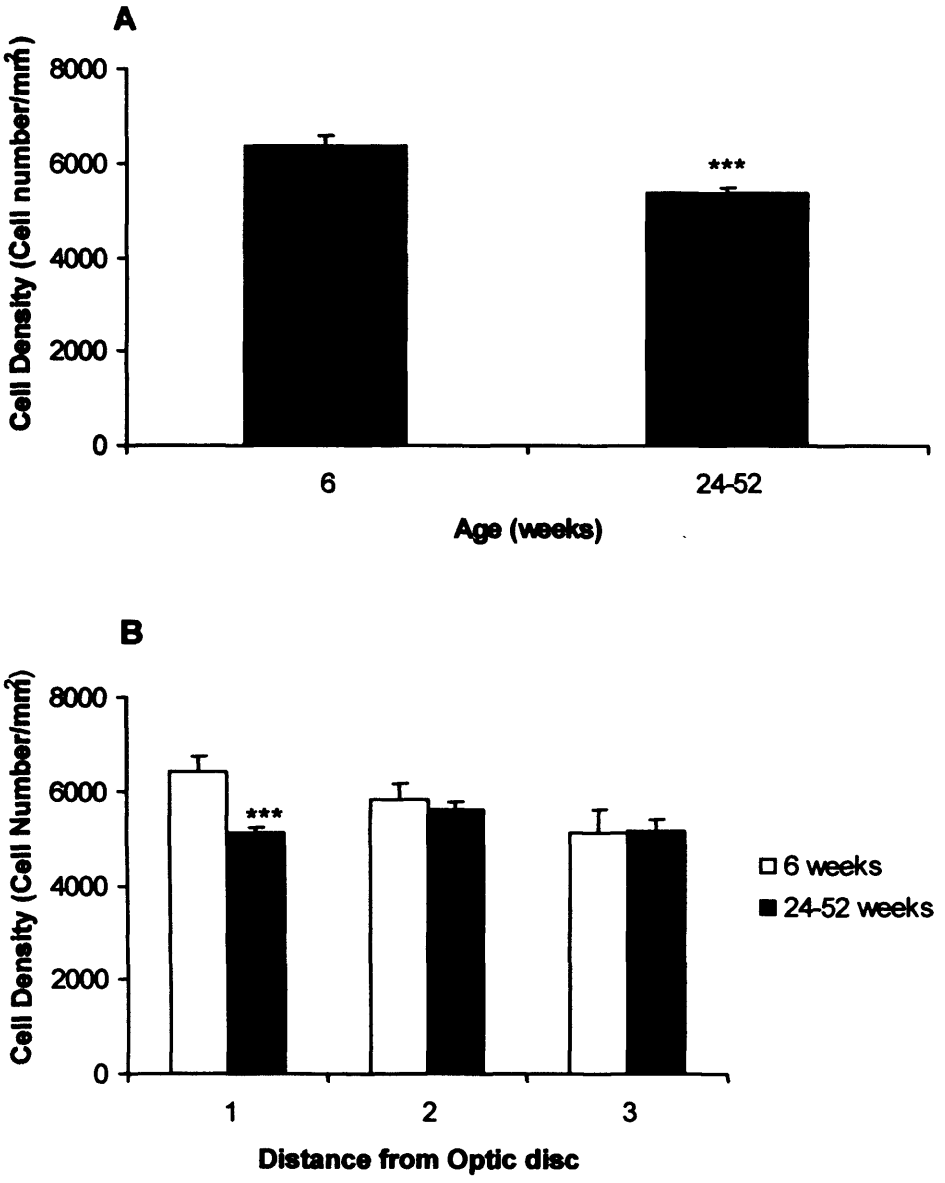

Figure 5.3. Decreased RGC density in the central but not peripheral BN retina during ageing. (A) RGC cell in three different areas of the retina in the two studied stages. There was a statistical significant reduction of RGC density in the central area (1mm from the Optic disc) of the retina of 24-52 compared to 6 week old retina. (B) The total RGC density in the whole retina was statistical significantly reduced. Mean and standard errors are shown on data from 4 animals per age (total 8 retinae per age) to produce the results (*** indicates $p < 0.001$ statistical comparison between the two ages, independent student's test).

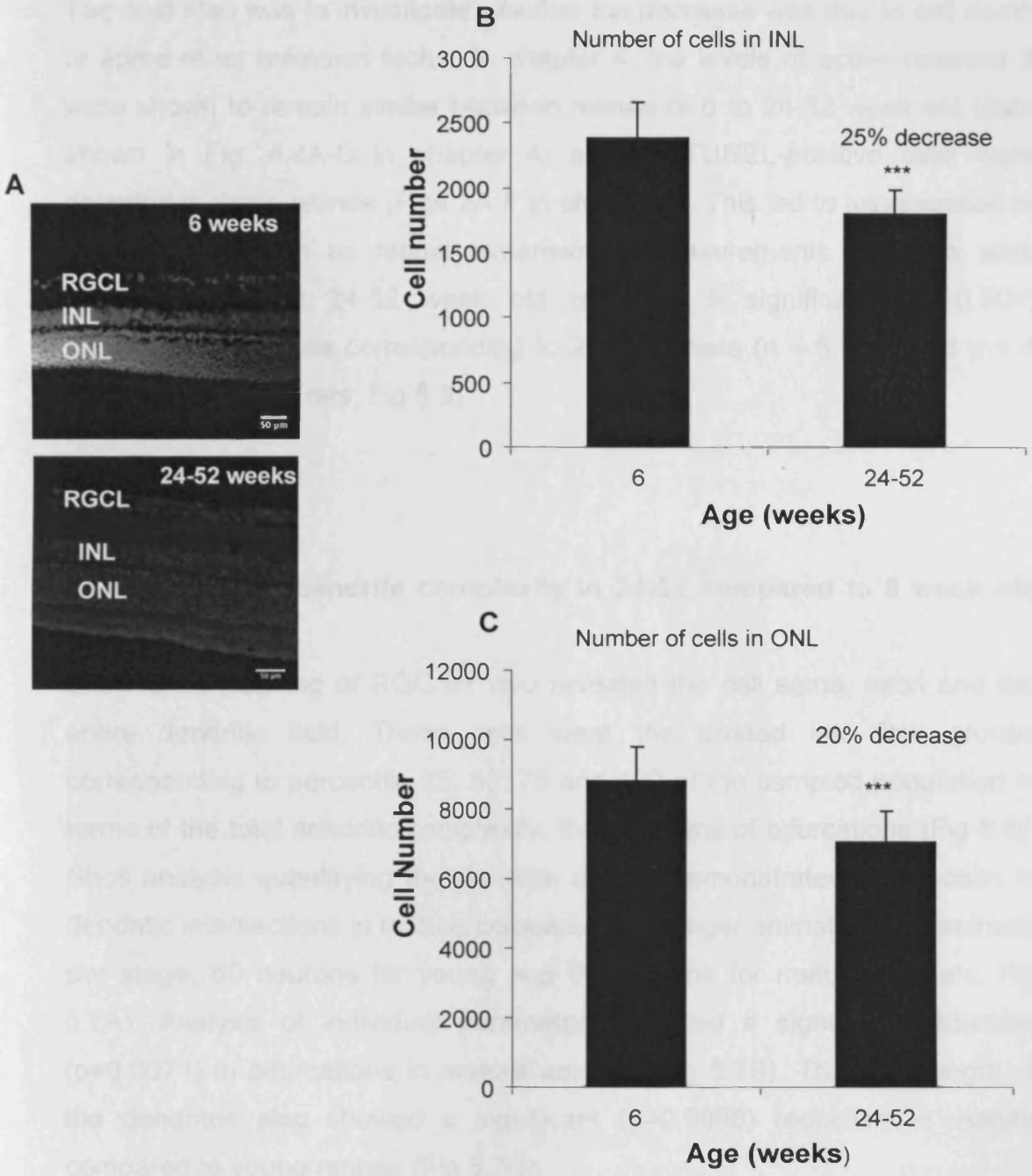

Figure 5.4. Reduced cell number of the cell in the inner and outer nuclear layer. Retinal sections stained for Hoeschst 3342 (A) . The INL (B) and ONL (C) cell number was statistical significant decreased during ageing. Mean and standard errors are shown on data from 5 sections per retina (n=6 eyes per age; total 30 sections per age) to produce the results (*** indicates $p < 0.001$ statistical comparison between the two ages, independent student's test). Abbreviations: INL, inner nuclear layer; ONL outer nuclear layer. Scale bar: 50µm

5.4.3 Retinal expansion during maturation

The next step was to investigate whether the decrease was due to cell death or some other unknown factor. In chapter 4, the levels of active caspase 3 were shown to remain similar between retinae of 6 to 24-52 week old (data shown in Fig. 4.4A-C in chapter 4) and no TUNEL-positive cells were detected in these retinae (Fig4.7A-F in chapter 4). This led to investigation of other factors such as retinal expansion. Measurements of retina area demonstrated that 24-52 week old rats had a significantly ($p>0.001$) increased retina area corresponding to 23% increase ($n = 5$ for 6 and $n = 4$ for 24-52 week old rats; Fig 5.5).

5.4.4 Decreased dendrite complexity in 24-52 compared to 6 week old retinae

Diolistic DiI labelling of RGC *ex vivo* revealed the cell soma, axon and the entire dendritic field. These cells were the divided into four groups corresponding to percentile 25, 50, 75 and 100 of the sampled population in terms of the total dendritic complexity, thus in terms of bifurcations (Fig 5.6). Sholl analysis quantifying the dendrite abours demonstrated a reduction in dendritic intersections in mature compared to younger animals ($n = 5$ animals per stage, 60 neurons for young and 64 neurons for mature animals; Fig 5.7A). Analysis of individual parameters revealed a significant reduction ($p=0.0071$) in bifurcations in mature animals (Fig 5.7B). The total length of the dendrites also showed a significant ($p=0.0098$) reduction in mature compared to young retinae (Fig 5.7C).

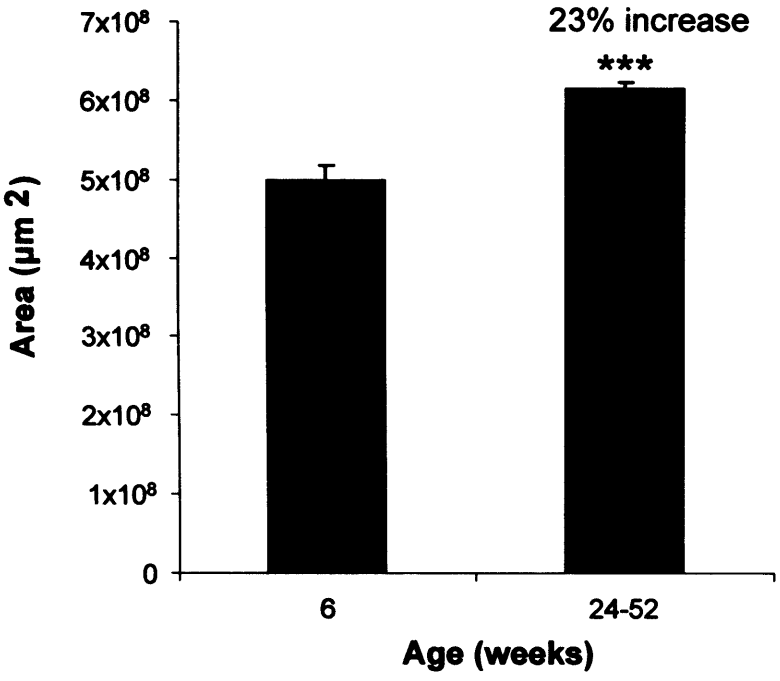

Figure 5.5. Increased retinal area in 24-52 weeks compared to 6 weeks. There was a statistical significant retinal expansion in 24-52 compared to 6 week old BN rat. The data represent mean and standard errors of 10 young and 8 mature retinae from 4-5 animals per stage (*** indicates $p < 0.001$, statistical comparison between the two ages, independent student's test).

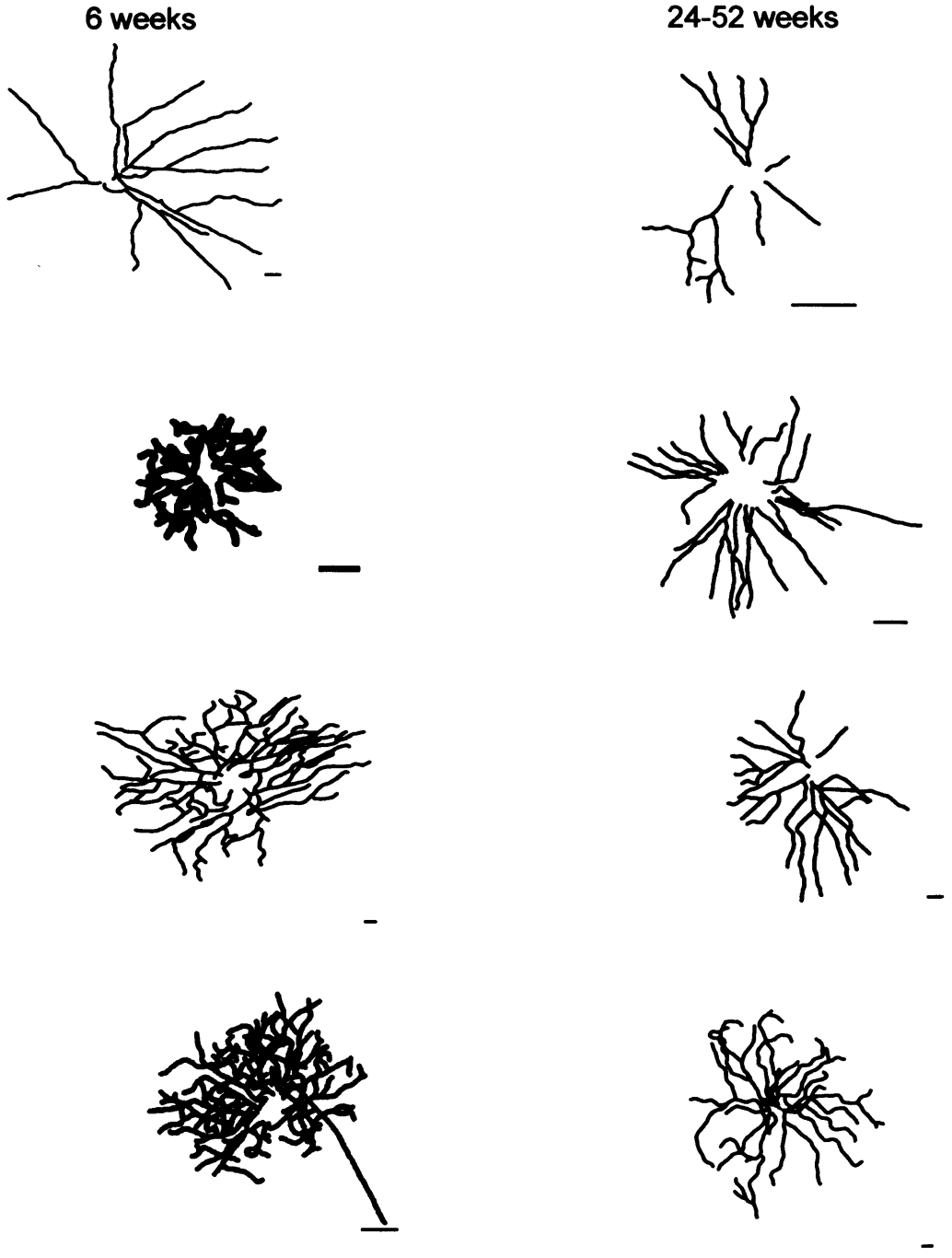

Figure 5.6 Schematic representation of the BN RGC. The figure illustrated morphology variety of the neurons in ages studied. RGC dendrite complexity is reduced in 24-52 (right panel) compared to 6 weeks (left panel) animals. The neurons shown correspond to percentiles 25, 50, 75 and 100 of the sampled population in terms of bifurcations. Scale bar: 20µm

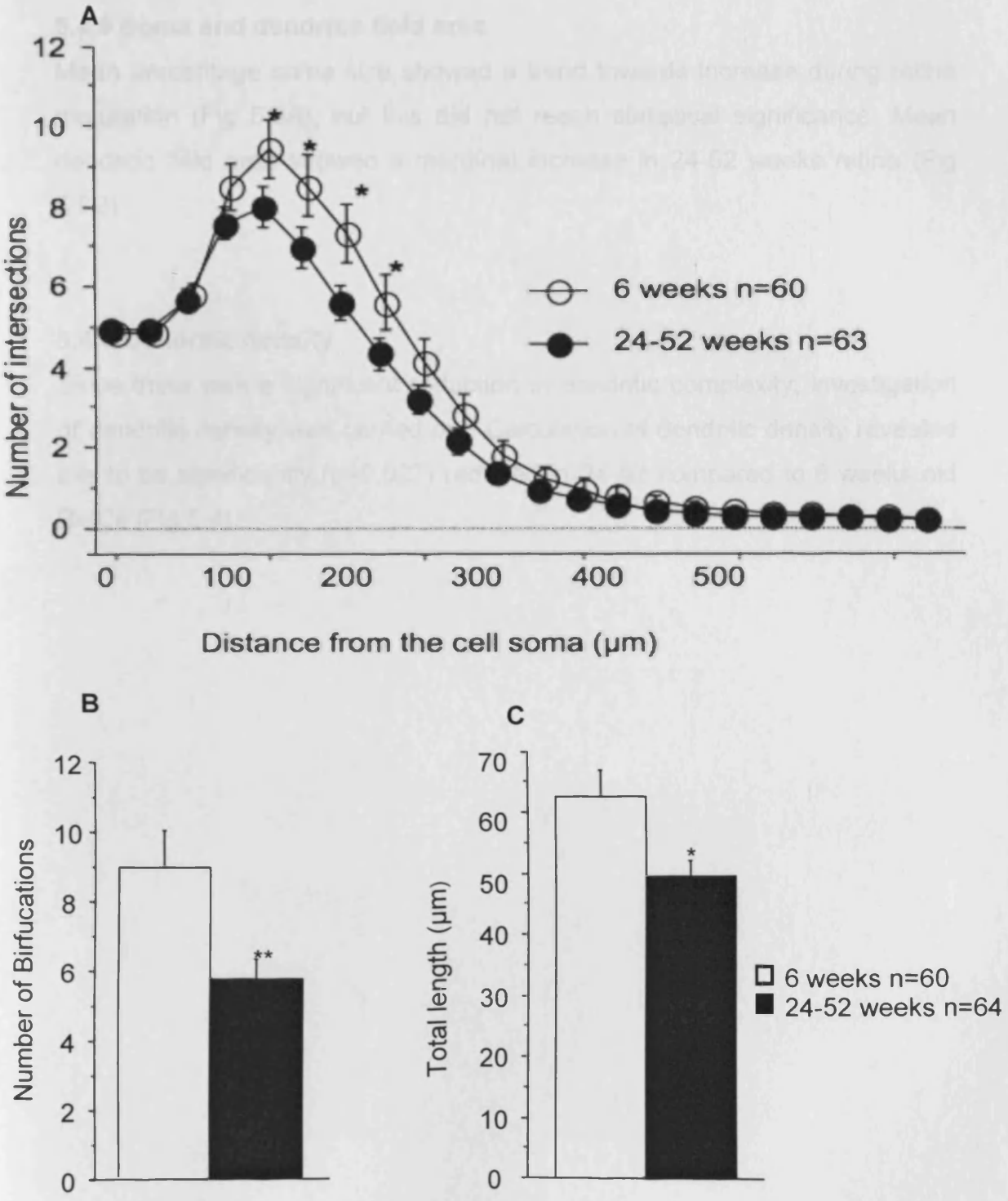

Figure 5.7. Reduced dendrite complexity in mature RGCs. (A) Photomicrographic of typical diolistically (DiI) labelled RGC. (B) Sholl analysis of RGCs dendrites morphology. (C) Number of birfucation was significantly ($p < 0.0071$) reduced in RGCs 24-52 weeks RGCs. (D) Total length of RGCs dendrites was also significantly ($p < 0.0098$) reduced in mature compared to younger RGC. The data represent mean and standard errors of 60 young and 64 mature neurons from 5 animals per stage (**indicates $p < 0.020$, statistical comparison between the two ages, independent student's test).

5.4.5 Soma and dendritic field area

Mean percentage soma size showed a trend towards increase during retina maturation (Fig 5.8A), but this did not reach statistical significance. Mean dendritic field area showed a marginal increase in 24-52 weeks retina (Fig 5.8B).

5.4.6 Dendritic density

Since there was a significant reduction in dendritic complexity, investigation of dendritic density was carried out. Calculation of dendritic density revealed this to be significantly ($p=0.027$) reduced in 24-52 compared to 6 weeks old RGCs (Fig 5.9).

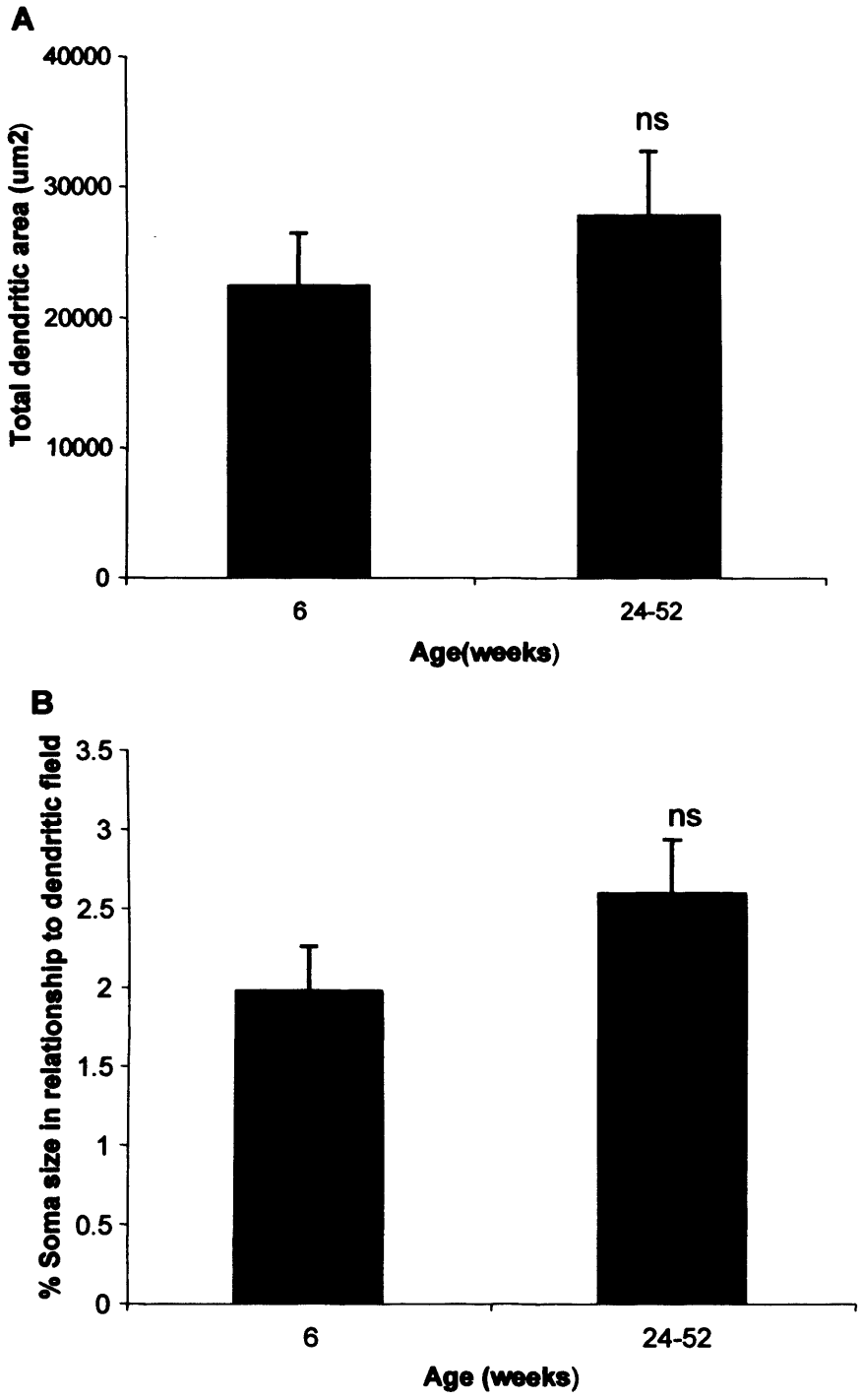

Figure 5.8. RGC soma remains similar during retina maturation. Both dendritic field (A) and percentage soma size (B) show a slight increase in mature compared to younger animals but this did not reach statistical differences. The data represent mean and standard errors of 50 young and 53 mature neurons from 5 animals per stage. Abbreviations; ns, non significant.

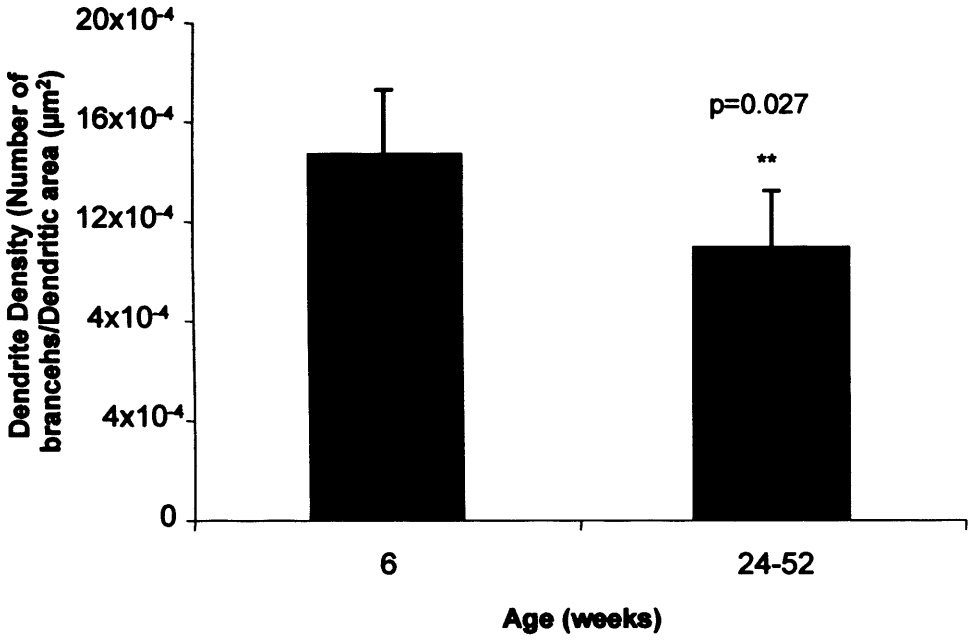

Figure 5.9. RGC dendrite density was significant decreased ($p < 0.025$) in 24-52 compared to 6 weeks retinae. The data represent mean and standard errors of 50 young and 53 mature neurons from 5 animals per stage (** indicates $p < 0.020$, statistical comparison between the two ages, independent student's test).

5.5 Discussion

The age-related decline in cognitive function has been well documented. Although there has been a large body of reports in the literature suggesting cognitive function decline with increase age, it is still unclear when these changes start occurring. The current study, explores the changes in the retinal cell population, along with number, density and architectural structure of neurons in young adult and mature BN rat retina. Furthermore, cell number in INL and ONL were determined. All retinal cell populations show a significant decrease in cell number and density with increasing age. Several groups have also reported reduction in retinal cell population as a function of age. For example, it was reported that there isan inherited age-related loss of RGCs in monkey (Sanchez et al., 1986, Jonas and Hayreh, 2000, Morrison and Hof, 1997) and human (Harman et al., 2000, Jonas et al., 1990, Kerrigan-Baumrind et al., 2000), but this loss in human differs from region to region.

The reduction in RGC density observed in this study confirms that cell reduction is more pronounced in the central compared to peripheral retina. These results corroborate that of other investigators showing that the distribution of RGCs in the rat is not homogenous (Urcola et al., 2006). Neuronal loss has been shown to also occur in the brain. A half of the neurons in somatosensory cortex are lost during ageing (Henderson et al., 1980). This effect is also seen in hippocampus (West et al., 1993) and visual cortex (Devaney and Johnson, 1980), where there is up to 50% of neuronal loss over the lifetime.Thus, the general understanding is that there is neuronal loss in CNS in human, primate and rodents (Flood and Coleman, 1993).

While the apparent cell loss observed in this study could reflect the degree of cell death changes, retinal area could also generate similar changes in cell density. In this study, there was an increased retinal area in the mature compared to younger animals studied here. These data are in line with a report suggesting that there is retinal expansion during adulthood (Harman et al., 2000). There were no TUNEL-positive cells detected in the present study.

In development, where 50% RGC undergo developmental apoptosis, usually less than 1% of TUNEL-positive is detected (Perry et al., 1983). The explanation for this could be that the phagocytosis of dead retinal cells has a clearance time of only a few hours suggesting that the negative results in this work observed by TUNEL could be a consequence of wrong timing.Investigation of human glaucomatous eyes by Kerrigan and colleagues revealed TUNEL-positive cells but DNA fragmentation was not detected and also the frequency of TUNEL-positive cells was very low (1/10000 cells; (Kerrigan et al., 1997). The data obtained in this work and data from other groups (Harman et al., 2000) strongly suggest that the decrease neuronal density in the retina is coursed by a small but continuous increase in retinal area and not cell death.

Interestingly, 0.3% axons loss occurs in the optic nerve per year in healthy humans (Jonas et al., 1990). The same observation has been made in human photoreceptors and pigment epithelium (Panda-Jonas et al., 1995). Progressive axonal loss occurs also in rodents. For instance, Wistars albino rats show over a third axonal loss during ageing process (Ricci et al., 1988). In contrast to this, relatively mild axonal loss in BN rats is observed, where just 12% by 30 months and none by 24 months (Cepurna et al., 2005) suggesting non-linear neuronal loss with age in BN rats. Clearly, the effect of age on retinal cell population, not only varies between species but also within species.

The work carried out here showed that neuronal network complexity is significantly reduced in mature compared to younger retinae. Taking in account retinal expansion and cell spreading out, in order to cover the increasing area, the likely hypothesis would be that neurons will extend there processes in order to maintain synaptic contact. However, this was not the case, suggesting that there is a reduction in synaptic contacts with age, which may be owing to visual impairment during the ageing process. Dendrites remain subjected to structural changes throughout adulthood (Johnston and Narayanan, 2008).

Thus, any alteration in dendrite geometry will significantly alter the physiological properties of any given neuron, even if the total number of synaptic input is stable thereby contributing to the cognitive changes that often accompany senescence (Barnes, 1979, Markowska et al., 1998). Nevertheless, it has been reported that similar changes occur in the brains of different species, where there is age-related decrease in dendrites stability, lengthening and regression (Grill and Riddle, 2002).

Dendrite growth has been suggested to terminate by age of 5 years in human prefrontal cortex (Koenderink and Uylings, 1995, Uylings and de Brabander, 2002) and by one month in rat visual cortex (Juraska, 1982). This could partially explain the observation obtained in the current work. Interestingly, there are some reports suggesting increasing dendritic extent between 3 and 12 months in rats supraoptic (Flood and Coleman, 1993) and in pyramidal neurons of macaca mulatta (Cupp and Uemura, 1980). Grill and Riddle showed an ongoing dendritic growth after 2 months and regression after 18 months in pyramidal neurons of BN rats (Grill and Riddle, 2002). This conflicting data could be owing to experimental set up. For example, housing condition has been shown to have an effect on the dendritic tree. Animals housed in more complex environment have a bigger and more elaborated dendritic field compared to those housed in less complex environment (Green et al., 1983).

The data provided here is informative for the effects of ageing on the development of glaucoma. BN rats are preferred models for experimental glaucoma, where RGC death occurs as early as two weeks after induction of glaucoma (Samsel et al., 2010). Since the RGCs are already "sick", this facilitates their death. This points out the importance of taking the animal's age in to consideration when evaluating the pathophysiology of glaucomatous eyes in animal models. Thus, BN are not susceptible to glaucoma as other rat strains such as Wistars due to neuronal death accompanying senescence but as a consequence of compromised RGC architectural structure.

Taken together, the results provided here suggest that neuronal cell loss that occurs as a result of the ageing process appears to be more marginal than it has been generally assumed. Although neuronal cells are subjected to ageing process it does not mean that the cell undergoes cell death (Harman et al., 2000).The architectural structural changes of the neurons may leave the cell viable with impaired physiological function. The changes are reflected in visual decline that is seen during ageing. The data provided here provide insights concerning the onset of these changes suggesting appropriate intervals for the use of therapeuric intervention the mitigation of RGC loss. It is clear that architectural structural changes of the CNS neurons occurs as early as middle age across all species. Also with animal models, it is important to have this information in order to correctly evaluate pathophysiology of a certain diseases.

Chapter 6

Expression of caspases and IAPs in the microbead model of experimental rat glaucoma

6.1 Introduction

Glaucoma is a neurodegenerative disease that leads to irreversible blindness. It is characterised by detrimental changes in the optic nerve and RGC death (Quigley et al., 1995, Kerrigan et al., 1997). The course of these detrimental effects is partially due to elevated intraocular pressure (IOP). Although glaucoma has been studied extensively for the past 30 years, molecular mechanism that governs RGC death has not been fully understood. The use of experimental glaucoma model has facilitated progress in this research field.

The development of an experimental rat glaucoma model has allowed the identification of genes and protein involved in glaucoma pathogenesis and disease progression (Johnson et al., 2000, Morrison, 2005, Morrison et al., 2005, Levkovitch-Verbin, 2004, McKinnon et al., 2002, Neufeld and Gachie, 2003). Different methods have been used to induce elevated IOP in rats. These include injection of phosphate buffer saline (Morrison et al., 1997), cauterisation of the episcleral vien (Kim and Park, 2005), laser energy delivery to the trabecular meshwork (Levkovitch-Verbin et al., 2006), injection of hypertonic saline into the limbal venous plexus (McKinnon et al., 2002) and injection of paramagnetic beads to the anterior chamber (Samsel et al., 2010). All these models strive to increase IOP by blocking outflow of the aqueous humor from the anterior chamber.

It is well documented that RGCs undergo apoptosis in glaucoma (Garcia-Valenzuela et al., 1995, Vrabec and Levin, 2007, Guerin et al., 2006, Quigley et al., 1995). Both human and animal model glaucoma shows TUNEL positivity in the RGCL (Kim and Park, 2005, Kerrigan et al., 1997). Moreover, activation of initiator caspase 8 and effector caspase 3 activation has been shown to occur in experimental glaucoma (McKinnon et al., 2002).

Discovery of IAP genes, which are conserved in viruses, insects and vertebrates and investigation of their function, has lead to a novel approach of caspase inhibition for neuroprotection in the retina (Liston et al., 2003). Furthermore, these molecules have shown capability to modulate activation

of survival pathways (Zarnegar et al., 2008). For instant, cIAP1 is involved in activation of nuclear factor kappa B (NF-kB) pathway (Zarnegar et al., 2008). Furthermore, it was demonstrated that overexpression of XIAP protects optic nerve (ON) axons of hypertension rat glaucoma model (McKinnon et al., 2002). Although extensive work has been performed to elucidate the function of IAP proteins, their roles in modulating glaucoma pathophysiology are still unclear.

Interestingly, both apoptotic and survival pathways are simultaneously activated in experimental glaucoma (Kim and Park, 2005, Levkovitch-Verbin et al., 2006, Levkovitch-Verbin et al., 2007, Yang et al., 2007), indicating that there is a delay in RGC death. It was shown that the proapoptotic genes from the p53 pathway *Gadd45a* and Ei24 were up-regulated in a photocoagulation model for experimental glaucoma (Levkovitch-Verbin et al., 2006). The MAP-kinase pathway was altered in experimental glaucoma (Levkovitch-Verbin et al., 2007).

6.2 Aim

The aim of the current study was to characterise the expression profile of pro-apoptotic and survival pathway molecules in glaucomatous eyes in order to identify molecules that can be targeted for therapeutic purposes in order to rescue RGC death. Since the apoptotic pathway has previously been shown to be the main mechanism of RGC death, molecules of apoptotic pathway were quantitatively investigated.

6.3 Experimental design

Elevated IOP was induced in 14 male BN rats by injecting paramagnetic microbeads into the anterior chamber of the left eye. The beads contain an Iron (II,III) oxide (Fe_3O_4) core, which is ferromagnetic, encapsulate by a polysterene with a carboxyl group (-COOH) link to it via a polyethylene glycol (PEG). The right (non-injected) eye was used as a control. IOP was

measured 24h after injection and every three days thereafter. Sustained elevated IOP for at least 14 days was desired, but some animals did not have increased IOP even after the injections therefore, up to 3 injections were required in some cases. Moreover, a minor number of animals did not have a sustained IOP elevation after multiple injections. These animals were not included in the protein analysis experiments.

After, at least 14 days of increased IOP, the animals were sacrificed by CO_2 inhilation. The retina was immediately dissected as described in section 2.2.1 for RNA analysis and 2.2.2 for protein isolation.

RNA extraction, quantification and cDNA synthesis was carried out as described in sections 2.4.3, 2.4.4 and 2.4.6 respectively.

Following evaluation of stability of the housekeeping genes, namely glyceraldehydes 3-phosphate dehydrogenase (GAPDH), beta-actin and beta-III tubulin in experimental and control eyes, real-time PCR was run as described in the methods and chapter 3. Caspase 3, 7 and 9 and IAPs genes, namely, NIAP, cIAP1, cIAP2, XIAP, Survivin, Bruce and Livin expression was evaluated.

Subsequently, caspase 3 activity was determined in glaucomatous eyes by Western blotting as described in section 2.6. The p53 pathway, which is involved in regulation of both pro- and anti- survival molecules pathway was evaluated by quantifying p53 protein levels in glaucomatous eyes.

Finally, statistical analysis between experimental and control eyes was performed using parametric analysis independent student t-test (SPSS16, Chicago, Illinois) after determining normal distribution (Shapiro-Wilk test) and equal variance (Lavene test) between the groups. All data are presented as means ± standard errors. Differences were considered significant for $p<0.05$.

6.4 Results

6.4.1 IOP profile

Injected paramagnetic beads can be seen in the live animal eye (Fig. 61A-B) and post-mortem H&E staining of the TM two weeks after injection (Fig 6.1C-F). The beads clearly blocked the outflow of the aqueous humour. Injection of the paramagnetic beads into the anterior chamber of the BN rats resulted in sustained elevated IOP in <50% of the injected animals for the period of investigation (≤ 30 days; Fig. 6.2, and 6.5). The remaining animals had fluctuating IOP (Fig. 6.2, and 6.5), but these animals were also included in the study since they all had an increase of IOP at some point. Previous work by our group has demonstrated that animals with fluctuating IOP also show RGC loss (Samsel et al., 2010). Mean IOPs of all animals are shown in table 6.1. The IOP increase was highly significant 1day post injection. At day 8 post injection the animals showed an increase in IOP but the statistical significance were modest. At day 16 and ≤ 30 days post injection the increase was significant but not as strong as 1day post injection (Table 6.1). IOP-integral differences were averaged for each animal and compared. The mean integral IOP was 326.14± 49.53, range 57.7-607.25 (±SEM).

Table 6.1. Intraocular pressure (IOP) history in rats with experimental glaucoma

Time point	Mean IOP (mmHg)		
	Glaucoma	Control*	p-values
1 day	34.95±11.2	19.05±4.56	P < 0.0114
8 days	31.29±12.83	21.55±3.31	P < 0.0540
16 days	32.35±12.17	22.77±3.40	P < 0.0467
≤ 30 days	31.21±10.59	23.34±2.07	P < 0.0413

Results are given as mean ±SD

*The animal's fellow eye

6.4.2 Evaluation of housekeeping genes stability

IOP profiles of the animals used for quantitative PCR are shown in figure 6.2 (n = 6). Animals in figures 6.2A, C and D had fluctuating IOP profiles whilst animals in figures 6.2B, D and F had sustained IOP profiles. Housekeeping gene expression was evaluated by plotting the ct values. The results show a trend towards a higher expression in glaucomatous eyes (n = 6) but the difference was marginal indicating that the expression of these housekeeping genes was not significantly altered following IOP elevation (Fig. 6.3).

6.4.3 mRNA expression of caspases and IAPs in glaucoma

Caspases 3,7 and 9 showed no alteration in their expression at the mRNA level (Fig. 6.4A, n = 6). By contrast, the majority of IAPs showed a trend towards an increased in expression (n = 6). These include NIAP, cIAP2, Survivin and Livin (Fig. 6.4B). NIAP and Livin were significantly up-regulated ($p<0.0001$ for both), up to 5-fold increase in glaucomatous compared to control eyes. Bruce was significantly down-regulated ($p<0.0001$; 2.5 fold) in experimental eyes while cIAP1 and XIAP remain similar between control and experimental eye (Fig. 6.4B).

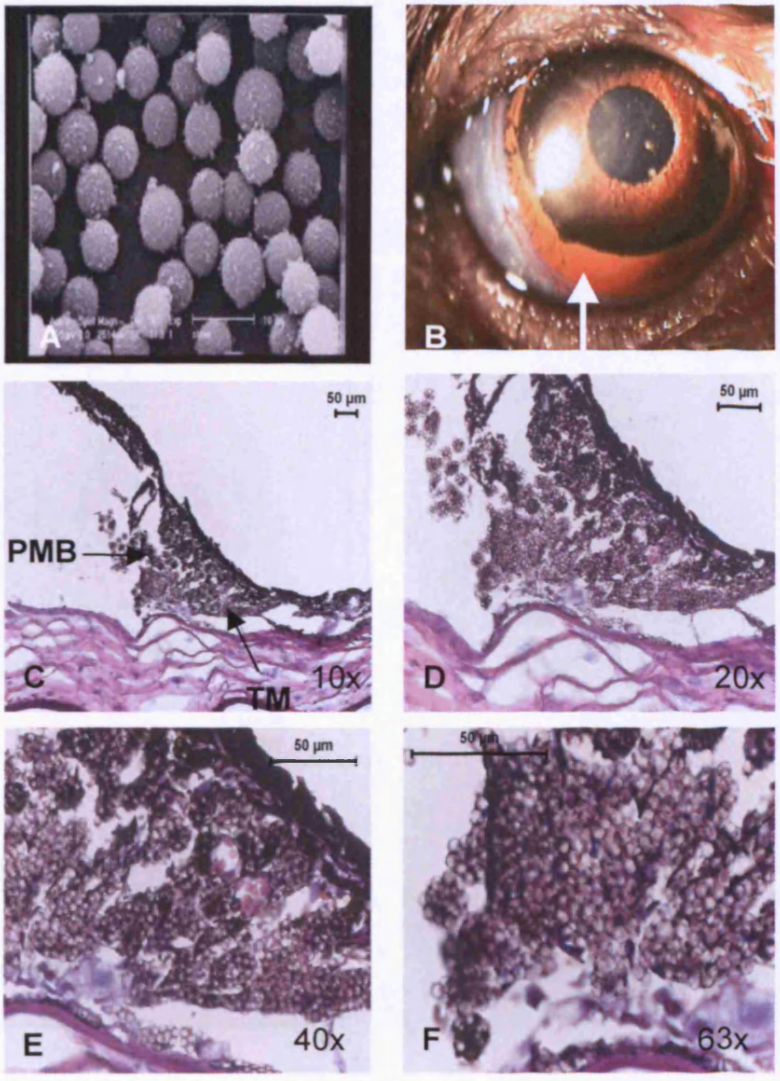

Figure 6.1. Paramagnetic beads in the trabecular meshwork (TM). A picture of he paramagnetic beads that were used to induce increased IOP in BN eyes (A). Beads in the iridocorneal angle as indicated by the arrow (B). Immunohistochemical analysis confirmed presence of the beads in the trabecular meshwork (C-F). Figure 6.1B is adapted from Samsel P, Kisiswa L et al., IOVS 2010, In press.. Abbreviations; TM, trebecular meshwork; PMB, paramagnetic beads.

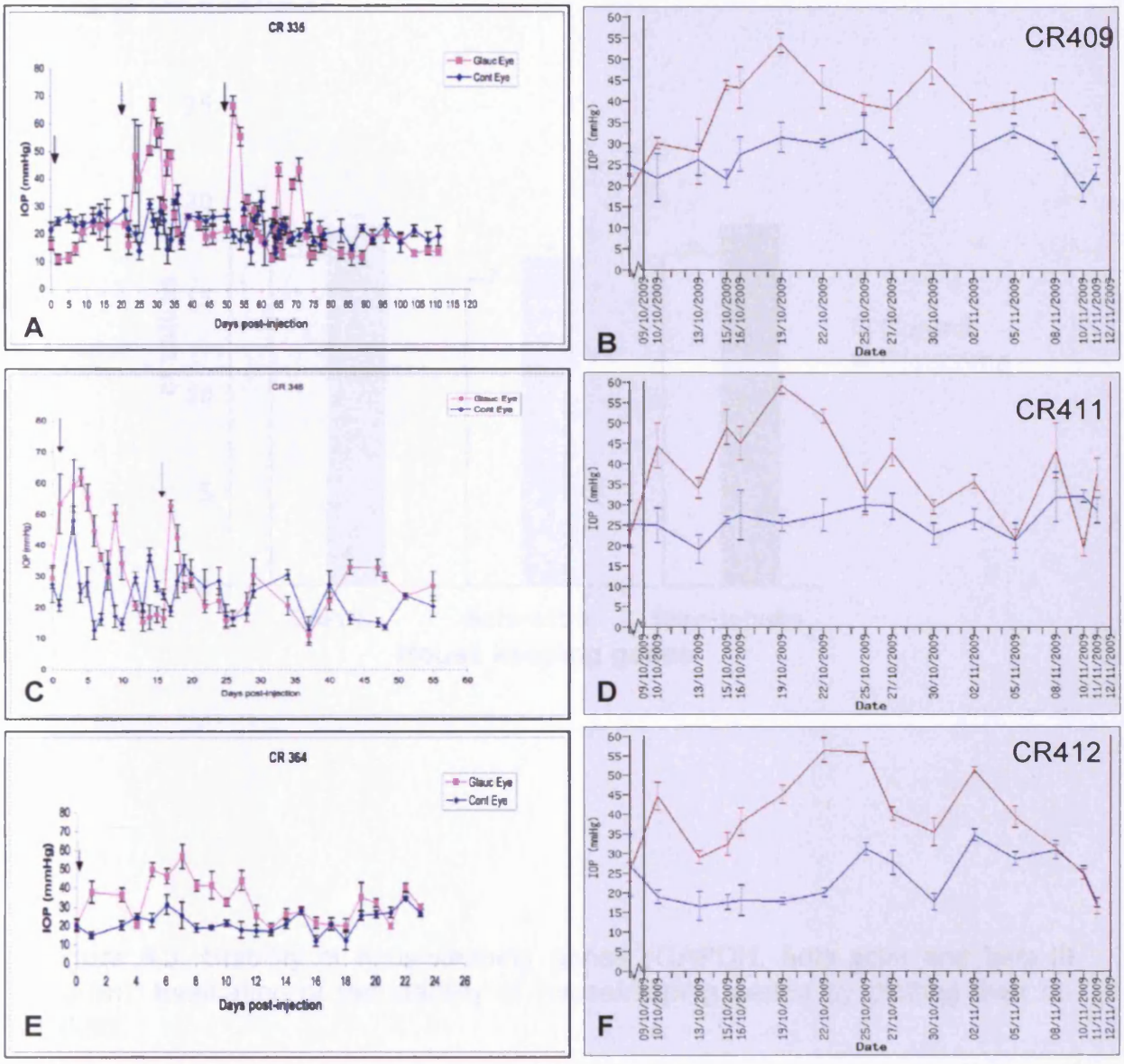

Figure 6.2. IOP profile of animals used for real-time PCR on expression profiles of caspases and IAPs in experimental rat glaucoma model. Some animals had sustained increased IOP (B,D-F) while other had fluctuation in IOP (A and C). Several animals required multiple injection (A and C)

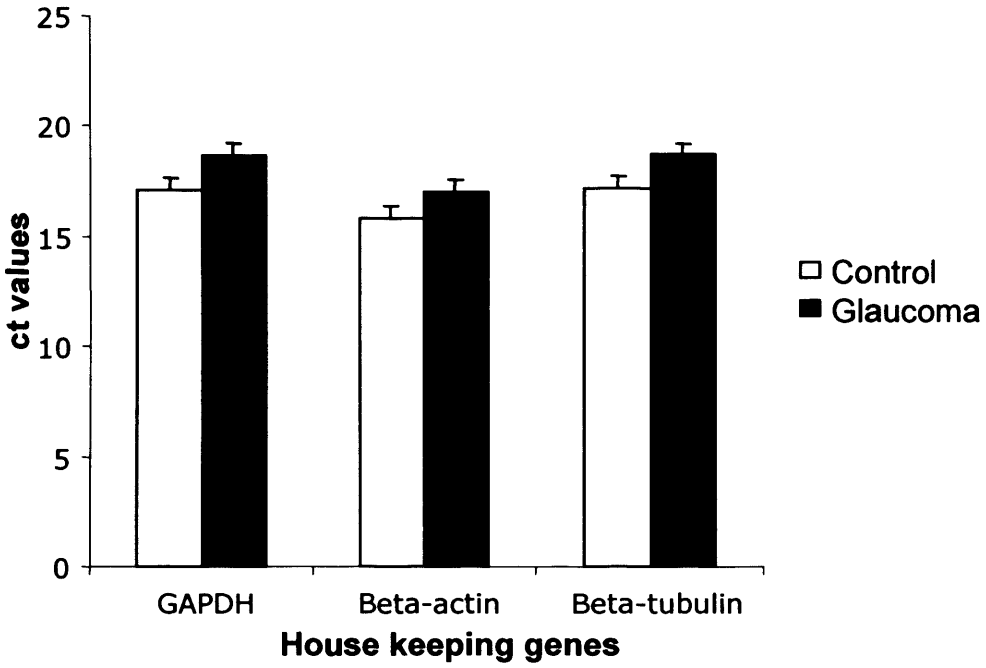

Figure 6.3. Stability of housekeeping genes (GAPDH, beta-actin and beta-III tubulin). Evaluation of the stability of housekeeping genes by plotting their ct-values.

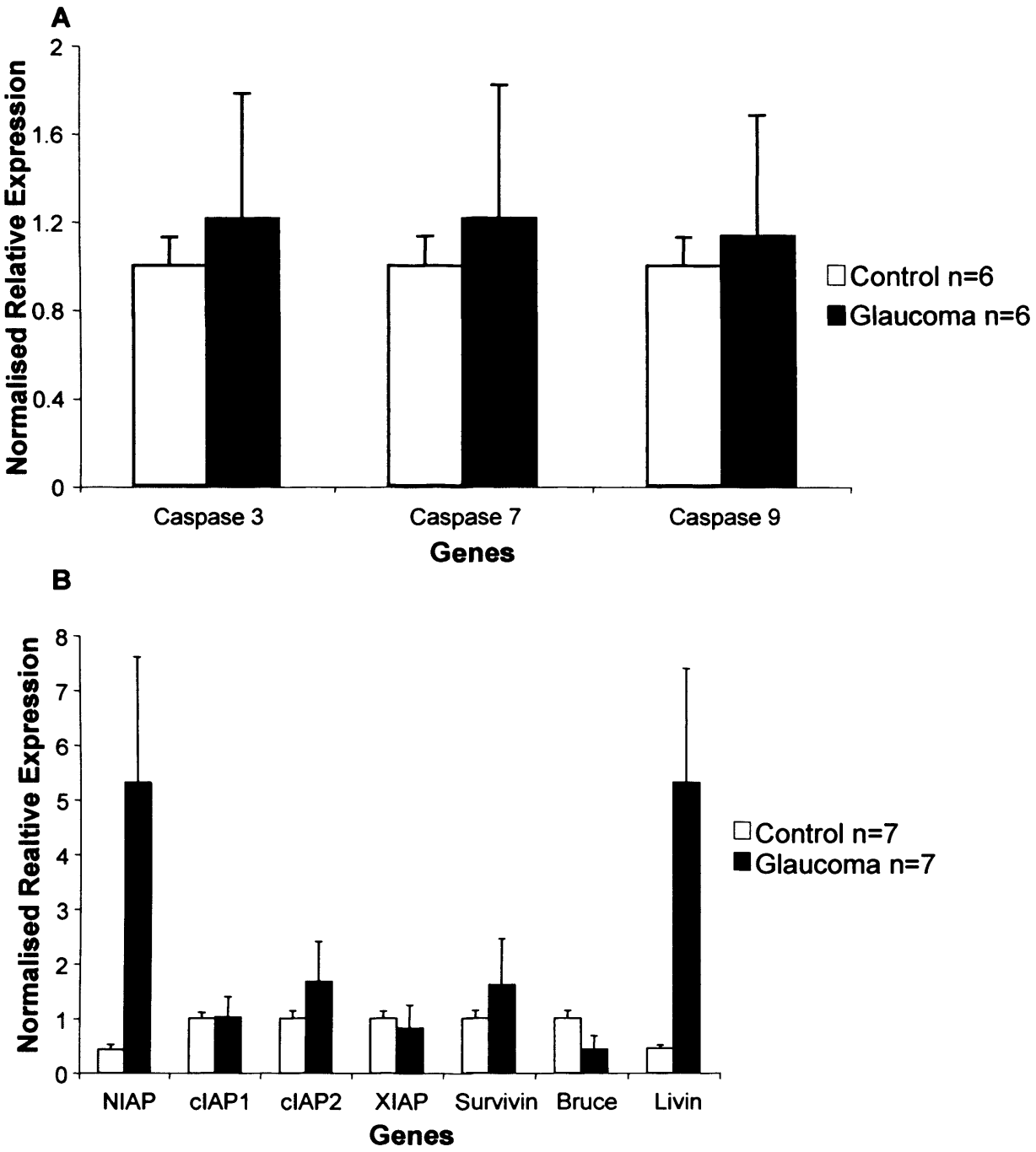

Figure 6.4. Real-time PCR on expression profiles of caspases (A) and IAPs (B) in experimental rat glaucoma model. Samples were taken from total retinal extraction (6 right (control) and 6 left (experimental) eyes, total 6 animals). The levels of mRNAs were calculated relative to three endogenous genes, namely, GAPHD, β-actin and β-tubulin mRNA. Mean and standard errors are shown.

6.4.3 Active caspase 3 in experimental eyes

Previously, it was reported that active caspase 3 is present in glaucomatous eyes using immunohistochemisty analysis. Western blotting analysis was performed to quantify active caspase 3 protein in the experimental glaucoma bead model. Thisese animals had a variable IOP profile (Fig. 6.5). Western blotting analysis demonstrated the presence of both inactive and active caspase 3 in the two groups (n = 7) studied (Fig 6.6A). Densitometric quantification revealed a significant ($p<0.001$) decrease in inactive caspase 3 in experimental (3.8 ± 1.8-fold; n = 7) compared to control (n = 7) eyes (Fig. 6.6B). The active form of caspase 3 also showed a trend towards reduction (2.3 ± 1.5-fold; n = 7; Fig. 6.6B) but this did not reach statistical significance.

6.4.3 Analysis of p53 protein levels in glaucomatous eyes

Although p53 gene expression was altered in experimental glaucoma by gene array analysis (Levkovitch-Verben et al. 2006), evaluation of p53 protein levels were measured here since mRNA levels of a particular gene do not always provide a consisten correlatation with protein levels. Protein levels of p53 in this study were statistically significantly ($p=0.02$, $n=7$) higher in the experimental eye of the bead model compared to the control eye (Fig. 6.7A-B).

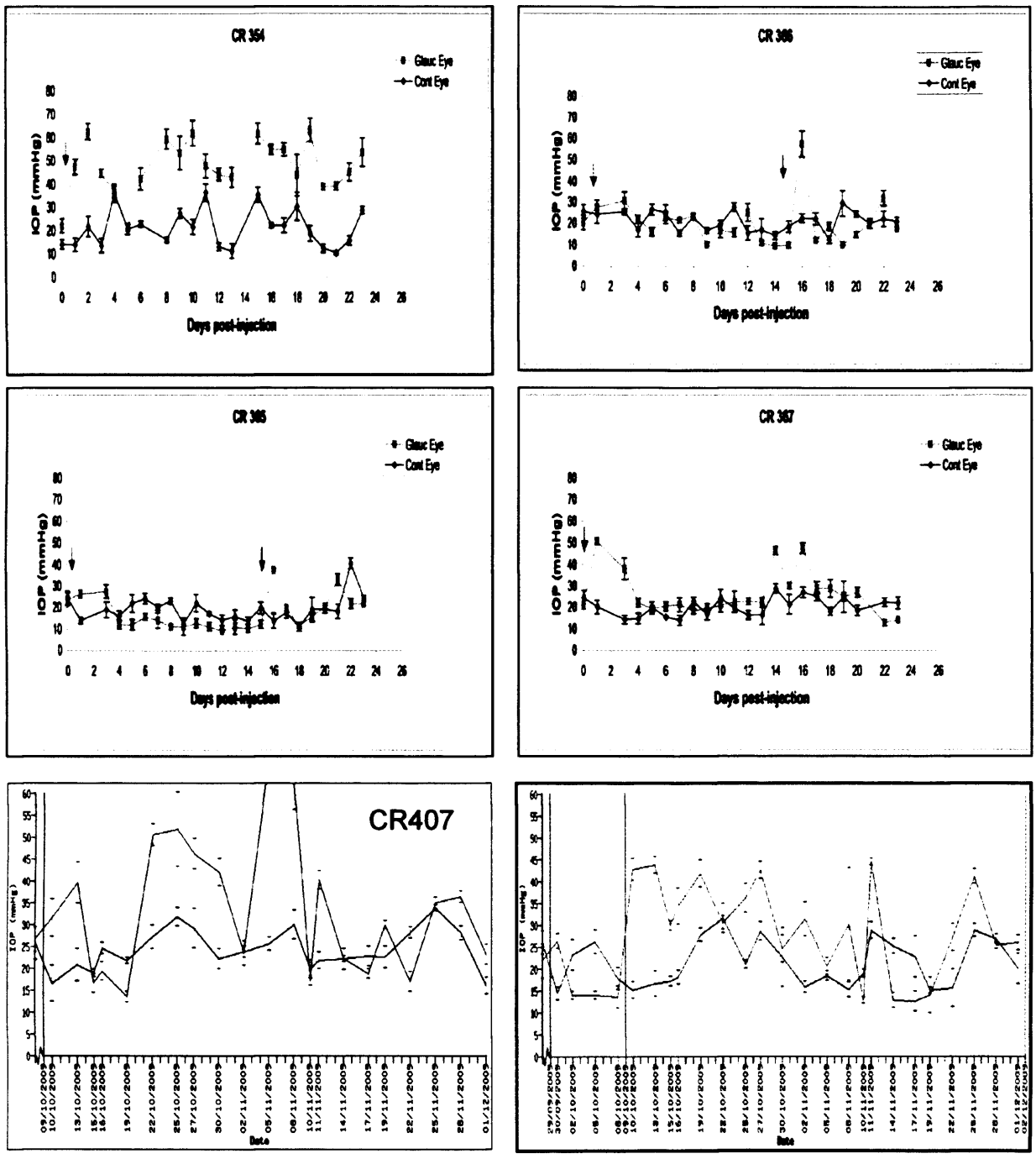

Figure 6.5. IOP profile (representative IOP profiles) of animals used for evaluating casapse 3 (pro-apoptotic), and p53 protein levels in experimental rat glaucoma model. Some animals had sustained increased IOP (B,D-F) while other had fluctuation in IOP (A and C). Several animals require multiple injection (A and C)

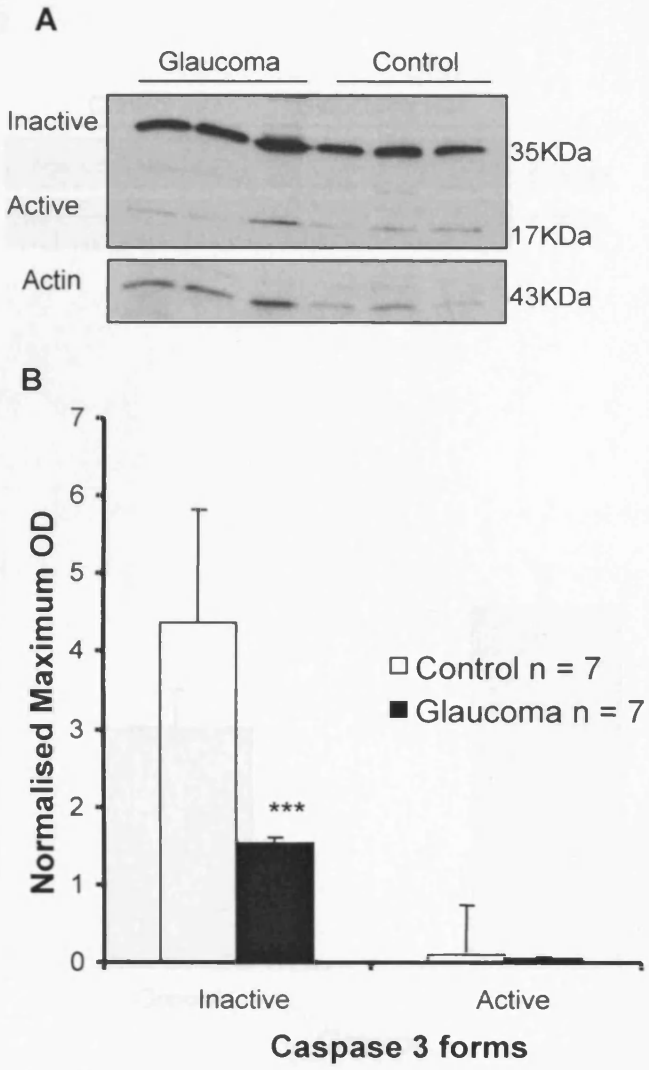

Figure 6.6. Increased active caspase 3 protein levels in experimental rat glaucoma model. (A) Blots showing reduction in levels of inactive caspase 3 in the left (experimental) compared to right (control) eye. (B) Quantification of the band density revealed a significant ($p<0.001$) reduction of inactive caspase 3 but active caspase 3 remained the same in both groups. The densitometry data reflect the expression level for each protein for each examined as a ratio value relative to actin levels (mean and standard errors, n=7 for each group (3 readings were taken for each animal; *** indicates $p <0.001$, statistical comparison between the two ages, independent student's test).

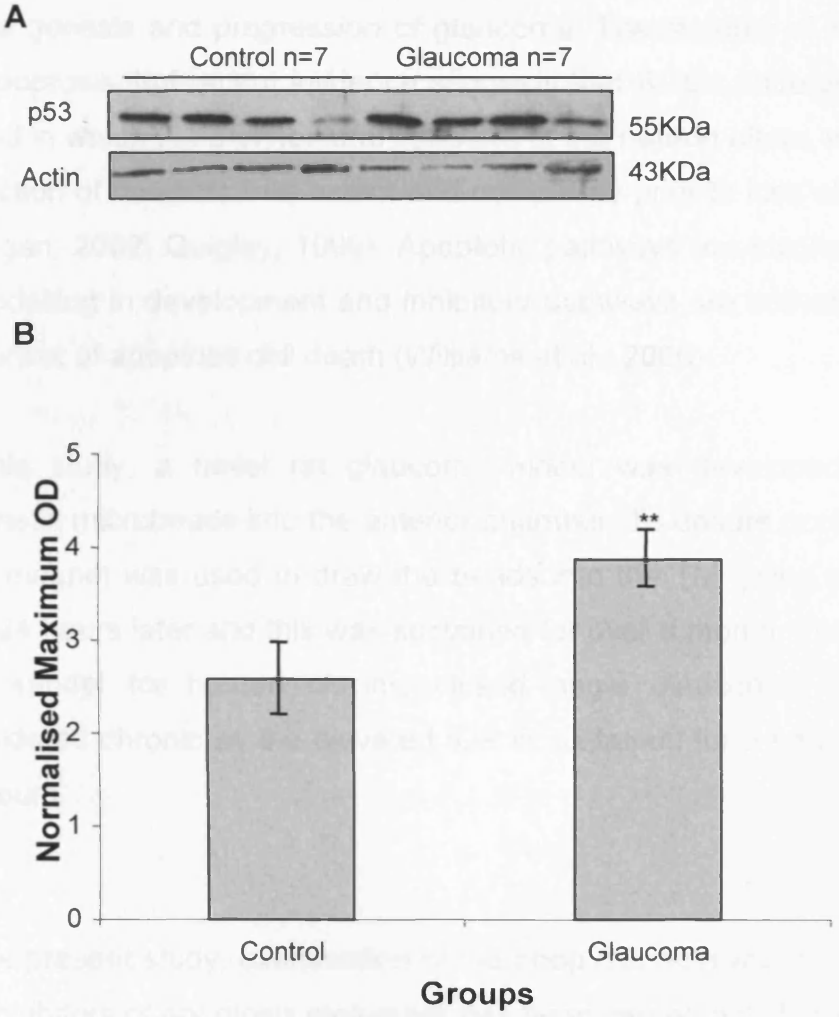

Figure 6.7. Increased p53 protein levels in experimental rat glaucoma model. (A) Blots showing an increased levels of p53 in the left (experimental) compared to right (control) eye. (B) Quantification of the band density revealed an increased in p53 protein levels. The densitometry data reflect the expression level for each protein for each examined as a ratio value relative to actin levels. Mean and standard errors, n=7 for each group (3 readings were recorded for each animal; **p=0.02).

6.5 Discussion

Susceptibility of getting glaucoma increases with age (Carter, 1994). Current work has focused on elucidating the molecular mechanisms that are involved in the genesis and progression of glaucoma. The majority of RGCs are lost by apoptosis, but recent evidence suggests that RGCs undergo a prolonged period in which the architectural structure of the neuron alters, which includes reduction of dendritic tree extent and complexity prior to loss of the cell body (Morgan, 2002, Quigley, 1999). Apoptotic pathways are involved in dendrite remodelling in development and inhibitory pathways are activated that retard the onset of apoptotic cell death (Williams et al., 2006).

In this study, a novel rat glaucoma model was developed by injecting magnetic microbeads into the anterior chamber. To ensure occlusion, a hand held magnet was used to draw the beads into the TM giving an increase in IOP 24 hours later and this was sustained for over a month. This bead model is a model for human chronic closed angle glaucoma. The model is considered chronic as the elevated IOP is sustained for a period longer than 24 hours.

In the present study, examination of the apoptotic pathway, concentrating on the inhibitors of apoptosis molecules has been carried out. The data provided here demonstrates that cIAP1, cIAP2, XIAP and Survivin expression on mRNA level remained similar in glaucomatous and normal eyes. Interestingly, Levkovitch-Verbin and colleagues showed cIAP1 (named IAP1 in the paper) and cIAP2 (named IAP2 in the paper) were up-regulated on the gene array but could only confirm the up-regulation for cIAP1 which was up-regulated 1.5-fold (Levkovitch-Verbin et al., 2006). These contradicting results may be owing to the fact that different rodent models were used in the two experiment and also that the method of inducing elevated IOP also differs between the experiments.

NIAP and Livin expression were increased 5-fold in glaucomatous compared to control eyes. Although, NIAP and Livin are structurally different, they have been suggested to bind caspase 3 and 9 (Liston et al., 2003). NIAP containing three BIR and Nucleotide Binding Domains (NBD) binds capsase 3 and 7 and hinders activation of these proteases (Liston et al., 2003). NIAP has been suggested to have a modulating function in spinal mascular atropy (SMA), a disease characterised by progressive loss of motor neurons (Gendron and MacKenzie, 1999, Xu et al., Liston et al., 2003). NIAP-deficient mice do not exhibit developmental malfunction or spinal mascular atrophy (Roy N et al., 1995; Holcik M, et al., 2000) suggesting that the mutation is not the primary cause of the disease (Gendron and MacKenzie, 1999). Taken together, the increase in the levels of NIAP shown in this study suggests that it may have a modulatory effect in glaucoma, possible by delaying RGC death.

By contrast, Livin contains only one BIR domain and a RING domain. The RING domain function is to encode ubiquitin protease activity. Thus, the RING domain is responsible for the transfer of ubiqutin into target proteins (Yang et al., 2000). There are two isoforms of Livin, the alpha (α) and the beta (β). Although they are structurally very similar, the two isoforms exhibit different cellular and tissue distribution and antiapoptotic characteristics (Wang et al., 2008b). Only the alpha isoform is expressed in the CNS (Ashhab et al., 2001).

Initially, Livin was suggested to inhibit caspase 3,7 and 9 showing a broader range of activity than any other IAP considering the fact that it has only one BIR domain (Kasof and Gomes, 2001, Liston et al., 2003). However, the inhibition has shown to be weak compared to XIAP (Vucic D et al., 2005) suggesting that Livin might bind to the proteases but has no or little effect on inhibiting their activity. Recent work reported that similarly to XIAP and cIAP1, Livin is involved in non-apoptotic pathway (Sanna et al., 2002, Dupoux et al., 2009, Li et al., 2002, Santoro et al., 2007, Rothe et al., 1995). Livin is capable of activating Jun NH2-terminal kinase 1 (JNK1) and activation of this molecule protects the cell from extrinsic apoptotic signals

(Sanna et al., 2002).

The linker region in XIAP between BIR1 and BIR2 has been suggested to be more important than BIR domain itself (Liston et al., 2003). The linker region spans the entire active site of caspase 3 and 7, hindering substrate entry (Liston et al., 2003). Also, XIAP has been suggested to inhibit directly and indirectly caspase 8. Activation of JNK1 has been implied to be the second role of XIAP (Sanna et al., 1998).Interestingly, overexpression of XIAP showed a protective effect of the optic nerve axons in rat glaucoma model (McKinnon et al., 2002).

But the group also observed expression of XIAP by cilliary bodies suggesting that overexpressing XIAP could have a protective effect in glaucoma by preventing pressure elevation by regulating production of aqueous humour (McKinnon et al., 2002). Thus, considering the fact that Livin and XIAP share 50% homology and function (activation of JKN1 and inhibition of caspase 3 and 7), it will be interesting to investigate whether the increase expression of Livin in glaucomatous eyes has a similar effect as XIAP and also to determine whether the expression is restricted to RCGL.

Interestingly, Bruce expression was decreased in glaucomatous eyes compared to control. Bruce, together with Survivin belongs to a group of IAPs with "Survivin like" BIR domain (Verhagen et al., 2001). Proteins with "Survivin like" BIR domains can also be found in *Caenorhabditis elegans* (*C. Elegance*) and yeast *Schizosaccharomyces pombe* (*S pombe*) indicating in evolutionary terms that these IAPs are older compared to the rest.

Furthermore, in these systems, the BIR domain in Bruce does not inhibit apoptosis but has been shown to modulate cell division (Silke and Vaux, 2001, Uren et al., 1996). Other reports suggest that Bruce promotes cell survival by inhibiting apoptosis by spontaneous release of second mitochondrial-derived activator of caspase (Smac) (Hao et al., 2004). For instance, Bruce has been shown to regulate apoptosis in mice (Hao et al., 2004, Ren et al., 2005) and in *Drosophilamelanogaster*(Vernooy et al., 2002). Recent work demonstrated that loss of Bruce function leads to up-regulation

of p53 (Ren et al., 2005). This work is line the work reported here. Although, no evidence of alterations in Bruce protein has been provided here, it is fair to postulate that down-regulation of gene expression seen in this work might contribute to the up-regulation/stabilisation of p53 as shown here.

Thus, Livin and NIAP up-regulation suggest that the cell is struggling to escape apoptosis while stabilisation of p53 as a consequence of down-regulation of Bruce indicates that apoptotic activity is taking place in glaucomatous eyes. But other forms of cell death such as autophagy cannot be ruled out.

In this work, p53 protein levels were increased in glaucomatous compared to control eyes. p53 is a transcriptional factor that positively and negatively regulates transcription of various genes (Laptenko and Prives, 2006). These genes include those that are essential for mediating apoptosis, senescence, and cell-cycle arrest (Vousden and Lane, 2007). These are the well understood activities of p53. However, recent work has demonstrated that p53 also regulates glycolysis (Bensaad et al., 2006, Matoba et al., 2006), the repair of genotoxic damage (Gatz and Wiesmuller, 2006), invasion and motility (Roger et al., 2006), angiongenesis (Teodoro et al., 2006) differentiation (Murray-Zmijewski et al., 2006), cellular senescence (Kortlever et al., 2006) and autophagy (Crighton et al., 2006).

Although a mechanistic basis of p53 in glaucoma has not been provided here, it can be speculated that the increase in p53 observed contributes to RGC death by apoptosis or autophagy. Although apoptosis has been shown to occur in glaucoma it is still debatable whether it is the only cell death mechanism that occurs in glaucoma. The evidence of p53 elevation hints that autophagy may be occurring in glaucoma. Since little is know to what extend the autophagy plays a role in glaucoma, it will be interesting to elucidate a role of p53 and autopaghy in glaucoma.

In summary, the present study has revealed up-regulation of two IAPs (NIAP and Livin) in an experimental rat glaucoma model (the bead model), of which one was previously shown to be up-regulated in a laser photocoagulation model for experimental glaucoma. Bruce, on the other hand, was down-regulated in the glaucomatous eyes. p53 protein levels were shown to be higher in the experimental eye suggesting that the down-regulation of Bruce might play a role in stabilisation of p53 protein in glaucoma. This in turn could lead to increased apoptosis activity and /or increased pro-survival activity in glaucoma.

Chapter 7

Final discussion, conclusion and future work

7.1 General discussion

The overall aim of the present study was to elucidate factors and mechanism that governs the maintenance and remodelling of RGC dendrites, as well as neuronal cell death in ageing and neurodegenerative diseases. Using PCR techniques, the expression pattern of molecules of the apoptotic pathway on mRNA level was determined in young adult, mature and diseased retinae. Furthermore, validation of the expression of these molecules on protein level was carried out using western blotting and immunoflouroscence techniques.

Rodent retinae were used in this study, which provide an excellent model because of its relative short lifespan enables ageing studies. Due to the availability of the ageing animals wistar albino rats were used for mRNA expression screening at late stage of the rat lifespan.

Using conventional PCR, caspases 3,6,7,8 and 9 expression in BN retina remain similar in two stages studied. IAPs expression, on the other hand, was generally decreased in mature compared to younger retina with an exception of cIAP1. cIAP1 was significantly down-regulated in mature retina compared to younger retina (Chapter 3). Real time PCR revealed a different expression pattern of the apoptotic pathway in ageing Wistar albino rats. Caspases 3,6,7,8 and 9 expressions were not altered during Wistar albino retina. NIAP, cIAP2 and XIAP and cIAP1 were decreased in older compared to younger Wistar albino retinae, while Survivin, Bruce and Livin we slightly increased with age (Chapter 3).

Correlation of cIAP1 mRNA levels, which showed a significant reduction in expression in BN rat, with protein was carried out. In deed, cIAP1 mRNA levels correlated with protein levels in the whole retina lysate. Using enriched RGCL cell sample, cIAP1 down-regulation was shown to be specific for RGCL. This was validated by immunoflouroscence. Reduction of cIAP1 did not alter caspase activity, which was shown using immunoflouroscence analysis and TUNEL assay. Impair survival pathway in retinae absent of cIAP1 was shown by quantifying TRAF2 using immuno blotting and fluroscence (Chapter 4).

Subsequently, dendrite pruning was determined in maturing BN rat retina revealing a reduction in dendrite complexity in what could be considered as middle-aged animals. The assessment of retinal cell loss demonstrated that there was reduction in cell density (unit per area) in all retinal layers but this was an offset of the retinal expansion (Chapter 5).

During this study, a new model of glaucoma was developed, where the injection of magnetic beads in the anterior chamber of the BN rat eyes was carried out. This lead to a sustained elevated IOP resulting in RGC cell death (Samsel et al., 2010). Once again, there was no alteration in caspase expression upon induction of glaucoma. Caspase 3 activity was slightly increased in the glaucomatous eyes. NIAP, cIAP2, Survivin and Livin were up-regulated, while Bruce was down-regulated in glaucomatous eyes. cIAP1 and XIAP expression remain similar between control and experimental eye (Chapter 6).

A summary of the results presented in this thesis is provided above. The following discussion offers general observations as to the importance of the differently expressed genes during ageing and neurodegenerative diseases and the consequences accompanying the alteration in expression of these identified molecules in this study. The outcome of compromising neuronal morphology and the importance of maintaining a complex dendritic tree in health and disease will also be discussed.

Two rat strain, namely BN and Wistar albino have been used in this study for several reasons. Firstly the availability of the rat in the group was a determining factor. Initial IAPs and caspases expression pattern was determined in both strains in order to evaluate whether the changes in expression was specific to the species or differed also within the species. BN were the favourable model for further studies commonly used and more representative of the human glaucoma. With this in mind it was logic to use the BN for the ageing study, which facilitated extrapolation of the aging studies with glaucoma studies.

Reduction in cIAP1 does not lead to cell death. Age-related cell loss in the CNS is well documented for the past decades. This was first reported by Brody back in 1955, where reduction in brain weight as a consiquence of scenescence was suggest to be coursed by cell loss (Brody, 1955). Since then, neuronal loss has been shown to occur in ageing human, non-human primate and rodent brain (Ball, 1977; Brizzee et al., 1980) and retina (Cano et al., 1986, Cavallotti et al., 2001, Curcio and Allen, 1990, Gao and Hollyfield, 1992, Katz and Robison, 1986, Weisse, 1995). Recent reports, including results provided in this thesis (Chapter 5) revealed no age-related neuronal cell loss occurs in rodent, human and non-human primates (Harman et al., 2000, Harman et al., 2003, Harman et al., 1999, Kim et al., 1996).

Earlier reports on cell death during ageing faced various technical and methodological difficulties, such as species and strain difference, tissue processing and sampling design. The stereological method used for this early studies were measuring neuronal density (unit per area) but not total neuronal number (Morrison and Hof, 1997). This type of measurements did not take in account developmental expansion and volume of the tissue.

The development of new stereological principles has greatly improved sampling strategy and also eliminates the confounding factors of the previous studies (Burke and Barnes, 2006). The principles consist of collection of rules that enables counting of the number of items in a three-dimensional structure independent of the size of the object (Burke and Barnes, 2006).

There are several issues that accompany the cell density data provided here. For instant, RGC density in the central part of the retina was reduced but this did not apply to the peripheral retinal areas. One explaination is that it reflects the uneven distribution of the retinal cells. For example, there are no cells at the optic disk and photoreceptors cells are contracted in the fovea and macula (Feng et al., 2007).

Moreover, the 7µm sections used in the study may result in overestimation of the number of cell (see chapter 2, section 2.7.2).The optical dissector method would have been better for sampling. The optical dissector, optically sections the sample area and directly estimates the cell number in each nuclear layer (Oorschot, 1994). The counting carried out here did not discriminate the amacrine cells. Amacrine cells make up to 50% of the cells in the RGCL (Perry et al., 1983). Thus, the data provided here show no changes in all retinal cell rather than retinal neuronal cells. Another limitation of the cell loss assessment carried out here is that the estimation of cell density did not account for the thickness of individual retina. Changes in retinal volume may vary topographically.

The advantage of this study is that the neuronal density measured took retinal expansion in account to estimate cells loss. For example the reduction in RGCL cell density was 16% whilst retinal expansion was 23%. Subtraction of percentage density reduction from percentage expansion showed no reduction. Thus neuronal loss is not a characteristic of normal ageing process in rodent retina to a certain age.

The cIAP1 reduction leads to accumulation of TRAF2, which suggest impaired survival pathway in the retina, specifically in the RGCL. TRAF2 is a key player in activation of NF-kB. In neurons activation of NF-kB leads to expression of NF-kB targeted genes (Table 7.1). The genes encodes for cell survival (Bcl-2 and Mn-SOD;), inhibition of apoptosis (IAPs), cell death (Bcl-x(S) and Bax), regulation of ion homeostasis (subunits of NMDAR, calbindin, calcium binding protein and voltage dependent calcium channels; (Camandola and Mattson, 2000, Camandola et al., 2000b, Camandola et al., 2000a, Chu et al., 1997, Furukawa and Mattson, 1998, Shou et al., 2002).

Although the cIAP1 expression data shown here do not exclude other cells such as glial cell, the suggestion put forward is that the reduction is mainly in

the neurons (amacrine and RGCs) since these cells form the major cell component of the RGCL (Perry et al., 1983).

Assessment of RGC dendrite complexity showed a reduction in dendritic complexity and this might be caused by a reduction in the survival response. Since the activation of survival pathway is impaired the cells are vulnerable to all kind of stress including deprivation of nutrients and more. Dendrites are more vulnerable to environmental changes, either intrinsic or extrinsic. As a consiquence to impaired survival pathway, in response to stress, they will be the first to go and that might explain the reduction in dendrite complexity seen here.

Impairment in activation of NF-kB also lead to reduced transcription of the genes that encode for cytoskeleton proteins including various filament proteins (Komine et al., 2000, Radoja et al., 2004, Wu et al., 2001, Wu et al., 1994). Reduction in the cytoskeletal genes might facilitate retraction of the dendrites.

The reductions in dendritic architecture may contribute to decline vision ability with age. Alterations in neuronal morphology have been suggested to be the main course of decline motor, sensory and cognitive function (Hofer et al., 2003, Mattson and Magnus, 2006). Although reduction in dendrite complexity is more pronounced in disease, these changes in the ageing rat retina are less marked and therefore likely to have comparably reduced physiological effects.

Similar changes have been reported in other parts of the CNS. In the hippocampus, CA1 pyramidal neurons demonstrate elevated Ca^{2+} conductance as a result of age-related dendritic pruning, which might result in alteration in Ca^{2+} homeostasis (Thibault and Landfield, 1996, Toescu et al., 2004), contributing to plasticity impairment accompanying scenescence (Foster and Norris, 1997, Landfield, 1988). The elevated Ca^{2+} result in prolonged depolarisation suggesting a decrease in the number of fired action

potential (Burke and Barnes, 2006). Indeed, using in vitro hippocampal slice cultures, CA1 neurons showed to be less excitable (Moyer et al., 1992).

The retina, as part of the CNS, is a good model for studying the CNS because of its easy access. The highly multilayered organisation of the retina facilitated enrichment of a particular neuronal population. Work carried out on retinal neurons can be extrapolated for other neuronal populations in the CNS and also in PNS. For example, impairment in NF-kB activation has been shown to inhibit dendrite growth in developing sympathetic neurons (Gavalda et al., 2009, Gutierrez et al., 2008). Furthermore, on the behavioural level, it was shown that mice lacking a subunit of NF-kB have a learning deficit (Meffert and Baltimore, 2005).

The animals used for induction of glaucoma in this study were 24-52 weeks old, which corresponds to the age range when reduction in dendrite complexity was observed. Thus, retinae of these animals have already compromised neurons. These neurons are clearly susceptible to insults such as increased IOP and this might explain why glaucoma is associated with age. Few studies have addressed the physiological impacts of these changes in the retina. In glaucoma, dendritic pruning has been reported as a consistent early feature (Morgan et al., 2006, Weber and Harman, 2005, Weber et al., 1998). In the primate glaucoma model, electrophysiological studies of RGC with dendritic pruning demonstrated a reduced response rate and changes consistent with impaired spatial summation (Weber and Harman, 2005).

The findings here contribute to the general knowledge to the change that might underlie the reduction in retinal sensitivity as a function of age. These observations are important in the study of neurodegenerative diseases such as glaucoma in which the retinal ganglion cell population is selectively damage. Investigations into the pathophysiology of these diseases and into the assessment of therapeutic measures should be conducted on age appropriate animals. It seems likely that neurons with age related

changes/degeneration would be more susceptible to damage compared with younger neurons.

For instant, RCG axons of older animals are more susceptible to increased intraocular (IOP) damage as a result of age-dependent decline of metabolic capacity in these retina (Baltan et al., 2006). Also, in contrast to young optic nerve, white matter in older optic nerves shows a higher vulnerability when subject to ischemic injury (Baltan et al., 2006). This clearly suggests that changes in experimental glaucoma in young animals may not reflect changes that would be seen in ageing eyes.

In conclusion, reduction in cIAP1, which leads to impairment in survival pathway might be the underlaying course of reduction in dendrite complexity observed in this study (Fig. 7.1). Compromised dendrite complexity could be the key factor in age-related visual decline. Compromised RGC morphology makes a preparatory platform for neurodegenerative process observed in glaucoma disease where age is a major risk factor.

7.2 Future work

Although this study shows a decrease in dendrite complexity, the extent to which these changes apply to all RGCs remains unclear. Thus, it will be of high interest to determine which type of RGC show a higher/less degree of dendrite remodelling during ageing.

Manipulation of cIAP1 in order to determine to what extend it is involved in dendrite pruning during retina maturation process should be carried out. For example down-regulation of cIAP1 in 6 weeks old retina using siRNA and measurement of RGC dendritic field will show whether cIAP1 is directly involved in dendritic pruning or whether the dendrite pruning observed during retinal maturation is a result of a collection of factors where reduction of cIAP1 is one of the factors.

Further work is needed to correlate IAPs mRNA levels observed in glaucomatous eyes with protein levels. This will give a better handle on the role of IAPs in glaucoma disease etiology.

The cell death has been well documented in glaucoma with the principal placed on events in the apoptototic pathways. In other neurodegenerative diseases such AD, recent report have suggest other cell death modes are involved in elimination of the neurons. It will be interesting to explore whether other cell death i.e. autophagy is responsible for cell death in glaucoma.

Table 7.1. NF-kB-responsive genes in the nervous system

Gene	Function	References
Mn-SOD1 and 2	Manganese superoxides dismutase	Das et al, 1995; Xu et al., 2007
Cu/Zn-SOD	superoxides dismutase	Rojo et al., 2004;
Bcl-2	Pro-survival factor	Catz and Johnson, 2001
Bax	Pro-apoptotic Bcl-2 homologue	Grimm et al., 2004
Bcl-xL	Pro-apoptotic Bcl-2 homologue	Chen et al., 1999; Lee et al., 1999
Bim	Pro-apoptotic Bcl-2 homolog	Wang et al., 2008
IAPs	Inhibitors of apoptosis	You et al., 1997; Stehlik et al., 1998a and 1998b; Turner et al., 2007
TRAF1	TNF-receptor associated factor	Schwenzer et al., 1999
TRAF2	TNF-receptor associated factor	Wang et al., 1998
TRAF2 binding protein (Carp)	TRAF2 binding protein	Chang et al.,2005
BDNF	Brain derived neurotrophic factor	Saha et al., 2007
NMDA receptor	Neural receptor for N-methyl-D aspartate	Ritcher et al., 2002; Begni et al., 2003
VDCC	Voltage-dependent calcium chanel	Cheng et al., 1994; Furukawa et al., 1998
Calbidin	Calcium binding protein	
Inducible NO-synthesis (Cano et al.)	Nitric oxide synthesis	Geller et al., 1993; Morris et al., 2003; Guo et al., 2006; Hudges et al., 2008
Nueronal nitric oxide synthesis (nNOS)	Nitric oxide synthesis	Nakata et al., 2006; Li et al., 2007
Amiloride-sensitive sodium channel	Sodium channel	Baines et al., 2002; Haddad, 2005

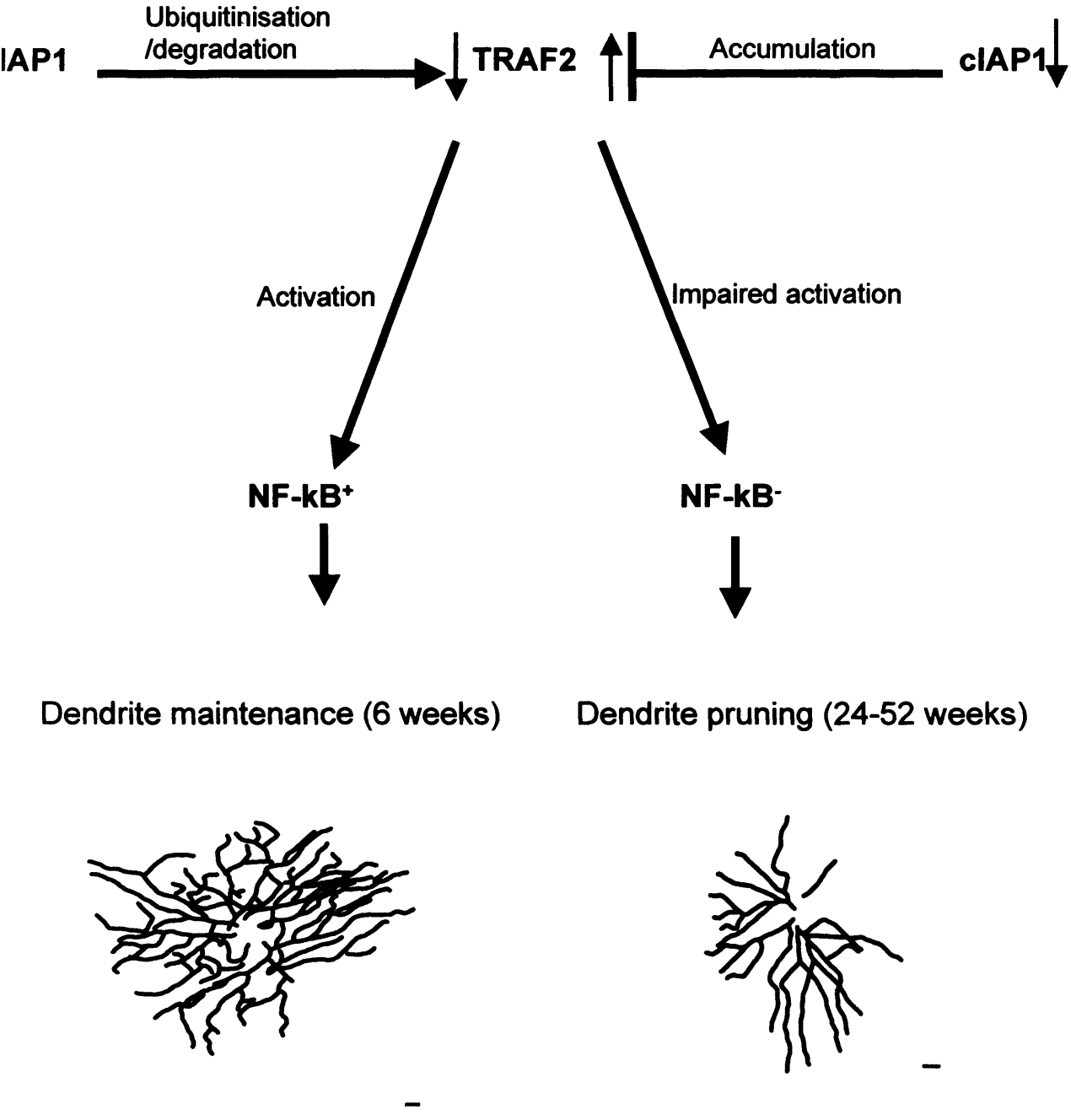

Figure 7.1. Schematic picture summarising cIAP1 role in neuronal plasticity. The traced neurons, represent 75% of dendrite complexity in respective populations. Scale bar, 20μm

References

A. KOIZUMA, T. J., RH MASLAND (2010) Spatial regularity of excitatory synapses within the inner plexiform layer. *ARVO abstract boklet.*

ADAMEC, E., MOHAN, P. S., CATALDO, A. M., VONSATTEL, J. P. & NIXON, R. A. (2000) Up-regulation of the lysosomal system in experimental models of neuronal injury: implications for Alzheimer's disease. *Neuroscience,* 100, 663-75.

ADAMS, I. (1987) Comparison of synaptic changes in the precentral and postcentral cerebral cortex of aging humans: a quantitative ultrastructural study. *Neurobiol Aging,* 8, 203-12.

ALAM, A., COHEN, L. Y., AOUAD, S. & SEKALY, R. P. (1999) Early activation of caspases during T lymphocyte stimulation results in selective substrate cleavage in nonapoptotic cells. *J Exp Med,* 190, 1879-90.

ALLEN, F. & WARNER, A. (1991) Gap junctional communication during neuromuscular junction formation. *Neuron,* 6, 101-11.

ALTIMUS, C. M., GULER, A. D., VILLA, K. L., MCNEILL, D. S., LEGATES, T. A. & HATTAR, S. (2008) Rods-cones and melanopsin detect light and dark to modulate sleep independent of image formation. *Proc Natl Acad Sci U S A,* 105, 19998-20003.

ASHHAB, Y., ALIAN, A., POLLIACK, A., PANET, A. & BEN YEHUDA, D. (2001) Two splicing variants of a new inhibitor of apoptosis gene with different biological properties and tissue distribution pattern. *FEBS Lett,* 495, 56-60.

ASHKENAZI, A. & DIXIT, V. M. (1998) Death receptors: signaling and modulation. *Science,* 281, 1305-8.

BALDWIN, A. S., JR. (1996) The NF-kappa B and I kappa B proteins: new discoveries and insights. *Annu Rev Immunol,* 14, 649-83.

BALL, M. J. (1977) Neuronal loss, neurofibrillary tangles and granulovacuolar degeneration in the hippocampus with ageing and dementia. A quantitative study. *Acta Neuropathol,* 37, 111-8.

BALOSSO, S., RAVIZZA, T., PEREGO, C., PESCHON, J., CAMPBELL, I. L., DE SIMONI, M. G. & VEZZANI, A. (2005) Tumor necrosis factor-alpha inhibits seizures in mice via p75 receptors. *Ann Neurol,* 57, 804-12.

BALTAN, S., INMAN, D. M., DANILOV, C. A., MORRISON, R. S., CALKINS, D. J. & HORNER, P. J. Metabolic vulnerability disposes retinal ganglion cell axons to dysfunction in a model of glaucomatous degeneration. *J Neurosci,* 30, 5644-52.

BARNARD, A. R., APPLEFORD, J. M., SEKARAN, S., CHINTHAPALLI, K., JENKINS, A., SEELIGER, M., BIEL, M., HUMPHRIES, P., DOUGLAS, R. H., WENZEL, A., FOSTER, R. G., HANKINS, M. W. & LUCAS, R. J. (2004) Residual photosensitivity in mice lacking both rod opsin and cone photoreceptor cyclic nucleotide gated channel 3 alpha subunit. *Vis Neurosci,* 21, 675-83.

BARNES, C. A. (1979) Memory deficits associated with senescence: a neurophysiological and behavioral study in the rat. *J Comp Physiol Psychol,* 93, 74-104.

BECKER, D., BONNESS, V. & MOBBS, P. (1998) Cell coupling in the retina: patterns and purpose. *Cell Biol Int,* 22, 781-92.

BECKER, D. L., BONNESS, V., CATSICAS, M. & MOBBS, P. (2002) Changing patterns of ganglion cell coupling and connexin expression during chick retinal development. *J Neurobiol,* 52, 280-93.

BECKER, D. L. & MOBBS, P. (1999) Connexin alpha1 and cell proliferation in the developing chick retina. *Exp Neurol,* 156, 326-32.

BENNETT, M. V., BARRIO, L. C., BARGIELLO, T. A., SPRAY, D. C., HERTZBERG, E. & SAEZ, J. C. (1991) Gap junctions: new tools, new answers, new questions. *Neuron,* 6, 305-20.

BENSAAD, K., TSURUTA, A., SELAK, M. A., VIDAL, M. N., NAKANO, K., BARTRONS, R., GOTTLIEB, E. & VOUSDEN, K. H. (2006) TIGAR, a p53-inducible regulator of glycolysis and apoptosis. *Cell,* 126, 107-20.

BERSON, D. M., DUNN, F. A. & TAKAO, M. (2002) Phototransduction by retinal ganglion cells that set the circadian clock. *Science,* 295, 1070-3.

BIZHEVA, K., PFLUG, R., HERMANN, B., POVAZAY, B., SATTMANN, H., QIU, P., ANGER, E., REITSAMER, H., POPOV, S., TAYLOR, J. R., UNTERHUBER, A., AHNELT, P. & DREXLER, W. (2006) Optophysiology: depth-resolved probing of retinal physiology with functional ultrahigh-resolution optical coherence tomography. *Proc Natl Acad Sci U S A,* 103, 5066-71.

BONHOEFFER, T. & YUSTE, R. (2002) Spine motility. Phenomenology, mechanisms, and function. *Neuron,* 35, 1019-27.

BRANNSTROM, T., HAVTON, L. & KELLERTH, J. O. (1992) Changes in size and dendritic arborization patterns of adult cat spinal alpha-motoneurons following permanent axotomy. *J Comp Neurol,* 318, 439-51.

BRODY, H. (1955) Organization of the cerebral cortex. III. A study of aging in the human cerebral cortex. *J Comp Neurol,* 102, 511-6.

BROWN, A. G. (2001) Nerve cells and nervous systems; An introduction to neuroscience. *New York, Springer,* Ed 2.

BURKE, S. N. & BARNES, C. A. (2006) Neural plasticity in the ageing brain. *Nat Rev Neurosci,* 7, 30-40.

BURTON, E. A., TINSLEY, J. M., HOLZFEIND, P. J., RODRIGUES, N. R. & DAVIES, K. E. (1999) A second promoter provides an alternative target for therapeutic up-regulation of utrophin in Duchenne muscular dystrophy. *Proc Natl Acad Sci U S A,* 96, 14025-30.

BUSTIN, S. A. (2000) Absolute quantification of mRNA using real-time reverse transcription polymerase chain reaction assays. *J Mol Endocrinol,* 25, 169-93.

CACERES, A., MAUTINO, J. & KOSIK, K. S. (1992) Suppression of MAP2 in cultured cerebellar macroneurons inhibits minor neurite formation. *Neuron,* 9, 607-18.

CAMANDOLA, S. & MATTSON, M. P. (2000) Pro-apoptotic action of PAR-4 involves inhibition of NF-kappaB activity and suppression of BCL-2 expression. *J Neurosci Res,* 61, 134-9.

CAMANDOLA, S., POLI, G. & MATTSON, M. P. (2000a) The lipid peroxidation product 4-hydroxy-2,3-nonenal increases AP-1-binding activity through caspase activation in neurons. *J Neurochem,* 74, 159-68.

CAMANDOLA, S., POLI, G. & MATTSON, M. P. (2000b) The lipid peroxidation product 4-hydroxy-2,3-nonenal inhibits constitutive and inducible activity of nuclear factor kappa B in neurons. *Brain Res Mol Brain Res,* 85, 53-60.

CANO, J., MACHADO, A. & REINOSO-SUAREZ, F. (1986) Morphological changes in the retina of ageing rats. *Arch Gerontol Geriatr,* 5, 41-50.

CAPRIOLI, J., KITANO, S. & MORGAN, J. E. (1996) Hyperthermia and hypoxia increase tolerance of retinal ganglion cells to anoxia and excitotoxicity. *Invest Ophthalmol Vis Sci,* 37, 2376-81.

CARLILE, G. W., SMITH, D. H. & WIEDMANN, M. (2004) Caspase-3 has a nonapoptotic function in erythroid maturation. *Blood,* 103, 4310-6.

CARTER, T. L. (1994) Age-related vision changes: a primary care guide. *Geriatrics,* 49, 37-42, 45; quiz 46-7.

CASTEDO, M., PERFETTINI, J. L., ROUMIER, T., ANDREAU, K., MEDEMA, R. & KROEMER, G. (2004) Cell death by mitotic catastrophe: a molecular definition. *Oncogene,* 23, 2825-37.

CAVALLOTTI, C., ARTICO, M., PESCOSOLIDO, N. & FEHER, J. (2001) Age-related changes in rat retina. *Jpn J Ophthalmol,* 45, 68-75.

CECCONI, F., ALVAREZ-BOLADO, G., MEYER, B. I., ROTH, K. A. & GRUSS, P. (1998) Apaf1 (CED-4 homolog) regulates programmed cell death in mammalian development. *Cell,* 94, 727-37.

CEPURNA, W. O., KAYTON, R. J., JOHNSON, E. C. & MORRISON, J. C. (2005) Age related optic nerve axonal loss in adult Brown Norway rats. *Exp Eye Res,* 80, 877-84.

CHAN, F. K., SHISLER, J., BIXBY, J. G., FELICES, M., ZHENG, L., APPEL, M., ORENSTEIN, J., MOSS, B. & LENARDO, M. J. (2003) A role for tumor necrosis factor receptor-2 and receptor-interacting protein in programmed necrosis and antiviral responses. *J Biol Chem,* 278, 51613-21.

CHEN, H. & WEBER, A. J. (2001) BDNF enhances retinal ganglion cell survival in cats with optic nerve damage. *Invest Ophthalmol Vis Sci,* 42, 966-74.

CHENG, L., SAPIEHA, P., KITTLEROVA, P., HAUSWIRTH, W. W. & DI POLO, A. (2002) TrkB gene transfer protects retinal ganglion cells from axotomy-induced death in vivo. *J Neurosci,* 22, 3977-86.

CHEUNG, Z. H., CHAN, Y. M., SIU, F. K., YIP, H. K., WU, W., LEUNG, M. C. & SO, K. F. (2004) Regulation of caspase activation in axotomized retinal ganglion cells. *Mol Cell Neurosci,* 25, 383-93.

CHINNAIYAN, A. M., O'ROURKE, K., TEWARI, M. & DIXIT, V. M. (1995) FADD, a novel death domain-containing protein, interacts with the death domain of Fas and initiates apoptosis. *Cell,* 81, 505-12.

CHU, Z. L., MCKINSEY, T. A., LIU, L., GENTRY, J. J., MALIM, M. H. & BALLARD, D. W. (1997) Suppression of tumor necrosis factor-induced cell death by inhibitor of apoptosis c-IAP2 is under NF-kappaB control. *Proc Natl Acad Sci U S A,* 94, 10057-62.

CHUN, H. J., ZHENG, L., AHMAD, M., WANG, J., SPEIRS, C. K., SIEGEL, R. M., DALE, J. K., PUCK, J., DAVIS, J., HALL, C. G., SKODA-SMITH, S., ATKINSON, T. P., STRAUS, S. E. & LENARDO, M. J. (2002) Pleiotropic defects in lymphocyte activation caused by caspase-8 mutations lead to human immunodeficiency. *Nature,* 419, 395-9.

CHUNG, J. Y., PARK, Y. C., YE, H. & WU, H. (2002) All TRAFs are not created equal: common and distinct molecular mechanisms of TRAF-mediated signal transduction. *J Cell Sci,* 115, 679-88.

CLEM, R. J. (2001) Baculoviruses and apoptosis: the good, the bad, and the ugly. *Cell Death Differ,* 8, 137-43.

COHEN, G. M. (1997) Caspases: the executioners of apoptosis. *Biochem J,* 326 (Pt 1), 1-16.

COLEMAN, P., FINCH, C. & JOSEPH, J. (1990) The need for multiple time points in aging studies. *Neurobiol Aging,* 11, 1-2.

COLEMAN, P. D. & FLOOD, D. G. (1987) Neuron numbers and dendritic extent in normal aging and Alzheimer's disease. *Neurobiol Aging,* 8, 521-45.

COOK, J. E. (1991) Correlated activity in the CNS: a role on every timescale? *Trends Neurosci,* 14, 397-401.

CRAIG, A. M. & BANKER, G. (1994) Neuronal polarity. *Annu Rev Neurosci,* 17, 267-310.

CRIGHTON, D., WILKINSON, S., O'PREY, J., SYED, N., SMITH, P., HARRISON, P. R., GASCO, M., GARRONE, O., CROOK, T. & RYAN, K. M. (2006) DRAM, a p53-induced modulator of autophagy, is critical for apoptosis. *Cell,* 126, 121-34.

CULPAN, D., CRAM, D., CHALMERS, K., CORNISH, A., PALMER, L., PALMER, J., HUGHES, A., PASSMORE, P., CRAIGS, D., WILCOCK, G. K., KEHOE, P. G. & LOVE, S. (2009) TNFR-associated factor-2 (TRAF-2) in Alzheimer's disease. *Neurobiol Aging,* 30, 1052-60.

CUPP, C. J. & UEMURA, E. (1980) Age-related changes in prefrontal cortex of Macaca mulatta: quantitative analysis of dendritic branching patterns. *Exp Neurol,* 69, 143-63.

CURCIO, C. A. & ALLEN, K. A. (1990) Topography of ganglion cells in human retina. *J Comp Neurol,* 300, 5-25.

DAILEY, M. E. & SMITH, S. J. (1996) The dynamics of dendritic structure in developing hippocampal slices. *J Neurosci,* 16, 2983-94.

DALLIMORE, E. J., CUI, Q., BEAZLEY, L. D. & HARVEY, A. R. (2002) Postnatal innervation of the rat superior colliculus by axons of late-born retinal ganglion cells. *Eur J Neurosci,* 16, 1295-304.

DANDONA, L. & DANDONA, R. (2006) What is the global burden of visual impairment? *BMC Med,* 4, 6.

DE BOEVER, S., VANGESTEL, C., DE BACKER, P., CROUBELS, S. & SYS, S. U. (2008) Identification and validation of housekeeping genes as internal control for gene expression in an intravenous LPS inflammation model in chickens. *Vet Immunol Immunopathol,* 122, 312-7.

DERISI, J. L. & IYER, V. R. (1999) Genomics and array technology. *Curr Opin Oncol,* 11, 76-9.

DEUTCH, A. Y. (2006) Striatal plasticity in parkinsonism: dystrophic changes in medium spiny neurons and progression in Parkinson's disease. *J Neural Transm Suppl*, 67-70.

DEVANEY, K. O. & JOHNSON, H. A. (1980) Neuron loss in the aging visual cortex of man. *J Gerontol,* 35, 836-41.

DEVERAUX, Q. L., TAKAHASHI, R., SALVESEN, G. S. & REED, J. C. (1997) X-linked IAP is a direct inhibitor of cell-death proteases. *Nature,* 388, 300-4.

DOUGLAS, G. R. (1998) Pathogenetic mechanisms of glaucoma not related to intraocular pressure. *Curr Opin Ophthalmol,* 9, 34-8.

DREHER, B., SEFTON, A. J., NI, S. Y. & NISBETT, G. (1985) The morphology, number, distribution and central projections of Class I retinal ganglion cells in albino and hooded rats. *Brain Behav Evol,* 26, 10-48.

DROUYER, E., DKHISSI-BENYAHYA, O., CHIQUET, C., WOLDEMUSSIE, E., RUIZ, G., WHEELER, L. A., DENIS, P. & COOPER, H. M. (2008) Glaucoma alters the circadian timing system. *PLoS One,* 3, e3931.

DUCKETT, C. S. (2005) IAP proteins: sticking it to Smac. *Biochem J,* 385, e1-2.

DUNAEVSKY, A., TASHIRO, A., MAJEWSKA, A., MASON, C. & YUSTE, R. (1999) Developmental regulation of spine motility in the mammalian central nervous system. *Proc Natl Acad Sci U S A,* 96, 13438-43.

DUPOUX, A., CARTIER, J., CATHELIN, S., FILOMENKO, R., SOLARY, E. & DUBREZ-DALOZ, L. (2009) cIAP1-dependent TRAF2 degradation regulates the differentiation of monocytes into macrophages and their response to CD40 ligand. *Blood,* 113, 175-85.

EARNSHAW, W. C., MARTINS, L. M. & KAUFMANN, S. H. (1999) Mammalian caspases: structure, activation, substrates, and functions during apoptosis. *Annu Rev Biochem,* 68, 383-424.

ECKELMAN, B. P. & SALVESEN, G. S. (2006) The human anti-apoptotic proteins cIAP1 and cIAP2 bind but do not inhibit caspases. *J Biol Chem,* 281, 3254-60.

EDINGER, A. L. & THOMPSON, C. B. (2004) Death by design: apoptosis, necrosis and autophagy. *Curr Opin Cell Biol,* 16, 663-9.

FALLS, D. L. (2005) Dasm1: a receptor that shapes neuronal dendrites and turns on silent synapses? *Sci STKE,* 2005, pe10.

FENG, L., SUN, Z., HAN, H., ZHOU, Y. & ZHANG, M. (2007) No age-related cell loss in three retinal nuclear layers of the Long-Evans rat. *Vis Neurosci,* 24, 799-803.

FENSTERMAKER, V., CHEN, Y., GHOSH, A., YUSTE, R. (2003) Regulation of dendritic length and branching by Semaphorin 3A. *J Neurobiol,* 58, 403-412.

FERRANTE, R. J., KOWALL, N. W. & RICHARDSON, E. P., JR. (1991) Proliferative and degenerative changes in striatal spiny neurons in Huntington's disease: a combined study using the section-Golgi method and calbindin D28k immunocytochemistry. *J Neurosci,* 11, 3877-87.

FIALA, J. C., SPACEK, J. & HARRIS, K. M. (2002) Dendritic spine pathology: cause or consequence of neurological disorders? *Brain Res Brain Res Rev,* 39, 29-54.

FINCH, C. E. (2009) The neurobiology of middle-age has arrived. *Neurobiol Aging,* 30, 515-20; discussion 530-33.

FISCHER, M., KAECH, S., KNUTTI, D. & MATUS, A. (1998) Rapid actin-based plasticity in dendritic spines. *Neuron,* 20, 847-54.

FLOOD, D. G. & COLEMAN, P. D. (1993) Dendritic regression dissociated from neuronal death but associated with partial deafferentation in aging rat supraoptic nucleus. *Neurobiol Aging,* 14, 575-87.

FOSTER, T. C. & NORRIS, C. M. (1997) Age-associated changes in Ca(2+)-dependent processes: relation to hippocampal synaptic plasticity. *Hippocampus,* 7, 602-12.

FREEDMAN, M. S., LUCAS, R. J., SONI, B., VON SCHANTZ, M., MUNOZ, M., DAVID-GRAY, Z. & FOSTER, R. (1999) Regulation of mammalian circadian behavior by non-rod, non-cone, ocular photoreceptors. *Science,* 284, 502-4.

FURUKAWA, K. & MATTSON, M. P. (1998) The transcription factor NF-kappaB mediates increases in calcium currents and decreases in NMDA- and AMPA/kainate-induced currents induced by tumor necrosis factor-alpha in hippocampal neurons. *J Neurochem,* 70, 1876-86.

GAASTERLAND, D. & KUPFER, C. (1974) Experimental glaucoma in the rhesus monkey. *Invest Ophthalmol,* 13, 455-7.

GALLI-RESTA, L. & ENSINI, M. (1996) An intrinsic time limit between genesis and death of individual neurons in the developing retinal ganglion cell layer. *J Neurosci,* 16, 2318-24.

GAN, L., WANG, S. W., HUANG, Z. & KLEIN, W. H. (1999) POU domain factor Brn-3b is essential for retinal ganglion cell differentiation and survival but not for initial cell fate specification. *Dev Biol,* 210, 469-80.

GAO, H. & HOLLYFIELD, J. G. (1992) Aging of the human retina. Differential loss of neurons and retinal pigment epithelial cells. *Invest Ophthalmol Vis Sci,* 33, 1-17.

GARCIA-VALENZUELA, E., SHAREEF, S., WALSH, J. & SHARMA, S. C. (1995) Programmed cell death of retinal ganglion cells during experimental glaucoma. *Exp Eye Res,* 61, 33-44.

GATZ, S. A. & WIESMULLER, L. (2006) p53 in recombination and repair. *Cell Death Differ,* 13, 1003-16.

GAVALDA, N., GUTIERREZ, H. & DAVIES, A. M. (2009) Developmental switch in NF-kappaB signalling required for neurite growth. *Development,* 136, 3405-12.

GENDRON, N. H. & MACKENZIE, A. E. (1999) Spinal muscular atrophy: molecular pathophysiology. *Curr Opin Neurol,* 12, 137-42.

GIBBS, R. A., WEINSTOCK, G. M., METZKER, M. L., MUZNY, D. M., SODERGREN, E. J., SCHERER, S., SCOTT, G., STEFFEN, D., WORLEY, K. C., BURCH, P. E., OKWUONU, G., HINES, S., LEWIS, L., DERAMO, C., DELGADO, O., DUGAN-ROCHA, S., MINER, G., MORGAN, M., HAWES, A., GILL, R., CELERA, HOLT, R. A., ADAMS, M. D., AMANATIDES, P. G., BADEN-TILLSON, H., BARNSTEAD, M., CHIN, S., EVANS, C. A., FERRIERA, S., FOSLER, C., GLODEK, A., GU, Z., JENNINGS, D., KRAFT, C. L., NGUYEN, T., PFANNKOCH, C. M., SITTER, C., SUTTON, G. G., VENTER, J. C., WOODAGE, T., SMITH, D., LEE, H. M., GUSTAFSON, E., CAHILL, P., KANA, A., DOUCETTE-STAMM, L., WEINSTOCK, K., FECHTEL, K., WEISS, R. B., DUNN, D. M., GREEN, E. D., BLAKESLEY, R. W., BOUFFARD, G. G., DE JONG, P. J., OSOEGAWA, K., ZHU, B., MARRA, M., SCHEIN, J., BOSDET, I., FJELL, C., JONES, S., KRZYWINSKI, M., MATHEWSON, C., SIDDIQUI, A., WYE, N., MCPHERSON, J., ZHAO, S., FRASER, C. M., SHETTY, J., SHATSMAN, S., GEER, K., CHEN, Y., ABRAMZON, S., NIERMAN, W. C., HAVLAK, P. H., CHEN, R., DURBIN, K. J., EGAN, A., REN, Y., SONG, X. Z., LI, B., LIU, Y., QIN, X., CAWLEY, S., WORLEY, K. C., COONEY, A. J., D'SOUZA, L. M., MARTIN, K., WU, J. Q., GONZALEZ-GARAY, M. L., JACKSON, A. R., KALAFUS, K. J., MCLEOD, M. P., MILOSAVLJEVIC, A., VIRK, D., VOLKOV, A., WHEELER, D. A., ZHANG, Z., BAILEY, J. A., EICHLER, E. E., et al. (2004) Genome sequence of the Brown Norway rat yields insights into mammalian evolution. *Nature,* 428, 493-521.

GILLOTEAUX, J., JAMISON, J. M., ARNOLD, D., ERVIN, E., ECKROAT, L., DOCHERTY, J. J., NEAL, D. & SUMMERS, J. L. (1998) Cancer cell necrosis by autoschizis: synergism of antitumor activity of vitamin C: vitamin K3 on human bladder carcinoma T24 cells. *Scanning,* 20, 564-75.

GILLOTEAUX, J., JAMISON, J. M., VENUGOPAL, M., GIAMMAR, D. & SUMMERS, J. L. (1995) Scanning electron microscopy and transmission electron microscopy aspects of synergistic antitumor activity of vitamin C - vitamin K3 combinations against human prostatic carcinoma cells. *Scanning Microsc,* 9, 159-73.

GILMAN, C. P. & MATTSON, M. P. (2002) Do apoptotic mechanisms regulate synaptic plasticity and growth-cone motility? *Neuromolecular Med,* 2, 197-214.

GLAZNER, G. W., CHAN, S. L., LU, C. & MATTSON, M. P. (2000) Caspase-mediated degradation of AMPA receptor subunits: a mechanism for preventing excitotoxic necrosis and ensuring apoptosis. *J Neurosci,* 20, 3641-9.

GLICK, D., BARTH, S. & MACLEOD, K. F. Autophagy: cellular and molecular mechanisms. *J Pathol,* 221, 3-12.

GOLSTEIN, P. & KROEMER, G. (2007) Cell death by necrosis: towards a molecular definition. *Trends Biochem Sci,* 32, 37-43.

GONZALEZ-MENENDEZ, I., CONTRERAS, F., CERNUDA-CERNUDA, R. & GARCIA-FERNANDEZ, J. M. No loss of melanopsin-expressing ganglion cells detected during postnatal development of the mouse retina. *Histol Histopathol,* 25, 73-82.

GOOLEY, J. J., LU, J., CHOU, T. C., SCAMMELL, T. E. & SAPER, C. B. (2001) Melanopsin in cells of origin of the retinohypothalamic tract. *Nat Neurosci,* 4, 1165.

GOOLEY, J. J., LU, J., FISCHER, D. & SAPER, C. B. (2003) A broad role for melanopsin in nonvisual photoreception. *J Neurosci,* 23, 7093-106.

GRAHAM, S. L., DRANCE, S. M., CHAUHAN, B. C., SWINDALE, N. V., HNIK, P., MIKELBERG, F. S. & DOUGLAS, G. R. (1996) Comparison of psychophysical and electrophysiological testing in early glaucoma. *Invest Ophthalmol Vis Sci,* 37, 2651-62.

GREEN, E. J., GREENOUGH, W. T. & SCHLUMPF, B. E. (1983) Effects of complex or isolated environments on cortical dendrites of middle-aged rats. *Brain Res,* 264, 233-40.

GREENBERG, A. H. (1996) Granzyme B-induced apoptosis. *Adv Exp Med Biol,* 406, 219-28.

GRILL, J. D. & RIDDLE, D. R. (2002) Age-related and laminar-specific dendritic changes in the medial frontal cortex of the rat. *Brain Res,* 937, 8-21.

GUERIN, M. B., MCKERNAN, D. P., O'BRIEN, C. J. & COTTER, T. G. (2006) Retinal ganglion cells: dying to survive. *Int J Dev Biol,* 50, 665-74.

GUPTA, N. & WEINREB, R. N. (1997) New definitions of glaucoma. *Curr Opin Ophthalmol,* 8, 38-41.

GUTIERREZ, H. & DAVIES, A. M. (2007) A fast and accurate procedure for deriving the Sholl profile in quantitative studies of neuronal morphology. *J Neurosci Methods,* 163, 24-30.

GUTIERREZ, H., HALE, V. A., DOLCET, X. & DAVIES, A. (2005) NF-kappaB signalling regulates the growth of neural processes in the developing PNS and CNS. *Development,* 132, 1713-26.

GUTIERREZ, H., O'KEEFFE, G. W., GAVALDA, N., GALLAGHER, D. & DAVIES, A. M. (2008) Nuclear factor kappa B signaling either stimulates or inhibits neurite growth depending on the phosphorylation status of p65/RelA. *J Neurosci,* 28, 8246-56.

HALL, A. (1998) Rho GTPases and the actin cytoskeleton. *Science,* 279, 509-14.

HAO, Y., SEKINE, K., KAWABATA, A., NAKAMURA, H., ISHIOKA, T., OHATA, H., KATAYAMA, R., HASHIMOTO, C., ZHANG, X., NODA, T., TSURUO, T. & NAITO, M. (2004) Apollon ubiquitinates SMAC and caspase-9, and has an essential cytoprotection function. *Nat Cell Biol,* 6, 849-60.

HARMAN, A., ABRAHAMS, B., MOORE, S. & HOSKINS, R. (2000) Neuronal density in the human retinal ganglion cell layer from 16-77 years. *Anat Rec,* 260, 124-31.

HARMAN, A. M., MACDONALD, A., MEYER, P. & AHMAT, A. (2003) Numbers of neurons in the retinal ganglion cell layer of the rat do not change throughout life. *Gerontology,* 49, 350-5.

HARMAN, A. M., MOORE, S., HOSKINS, R. & KELLER, P. (1999) Horse vision and an explanation for the visual behaviour originally explained by the 'ramp retina'. *Equine Vet J,* 31, 384-90.

HARRINGTON, C. A., ROSENOW, C. & RETIEF, J. (2000) Monitoring gene expression using DNA microarrays. *Curr Opin Microbiol,* 3, 285-91.

HATTAR, S., KUMAR, M., PARK, A., TONG, P., TUNG, J., YAU, K. W. & BERSON, D. M. (2006) Central projections of melanopsin-expressing retinal ganglion cells in the mouse. *J Comp Neurol,* 497, 326-49.

HATTAR, S., LIAO, H. W., TAKAO, M., BERSON, D. M. & YAU, K. W. (2002) Melanopsin-containing retinal ganglion cells: architecture, projections, and intrinsic photosensitivity. *Science,* 295, 1065-70.

HE, Z., WANG, K. C., KOPRIVICA, V., MING, G. & SONG, H. J. (2002) Knowing how to navigate: mechanisms of semaphorin signaling in the nervous system. *Sci STKE,* 2002, RE1.

HENDERSON, G., TOMLINSON, B. E. & GIBSON, P. H. (1980) Cell counts in human cerebral cortex in normal adults throughout life using an image analysing computer. *J Neurol Sci,* 46, 113-36.

HERZOG, K. H. & VON BARTHELD, C. S. (1998) Contributions of the optic tectum and the retina as sources of brain-derived neurotrophic factor for retinal ganglion cells in the chick embryo. *J Neurosci,* 18, 2891-906.

HICKMOTT, P. W. & ETHELL, I. M. (2006) Dendritic plasticity in the adult neocortex. *Neuroscientist,* 12, 16-28.

HOFER, S. M., BERG, S. & ERA, P. (2003) Evaluating the interdependence of aging-related changes in visual and auditory acuity, balance, and cognitive functioning. *Psychol Aging,* 18, 285-305.

HOFMANN, K., BUCHER, P. & TSCHOPP, J. (1997) The CARD domain: a new apoptotic signalling motif. *Trends Biochem Sci,* 22, 155-6.

HORIKOSHI, T., DANENBERG, K. D., STADLBAUER, T. H., VOLKENANDT, M., SHEA, L. C., AIGNER, K., GUSTAVSSON, B., LEICHMAN, L., FROSING, R., RAY, M. & ET AL. (1992) Quantitation of thymidylate synthase, dihydrofolate reductase, and DT-diaphorase gene expression in human tumors using the polymerase chain reaction. *Cancer Res,* 52, 108-16.

HSU, H., SHU, H. B., PAN, M. G. & GOEDDEL, D. V. (1996) TRADD-TRAF2 and TRADD-FADD interactions define two distinct TNF receptor 1 signal transduction pathways. *Cell,* 84, 299-308.

HSU, H., XIONG, J. & GOEDDEL, D. V. (1995) The TNF receptor 1-associated protein TRADD signals cell death and NF-kappa B activation. *Cell,* 81, 495-504.

HUANG, E. J. & REICHARDT, L. F. (2003) Trk receptors: roles in neuronal signal transduction. *Annu Rev Biochem,* 72, 609-42.

HUANG, Y., CEN, L. P., LUO, J. M., WANG, N., ZHANG, M. Z., VAN ROOIJEN, N., PANG, C. P. & CUI, Q. (2008) Differential roles of phosphatidylinositol 3-kinase/akt pathway in retinal ganglion cell survival in rats with or without acute ocular hypertension. *Neuroscience,* 153, 214-25.

ILIA, M. & JEFFERY, G. (1996) Delayed neurogenesis in the albino retina: evidence of a role for melanin in regulating the pace of cell generation. *Brain Res Dev Brain Res,* 95, 176-83.

ISENMANN, S., KRETZ, A. & CELLERINO, A. (2003) Molecular determinants of retinal ganglion cell development, survival, and regeneration. *Prog Retin Eye Res,* 22, 483-543.

ISHII, T., WALLACE, A. M., ZHANG, X., GOSSELINK, J., ABBOUD, R. T., ENGLISH, J. C., PARE, P. D. & SANDFORD, A. J. (2006) Stability of housekeeping genes in alveolar macrophages from COPD patients. *Eur Respir J,* 27, 300-6.

ISHIZAKI, Y., JACOBSON, M. D. & RAFF, M. C. (1998) A role for caspases in lens fiber differentiation. *J Cell Biol,* 140, 153-8.

JAATTELA, M. & TSCHOPP, J. (2003) Caspase-independent cell death in T lymphocytes. *Nat Immunol,* 4, 416-23.

JACOBSON, M. (1991) Developmental biology. *New york: Plenum press.*

JAKOBS, T. C., LIBBY, R. T., BEN, Y., JOHN, S. W. & MASLAND, R. H. (2005) Retinal ganglion cell degeneration is topological but not cell type specific in DBA/2J mice. *J Cell Biol,* 171, 313-25.

JAMISON, J. M., GILLOTEAUX, J., TAPER, H. S., CALDERON, P. B. & SUMMERS, J. L. (2002) Autoschizis: a novel cell death. *Biochem Pharmacol,* 63, 1773-83.

JAN, Y. N. & JAN, L. Y. (2003) The control of dendrite development. *Neuron,* 40, 229-42.

JIA, L., CEPURNA, W. O., JOHNSON, E. C. & MORRISON, J. C. (2000) Effect of general anesthetics on IOP in rats with experimental aqueous outflow obstruction. *Invest Ophthalmol Vis Sci,* 41, 3415-9.

JIANG, X. & WANG, X. (2004) Cytochrome C-mediated apoptosis. *Annu Rev Biochem,* 73, 87-106.

JIN, S. (2006) Autophagy, mitochondrial quality control, and oncogenesis. *Autophagy,* 2, 80-4.

JOHN, S. W., ANDERSON, M. G. & SMITH, R. S. (1999) Mouse genetics: a tool to help unlock the mechanisms of glaucoma. *J Glaucoma,* 8, 400-12.

JOHN, S. W., SMITH, R. S., SAVINOVA, O. V., HAWES, N. L., CHANG, B., TURNBULL, D., DAVISSON, M., RODERICK, T. H. & HECKENLIVELY, J. R. (1998) Essential iris atrophy, pigment dispersion, and glaucoma in DBA/2J mice. *Invest Ophthalmol Vis Sci,* 39, 951-62.

JOHNSON, C. A. (1994) Selective versus non-selective losses in glaucoma. *J Glaucoma,* 3, 532-4.

JOHNSON, C. A., CIOFFI, G. A., LIEBMANN, J. R., SAMPLE, P. A., ZANGWILL, L. M. & WEINREB, R. N. (2000) The relationship between structural and functional alterations in glaucoma: a review. *Semin Ophthalmol,* 15, 221-33.

JOHNSON, E. C., MORRISON, J. C., FARRELL, S., DEPPMEIER, L., MOORE, C. G. & MCGINTY, M. R. (1996) The effect of chronically elevated intraocular pressure on the rat optic nerve head extracellular matrix. *Exp Eye Res,* 62, 663-74.

JOHNSTON, D. & NARAYANAN, R. (2008) Active dendrites: colorful wings of the mysterious butterflies. *Trends Neurosci,* 31, 309-16.

JONAS, J. B. & HAYREH, S. S. (2000) Ophthalmoscopic appearance of the normal optic nerve head in rhesus monkeys. *Invest Ophthalmol Vis Sci,* 41, 2978-83.

JONAS, J. B., MULLER-BERGH, J. A., SCHLOTZER-SCHREHARDT, U. M. & NAUMANN, G. O. (1990) Histomorphometry of the human optic nerve. *Invest Ophthalmol Vis Sci,* 31, 736-44.

JONAS, J. B., NGUYEN, N. X. & NAUMANN, G. O. (1989) The retinal nerve fiber layer in normal eyes. *Ophthalmology,* 96, 627-32.

JURASKA, J. M. (1982) The development of pyramidal neurons after eye opening in the visual cortex of hooded rats: a quantitative study. *J Comp Neurol,* 212, 208-13.

KALLONIATIS, M., HARWERTH, R. S., SMITH, E. L., 3RD & DESANTIS, L. (1993) Colour vision anomalies following experimental glaucoma in monkeys. *Ophthalmic Physiol Opt,* 13, 56-67.

KARIN, M. (1996) The regulation of AP-1 activity by mitogen-activated protein kinases. *Philos Trans R Soc Lond B Biol Sci,* 351, 127-34.

KASOF, G. M. & GOMES, B. C. (2001) Livin, a novel inhibitor of apoptosis protein family member. *J Biol Chem,* 276, 3238-46.

KATZ, M. L. & ROBISON, W. G., JR. (1986) Evidence of cell loss from the rat retina during senescence. *Exp Eye Res,* 42, 293-304.

KEGEL, K. B., KIM, M., SAPP, E., MCINTYRE, C., CASTANO, J. G., ARONIN, N. & DIFIGLIA, M. (2000) Huntingtin expression stimulates endosomal-lysosomal activity, endosome tubulation, and autophagy. *J Neurosci,* 20, 7268-78.

KENNEDY, N. J., KATAOKA, T., TSCHOPP, J. & BUDD, R. C. (1999) Caspase activation is required for T cell proliferation. *J Exp Med,* 190, 1891-6.

KERR, J. F., WYLLIE, A. H. & CURRIE, A. R. (1972) Apoptosis: a basic biological phenomenon with wide-ranging implications in tissue kinetics. *Br J Cancer,* 26, 239-57.

KERRIGAN, L. A., ZACK, D. J., QUIGLEY, H. A., SMITH, S. D. & PEASE, M. E. (1997) TUNEL-positive ganglion cells in human primary open-angle glaucoma. *Arch Ophthalmol,* 115, 1031-5.

KERRIGAN-BAUMRIND, L. A., QUIGLEY, H. A., PEASE, M. E., KERRIGAN, D. F. & MITCHELL, R. S. (2000) Number of ganglion cells in glaucoma eyes compared with threshold visual field tests in the same persons. *Invest Ophthalmol Vis Sci,* 41, 741-8.

KHAW, P. T., SHAH, P. & ELKINGTON, A. R. (2004) Glaucoma--1: diagnosis. *BMJ,* 328, 97-9.

KIM, C. B., TOM, B. W. & SPEAR, P. D. (1996) Effects of aging on the densities, numbers, and sizes of retinal ganglion cells in rhesus monkey. *Neurobiol Aging,* 17, 431-8.

KIM, H. S. & PARK, C. K. (2005) Retinal ganglion cell death is delayed by activation of retinal intrinsic cell survival program. *Brain Res,* 1057, 17-28.

KINBARA, K., ISHIURA, S., TOMIOKA, S., SORIMACHI, H., JEONG, S. Y., AMANO, S., KAWASAKI, H., KOLMERER, B., KIMURA, S., LABEIT, S. & SUZUKI, K. (1998) Purification of native p94, a muscle-specific calpain, and characterization of its autolysis. *Biochem J,* 335 (Pt 3), 589-96.

KISISWA, L., DERVAN, A. G., ALBON, J., MORGAN, J. E. & WRIDE, M. A. (2009) Retinal Ganglion Cell Death Postponed: Giving Apoptosis a Break? *Ophthalmic Res,* 43, 61-78.

KNOBLOCH, M. & MANSUY, I. M. (2008) Dendritic spine loss and synaptic alterations in Alzheimer's disease. *Mol Neurobiol,* 37, 73-82.

KOENDERINK, M. J. & UYLINGS, H. B. (1995) Postnatal maturation of layer V pyramidal neurons in the human prefrontal cortex. A quantitative Golgi analysis. *Brain Res,* 678, 233-43.

KOLB, B. & WHISHAW, I. Q. (1998) Brain plasticity and behavior. *Annu Rev Psychol,* 49, 43-64.

KOMINE, M., RAO, L. S., KANEKO, T., TOMIC-CANIC, M., TAMAKI, K., FREEDBERG, I. M. & BLUMENBERG, M. (2000) Inflammatory versus proliferative processes in epidermis. Tumor necrosis factor alpha induces K6b keratin synthesis through a transcriptional complex containing NFkappa B and C/EBPbeta. *J Biol Chem,* 275, 32077-88.

KORTLEVER, R. M., HIGGINS, P. J. & BERNARDS, R. (2006) Plasminogen activator inhibitor-1 is a critical downstream target of p53 in the induction of replicative senescence. *Nat Cell Biol,* 8, 877-84.

KRETZ, A., MARTICKE, J. K., HAPPOLD, C. J., SCHMEER, C. & ISENMANN, S. (2007) A primary culture technique of adult retina for regeneration studies on adult CNS neurons. *Nat Protoc,* 2, 131-40.

KUEHN, M. H., FINGERT, J. H. & KWON, Y. H. (2005) Retinal ganglion cell death in glaucoma: mechanisms and neuroprotective strategies. *Ophthalmol Clin North Am,* 18, 383-95, vi.

KUGLER, S., KLOCKER, N., KERMER, P., ISENMANN, S. & BAHR, M. (1999) Transduction of axotomized retinal ganglion cells by adenoviral vector administration at the optic nerve stump: an in vivo model system for the inhibition of neuronal apoptotic cell death. *Gene Ther,* 6, 1759-67.

KUGLER, S., STRATEN, G., KREPPEL, F., ISENMANN, S., LISTON, P. & BAHR, M. (2000) The X-linked inhibitor of apoptosis (XIAP) prevents cell death in axotomized CNS neurons in vivo. *Cell Death Differ,* 7, 815-24.

KUO, C. T., JAN, L. Y. & JAN, Y. N. (2005) Dendrite-specific remodeling of Drosophila sensory neurons requires matrix metalloproteases, ubiquitin-proteasome, and ecdysone signaling. *Proc Natl Acad Sci U S A,* 102, 15230-5.

KUO, C. T., ZHU, S., YOUNGER, S., JAN, L. Y. & JAN, Y. N. (2006) Identification of E2/E3 ubiquitinating enzymes and caspase activity regulating Drosophila sensory neuron dendrite pruning. *Neuron,* 51, 283-90.

KURANAGA, E., KANUKA, H., TONOKI, A., TAKEMOTO, K., TOMIOKA, T., KOBAYASHI, M., HAYASHI, S. & MIURA, M. (2006) Drosophila IKK-related kinase regulates nonapoptotic function of caspases via degradation of IAPs. *Cell,* 126, 583-96.

LANDFIELD, P. W. (1988) Hippocampal neurobiological mechanisms of age-related memory dysfunction. *Neurobiol Aging,* 9, 571-9.

LAPTENKO, O. & PRIVES, C. (2006) Transcriptional regulation by p53: one protein, many possibilities. *Cell Death Differ,* 13, 951-61.

LEE, M. S., KWON, Y. T., LI, M., PENG, J., FRIEDLANDER, R. M. & TSAI, L. H. (2000) Neurotoxicity induces cleavage of p35 to p25 by calpain. *Nature,* 405, 360-4.

LEVINE, B. & KLIONSKY, D. J. (2004) Development by self-digestion: molecular mechanisms and biological functions of autophagy. *Dev Cell,* 6, 463-77.

LEVKOVITCH-VERBIN, H. (2004) Animal models of optic nerve diseases. *Eye,* 18, 1066-74.

LEVKOVITCH-VERBIN, H., DARDIK, R., VANDER, S., NISGAV, Y., KALEV-LANDOY, M. & MELAMED, S. (2006) Experimental glaucoma and optic nerve transection induce simultaneous upregulation of proapoptotic and prosurvival genes. *Invest Ophthalmol Vis Sci,* 47, 2491-7.

LEVKOVITCH-VERBIN, H., HARIZMAN, N., DARDIK, R., NISGAV, Y., VANDER, S. & MELAMED, S. (2007) Regulation of cell death and survival pathways in experimental glaucoma. *Exp Eye Res,* 85, 250-8.

LEVKOVITCH-VERBIN, H., QUIGLEY, H. A., MARTIN, K. R., VALENTA, D., BAUMRIND, L. A. & PEASE, M. E. (2002) Translimbal laser photocoagulation to the trabecular meshwork as a model of glaucoma in rats. *Invest Ophthalmol Vis Sci,* 43, 402-10.

LI, H., ZHU, H., XU, C. J. & YUAN, J. (1998) Cleavage of BID by caspase 8 mediates the mitochondrial damage in the Fas pathway of apoptosis. *Cell,* 94, 491-501.

LI, K. Z., LINDENBERGER, U., FREUND, A. M. & BALTES, P. B. (2001) Walking while memorizing: age-related differences in compensatory behavior. *Psychol Sci,* 12, 230-7.

LI, R. S., CHEN, B. Y., TAY, D. K., CHAN, H. H., PU, M. L. & SO, K. F. (2006) Melanopsin-expressing retinal ganglion cells are more injury-resistant in a chronic ocular hypertension model. *Invest Ophthalmol Vis Sci,* 47, 2951-8.

LI, X., YANG, Y. & ASHWELL, J. D. (2002) TNF-RII and c-IAP1 mediate ubiquitination and degradation of TRAF2. *Nature,* 416, 345-7.

LIETS, L. C., ELIASIEH, K., VAN DER LIST, D. A. & CHALUPA, L. M. (2006) Dendrites of rod bipolar cells sprout in normal aging retina. *Proc Natl Acad Sci U S A,* 103, 12156-60.

LIN, J. H., WEIGEL, H., COTRINA, M. L., LIU, S., BUENO, E., HANSEN, A. J., HANSEN, T. W., GOLDMAN, S. & NEDERGAARD, M. (1998) Gap-junction-mediated propagation and amplification of cell injury. *Nat Neurosci,* 1, 494-500.

LIPPMAN, J. & DUNAEVSKY, A. (2005) Dendritic spine morphogenesis and plasticity. *J Neurobiol,* 64, 47-57.

LISTON, P., FONG, W. G., KELLY, N. L., TOJI, S., MIYAZAKI, T., CONTE, D., TAMAI, K., CRAIG, C. G., MCBURNEY, M. W. & KORNELUK, R. G. (2001) Identification of XAF1 as an antagonist of XIAP anti-Caspase activity. *Nat Cell Biol,* 3, 128-33.

LISTON, P., FONG, W. G. & KORNELUK, R. G. (2003) The inhibitors of apoptosis: there is more to life than Bcl2. *Oncogene,* 22, 8568-80.

LIU, Q. A. & HENGARTNER, M. O. (1999) The molecular mechanism of programmed cell death in C. elegans. *Ann N Y Acad Sci,* 887, 92-104.

LIVAK, K. J. & SCHMITTGEN, T. D. (2001) Analysis of relative gene expression data using real-time quantitative PCR and the 2(-Delta Delta C(T)) Method. *Methods,* 25, 402-8.

LOCKEY, C., OTTO, E. & LONG, Z. (1998) Real-time fluorescence detection of a single DNA molecule. *Biotechniques,* 24, 744-6.

LU, C., FU, W., SALVESEN, G. S. & MATTSON, M. P. (2002) Direct cleavage of AMPA receptor subunit GluR1 and suppression of AMPA currents by caspase-3: implications for synaptic plasticity and excitotoxic neuronal death. *Neuromolecular Med,* 1, 69-79.

LU, C., WANG, Y., FURUKAWA, K., FU, W., OUYANG, X. & MATTSON, M. P. (2006) Evidence that caspase-1 is a negative regulator of AMPA receptor-mediated long-term potentiation at hippocampal synapses. *J Neurochem,* 97, 1104-10.

LUCAS, R. J., DOUGLAS, R. H. & FOSTER, R. G. (2001) Characterization of an ocular photopigment capable of driving pupillary constriction in mice. *Nat Neurosci,* 4, 621-6.

LUCAS, R. J., FREEDMAN, M. S., MUNOZ, M., GARCIA-FERNANDEZ, J. M. & FOSTER, R. G. (1999) Regulation of the mammalian pineal by non-rod, non-cone, ocular photoreceptors. *Science,* 284, 505-7.

LUPI, D., OSTER, H., THOMPSON, S. & FOSTER, R. G. (2008) The acute light-induction of sleep is mediated by OPN4-based photoreception. *Nat Neurosci,* 11, 1068-73.

MABUCHI, F., AIHARA, M., MACKEY, M. R., LINDSEY, J. D. & WEINREB, R. N. (2003) Optic nerve damage in experimental mouse ocular hypertension. *Invest Ophthalmol Vis Sci,* 44, 4321-30.

MAHONEY, D. J., CHEUNG, H. H., MRAD, R. L., PLENCHETTE, S., SIMARD, C., ENWERE, E., ARORA, V., MAK, T. W., LACASSE, E. C., WARING, J. & KORNELUK, R. G. (2008) Both cIAP1 and cIAP2 regulate TNFalpha-mediated NF-kappaB activation. *Proc Natl Acad Sci U S A,* 105, 11778-83.

MANN, D. M. (1996) Pyramidal nerve cell loss in Alzheimer's disease. *Neurodegeneration,* 5, 423-7.

MARKOWSKA, A. L., SPANGLER, E. L. & INGRAM, D. K. (1998) Behavioral assessment of the senescence-accelerated mouse (SAM P8 and R1). *Physiol Behav,* 64, 15-26.

MARTIN, K. R., LEVKOVITCH-VERBIN, H., VALENTA, D., BAUMRIND, L., PEASE, M. E. & QUIGLEY, H. A. (2002) Retinal glutamate transporter changes in experimental glaucoma and after optic nerve transection in the rat. *Invest Ophthalmol Vis Sci,* 43, 2236-43.

MASLAND, R. H. (2001) The fundamental plan of the retina. *Nat Neurosci,* 4, 877-86.

MASLIM, J., WEBSTER, M. & STONE, J. (1986) Stages in the structural differentiation of retinal ganglion cells. *J Comp Neurol,* 254, 382-402.

MATOBA, S., KANG, J. G., PATINO, W. D., WRAGG, A., BOEHM, M., GAVRILOVA, O., HURLEY, P. J., BUNZ, F. & HWANG, P. M. (2006) p53 regulates mitochondrial respiration. *Science,* 312, 1650-3.

MATTSON, M. P. (2006) Neuronal life-and-death signaling, apoptosis, and neurodegenerative disorders. *Antioxid Redox Signal,* 8, 1997-2006.

MATTSON, M. P. & DUAN, W. (1999) "Apoptotic" biochemical cascades in synaptic compartments: roles in adaptive plasticity and neurodegenerative disorders. *J Neurosci Res,* 58, 152-66.

MATTSON, M. P. & MAGNUS, T. (2006) Ageing and neuronal vulnerability. *Nat Rev Neurosci,* 7, 278-94.

MCALLISTER, A. K. (2000) Cellular and molecular mechanisms of dendrite growth. *Cereb Cortex,* 10, 963-73.

MCALLISTER, A. K., LO, D. C. & KATZ, L. C. (1995) Neurotrophins regulate dendritic growth in developing visual cortex. *Neuron,* 15, 791-803.

MCARDLE, J. J., FERRER-CAJA, E., HAMAGAMI, F. & WOODCOCK, R. W. (2002) Comparative longitudinal structural analyses of the growth and decline of multiple intellectual abilities over the life span. *Dev Psychol,* 38, 115-42.

MCKERNAN, D. P., CAPLIS, C., DONOVAN, M., O'BRIEN C, J. & COTTER, T. G. (2006) Age-dependent susceptibility of the retinal ganglion cell layer to cell death. *Invest Ophthalmol Vis Sci,* 47, 807-14.

MCKINNON, S. J., LEHMAN, D. M., TAHZIB, N. G., RANSOM, N. L., REITSAMER, H. A., LISTON, P., LACASSE, E., LI, Q., KORNELUK, R. G. & HAUSWIRTH, W. W. (2002) Baculoviral IAP repeat-containing-4 protects optic nerve axons in a rat glaucoma model. *Mol Ther,* 5, 780-7.

MCNEILL, T. H., BROWN, S. A., RAFOLS, J. A. & SHOULSON, I. (1988) Atrophy of medium spiny I striatal dendrites in advanced Parkinson's disease. *Brain Res,* 455, 148-52.

MEFFERT, M. K. & BALTIMORE, D. (2005) Physiological functions for brain NF-kappaB. *Trends Neurosci,* 28, 37-43.

MELLONI, E., MICHETTI, M., SALAMINO, F., MINAFRA, R. & PONTREMOLI, S. (1996) Modulation of the calpain autoproteolysis by calpastatin and phospholipids. *Biochem Biophys Res Commun,* 229, 193-7.

MERRY, D. E. & KORSMEYER, S. J. (1997) Bcl-2 gene family in the nervous system. *Annu Rev Neurosci,* 20, 245-67.

MOGI, M. & TOGARI, A. (2003) Activation of caspases is required for osteoblastic differentiation. *J Biol Chem,* 278, 47477-82.

MONTELL, D. J. (2006) A kinase gets caspases into shape. *Cell,* 126, 450-2.
MONTGOMERY, S. M. (2009) In situ Hybridization.

MOOLMAN, D. L., VITOLO, O. V., VONSATTEL, J. P. & SHELANSKI, M. L. (2004) Dendrite and dendritic spine alterations in Alzheimer models. *J Neurocytol,* 33, 377-87.

MOORE, C. G., EPLEY, D., MILNE, S. T. & MORRISON, J. C. (1995) Long-term non-invasive measurement of intraocular pressure in the rat eye. *Curr Eye Res,* 14, 711-7.

MOREIRA, P. I., SIEDLAK, S. L., WANG, X., SANTOS, M. S., OLIVEIRA, C. R., TABATON, M., NUNOMURA, A., SZWEDA, L. I., ALIEV, G., SMITH, M. A., ZHU, X. & PERRY, G. (2007) Autophagocytosis of mitochondria is prominent in Alzheimer disease. *J Neuropathol Exp Neurol,* 66, 525-32.

MORGAN, J., CAPRIOLI, J. & KOSEKI, Y. (1999a) Nitric oxide mediates excitotoxic and anoxic damage in rat retinal ganglion cells cocultured with astroglia. *Arch Ophthalmol,* 117, 1524-9.

MORGAN, J. E. (1994) Selective cell death in glaucoma: does it really occur? *Br J Ophthalmol,* 78, 875-9; discussion 879-80.

MORGAN, J. E. (2002) Retinal ganglion cell shrinkage in glaucoma. *J Glaucoma,* 11, 365-70.

MORGAN, J. E., DATTA, A. V., ERICHSEN, J. T., ALBON, J. & BOULTON, M. E. (2006) Retinal ganglion cell remodelling in experimental glaucoma. *Adv Exp Med Biol,* 572, 397-402.

MORGAN, J. E., UCHIDA, H. & CAPRIOLI, J. (2000) Retinal ganglion cell death in experimental glaucoma. *Br J Ophthalmol,* 84, 303-10.

MORGAN, T. E., XIE, Z., GOLDSMITH, S., YOSHIDA, T., LANZREIN, A. S., STONE, D., ROZOVSKY, I., PERRY, G., SMITH, M. A. & FINCH, C. E. (1999b) The mosaic of brain glial hyperactivity during normal ageing and its attenuation by food restriction. *Neuroscience,* 89, 687-99.

MORIN, L. P., BLANCHARD, J. H. & PROVENCIO, I. (2003) Retinal ganglion cell projections to the hamster suprachiasmatic nucleus, intergeniculate leaflet, and visual midbrain: bifurcation and melanopsin immunoreactivity. *J Comp Neurol,* 465, 401-16.

MORRISON, J., FARRELL, S., JOHNSON, E., DEPPMEIER, L., MOORE, C. G. & GROSSMANN, E. (1995) Structure and composition of the rodent lamina cribrosa. *Exp Eye Res,* 60, 127-35.

MORRISON, J. C. (2005) Elevated intraocular pressure and optic nerve injury models in the rat. *J Glaucoma,* 14, 315-7.

MORRISON, J. C., CORK, L. C., DUNKELBERGER, G. R., BROWN, A. & QUIGLEY, H. A. (1990) Aging changes of the rhesus monkey optic nerve. *Invest Ophthalmol Vis Sci,* 31, 1623-7.

MORRISON, J. C., JOHNSON, E. C., CEPURNA, W. & JIA, L. (2005) Understanding mechanisms of pressure-induced optic nerve damage. *Prog Retin Eye Res,* 24, 217-40.

MORRISON, J. C., MOORE, C. G., DEPPMEIER, L. M., GOLD, B. G., MESHUL, C. K. & JOHNSON, E. C. (1997) A rat model of chronic pressure-induced optic nerve damage. *Exp Eye Res,* 64, 85-96.

MORRISON, J. H. & HOF, P. R. (1997) Life and death of neurons in the aging brain. *Science,* 278, 412-9.

MOUATT-PRIGENT, A., KARLSSON, J. O., AGID, Y. & HIRSCH, E. C. (1996) Increased M-calpain expression in the mesencephalon of patients with Parkinson's disease but not in other neurodegenerative disorders involving the mesencephalon: a role in nerve cell death? *Neuroscience,* 73, 979-87.

MOYER, J. R., JR., THOMPSON, L. T., BLACK, J. P. & DISTERHOFT, J. F. (1992) Nimodipine increases excitability of rabbit CA1 pyramidal neurons in an age- and concentration-dependent manner. *J Neurophysiol,* 68, 2100-9.

MURPHY, L. D., HERZOG, C. E., RUDICK, J. B., FOJO, A. T. & BATES, S. E. (1990) Use of the polymerase chain reaction in the quantitation of mdr-1 gene expression. *Biochemistry,* 29, 10351-6.

assembly and interacts with Drosophila IAP1 in cellular morphogenesis. *Curr Biol,* 16, 1531-7.

PAN, T., KONDO, S., ZHU, W., XIE, W., JANKOVIC, J. & LE, W. (2008) Neuroprotection of rapamycin in lactacystin-induced neurodegeneration via autophagy enhancement. *Neurobiol Dis,* 32, 16-25.

PANDA-JONAS, S., JONAS, J. B. & JAKOBCZYK-ZMIJA, M. (1995) Retinal photoreceptor density decreases with age. *Ophthalmology,* 102, 1853-9.

PANG, I. H. & CLARK, A. F. (2007) Rodent models for glaucoma retinopathy and optic neuropathy. *J Glaucoma,* 16, 483-505.

PAUL, D. L., YU, K., BRUZZONE, R., GIMLICH, R. L. & GOODENOUGH, D. A. (1995) Expression of a dominant negative inhibitor of intercellular communication in the early Xenopus embryo causes delamination and extrusion of cells. *Development,* 121, 371-81.

PERRY, V. H., HENDERSON, Z. & LINDEN, R. (1983) Postnatal changes in retinal ganglion cell and optic axon populations in the pigmented rat. *J Comp Neurol,* 219, 356-68.

PFAFFL, M. W. (2003) Livestock Transcriptomics; Quantitative mRNA Analytics in Molecular Endrocrinology and Physiology.

PHAM, C. T. & LEY, T. J. (1997) The role of granzyme B cluster proteases in cell-mediated cytotoxicity. *Semin Immunol,* 9, 127-33.

POE, B. H., LINVILLE, C. & BRUNSO-BECHTOLD, J. (2001) Age-related decline of presumptive inhibitory synapses in the sensorimotor cortex as revealed by the physical disector. *J Comp Neurol,* 439, 65-72.

POLLEUX, F., MORROW, T. & GHOSH, A. (2000) Semaphorin 3A is a chemoattractant for cortical apical dendrites. *Nature,* 404, 567-73.

PROVENCIO, I., RODRIGUEZ, I. R., JIANG, G., HAYES, W. P., MOREIRA, E. F. & ROLLAG, M. D. (2000) A novel human opsin in the inner retina. *J Neurosci,* 20, 600-5.

PRUNELL, G. F. & TROY, C. M. (2004) Balancing neuronal death. *J Neurosci Res,* 78, 1-6.

QU, Y. & BOUTJDIR, M. (2007) RNase protection assay for quantifying gene expression levels. *Methods Mol Biol,* 366, 145-58.

QUIGLEY, H. A. (1983) Experimental glaucoma damage mechanism. *Arch Ophthalmol,* 101, 1301-2.

QUIGLEY, H. A. (1999) Neuronal death in glaucoma. *Prog Retin Eye Res,* 18, 39-57.

QUIGLEY, H. A. & ADDICKS, E. M. (1980a) Chronic experimental glaucoma in primates. I. Production of elevated intraocular pressure by anterior chamber injection of autologous ghost red blood cells. *Invest Ophthalmol Vis Sci,* 19, 126-36.

QUIGLEY, H. A. & ADDICKS, E. M. (1980b) Chronic experimental glaucoma in primates. II. Effect of extended intraocular pressure elevation on optic nerve head and axonal transport. *Invest Ophthalmol Vis Sci,* 19, 137-52.

QUIGLEY, H. A., NICKELLS, R. W., KERRIGAN, L. A., PEASE, M. E., THIBAULT, D. J. & ZACK, D. J. (1995) Retinal ganglion cell death in experimental glaucoma and after axotomy occurs by apoptosis. *Invest Ophthalmol Vis Sci,* 36, 774-86.

RADOJA, N., STOJADINOVIC, O., WASEEM, A., TOMIC-CANIC, M., MILISAVLJEVIC, V., TEEBOR, S. & BLUMENBERG, M. (2004) Thyroid hormones and gamma interferon specifically increase K15 keratin gene transcription. *Mol Cell Biol,* 24, 3168-79.

RADONIC, A., THULKE, S., MACKAY, I. M., LANDT, O., SIEGERT, W. & NITSCHE, A. (2004) Guideline to reference gene selection for quantitative real-time PCR. *Biochem Biophys Res Commun,* 313, 856-62.

RAVIKUMAR, B., VACHER, C., BERGER, Z., DAVIES, J. E., LUO, S., OROZ, L. G., SCARAVILLI, F., EASTON, D. F., DUDEN, R., O'KANE, C. J. & RUBINSZTEIN, D. C. (2004) Inhibition of mTOR induces autophagy and reduces toxicity of polyglutamine expansions in fly and mouse models of Huntington disease. *Nat Genet,* 36, 585-95.

REDMOND, L. & GHOSH, A. (2005) Regulation of dendritic development by calcium signaling. *Cell Calcium,* 37, 411-6.

REDMOND, L., KASHANI, A. H. & GHOSH, A. (2002) Calcium regulation of dendritic growth via CaM kinase IV and CREB-mediated transcription. *Neuron,* 34, 999-1010.

REITSAMER, H. A., KIEL, J. W., HARRISON, J. M., RANSOM, N. L. & MCKINNON, S. J. (2004) Tonopen measurement of intraocular pressure in mice. *Exp Eye Res,* 78, 799-804.

REN, J., SHI, M., LIU, R., YANG, Q. H., JOHNSON, T., SKARNES, W. C. & DU, C. (2005) The Birc6 (Bruce) gene regulates p53 and the mitochondrial pathway of apoptosis and is essential for mouse embryonic development. *Proc Natl Acad Sci U S A,* 102, 565-70.

RICCI, A., BRONZETTI, E. & AMENTA, F. (1988) Effect of ageing on the nerve fibre population of rat optic nerve. *Gerontology,* 34, 231-5.

ROACH, H. I., AIGNER, T. & KOURI, J. B. (2004) Chondroptosis: a variant of apoptotic cell death in chondrocytes? *Apoptosis,* 9, 265-77.

ROBINSON, G. A. & MADISON, R. D. (2004) Axotomized mouse retinal ganglion cells containing melanopsin show enhanced survival, but not enhanced axon regrowth into a peripheral nerve graft. *Vision Res,* 44, 2667-74.

ROGER, L., GADEA, G. & ROUX, P. (2006) Control of cell migration: a tumour suppressor function for p53? *Biol Cell,* 98, 141-52.

ROTHE, M., PAN, M. G., HENZEL, W. J., AYRES, T. M. & GOEDDEL, D. V. (1995) The TNFR2-TRAF signaling complex contains two novel proteins related to baculoviral inhibitor of apoptosis proteins. *Cell,* 83, 1243-52.

ROY, N., DEVERAUX, Q. L., TAKAHASHI, R., SALVESEN, G. S. & REED, J. C. (1997) The c-IAP-1 and c-IAP-2 proteins are direct inhibitors of specific caspases. *Embo J,* 16, 6914-25.

SADOWSKI-DEBBING, K., COY, J. F., MIER, W., HUG, H. & LOS, M. (2002) Caspases--their role in apoptosis and other physiological processes as revealed by knock-out studies. *Arch Immunol Ther Exp (Warsz),* 50, 19-34.

SAFTIG, P., BEERTSEN, W. & ESKELINEN, E. L. (2008) LAMP-2: a control step for phagosome and autophagosome maturation. *Autophagy,* 4, 510-2.

SALTHOUSE, T. A. (2009) When does age-related cognitive decline begin? *Neurobiol Aging,* 30, 507-14.

SAMSEL, P. A., KISISWA, L., ERICHSEN, J. T., CROSS, S. D. & MORGAN, J. E. A novel method for the induction of experimental glaucoma using magnetic microspheres. *Invest Ophthalmol Vis Sci.*

SAMUEL, T., WELSH, K., LOBER, T., TOGO, S. H., ZAPATA, J. M. & REED, J. C. (2006) Distinct BIR domains of cIAP1 mediate binding to and ubiquitination of tumor necrosis factor receptor-associated factor 2 and second mitochondrial activator of caspases. *J Biol Chem,* 281, 1080-90.

SANCHEZ, R. M., DUNKELBERGER, G. R. & QUIGLEY, H. A. (1986) The number and diameter distribution of axons in the monkey optic nerve. *Invest Ophthalmol Vis Sci,* 27, 1342-50.

SANNA, M. G., DA SILVA CORREIA, J., DUCREY, O., LEE, J., NOMOTO, K., SCHRANTZ, N., DEVERAUX, Q. L. & ULEVITCH, R. J. (2002) IAP suppression of apoptosis involves distinct mechanisms: the TAK1/JNK1 signaling cascade and caspase inhibition. *Mol Cell Biol,* 22, 1754-66.

SANNA, M. G., DUCKETT, C. S., RICHTER, B. W., THOMPSON, C. B. & ULEVITCH, R. J. (1998) Selective activation of JNK1 is necessary for the anti-apoptotic activity of hILP. *Proc Natl Acad Sci U S A,* 95, 6015-20.

SANTORO, M. M., SAMUEL, T., MITCHELL, T., REED, J. C. & STAINIER, D. Y. (2007) Birc2 (clap1) regulates endothelial cell integrity and blood vessel homeostasis. *Nat Genet,* 39, 1397-402.

SARKAR, S., DAVIES, J. E., HUANG, Z., TUNNACLIFFE, A. & RUBINSZTEIN, D. C. (2007) Trehalose, a novel mTOR-independent autophagy enhancer, accelerates the clearance of mutant huntingtin and alpha-synuclein. *J Biol Chem,* 282, 5641-52.

SAWADA, A. & NEUFELD, A. H. (1999) Confirmation of the rat model of chronic, moderately elevated intraocular pressure. *Exp Eye Res,* 69, 525-31.

SCHENA, M., SHALON, D., DAVIS, R. W. & BROWN, P. O. (1995) Quantitative monitoring of gene expression patterns with a complementary DNA microarray. *Science,* 270, 467-70.

SCHWERK, C. & SCHULZE-OSTHOFF, K. (2003) Non-apoptotic functions of caspases in cellular proliferation and differentiation. *Biochem Pharmacol,* 66, 1453-8.

SCOTT, E. K. & LUO, L. (2001) How do dendrites take their shape? *Nat Neurosci,* 4, 359-65.

SEKARAN, S., LUPI, D., JONES, S. L., SHEELY, C. J., HATTAR, S., YAU, K. W., LUCAS, R. J., FOSTER, R. G. & HANKINS, M. W. (2005) Melanopsin-dependent photoreception provides earliest light detection in the mammalian retina. *Curr Biol,* 15, 1099-107.

SELZNICK, L. A., ZHENG, T. S., FLAVELL, R. A., RAKIC, P. & ROTH, K. A. (2000) Amyloid beta-induced neuronal death is bax-dependent but caspase-independent. *J Neuropathol Exp Neurol,* 59, 271-9.

SEMO, M., PEIRSON, S., LUPI, D., LUCAS, R. J., JEFFERY, G. & FOSTER, R. G. (2003) Melanopsin retinal ganglion cells and the maintenance of circadian and pupillary responses to light in aged rodless/coneless (rd/rd cl) mice. *Eur J Neurosci,* 17, 1793-801.

SEVERSON, J. A. & FINCH, C. E. (1980) Reduced dopaminergic binding during aging in the rodent striatum. *Brain Res,* 192, 147-62.

SGORBISSA, A., BENETTI, R., MARZINOTTO, S., SCHNEIDER, C. & BRANCOLINI, C. (1999) Caspase-3 and caspase-7 but not caspase-6 cleave Gas2 in vitro: implications for microfilament reorganization during apoptosis. *J Cell Sci,* 112 (Pt 23), 4475-82.

SHAREEF, S. R., GARCIA-VALENZUELA, E., SALIERNO, A., WALSH, J. & SHARMA, S. C. (1995) Chronic ocular hypertension following episcleral venous occlusion in rats. *Exp Eye Res,* 61, 379-82.

SHI, S. H., CHENG, T., JAN, L. Y. & JAN, Y. N. (2004a) The immunoglobulin family member dendrite arborization and synapse maturation 1 (Dasm1) controls excitatory synapse maturation. *Proc Natl Acad Sci U S A,* 101, 13346-51.

SHI, S. H., COX, D. N., WANG, D., JAN, L. Y. & JAN, Y. N. (2004b) Control of dendrite arborization by an Ig family member, dendrite arborization and synapse maturation 1 (Dasm1). *Proc Natl Acad Sci U S A,* 101, 13341-5.

SHOU, T., LIU, J., WANG, W., ZHOU, Y. & ZHAO, K. (2003) Differential dendritic shrinkage of alpha and beta retinal ganglion cells in cats with chronic glaucoma. *Invest Ophthalmol Vis Sci,* 44, 3005-10.

SHOU, Y., LI, N., LI, L., BOROWITZ, J. L. & ISOM, G. E. (2002) NF-kappaB-mediated up-regulation of Bcl-X(S) and Bax contributes to cytochrome c release in cyanide-induced apoptosis. *J Neurochem,* 81, 842-52.

SHU, H. B., TAKEUCHI, M. & GOEDDEL, D. V. (1996) The tumor necrosis factor receptor 2 signal transducers TRAF2 and c-IAP1 are components of the tumor necrosis factor receptor 1 signaling complex. *Proc Natl Acad Sci U S A,* 93, 13973-8.

SILKE, J. & VAUX, D. L. (2001) Two kinds of BIR-containing protein - inhibitors of apoptosis, or required for mitosis. *J Cell Sci,* 114, 1821-7.

SILVER, J. & HUGHES, A. F. (1973) The role of cell death during morphogenesis of the mammalian eye. *J Morphol,* 140, 159-70.

SILVER, J. & ROBB, R. M. (1979) Studies on the development of the eye cup and optic nerve in normal mice and in mutants with congenital optic nerve aplasia. *Dev Biol,* 68, 175-90.

SLEE, E. A., HARTE, M. T., KLUCK, R. M., WOLF, B. B., CASIANO, C. A., NEWMEYER, D. D., WANG, H. G., REED, J. C., NICHOLSON, D. W., ALNEMRI, E. S., GREEN, D. R. & MARTIN, S. J. (1999) Ordering the cytochrome c-initiated caspase cascade: hierarchical activation of caspases-2, -3, -6, -7, -8, and -10 in a caspase-9-dependent manner. *J Cell Biol,* 144, 281-92.

SOHL, G., DEGEN, J., TEUBNER, B. & WILLECKE, K. (1998) The murine gap junction gene connexin36 is highly expressed in mouse retina and regulated during brain development. *FEBS Lett,* 428, 27-31.

SOKOLOV, M., LYUBARSKY, A. L., STRISSEL, K. J., SAVCHENKO, A. B., GOVARDOVSKII, V. I., PUGH, E. N., JR. & ARSHAVSKY, V. Y. (2002) Massive light-driven translocation of transducin between the two major compartments of rod cells: a novel mechanism of light adaptation. *Neuron,* 34, 95-106.

SOLIS, O., LIMON, D. I., FLORES-HERNANDEZ, J. & FLORES, G. (2007) Alterations in dendritic morphology of the prefrontal cortical and striatum neurons in the unilateral 6-OHDA-rat model of Parkinson's disease. *Synapse,* 61, 450-8.

SOLLARS, P. J., SMERASKI, C. A., KAUFMAN, J. D., OGILVIE, M. D., PROVENCIO, I. & PICKARD, G. E. (2003) Melanopsin and non-melanopsin expressing retinal ganglion cells innervate the hypothalamic suprachiasmatic nucleus. *Vis Neurosci,* 20, 601-10.

SONG, H., MING, G., HE, Z., LEHMANN, M., MCKERRACHER, L., TESSIER-LAVIGNE, M. & POO, M. (1998) Conversion of neuronal growth cone responses from repulsion to attraction by cyclic nucleotides. *Science,* 281, 1515-8.

SORDET, O., REBE, C., PLENCHETTE, S., ZERMATI, Y., HERMINE, O., VAINCHENKER, W., GARRIDO, C., SOLARY, E. & DUBREZ-DALOZ, L. (2002) Specific involvement of caspases in the differentiation of monocytes into macrophages. *Blood,* 100, 4446-53.

SPANAKIS, E. (1993) Problems related to the interpretation of autoradiographic data on gene expression using common constitutive transcripts as controls. *Nucleic Acids Res,* 21, 3809-19.

SPEAR, P. D. (1993) Neural bases of visual deficits during aging. *Vision Res,* 33, 2589-609.

SPERANDIO, S., POKSAY, K., DE BELLE, I., LAFUENTE, M. J., LIU, B., NASIR, J. & BREDESEN, D. E. (2004) Paraptosis: mediation by MAP kinases and inhibition by AIP-1/Alix. *Cell Death Differ,* 11, 1066-75.

SPROTT, R. L. & AUSTAD, S. N. (1995) Animal models for aging research. *E.L Scdneider, J.W.Rowe (Eds), Handbook of the Biology of aging, 4th Edition, Academic Press, San Diego,* 3-24.

SRINIVASULA, S. M. & ASHWELL, J. D. (2008) IAPs: what's in a name? *Mol Cell,* 30, 123-35.

STREIT, S., MICHALSKI, C. W., ERKAN, M., KLEEFF, J. & FRIESS, H. (2009) Northern blot analysis for detection and quantification of RNA in pancreatic cancer cells and tissues. *Nat Protoc,* 4, 37-43.

STUART, G., SPRUSTON, N. AND HAUSSER, M. (2008) Dendrites. *Oxford University Press, Oxford, UK.*

SUN, W., LI, N. & HE, S. (2002) Large-scale morophological survey of rat retinal ganglion cells. *Vis Neurosci,* 19, 483-93.

SUZUKI, T., HIGGINS, P. J. & CRAWFORD, D. R. (2000) Control selection for RNA quantitation. *Biotechniques,* 29, 332-7.

TAHZIB, N. G., RANSOM, N. L., REITSAMER, H. A. & MCKINNON, S. J. (2004) Alpha-fodrin is cleaved by caspase-3 in a chronic ocular hypertensive (COH) rat model of glaucoma. *Brain Res Bull,* 62, 491-5.

TANG, E. D., WANG, C. Y., XIONG, Y. & GUAN, K. L. (2003) A role for NF-kappaB essential modifier/IkappaB kinase-gamma (NEMO/IKKgamma) ubiquitination in the activation of the IkappaB kinase complex by tumor necrosis factor-alpha. *J Biol Chem,* 278, 37297-305.

TEODORO, J. G., PARKER, A. E., ZHU, X. & GREEN, M. R. (2006) p53-mediated inhibition of angiogenesis through up-regulation of a collagen prolyl hydroxylase. *Science,* 313, 968-71.

TEZEL, G., LI, L. Y., PATIL, R. V. & WAX, M. B. (2001) TNF-alpha and TNF-alpha receptor-1 in the retina of normal and glaucomatous eyes. *Invest Ophthalmol Vis Sci,* 42, 1787-94.

THANOS, S. (1988) Alterations in the morphology of ganglion cell dendrites in the adult rat retina after optic nerve transection and grafting of peripheral nerve segments. *Cell Tissue Res,* 254, 599-609.

THELLIN, O., ZORZI, W., LAKAYE, B., DE BORMAN, B., COUMANS, B., HENNEN, G., GRISAR, T., IGOUT, A. & HEINEN, E. (1999) Housekeeping genes as internal standards: use and limits. *J Biotechnol,* 75, 291-5.

THIBAULT, O. & LANDFIELD, P. W. (1996) Increase in single L-type calcium channels in hippocampal neurons during aging. *Science,* 272, 1017-20.

THOMPSON, S., FOSTER, R. G., STONE, E. M., SHEFFIELD, V. C. & MROSOVSKY, N. (2008) Classical and melanopsin photoreception in irradiance detection: negative masking of locomotor activity by light. *Eur J Neurosci,* 27, 1973-9.

THORNBERRY, N. A., RANO, T. A., PETERSON, E. P., RASPER, D. M., TIMKEY, T., GARCIA-CALVO, M., HOUTZAGER, V. M., NORDSTROM, P. A., ROY, S., VAILLANCOURT, J. P., CHAPMAN, K. T. & NICHOLSON, D. W. (1997) A combinatorial approach defines specificities of members of the caspase family and granzyme B. Functional relationships established for key mediators of apoptosis. *J Biol Chem,* 272, 17907-11.

TOESCU, E. C., VERKHRATSKY, A. & LANDFIELD, P. W. (2004) Ca2+ regulation and gene expression in normal brain aging. *Trends Neurosci,* 27, 614-20.

TURMAINE, M., RAZA, A., MAHAL, A., MANGIARINI, L., BATES, G. P. & DAVIES, S. W. (2000) Nonapoptotic neurodegeneration in a transgenic mouse model of Huntington's disease. *Proc Natl Acad Sci U S A,* 97, 8093-7.

UEDA, J., SAWAGUCHI, S., HANYU, T., YAOEDA, K., FUKUCHI, T., ABE, H. & OZAWA, H. (1998) Experimental glaucoma model in the rat induced by laser trabecular photocoagulation after an intracameral injection of India ink. *Jpn J Ophthalmol,* 42, 337-44.

URCOLA, J. H., HERNANDEZ, M. & VECINO, E. (2006) Three experimental glaucoma models in rats: comparison of the effects of intraocular pressure elevation on retinal ganglion cell size and death. *Exp Eye Res,* 83, 429-37.

UREN, A. G., PAKUSCH, M., HAWKINS, C. J., PULS, K. L. & VAUX, D. L. (1996) Cloning and expression of apoptosis inhibitory protein homologs that function to inhibit apoptosis and/or bind tumor necrosis factor receptor-associated factors. *Proc Natl Acad Sci U S A,* 93, 4974-8.

UYLINGS, H. B. & DE BRABANDER, J. M. (2002) Neuronal changes in normal human aging and Alzheimer's disease. *Brain Cogn,* 49, 268-76.

VANDESOMPELE, J., DE PRETER, K., PATTYN, F., POPPE, B., VAN ROY, N., DE PAEPE, A. & SPELEMAN, F. (2002) Accurate normalization of real-time quantitative RT-PCR data by geometric averaging of multiple internal control genes. *Genome Biol,* 3, RESEARCH0034.

VARFOLOMEEV, E., BLANKENSHIP, J. W., WAYSON, S. M., FEDOROVA, A. V., KAYAGAKI, N., GARG, P., ZOBEL, K., DYNEK, J. N., ELLIOTT, L. O., WALLWEBER, H. J., FLYGARE, J. A., FAIRBROTHER, W. J., DESHAYES, K., DIXIT, V. M. & VUCIC, D. (2007) IAP antagonists induce autoubiquitination of c-IAPs, NF-kappaB activation, and TNFalpha-dependent apoptosis. *Cell,* 131, 669-81.

VARFOLOMEEV, E. & VUCIC, D. (2008) (Un)expected roles of c-IAPs in apoptotic and NFkappaB signaling pathways. *Cell Cycle,* 7, 1511-21.

VARFOLOMEEV, E., WAYSON, S. M., DIXIT, V. M., FAIRBROTHER, W. J. & VUCIC, D. (2006) The inhibitor of apoptosis protein fusion c-IAP2.MALT1 stimulates NF-kappaB activation independently of TRAF1 AND TRAF2. *J Biol Chem,* 281, 29022-9.

VERHAGEN, A. M., COULSON, E. J. & VAUX, D. L. (2001) Inhibitor of apoptosis proteins and their relatives: IAPs and other BIRPs. *Genome Biol,* 2, REVIEWS3009.

VERNOOY, S. Y., CHOW, V., SU, J., VERBRUGGHE, K., YANG, J., COLE, S., OLSON, M. R. & HAY, B. A. (2002) Drosophila Bruce can potently suppress Rpr- and Grim-dependent but not Hid-dependent cell death. *Curr Biol,* 12, 1164-8.

VINCE, J. E., WONG, W. W., KHAN, N., FELTHAM, R., CHAU, D., AHMED, A. U., BENETATOS, C. A., CHUNDURU, S. K., CONDON, S. M., MCKINLAY, M., BRINK, R., LEVERKUS, M.,

TERGAONKAR, V., SCHNEIDER, P., CALLUS, B. A., KOENTGEN, F., VAUX, D. L. & SILKE, J. (2007) IAP antagonists target cIAP1 to induce TNFalpha-dependent apoptosis. *Cell,* 131, 682-93.

VONSATTEL, J. P., MYERS, R. H., STEVENS, T. J., FERRANTE, R. J., BIRD, E. D. & RICHARDSON, E. P., JR. (1985) Neuropathological classification of Huntington's disease. *J Neuropathol Exp Neurol,* 44, 559-77.

VOUSDEN, K. H. & LANE, D. P. (2007) p53 in health and disease. *Nat Rev Mol Cell Biol,* 8, 275-83.

VRABEC, J. P. & LEVIN, L. A. (2007) The neurobiology of cell death in glaucoma. *Eye (Lond),* 21 Suppl 1, S11-4.

WAJANT, H., PFIZENMAIER, K. & SCHEURICH, P. (2003) Tumor necrosis factor signaling. *Cell Death Differ,* 10, 45-65.

WALTON, K. D. & NAVARRETE, R. (1991) Postnatal changes in motoneurone electrotonic coupling studied in the in vitro rat lumbar spinal cord. *J Physiol,* 433, 283-305.

WANG, H. Z., LU, Q. J., WANG, N. L., LIU, H., ZHANG, L. & ZHAN, G. L. (2008a) Loss of melanopsin-containing retinal ganglion cells in a rat glaucoma model. *Chin Med J (Engl),* 121, 1015-9.

WANG, L., ZHANG, Q., LIU, B., HAN, M. & SHAN, B. (2008b) Challenge and promise: roles for Livin in progression and therapy of cancer. *Mol Cancer Ther,* 7, 3661-9.

WANG, R. F., SCHUMER, R. A., SERLE, J. B. & PODOS, S. M. (1998) A comparison of argon laser and diode laser photocoagulation of the trabecular meshwork to produce the glaucoma monkey model. *J Glaucoma,* 7, 45-9.

WANG, X., TAY, S. S. & NG, Y. K. (2000) An immunohistochemical study of neuronal and glial cell reactions in retinae of rats with experimental glaucoma. *Exp Brain Res,* 132, 476-84.

WARRINGTON, J. A., NAIR, A., MAHADEVAPPA, M. & TSYGANSKAYA, M. (2000) Comparison of human adult and fetal expression and identification of 535 housekeeping/maintenance genes. *Physiol Genomics,* 2, 143-7.

WATTS, R. J., HOOPFER, E. D. & LUO, L. (2003) Axon pruning during Drosophila metamorphosis: evidence for local degeneration and requirement of the ubiquitin-proteasome system. *Neuron,* 38, 871-85.

WEBER, A. J. & HARMAN, C. D. (2005) Structure-function relations of parasol cells in the normal and glaucomatous primate retina. *Invest Ophthalmol Vis Sci,* 46, 3197-207.

WEBER, A. J., KAUFMAN, P. L. & HUBBARD, W. C. (1998) Morphology of single ganglion cells in the glaucomatous primate retina. *Invest Ophthalmol Vis Sci,* 39, 2304-20.

WEINREB, R. N. & LINDSEY, J. D. (2005) The importance of models in glaucoma research. *J Glaucoma,* 14, 302-4.

WEISSE, I. (1995) Changes in the aging rat retina. *Ophthalmic Res,* 27 Suppl 1, 154-63.

WENK, G. L. (2003) Neuropathologic changes in Alzheimer's disease. *J Clin Psychiatry,* 64 Suppl 9, 7-10.

WHITMORE, A. V., LIBBY, R. T. & JOHN, S. W. (2005) Glaucoma: thinking in new ways-a role for autonomous axonal self-destruction and other compartmentalised processes? *Prog Retin Eye Res,* 24, 639-62.

WILLIAMS, D. W., KONDO, S., KRZYZANOWSKA, A., HIROMI, Y. & TRUMAN, J. W. (2006) Local caspase activity directs engulfment of dendrites during pruning. *Nat Neurosci,* 9, 1234-6.

WOLSZON, L. R., REHDER, V., KATER, S. B. & MACAGNO, E. R. (1994) Calcium wave fronts that cross gap junctions may signal neuronal death during development. *J Neurosci,* 14, 3437-48.

WONG, R. O. & GHOSH, A. (2002) Activity-dependent regulation of dendritic growth and patterning. *Nat Rev Neurosci,* 3, 803-12.

WONG, T. P., CAMPBELL, P. M., RIBEIRO-DA-SILVA, A. & CUELLO, A. C. (1998) Synaptic numbers across cortical laminae and cognitive performance of the rat during ageing. *Neuroscience,* 84, 403-12.

WRIDE, M. A. (2000) Minireview: apoptosis as seen through a lens. *Apoptosis,* 5, 203-9.

WRIDE, M. A., GEATRELL, J. & GUGGENHEIM, J. A. (2006) Proteases in eye development and disease. *Birth Defects Res C Embryo Today,* 78, 90-105.

WRIDE, M. A., PARKER, E. & SANDERS, E. J. (1999) Members of the bcl-2 and caspase families regulate nuclear degeneration during chick lens fibre differentiation. *Dev Biol,* 213, 142-56.

WU, G. Y., DEISSEROTH, K. & TSIEN, R. W. (2001) Spaced stimuli stabilize MAPK pathway activation and its effects on dendritic morphology. *Nat Neurosci,* 4, 151-8.

WU, R. L., CHEN, T. T. & SUN, T. T. (1994) Functional importance of an Sp1- and an NFkB-related nuclear protein in a keratinocyte-specific promoter of rabbit K3 keratin gene. *J Biol Chem,* 269, 28450-9.

XILOURI, M., VOGIATZI, T., VEKRELLIS, K., PARK, D. & STEFANIS, L. (2009) Abberant alpha-synuclein confers toxicity to neurons in part through inhibition of chaperone-mediated autophagy. *PLoS One,* 4, e5515.

XU, H. P., CHEN, H., DING, Q., XIE, Z. H., CHEN, L., DIAO, L., WANG, P., GAN, L., CRAIR, M. C. & TIAN, N. The immune protein CD3zeta is required for normal development of neural circuits in the retina. *Neuron,* 65, 503-15.

YAMASHIMA, T. (2000) Implication of cysteine proteases calpain, cathepsin and caspase in ischemic neuronal death of primates. *Prog Neurobiol,* 62, 273-95.

YAMASHIMA, T. (2004) Ca2+-dependent proteases in ischemic neuronal death: a conserved 'calpain-cathepsin cascade' from nematodes to primates. *Cell Calcium,* 36, 285-93.

YANG, Y., FANG, S., JENSEN, J. P., WEISSMAN, A. M. & ASHWELL, J. D. (2000) Ubiquitin protein ligase activity of IAPs and their degradation in proteasomes in response to apoptotic stimuli. *Science,* 288, 874-7.

YANG, Z., QUIGLEY, H. A., PEASE, M. E., YANG, Y., QIAN, J., VALENTA, D. & ZACK, D. J. (2007) Changes in gene expression in experimental glaucoma and optic nerve transection: the equilibrium between protective and detrimental mechanisms. *Invest Ophthalmol Vis Sci,* 48, 5539-48.

YAWO, H. (1987) Changes in the dendritic geometry of mouse superior cervical ganglion cells following postganglionic axotomy. *J Neurosci,* 7, 3703-11.

YOUNG, R. W. (1985) Cell differentiation in the retina of the mouse. *Anat Rec,* 212, 199-205.

YUAN, J., LIPINSKI, M. & DEGTEREV, A. (2003) Diversity in the mechanisms of neuronal cell death. *Neuron,* 40, 401-13.

YUCEL, Y. H., GUPTA, N., ZHANG, Q., MIZISIN, A. P., KALICHMAN, M. W. & WEINREB, R. N. (2006) Memantine protects neurons from shrinkage in the lateral geniculate nucleus in experimental glaucoma. *Arch Ophthalmol,* 124, 217-25.

YUCEL, Y. H., ZHANG, Q., WEINREB, R. N., KAUFMAN, P. L. & GUPTA, N. (2003) Effects of retinal ganglion cell loss on magno-, parvo-, koniocellular pathways in the lateral geniculate nucleus and visual cortex in glaucoma. *Prog Retin Eye Res,* 22, 465-81.

ZAJA-MILATOVIC, S., MILATOVIC, D., SCHANTZ, A. M., ZHANG, J., MONTINE, K. S., SAMII, A., DEUTCH, A. Y. & MONTINE, T. J. (2005) Dendritic degeneration in neostriatal medium spiny neurons in Parkinson disease. *Neurology,* 64, 545-7.

ZARNEGAR, B. J., WANG, Y., MAHONEY, D. J., DEMPSEY, P. W., CHEUNG, H. H., HE, J., SHIBA, T., YANG, X., YEH, W. C., MAK, T. W., KORNELUK, R. G. & CHENG, G. (2008) Noncanonical NF-kappaB activation requires coordinated assembly of a regulatory complex of the adaptors cIAP1, cIAP2, TRAF2 and TRAF3 and the kinase NIK. *Nat Immunol,* 9, 1371-8.

ZHANG, X., CHEN, J., GRAHAM, S. H., DU, L., KOCHANEK, P. M., DRAVIAM, R., GUO, F., NATHANIEL, P. D., SZABO, C., WATKINS, S. C. & CLARK, R. S. (2002) Intranuclear localization of apoptosis-inducing factor (AIF) and large scale DNA fragmentation after traumatic brain injury in rats and in neuronal cultures exposed to peroxynitrite. *J Neurochem,* 82, 181-91.

Appendices

Appendix I

List of publications and related papers

Kisiswa L., Albon J., Morgan JE., Wride MA., Cellular inhibitor of apoptosis (cIAP1) is down-regulated during retinal ganglion cell (RGC) maturation. Exp Eye Res. 2010 Nov;91(5):739-47.

Samsel PA., **Kisiswa L.,** Erichsen JT., Cross SD., Morgan JE. A novel method for the induction of experimental glaucoma using magnetic Microspheres. Invest Ophthalmol Vis Sci. 2010 Oct. Ahead of print.

Kisiswa L., Dervan AG., Albon J., Morgan JE., Wride MA. Retinal Ganglion Cell Death Postponed: Giving Apoptosis a Break? Ophthalmic Res. 2009 Oct 15;43(2):61-78.

Geatrell JC., Gan PM., Mansergh FC., **Kisiswa L.,** Jarrin M., Williams LA., Evans MJ., Boulton ME., Wride MA. Apoptosis gene profiling reveals spatio-temporal regulated expression of the p53/Mdm2 pathway during lens development. Exp Eye Res. 2009 Jun;88 (6):1137-51

Goodall N., **Kisiswa L.,** Prashar A., Faulkner S., Tokarczuk P., Singh K., Erichsen JT., Guggenheim J., Halfter W., Wride MA. 3-Dimensional Modelling of Chick Embryo Eye Development and Growth Using High Resolution Magnetic Resonance Imaging. Exp Eye Res. 2009 Oct;89(4):511-21.

List of published abstracts

1. Age-related dendrite pruning in the adult Brown Norway (BN) rat retina. Association for Research in Vision and Ophthalmology's (ARVO) 2010 Annual Meeting. Fort Lauderdale, USA.

2. Impaired survival pathway activation in mature retinal ganglion cells (RGCs). The 8th Retinal Ganglion cell meeting, a pre-ARVO meeting, 2010. Fort Lauderdale, USA.

3. Age-dependent reduction in the expression of inhibitors of apoptosis (IAPs) in the retina: implication for age-related retinal degeneration. Society for Neuroscience Annual Meeting, 2009. Chicago, USA.

4. Retina conference 2nd October 2009. Cellular inhibitor of apoptosis (cIAP1) is down-regulated in ageing rat retina. Retina conference, 2009. Dublin, Ireland,.

5. Age-dependent reduction in the expression of inhibitors of apoptosis (IAPs) in the retina: implication for age-related retinal degeneration. Cardiff tissue engineering and repair (CITER) meeting, 2009. Cardiff University, Wales, UK

6.Age-dependent reduction in the expression of inhibitors of apoptosis (IAPs) in the retina: implication for age-related retinal degeneration. Gene expression in neuronal diseases, 2009. Conference organised by the international society of Biochemistry, Cardiff University, Wales, UK

Appendix II

RT-PCR/REAL-TIME PCR

10x MOPS electrophoresis buffer

50mM sodium acetat,

0.2 4-Morpholinepropanesulfonic acid (MOPS)

1mM EDTA.

Adjust to pH7.0 with NaOH

RNA denaturing gel [100ml]

18ml formaldehyde

10ml 10x MOPS

72ml ddH_2O

1.5g agarose

RNA running buffer [1L]

83ml formaldehyde

100ml 10x MOPS

817ml ddH_2O

Working RTL

10µl β-Mecarptoethanol

1ml RTL buffer

Working RPE

4 volumes of 100% ethanol

RPE

EDTA (0.5M)

93.05g EDTA (FW-372.2)

500ml ddH_2O

NaOH to pH 8.5

TAE (50x) Buffer

242g Tris base (FW=121.14)

100ml 0.5M EDTA (pH8.0)

57.1ml Glacial acid

750ml ddH_2O.

HISTOLOGY/HISTOCHEMISTRY

10X PBS [1L]

80g NaCl

2g KCl

14.4g Na_2PO_4

2.4g KH_2PO_4

HCl to pH 7.4

1000ml dH_2O

4% Paraformaldehyde (PFA) solution [100ml]

4 g PFA

99ml 1x PBS.

1 ml 1M NaOH

Peroxidase sunstrate [5ml]

1 tablet of DAB/Cobalt [0.5mg/ml]

1 tablet of Urea Hydrogen Peroxidase/Tris Buffer

5ml dH_2O

DNaseI [per slide]

100µl1x Reaction Buffer

100µl DNaseI stock

Inactive caspase 3 blocking solution

1X PBS

0.1% Tween 20

5% donkey serum.

WESTERN BLOTTING

10X TBS pH 7.6 (1L)

12.1g 10mM Tris

8.7g 150mM NaCl

1000ml dH_2O

HCL to pH 7.6

1x TBS/Tween 20 [1L]

100ml 10x TBS

900ml dH_2O

1ml Tween 20

pH 7.4

10% APS [10ml]

10g Ammonium persulphate

10ml dH_2O

10x SDS

10g SDS

100ml dH_2O

1.5M Tris-HCL pH 8.8 [150ml]

27,23g Tris base

150 dH_2O

HCL to pH 8.8

0.5M Tris-HCL pH 6.8 [100ml]

6g Tris base

100ml dH_2O

HCL to pH 6.8

Working sample buffer [100µl]

95µl Laemlli buffer

5µl β-Mecarptoethanol

Running buffer [1L]

100ml 10x Tris/glycin/SDS

900ml dH_2O

1X Transfer buffer (1L)

100mlTris/glycine buffer (Bio-Rad)

200ml Methanol

700ml dH_2O

Mild stripping buffer, 1L

15g glycine

1g sodium deocyl sulphate (SDS)

10ml Tween 20

HCL to pH 2.2

1000ml dH_2O

Antigen retrival solution [1L]

1.92 Citric acid anhydrous

1000ml dH_2O

SDS-PAGE

1. Resolving Gel to a final volume of 10ml

Final % Gel	**6%**	**6.5%**	**7%**	**7.5%**	**8%**	**10%**	**12%**	**15%**
Range (Mw)				70-200		20-100	10-70	8-50
Acrylamide (30%)	2.0	2.2	2.3	2.5	2.7	3.3	4.0	5.0
Water	5.3	5.1	5	4.8	4.6	4	3.3	2.3
1.5M Tris pH8.8	2.5	2.5	2.5	2.5	2.5	2.5	2.5	2.5
10% SDS	0.1	0.1	0.1	0.1	0.1	0.1	0.1	0.1
10% APS	100µl	100µl	100µl	100µl	100µl	100µl	100µl	100µl
TEMED	20µl	20µl	20µl	20µl	20µl	20µl	20µl	20µl

2. Stacking Gel to a final volume of 10ml

Acrylamide (30%)	1.67
Water	5.83
0.5M Tris pH 6.6	2.5
10% SDS	0.1
10% APS	50µl
TEMED	10µl

COMPOSITIONS OF SOLUTIONS PROVIDED WITH KITS

ApopTag® Peroxidase in situ Apoptosis Detection Kit, Chemicon

Equlibration buffer: contains potassium cacodylate (dimethylarsinic acid)
Reaction buffer: contains potassium cacodylate (dimethylarsinic acid)

BCA™ Protein Assay, Pierce

Reagent A: Sodium carbonate, sodium bicarbonate, bicinchonic acid and sodium tartrate in 0.1M sodium hydroxide
Reagent B: 4% cupric sulphate
Albumin Standard Ampluse 2 mg/ml: bovine serum albumin at 2.0mg/ml in 0.9% saline and 0.05% sodium azide

cDNA kit, BIOLINE

Oligo $(dT)_{18}$
Random Hexamers
2.5 mM dNTP
5x RT buffer
30Units RNase inhibitors
150 units Reverse trascriptase
1µg/µl Control RNA templet

ECL Plus. Amersham

Solution A: ECL Plus substrate solution containing tris buffer
Solution B. Stock Acridam solution in Dioxane and Ethenol

RNeasy® Mini Kit, Qiagen

RTL buffer: containing guanidinium thicyanate
RPE buffer: containing ethanol
RW1 buffer: containing guanidinium thicyanate, ethanol

VECTASTAIN® Elite® ABC KIT, Vector Laboratories

Reagent A: Avadin

Reagent B: Biotinylated enzyme

QPCR Kit, Sigma

Master mix containing 20 mM Tris-HCl, pH 8.3, 100 mM KCl, 7 mM MgCl2, 0.4 mM each dNTP (dATP, dCTP, dGTP, TTP), stabilizers, 0.05 unit/ml Taq DNA Polymerase, JumpStart Taq antibody, and SYBR Green I.

Internal Reference Dye

Appendix III

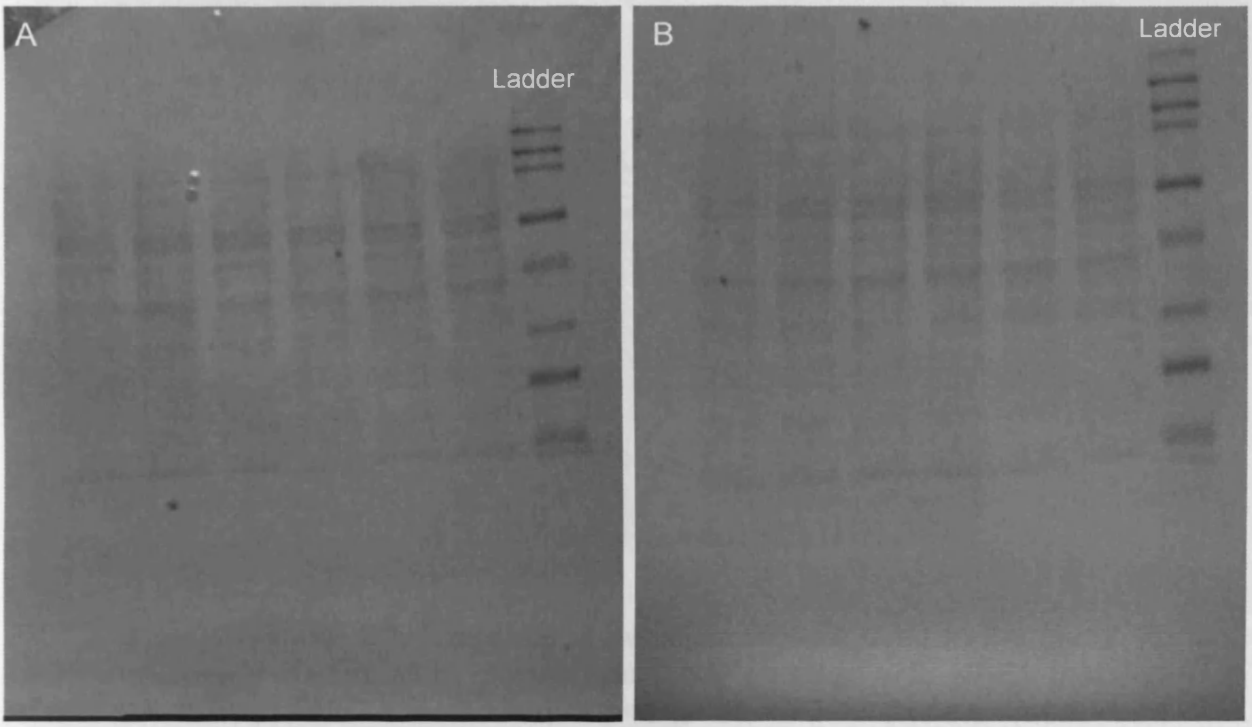

Figure S1. Visualisation of successful transfer utilising Ponceau S. Ladder (Bio Rad)

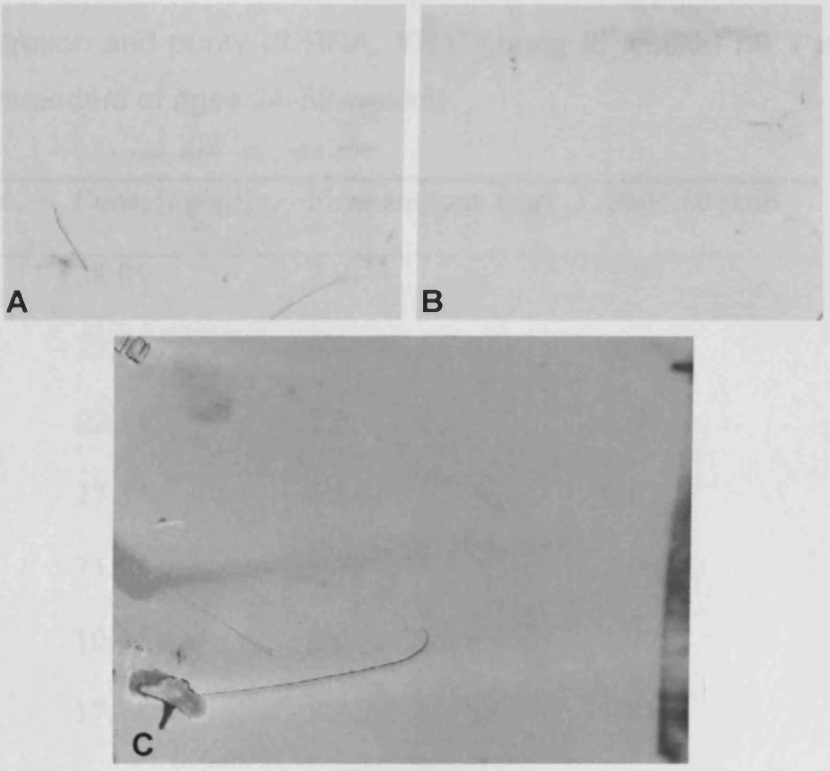

Figure S2. Exampes of negative controls used in the study. A. Pre-incubation of cIAP1 antibody together with cIAP1 blocking peptide showed no staining of cIAP1 on the membrane confirming specificity of primary antibody. B.Rabbit immunoglobulins (IgG) control. C. Secondary antibody omission.

Table S1. Concentration and purity of RNA. YR1, young (6 weeks) rat 1 and OR1 is old (retired breeders of ages 24-52 weeks).

Animal	Sample nr.	Conc. [ng/ µl]	Final amount [µg]	260/280 ratio
YR1	1	28.05	7.0	1.95
	2	25.85	6.0	1.94
YR2	3	22.14	5.0	1.99
	4	27.34	6.8	2.05
YR3	5	23.12	5.78	2.09
	6	10.45	2.6	2.27
OR1	7	17.75	4.4	1.81
	8	11.50	2.86	2.35
OR2	9	10.65	2.66	1.91
	10	21.95	5.5	2.05
OR3	11	9.22	2.3	2.18
	12	6.18	1.54	2.07

Table S2. An example of protein quantification. Absorbance and concentration of the unknown samples. The concentrations were calculated using the equation (y = 0.0008x + 0.135) obtained from the standard curve (Fig. 10).

Sample	Absorbance	Conc.(μg/ml)	Conc.(μg/ml) x 10 (dilution factor)	Conc.(mg/ml)
YR1	0.789	817.5	8175	8.175
YR2	0.8985	954.375	9543.75	9.544
YR3	0.596	576.25	5762.5	5.763
OR1	0.872	921.25	9212.5	9.213
OR2	0.9345	999.375	9993.75	10
OR3	0.9055	963.125	9631.25	9.631

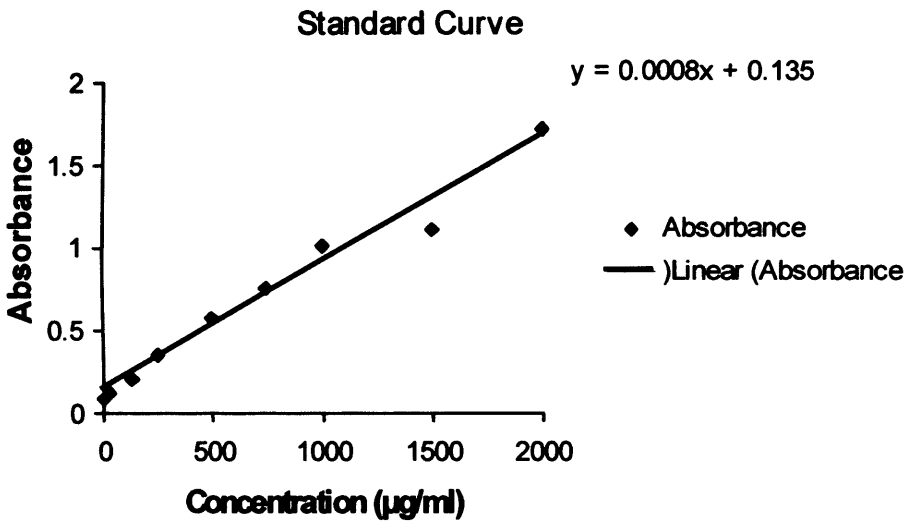

Figure S3. Standard curve. Abbreviations: y, Absorbance: x, concentration.

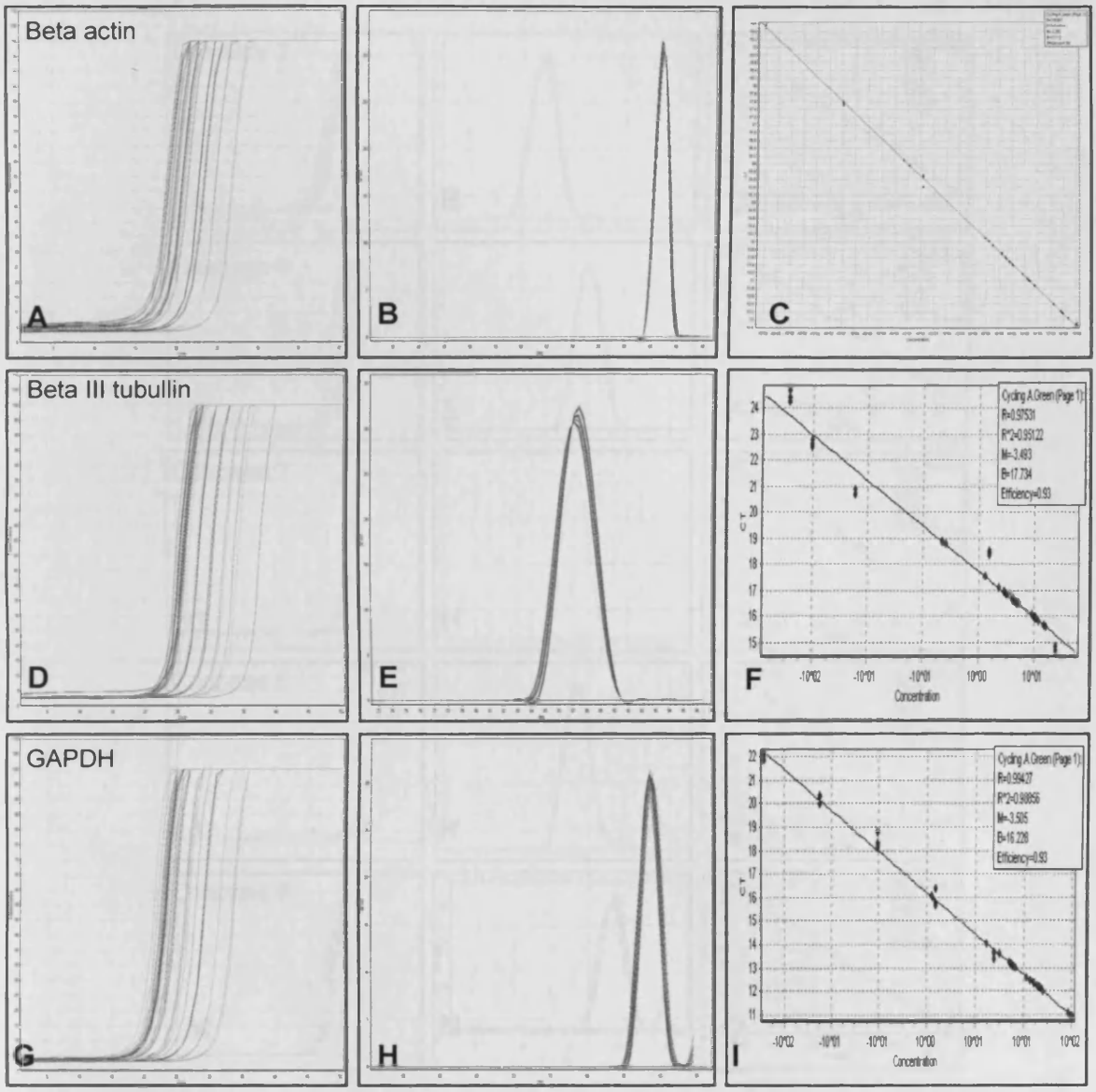

Figure S4: Amplification plot, melting curve and Standard curve of beta actin (A-C). Beta III tubulin (D-F) and GAPDH (G-I)

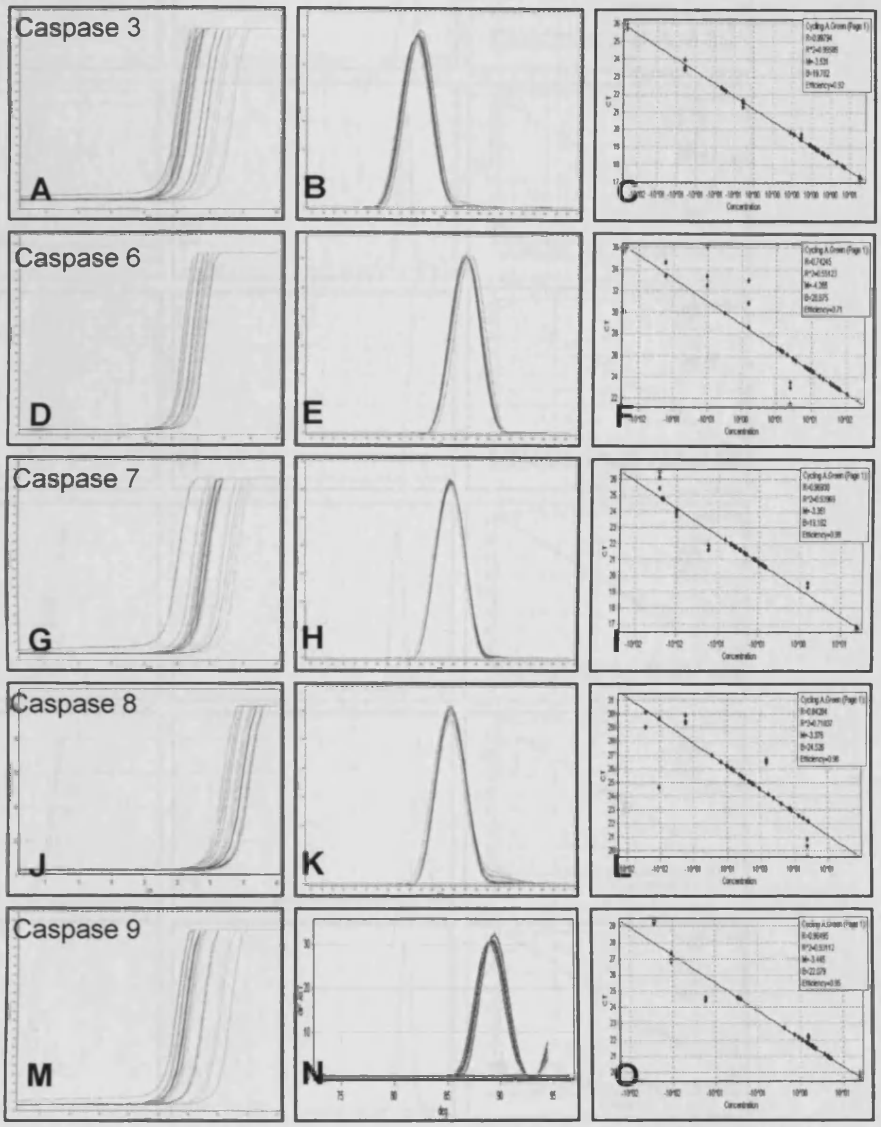

Figure S5: Amplification plot, melting curve and Standard curve of Caspase 3 (A-C). 6 (D-F), 7 (G-I). 8 (J-L) and 9 (M-N).

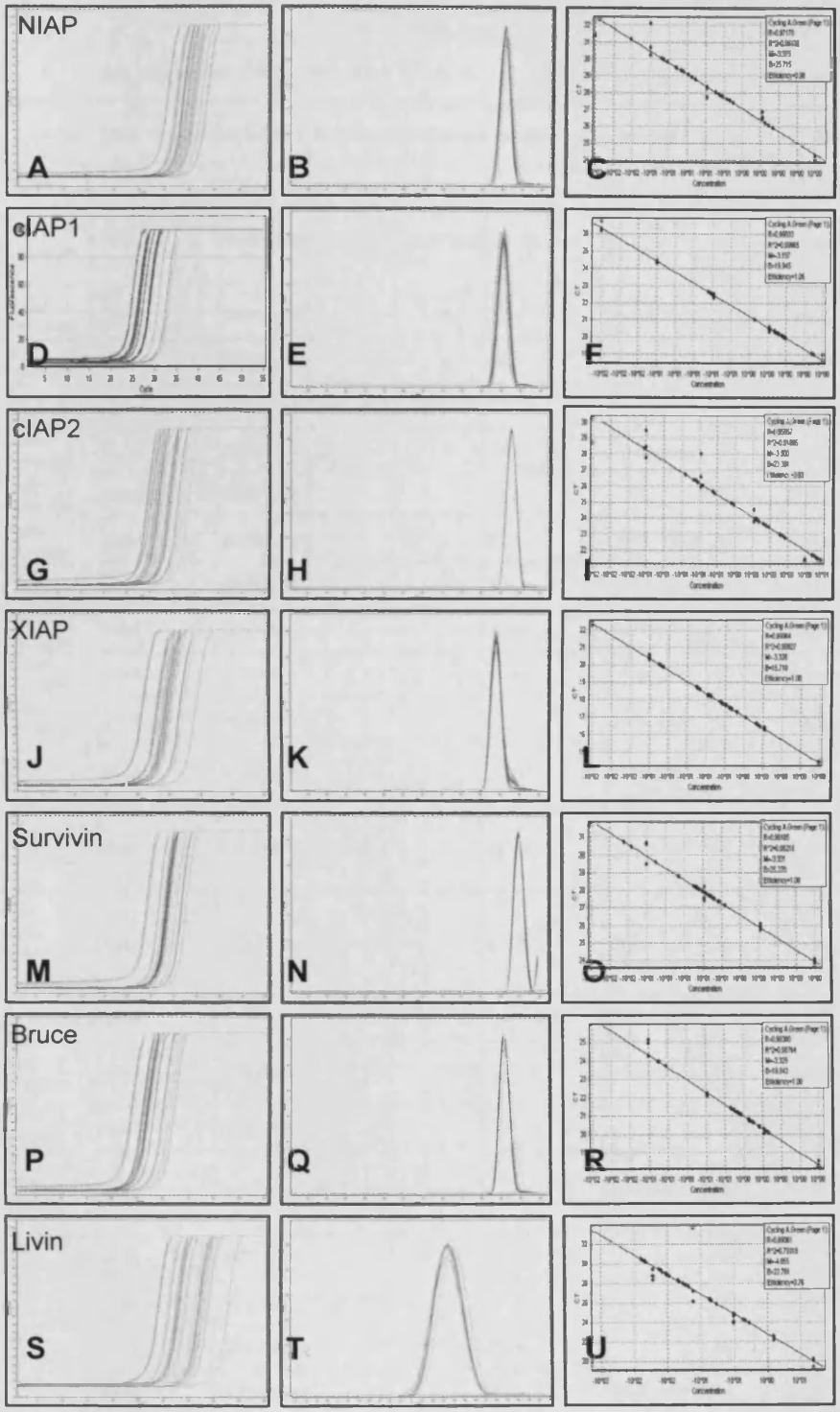

Figure S6: Amplification plot, melting curve and Standard curve of NIAP (A-C). cIAP1 (D-F), cIAP2 (G-I). XIAP (J-L), Survivin (M-N), Bruce (P-R) and Livin (S-U)

Critters 1.0

You are logged in as KISISWA L (kisiswa)
Home | Change Password | Log out

Add a new critter | Print this table | Filter All Go | Export as CSV file Go

ID	Species	Status	Injection Type	Injection 1	Injection 2	Injection 3	Integrated IOP	Termination	Days since 1st injection	Type	Comments
424	Rat	Ready	Bead						-	Explant	
CR400	Rat	Under Procedure	Bead	09/07/2009	18/07/2009	28/07/2009	279.56		362	Explant	OCT.08.07.1st Paulina inj.5um beads,10ul,bad distribution of beads 2nd P,10ul,good.5um 3rd P inj.10u
489	Rat	Under Procedure	Bead	28/05/2010			56.8	14/06/2010	17	Other	20um BSS only control
488	Rat	Under Procedure	Bead	28/05/2010			48.1	14/06/2010	17	Other	20um BSS only control
487	Rat	Under Procedure	Bead						-	Other	
486	Rat	Under Procedure	Bead	28/05/2010			72.5	14/06/2010	17	Other	20um BSS only control
485	Rat	Under Procedure	Bead	28/05/2010			60.3		39	Other	20um BSS only control
484	Rat	Under Procedure	Bead	28/05/2010			65.5	14/06/2010	17	Other	20um No Magnet Control
483	Rat	Under Procedure	Bead	28/05/2010			68.6	14/06/2010	17	Other	20um No Magnet Control
482	Rat	Under Procedure	Bead	28/05/2010			23.5	14/06/2010	17	Other	20um No Magnet Control
481	Rat	Under Procedure	Bead	28/05/2010			12.3	14/06/2010	17	Other	20um No Magnet Control
480	Rat	Under Procedure	Bead	28/05/2010			37.7	14/06/2010	17	Other	20um No Magnet Control
CR401	Rat	Under Procedure	Bead	09/07/2009			288.11	24/08/2009	46	Explant	OCT.08.07,10.08.09.1st Paulina inj.5um beads,10ul,v.good.
CR402	Rat	Under Procedure	Bead	09/07/2009	18/07/2009		873.045	21/09/2009	74	Explant	OCT.08.07,10.08.09.1st Paulina inj.5um beads,10ul,v.good,2nd P,10ul,v.good,5um
CR403	Rat	Under Procedure	Bead	09/07/2009	18/07/2009		810.7	21/09/2009	74	Explant	OCT.08/07,10.08.09.1st Paulina inj.5um beads,15ul,bad beads distribution,2nd P,10ul,5um.good
CTS4	Tree shrew	Acclimatising	Bead					20/11/2009	-	Perfusion (imaging)	Died of illness
CR404	Rat	Under Procedure	Bead	09/07/2009			540.12	21/09/2009	74	Explant	OCT.08/07,10/08/09.1st Paulina inj.5um beads,10ul,v.good.
CTS5	Tree shrew	Under Procedure	Bead	05/03/2009			29.7		488	Perfusion (imaging)	
CR405	Rat	Under Procedure	Bead	29/09/2009	09/10/2009	03/11/2009	57.7	02/12/2009	64	Other	Bad injections. Got lots of saline in because the beads had settled Bleeding. 20um injected
CTS6	Tree shrew	Under Procedure	Bead	05/03/2009			7.8		488	Perfusion (imaging)	
Cts7	Tree shrew	Under Procedure	Bead	23/01/2009	05/03/2009		154.8		529	Perfusion (other)	
CTS8	Tree shrew	Under Procedure	Bead	22/01/2009			428.4		530	Perfusion (imaging)	
CTS9	Tree shrew	Under Procedure	Bead	22/01/2009			95.4	14/02/2009	23	Perfusion (imaging)	
CTS10	Tree shrew	Under Procedure	Bead	22/01/2009			295.1	14/02/2009	23	Perfusion (imaging)	
CTS11	Tree shrew	Under Procedure	Bead	03/12/2009	18/12/2009		259.82	20/12/2009	17	Perfusion (imaging)	
CTS12	Tree shrew	Acclimatising	Bead	11/01/2010			112.33		176	Perfusion (imaging)	Likely to need further injections to keep IOP up JEM
CTS13	Tree shrew	Ready	Bead	04/02/2010	22/03/2010	16/04/2010	363.5		152	Perfusion (imaging)	

Figure S7. An example of critter database for IOP records. Image taken from critter1.cf.ac.uk. Accessed on 6.7.10